Synthesis and Characterization of Biodegradable Polymers

A Thesis Submitted to

The University of Pune

for the degree of

DOCTOR OF PHILOSOPHY

(IN CHEMISTRY)

by

Asutosh Kumar Pandey

Polymer Science and Engineering Division

National Chemical Laboratory

PUNE - 411 008, INDIA.

March 2009

DEDICATED TO MY FAMILY

Acknowledgements

I convey my deep sense of gratitude to my supervisor Dr. (Mrs). Baijayantimala. Garnaik for her constant guidance and her valuable advices that has enabled me to complete my research work successfully. I consider myself fortunate for having a chance of working with a person like her, who is a rare blend of many unique qualities. The tremendous faith on her students sets her apart from others.

I take this opportunity to thank Dr. (Mrs). B. Garnaik for her tremendous help and cooperation throughout my research tenure. I have learnt from her the necessity to be hard-working and sincere, to be honest and critical, and in order to be an accomplished scientist. I am grateful her for all her contribution towards my research work. I am thankful to all my lab-mates, Smita, Balaji, Rahul Jadhav, Dnyaneshwar, Taiseen, Edna Joseph, V.K. Rana and special thanks to lab assistant S .S. Jadhav, Zine, Shelar and Mahesh for their extensive help and cooperation through the entire period of my research at NCL. I also convey my sincerest thanks to Dr. R. P Singh, Dr .B. B. Idage, Dr. C. V. Avadhani, Dr. P.P. Wadgaonkar, Dr D. R. Sani, Mr. Menon and Mrs. D. A. Dhoble for their helpful attitude at all times of need. I am also thankful to all members of Polymer Science and Engineering Division, NCL, for maintaining a warm and friendly atmosphere that helped me to overcome the pain of staying away from all the near and dear ones of my family. My special thanks to Dr. P. Rajmohan for NMR facility, NCL, for his prompt help, whenever sought for. I thank all my friends, Manish Singh, Chandrmaulli Jha, Ananad Chubay, Shrikant Singh, Suraj Agrawa, Chitrasen Gupta and many more, for their friendship, love and cooperation. I am at a loss of words while expressing my feeling of gratitude towards my family brother (Nishitosh kumar Pandey), sister (Anupama Pandey), mother (Smt. Usha Pandey), father (Shri.Dinesh kumar Pandey), son (Yash Pandey) and my wife (Nidhi Pandey) and special thanks to Dr. Gyanandra Prakesh and Shikhar C. Bapna. The patience and encouragement of my parents has been a major driving force for me during the last few years of my research career. I am equally indebted to my wife, who had been a constant source of inspiration for me that gave me the moral boost to win against odds. I am thankful to all other members of my family for their affection and faith they have been keeping on me since years. Finally I thank UGC for the junior and senior research fellowship and the Director (Dr. S. Sivaram) NCL for allowing me to carry out this in the form of a thesis to the University of Poona, to whom again I am grateful for my registration towards the eligibility of a dissertation.

(ASUTOSH KUMAR PANDEY)

DECLARATION

Certified that the work incorporated in this thesis **"Synthesis and Characterization of Biodegradable Polymers"** submitted by Mr. Asutosh Kumar Pandey was carried out by the candidate under my supervision. Such materials as have been obtained from other sources have been duly acknowledged.

(Baijayantimala Garnaik)
Research Supervisor

A B S T R A C T

The thesis highlights the results of dehydropolycondensation of L-lactic acid in to poly (L-lactic acid) (PLA oligomers) followed by post polymerization in presence of various zeolites i.e. ZSM-5, ZSM-12 and β-zeolites. The dehydropolycondensation was achieved under various reaction conditions of temperature, solvents and using various Lewis acid catalysts. The oligomeric product of such dehydropolycondensation were characterized for their thermal and crystalline properties as well as for molecular weight and end groups, using SEC, DSC, powder XRD, NMR and MALDI-ToF spectroscopy. It has been observed that properties of PLA oligomers as well as molecular weights can be controlled by varying these reaction parameters. The analysis of end groups is of importance for the successes of any post polymerization process.

Formation of macrocyclic oligomers was identified by MALDI-ToF at higher temperature. The probability of macrocyclic compounds formation were found to increase with increasing temperature and with the use of solvent in performing the dehydropolycondensation reaction temperature and the use of solvent in performing dehydropolycondensation reaction. The reaction done at temperature ~ 145 ^{0}C or at high temperature but with out solvent were found to result in linear oligomers with both hydroxyl and carboxyl end groups. PLA oligomers which posses both hydroxyl and carboxylic end groups and which are semicrystalline were subjected to post polymerization using dehydropolycondensation techniques.

The post polycondensation was carried out under different reaction condition such as temperature, solvents and using different Lewis acid catalysts. It was found that the molecular weight increased thirteen folds using decaline as a solvent and $SnCl_2.2H_2O$ as a catalyst in 5h. The results obtained using β-zeolite was promising in comparison with other zeolites such as ZSM-5 and ZSM-12.

The sequence determination of resulting polymers showed hexad using ^{13}C quantitative NMR (125 MHz). The sequence results obtained from carbonyl (C=O) and methine regions conform the presence of recemization and transesterification reactions respectively.

Poly (aleuritic acid) and L-lactic acid-co-aleuritic acid were prepared by dehydropolycondensation using protection and deprotection method. A linear poly

(aleuritic acid) with $\bar{M}_w$ =12,000 was prepared. Aggregation behavior of PAA showed micelle type structure in various solvents. The copolymers of L-lactic acid and aleuritic acid are soluble in organic and also mixed solvents. The copolymers also assembled micelle like structure in various organic solvents and combination of two solvents at various compositions.

The grafting reaction of L-lactic acid, PLA oligomers and L-lactic acid-co-12-hydroxy stearic acid copolymer were on the surface of functionalized MWCNTs using dehydropolycondensation in presence of Lewis acid catalyst. Thermal studies revel that the PLA-g-MWCNTS has the effect of plasticizing the PLA matrix and also suggest the formation of new crystalline domains, which is likely to be induced in the proximity of functionalized MWCNTs. The homogeneous distribution of MWCNTs was observed by AFM and ultimately improves the mechanical and electrical properties of PLA polymers.

PLA oligomers with $\bar{M}_w$ 2900-5100 were obtained using ring opening polymerization in presence of zinc L-prolinate catalyst. A series of linear copolymers of L, L-lactide with ε-caprolactone with $\bar{M}_w$ 9000 to 30,000 were also obtained by ROP using the same catalyst. Block copolymer of L, L-lactide with ε-caprolactone was prepared by sequential addition of ε-caprolactone and L, L-lactide and $\bar{M}_w$ was found to be 52,000. ^{13}C NMR results also proved the nature of copolymers were random as well as blocky depending on the comonomer addition during copolymerization reaction.

GLOSSARY

LA	**Lactic acid**
L-LA	**L-Lactic acid**
PLA	**Poly (L-lactic acid)**
TPT	**Tetraphenyltin**
ROP	**Ring opening polymerization**
AL	**Aleuritic acid**
proAL	**Protected aleuritic acid**
PAL	**Protected poly (aleuritic acid)**
PAA	**poly (aleuritic acid)**
PTSA	**p-Toluene sulphonic acid**
CNTs	**Carbon nanotubes**
MWCNTs	**Multiwalled Carbon nanotubes**
12-HSA	**12-Hydroxystearic acid**
CL	**ε-Caprolactone**
PCL	**Poly (ε-caprolactone)**
M_n	**Number average molecular weight**
M_w	**Weight average molecular weight**
M_v	**Viscosity average molecular weight**
MWD	**Molecular weight distribution**
[η]	**Intrinsic viscosity**
T_g	**Glass transition temperature**
T_m	**Melting point**
m.p.	**Melting point (of an organic compound)**
b.p.	**Boiling point**

LIST OF TABLES

LIST OF FIGURES

C O N T E N T S

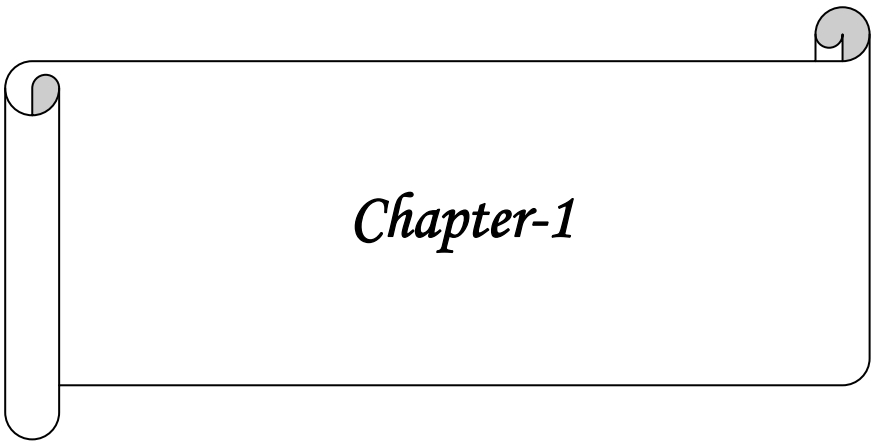
Chapter-1

CHAPTER – 1: SYNTHESIS, CHARACTERIZATION AND APPLICATION OF BIODEGRADABLE POLYESTERS

1.1. Introduction:

Synthetic petrochemical-based polymers have had a tremendous industrial impact since the 1940s. Despite the numerous advantages of these materials, two major drawbacks remain to be solved, namely, the use of nonrenewable resources in their production and the ultimate fate of these large-scale commodity polymers. Due to their unique properties, biodegradable **[1]**, polymers have long been considered as alternative environmentally friendly polymers, and the spectacular advances achieved over the last 30 years in the synthesis, manufacture, and processing of these materials have given rise to a broad range of practical applications from packaging to more sophisticated biomedical devices **[2-8]**. The variety of biodegradable polymers known, linear aliphatic polyesters are particularly attractive and most used, especially those derived from lactic acid (LA).

International organizations such as the American Society for Testing and Materials (ASTM), the Institute for Standards Research (ISR), the European Standardization Committee (CEN), the International Standardization Organization (ISO), the German Institute for Standardization (DIN), the Italian Standardization Agency (UNI), and the Organic Reclamation and Composting Association (ORCA), are all actively involved in developing definitions and tests of biodegradability in different environments and compostability **[9, 10]**. Although a standard, global definition for biodegradable plastics has so far not evolved, each available definition (ASTM, CEN, ISO) correlates the degradability of a material with a specific disposal environment and to a specific standard test method.

Biodegradability must be looked at as a supplementary property for a thermoplastic product whose primary characteristic has to be a material, which is stable during its first use and then, after a certain induction time, becomes degradable until its complete assimilation in the biological cycle of nature.

Poly (lactic acid) (PLA, **1.1**) consists of aliphatic ester linkages, which are prone to both chemical and enzymatic hydrolysis. PLA is hydrolyzed by many enzymes such as protease, proteinase K, bromelain, esterase and trypsin **[11-16]**. But these ester linkages

start hydrolyzing only when in contact with water and under certain specific conditions of pH and temperature. The primary degradation phase is purely hydrolytic, where no microorganisms are involved. Only after the weight average molecular weight goes down below approximately 10,000, microorganisms begin to digest the lower molecular weight lactic acid oligomers, producing carbon dioxide and water.

This two-stage mechanism of degradation is a distinct advantage of PLA over other biodegradable polymers, which typically degrade by a single-step process involving bacterial attack on the polymeric device itself. This is a useful attribute, particularly for product storage and in applications requiring food contact. PLA degrades rapidly in the composting atmosphere of high humidity and temperature (55 - 70 ^{0}C). But, at lower temperatures and/ or lower humidity, the storage stability of PLA products is considerably high.

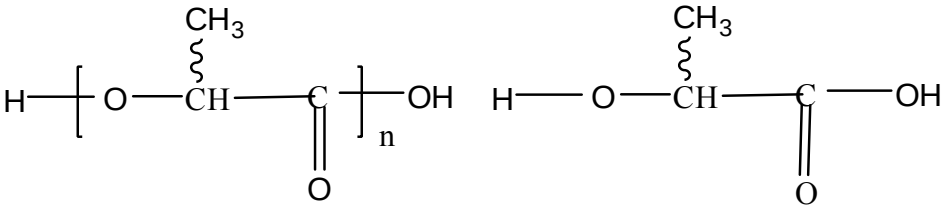

1.1
Poly(lactic acid)

1.2
Lactic acid

The building block of poly (lactic acid) is lactic acid or 2-hydroxypropanoic acid (lactic acid **1.2**), in which the carbon in between the carboxylic acid and hydroxyl functional groups is chiral, which gives rise to the possibility of diastereoisomeric (isotactic, syndiotactic and hetero- or atactic) polymer chains of PLA, depending on the direction of the methyl group with respect to the direction of propagation of the chain. PLA polymers range from amorphous glassy polymers with a glass transition temperature of about 50 – 60 ^{0}C to semicrystalline products with melting points ranging from 130 to 180 ^{0}C, depending on the sequence of enantiomeric repeating units (L and D) in the polymer backbone. A careful selection of stoichiometry of repeat units coupled with judicious plasticizer selection, therefore, allows flexible blown and cast film products to be successfully manufactured. Nucleated crystalline products of PLA are essentially opaque, whereas stress-induced crystalline materials are transparent. In summary, the basic

properties of PLA lie between those of crystalline polystyrene and PET. In particular, certain properties worth noting include:

- Flexural modulus > polystyrene
- Fat barrier properties, comparable to PET
- Excellent gas barrier properties
- Good heat stability
- Clarity and gloss of amorphous and biaxial films exceeding those of PET and PP
- High surface energy allowing easy printability.

United State demand for biodegradable plastic will grow 15.5 percent annually through 2012. Gains will be driven by escalating costs for petroleum-based resins and growing initiatives that favor renewable resources. Polyester-based and poly lactic acid resins will grow the fastest, while starch-based types remain the largest segment **[17]**, and PLA was clearly among the most promising ones. In an attempt to figure out its potential in near future, one may reasonably extrapolate a PLA only share of 720 million pounds in year 2012 and 2017, valued at $ 845 million **[17]**.

Poly (lactic acid) marked its beginning when Carothers made it in 1932 **[18]**, although with a low molecular weight and poor mechanical properties. In the following years research and development activity about lactic acid production has come a long way, so that today a number of major players of the global chemical industry are into the production of lactic acid and PLA polymers. The major companies dealing in lactic acid are listed in the Table 1.1.

1.2. Source of monomer:

1.2.1. Source of L-lactic acid: Lactic acid or 2-hydroxypropanoic acid ($C_3H_6O_3$) and L, L-lactide, which is the monomer for poly (lactide), is present in almost every form of organized life. Its most important function in animals and humans is related to the supply of energy to muscle tissues. This is a water soluble and highly hygroscopic aliphatic acid, and exists in two enantiomeric forms. Almost all the lactic acid found in natural sources is dextrorotatory L (+), the D (-) form, on the contrary, being very uncommon. Lactic

acid can be obtained in large, commercial scale from two different sources. One is the petrochemical source (**Scheme 1.1**) in which lactic acid is chemically synthesized by hydrolysis of lactonitrile and results in a 50/50 or racemic form.

Table 1.1: Lactic acid production: Global Scenario

Company	Plant location	Production capacity (in tons)
Purac	Holland, Spain, Brazil	80,000
Purac / Cargill	USA	34,000
Galactic	Belgium	15,000
ADM	USA	10,000
Mitsubishi	Japan	8000

On the contrary, lactic acid from the second source, that is fermentation broth of sugar and starch using different lactic acid bacteria (LAB), exists almost exclusively as the dextrorotatory (D or L (+)) form. Of the 100,000 tons of lactic acid that is produced worldwide every year about 90 % is made by lactic acid bacterial fermentation and the rest is produced synthetically. Presently, Musahino, Japan, is the sole producer of the synthetic variety.

Fermentative source has the advantage that by choosing a strain of lactic acid bacteria (LAB) producing only one of the isomers, an optically pure product can be obtained. The ability to produce an enantiomerically pure lactic acid has important ramifications in the ultimate structure-property relationship of the PLA. Besides, Cellulose, hemicellulose and starch are abundantly available in nature, and when hydrolyzed to mainly glucose they are fermentable by a number of microorganisms of to produce Lactic acid [**19-25]**. On the top of that these resources do not give any net contribution of carbon dioxide to the atmosphere, because they necessitate uptake of carbon dioxide for their own photosynthesis and growth.

1.3. Production of L-lactic acid: The product of lactic acid from renewable natural resources is more significant from the industrial and economic as well as environmental point of view.

1.3.1. Fermentation route to lactic acid: Lactic acid is produced in the metabolic cycle of a group of bacteria, which are called the lactic acid bacteria (LAB). Lactic acid bacteria (LAB) consist of the following genera: *Carnobacterium*, *Enterococcus*, *Lactobacillus*, *Lacticoccus*, *Leuconostoc*, *Oenococcus*, *Pediococcus*, *Streptococcus*, *Tetragenococcus*, *Vagococcus* and *Weissella* **[26]**.

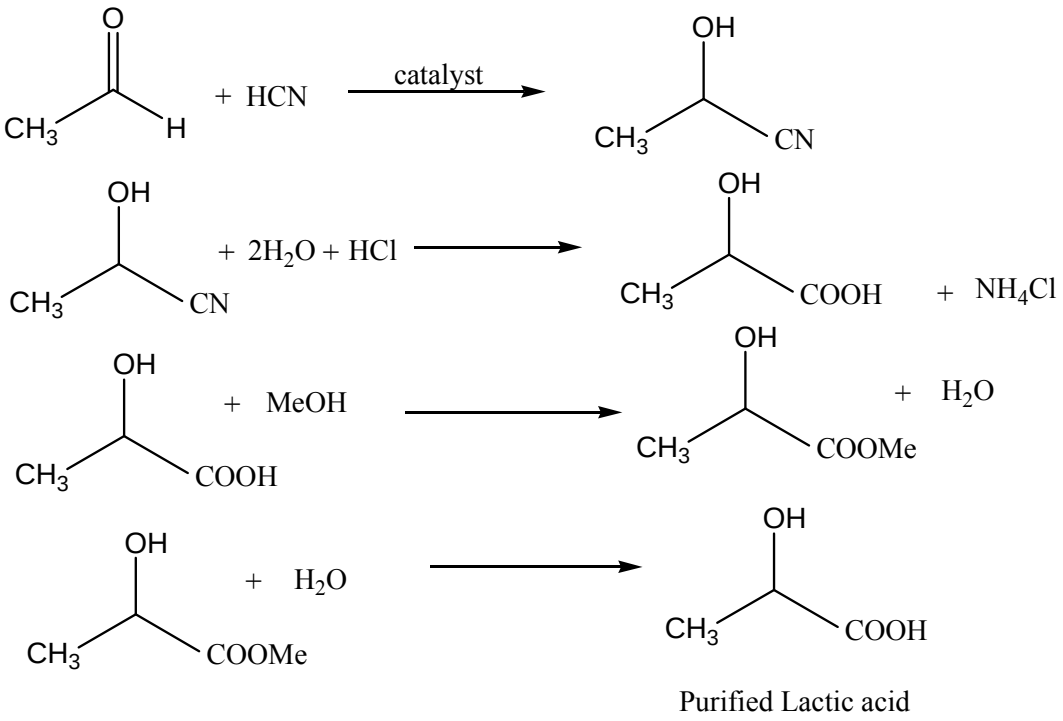

Scheme 1.1: The synthetic route to lactic acid monomer through acetaldehyde

LAB is unable to synthesize ATP (adenocine triphosphate), instead produce lactic acid as the major end product from anabolic (energy-conserving) fermentation of sugars. Most of them are facultative anaerobes and are highly acid-tolerant (down to pH. 5 and lower). Their optimal temperature for growth varies from 20 to 45 ^{0}C (from genera to genera) **[27, 28]**. Most of them are considered GRAS (**g**enerally **r**egarded **a**s **s**afe), but some strains, e.g. streptococci, are pathogenic. Another common and very important characteristic of all the LAB is that they do not synthesize vitamins-B and amino acids **[29]**, which

renders them able to grow in a complex nutrient environment and metabolize many different carbohydrates **[30]**.

Lactic acid bacteria (LAB) and some filamentous fungi are the chief microbial sources of lactic acid. On the basis of the nature of fermentation, LAB is classified into (1) homofermentative and (2) heterofermentative. Homofermentative LAB produces virtually a single product, i.e., lactic acid, whereas the heterofermentative LAB produce other products such as ethanol, diacetyl formate, acetoin or acetic acid, and carbon dioxide along with lactic acid.

Depending on the pH and temperature and also depending on the sugar which is fermented, LAB may produce either lactic acid only (homofermentation, for example, by *Lactobacillus delbrueckii*), or an equimolar mixture of lactic acid, carbon dioxide and ethanol or acetate (Heterofermentation), or a mixture of lactic acid, ethanol, acetate and formate (Mixed acid fermentation) **[31]**. All other LAB except *lactrobacilli* of type I **[32, 33]**, (e.g. *lactobacillus casei*) are facultative heterofermenters. Homofermenters start carrying out mixed acid fermentation when the sugar is other than glucose or when glucose is in short supply. Lactic acid-producing organisms, most of which are anaerobic, utilize pyruvic acid, which is the end product of Embden–Meyerhof pathway. The conversion of pyruvic acid to lactate can be effected by either of the two enzymes, L-lactate dehydrogenase or D-lactate dehydrogenase. The stereospecificity of the lactic acid depends on the type of organism, whose enzyme is involved in the process of lactic acid production. The major homofermentative LAB used in the lactic acid production from different carbon sources are Lactococcus lactis (Nolasco-Hipolito et al.) **[34]**.

In search of a new large-scale fermentation process for lactic acid, much effort has been put in to utilize cheaper medium components. For the carbon source to be converted to lactic acid, most of the attention has been paid to renewable glucose and lactose available from cheese whey permeate **[35-37]**.

However, the fastidious nature of lactic acid bacteria is still the main impediment to the economical feasibility of the fermentation process. Most lactic acid bacteria require a wide range of growth factors including amino acids, vitamins, fatty acids, purines and pyrimidines for their growth and biological activity **[38, 39]**. It has been found from a number of studies worldwide that the more supplemented the medium, the higher the

productivity of lactic acid. Among various complex nitrogen sources, yeast extract (YE) is generally considered to be the best choice for both microbial growth and lactic acid production **[40, 41]**. However, for the production of lactic acid as a source for commodity chemicals and materials, YE are not cost effective. YE is found to contribute over 30 % to the total cost of lactic acid or further downstream materials **[42, 43]**, which suggests an obvious need for a cheaper alternative.

There have been a number of efforts to utilize other nitrogen sources from industrial byproducts as growth factors to achieve a partial or complete replacement of YE **[44, 45]**. Barley malt sprout has been found to be a feasible, partial replacement **[46]**. Besides, a newly screened strain similar to *Lactococcus lactis* has been found to provide with a clear advantage of replacing YE by utilizing dairy sewage (whey) protein as a measure for cost-effectiveness **[47]**. Soybean hydrolyzate has been found to be capable of being used as the sole source of nitrogen by *Lactobacillus rhamnosus*, giving a complete replacement of YE. Further enhancement of lactic acid production using this nitrogen source has also been found by supplementation with 7 specific vitamins as additional growth factors, and the process has been found to more cost-effective than the YE process by 41 %.

Direct conversion of starch into enantiopure L- (+)-lactic acid has been achieved with the help of certain strains, for example of *Lactobacillus amylophillus* GV6 and *Rhizopus oryzae* Rojan et al **[48]**.

Maintaining pH by neutralizing lactic acid with NaOH is generally found to improve the growth, glucose consumption and lactic acid production by *Lactobacillus casei*. But maintaining pH with $CaCO_3$ is found to be effective also at high glucose concentration, which is generally found to impose a decrease in the growth rate **[49]**.

Sugarcane bagasse is reported to use as support for lactic acid production by R. oryzae and Lactobacillus in solid-state fermentation (SSF) by supplementing sugars or starch hydrolyzate as carbon source (Soccol et al.) **[50]**. The major manufacturers of fermentative lactic acid include Nature Works LLC, Purac (The Netherlands), Galactic (Belgium), Cargill (USA), and several Chinese companies (Wee et al.) **[51]**.

1.3.2. Isolation of lactic acid: Lactic acid the basic protocol is to extract the lactic acid from the fermentation broth by reactive extraction with a suitable extracting agent at a particular pH. Over 50 % yield of lactic acid was obtained from in a single extraction step, when using tertiary amine Hostarex A327 as the extractant, 1-decanol as the diluent and trimethylamine (TMA) as the stripping solution **[52]**. Mixtures of tripropylamine (TPA) and tripctylamine (TOA) dissolved in 1-octanol/n-heptane have been found to be successful in reactive extraction of L(+)-lactic acid I aqueous solution **[53]**. Maximum distribution coefficients were obtained in the range from 6:4 to 8:2 weight ratios of TPA/TOA at 5 % (w/w) lactic acid in aqueous phase and their extraction efficiencies were above 90 %.

Another extracting agent is poly (vinyledene fluoride)-supported liquid membrane containing 40 vol. % trialkyl phosphine oxide (TRPO) in kerosine as a carrier **[54]**. Alumina ceramic filters with mean pore diameter of 1.6 μm have also been successfully applied for continuous removal of lactic acid form the culture broth **[55]**.

Controlling pH is essential to keep the productivity high. One way is to add basic materials. But the other viable alternative is to continually isolate the lactic acid from the fermentation broth by means of extraction, adsorption or electro-dialysis. The optimum pH for lactic acid production varies between 5 and 7, but a pH necessarily below 5.7 is optimal for lactobacillus strains, which are more acid tolerant than the other **[56]**.

1.4. Purity and impurities in lactic acid:

1.4.1. Chemical purity: Chemical purity of the lactic acid is of utmost importance from the viewpoint of polymerization. Total impurities above a limit of about 100 ppm limit the maximum attainable molecular weight very drastically. A detailed study on this subject is reported in the literature **[57]**. The lactic acid obtained by working up the fermentation product has 98 % or more of optical (enantiomeric) purity. But the product still contains, besides residual sugars and various biological impurities, certain alcohols like methanol and ethanol, mono and dicarboxylic acids like acetic, pyruvic, oxalic and succinic acids and esters of lactic acid such as methyl and ethyl lactate. This product is yellow in color, turns black on heating, and is absolutely unsuitable for polymerization.

1.4.1a. Purification of fermentation-produced lactic acid: Complete esterification is a viable means of purification. But that reduces the enantiomeric purity due to associated racemization of various extents. Besides, traces of the esterifying alcohol remain as impurity. Various other methods, largely physical, have been reported over a long period of time, including solvent extraction, steam distillation, electro-dialysis and fractional crystallization **[58-64]**.

Industrial effort of lactic acid purification has quite a long history, dating back to as early as the 1930s. The oldest reference discusses purification by a fractional crystallization from a concentrated lactic solution obtained through thin film evaporation and distillation followed by fractional crystallization under high vacuum **[65]**. But the process is applicable only for small amounts to avoid large material loss and is too tricky to be industrially viable. Enantiomerically pure, crystalline L-lactic acid with more than 99 % purity and less than 1 % moisture content, and with solved crystal structure has been known only in the early 1990s and has been marketed on a commercial scale by Fluka and Sigma chemical companies **[66-68]**.

By now the best processes of industrial scale purification of fermentation-derived lactic acid have been known, which can give a crystalline lactic acid, which is colorless, chemically pure as well as enantiomerically pure. The processes are basically distillation under reduced pressure followed by crystallization. Oligomers and possible anhydrides are saponified completely into the monomer before concentration and distillation. The lactic acid thus obtained is reported more than 99 % chemically pure and 99.8 % enantiopure (99.6 % enantiomeric excess), having alcohol < 250 ppm, N_2 < 5 ppm, sugar < 100 ppm and other COOH < 250 ppm **[64]**. The basic technique of crystal formation that is followed is adiabatic cooling. These lactic acid crystals are immediately dissolved in water and commercially exploited in the form of 80 – 90 % aqueous solutions.

1.4.1b. Analytical methods for purity determination: Purity of the LAB strain is an important parameter in controlling production and purity of the lactic acid. FTIR has been found to be a potentially suitable tool for identifying LAB in dairy products. 20 species and 9 subspecies altogether of the LAB *Lactobacillus*, *Lactococcus*, *Leuconostoc*, *Weissella* and *Streptococcus* have been identified in soft cheese, with good correlation with other methods. A more complete database of all LABS is in process of making **[69]**.

Next comes the question of determining the purity of the lactic acid that is produced. In a broad survey of different analytical methods including titration, photometry, fluorometry and enzymatic assays, an HPLC method, using a Sepharon SGX-C18 column, mobile phase of 2 % $(NH_4)_2HPO_4$ / H_3PO_4, pH 3.5 and differential refractometric detector, was proved more suitable and a practical one **[70]**. This method is also suitable for on-line monitoring the course, rate and completion of the fermentation process. Other columns, mobile phases and detectors have also been exploited for HPLC analysis of aqueous lactic acid solutions **[71]**. Packed column gas-liquid chromatography **[72]**, indirect polarography based on the inhibition of the catalytic wave of Mo (IV) reduction in presence of sodium nitrate **[73]**, and capillary electrophoresis **[74]**, have also been reported as nice processes of simultaneous qualitative as well as quantitative determination of lactic acid in presence of other impurities especially other carboxylic acids. The indirect polarographic method is reported to be particularly sensitive for quantitative detection with detection limits down to 2×10^{-8} moles/100 mL. HPLC result of L-lactic acid showed an acid impurity like oxalic acid, pyruvic acid, acetic acid, succinic acid, fumaric acid, acrylic acid etc. Alcohol impurities like methanol, ethanol, propanol etc, and ester of lactic acid such as methyl and ethyl lactate.

1.4.2. Optical purity: Optical purity of the monomer has a great deal to do with the structure property relationship in the final polymer. For example, pure poly (L-lactic acid) (PLLA) and pure poly (D-lactic acid) (PDLA), which are isotactic, are semicrystalline; poly (D, L-lactic acid) (PDLLA) is amorphous.

Chiral resolution of D- and L-lactic acids has been performed by capillary electrophoresis using 2-hydroxypropyl-β-cyclodextrin as a chiral selector in a 90 mM phosphate buffer (pH 6.0) **[74 ab]**. Another novel and recently developed method for enantiomeric purification of lactic acid is chiral recognition by macrocyclic receptors **[75]**. A chiral HPLC technique **[76]**, has also been reported for identification of lactic acid isomers. In fact, this technique has been employed to investigate the chiral selectivity of an enzyme-catalyzed lactic acid polymerization.

1.5. Production and purification of lactide: A process for the continuous production of substantially purified lactide and lactide polymers from lactic acid or an ester of lactic acid comprises the steps of forming crude poly lactic acid, preferably in the presence of a

catalyst means in the case of the ester of lactic acid, to form a condensation reaction byproduct and poly lactic acid, and depolymerizing the poly (lactic acid) in a lactide reactor to form crude lactide **[77, 78]**. The first process disclosure to make commercially viable, polymer grade lactide with chemical as well as enantiomeric purity, from crude unpurified lactic acid came from Cargill. Incorporation, which brought in a continuous process for large-scale production, where the crude lactic acid could be any ester of lactic acid or mixtures of several esters including self-esters, where racemization was taken care of and oxidation was prohibited by use of phosphite-containing organic compounds and hindered phenols as thermal stabilizers, and where diastereoisomeric impurities were removed by fractional distillation in the production line itself instead of fractional crystallization off-line. To date, Cargill, Inc. manufactures, utilizes and sells the largest volume of polymer grade dilactide.

The basic technique is to depolymerize a lactic acid oligomer at high temperature in presence of certain catalysts (**Scheme 1.2**). The process is equilibrium one and necessitates constant or phased removal of the product. Its synthetic feasibility, thermodynamic stability and properties have been thoroughly discussed **[79]**, while detailed studies of reaction parameters, of different possible catalysts and their relative effectiveness and of racemization processes yielding varying percentages of L, L-, D, L- and D, D-lactides have been carried out relatively recently **[80]**. Favorable depolymerization temperatures are 190 – 260 °C and catalysts are various, for example zinc octoate, zinc oxalate, Sn-phthalocyanin, Sn-acetate, Zn (II) oxide, stannous octoate, dibutyltin oxide, Zinc (IV) oxide, Zn-powder and zinc lactate. The lactides are all volatile solids, which are to be condensed as sublimate between 20 and 35 ^{0}C. Industrial response towards this material remained scant for a long time in its total history, which is but as old as having its first reference dating back to the first decade of the last century **[81]**. Figure 1.1 shows the stereoisomer of lactide.

Although there have been passing references here and there to this nice organic compound **[82]**, heightened activity with this as a material for polymerization started only as recently as in the 1980s **[83]**. Various aspects of lactide synthesis have seen competitive amounts of research activity by each passing day. Fluorocarbon compounds have been mixed with the de-polymerizing oligomers **[84]**, and thin film evaporation

technique has been employed **[85]**, to increase the interfacial area between the lactide and the oligomer in order for better stripping of the lactide from the oligomer, NaOH as a catalyst **[86]**, yielded an isomeric lactide ratio of DL : LL : DD = 36 : 32 : 32.

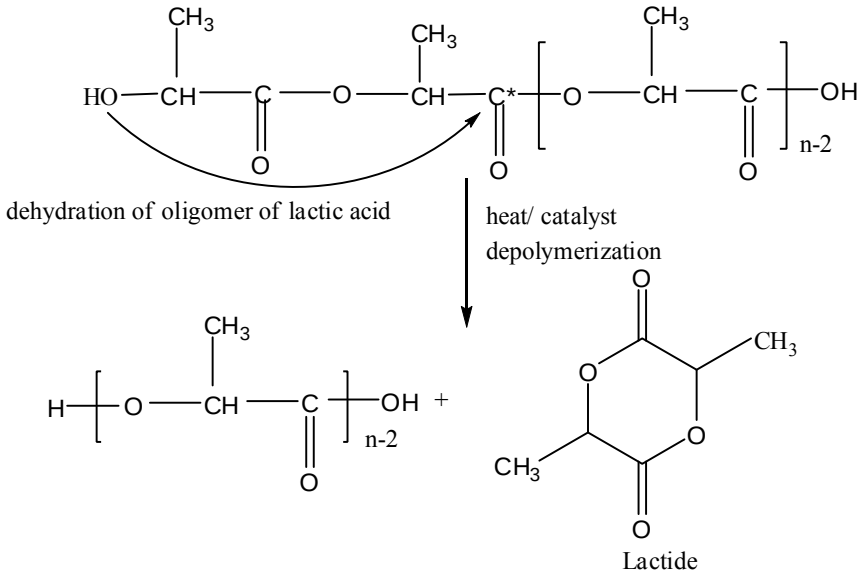

Scheme 1.2: Production of lactide from lactic acid oligomers by backbiting

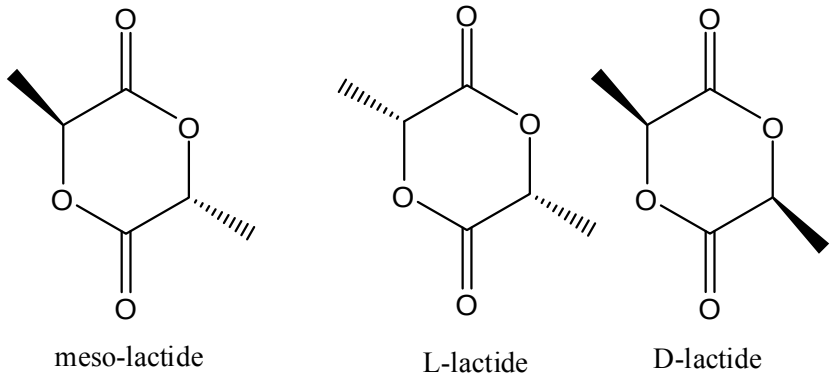

Figure 1.1: Stereoisomers of lactide.

Lactide synthesized by depolymerization of poly (L-lactic acid) by using Al, Ti, Zn and Zr compounds i.e. their metal alkoxides, organic acid and enolate salts, resulting in L,L-lactide, meso-lactide and D,D-lactide by gas chromatography using a b'-cyclodexstrin chiral stationary phase capillary column **[87]**. In presence of zinc alkoxide, lactic acid was heated at 190 ^{0}C under reduced pressure (100-25 Torr) to give lactic acid oligomers.

Tri-Bu tin ethoxide was added, and the reaction mixture was heated at 190 ^{0}C (7.5 torr) to give 95% lactide and 89% yield **[88]**. Depolymerization of oligomer at 220-250 ^{0}C using ZnO as dehydrating agent and depolymerization agent for the lactide synthesis characterized by IR and ^{1}H NMR **[89]**. L-lactic acid oligomer (M_w = 1700 and optical purity 98.5%) was heated at 200 ^{0}C under 3 Torr and depolymerized, using tin octylate at 160 ^{0}C for 1 hr to give 89.0% L, L-lactide **[90]**. Tin octanoate was used as catalyst at 200 ^{0}C gives 91.7% optically pure L,L-lactide **[91]**. Dibutyl tin chloride at 160^0 C gives 57% L,L-lactide **[92]**, whereas Sn-powder **[93, 94]**, gave exclusively L,L-lactide with high enantiomeric purity (enantiomeric excess > 99 %) from L-lactic acid. Other tin compounds like $SnCl_2.2H_2O$ and Sn $(OH)_2$ have also been used as catalysts (enantio-purity not reported) **[95]**. Rare earth metals, for example La $(OAc)_3$, have also been employed as catalysts to improve enantiomeric purity **[96]**.

1.6. Synthesis and characterization of poly (lactic Acid):

PLA is synthesized mostly in two ways. One is direct dehydropolycondensation in melt or solution phase to from oligomers followed by various post polymerization processes (**Scheme 1.3**) for example melt or solution phase polycondensation, which basically means extension of the process of oligomer synthesis itself.

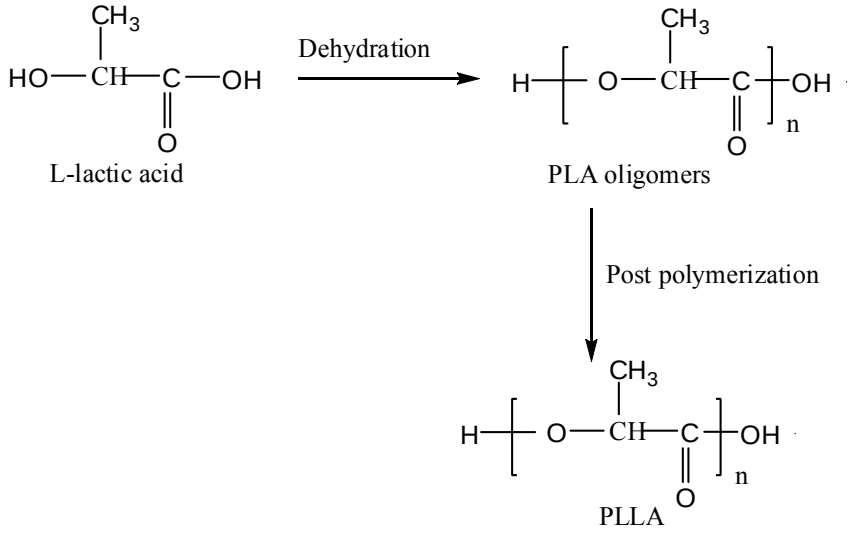

Scheme 1.3: Dehydropolycondensation followed by post polymerization.

The other means is to perform cationic, anionic or co-ordination (Lewis acidic) ring opening polymerization (ROP) of the lactide. Although studies on lactide polymerization

with cationic and anionic initiators such as triflic acid/ methyl triflate initiators and potassium alkoxide initiators (strong nucleophiles yet weak base) initiators, respectively, have been done from an academic viewpoint, they have been found to be plagued by high degrees of racemization and transesterification because of very high reactivity of the lactide in presence of such initiators. These mechanisms are also relatively highly susceptible to impurity levels. On the contrary, bulk melt polymerization of lactides in presence of non-ionic, Lewis acidic initiators (also called catalysts) through a co-ordination insertion mechanism are free of the above problems, while the reactions are relatively slow. Less reactive metal carboxylates, oxides and alkoxides fall in this category of initiator.

1.6.1. Dehydropolycondensation of lactic acid: One of the ways of producing poly (lactic acid) at least up to the level of oligomers is direct dehydropolycondensation of chemically pure lactic acid. The subject has seen extensive amount of research and development activity, but the literature is mostly scattered in numerous patents. Number of published literature is relatively few.

The process is basically an acid-catalyzed intermolecular esterification of the hydroxyl and carboxylic acid groups of lactic acid, in which numerous Lewis acids as well as protonic acids have been used for trials. Ajioka et al **[97]**, have accumulated results of lactic acid dehydropolycondensation with various catalysts and compared the results. They have synthesized poly (L-lactic acid) (PLA) by dehydropolycondensation of L-lactic acid in biphenyl ether solvent at different temperatures using various catalysts and compared weight average molecular weights, to find that higher the temperature of reaction higher the molecular weight, in case all other parameters were kept constant. The effect of normal boiling point of the solvent used and effect of negative pressure (to make the solvent reflux at a desired temperature) on the dehydropolycondensation rate were observed. Results of characterization of molecular weights by GPC and thermal degradation leading to cyclic oligomers by MALDI-ToF spectroscopy and results of characterization of thermal as well of mechanical properties have been gathered.

Young Ha investigated a number of Lewis acids and different reaction conditions also. et al **[98]**, for the direct dehydropolycondensation of L-lactic acid to make PLA, and the polymers prepared thereof were characterized for molecular weight as well as conversion,

cyclic dimer formation and racemization by proton NMR and for crystallinity by thermal analysis. 98 % H_2SO_4 was found to be the best polycondensation catalyst, which yielded a PLA of number average molecular weight 31,000, and minimum or no racemization. Sn $(Oct)_2$, which is a good Lewis acid and widely used in the coordination ring opening polymerization of the cyclic dimer of lactic acid, yielded a number average molecular weight of 30,000 in dehydropolycondensation, but racemization with this catalyst was high (about 48 mol%) and the product polymer consequently completely amorphous.

Sn (II) Lewis acid catalysts such as SnO, $SnCl_2.2H_2O$ etc, which are commonly used as catalysts for dehydropolycondensation of lactic acids are found to be activated by various proton acids **[99-101]**. Such activated catalysts have been found to produce PLA with high weight average molecular weight of about 100,000 in relatively short reaction time (15 h), compared to reactions catalyzed by non-activated catalysts as mentioned above, which produce weight average molecular weight of around 30,000 in 20 h. Such activated catalysts are also reported to give less racemization.

The lactic acid dehydropolycondensation, like any other esterification reaction, is an equilibrium-controlled process, in which both esterification of the alcohol and carboxylic group and hydrolysis of the ester linkages by water, which is a by-product of esterification, proceed simultaneously, thereby limiting the attainable molecular weight unless the by-product water is removed from the system very efficiently. A new type of tin-based Lewis acid catalyst, tetrabutyl distannoxane, which can retard the hydrolysis, has been exploited for lactic acid dehydropolycondensation reaction by Kobayashi et al **[102]**, where a maximum weight average molecular weight of 126,000 has been attained.

1.6.2. Dehyropolycondensation of L-lactic acid using zeolites: Transesterification of aromatic diesters forming derivatives with glycols in the presence of metal catalysts have been reported and synthetic zeolite has been used for removal of metal catalysts. Finally the product has been further polymerized in presence of Me_3PO_4 and Sb_2O_3. There are few literature reports where molecular sieves of various pore sizes have been used in dehydropolycondensation reactions by raising temperature as well as vacuum **[103]**. The polymer yield varied from 70 to 78 %. Woo et al **[104]**, have studied the effect of desiccating agents i.e. molecular sieves $3A^0$ using various catalyst systems such as $SnCl_2.2H_2O$, SnO, tin powder, trifluoro methanesulphonate and found that $\bar{M}_v$ of PLA

synthesized with molecular sieves is slightly higher than that of PLA synthesized in solution. The other catalysts such as SnO, Sn powder and trifluoro methanesulphonate did not show any increase in $\bar{M}_v$ of PLA with $3A^0$ molecular sieves because it is an irreversible process where molecular sieve will get saturated as polymerization proceeds even though molecular sieves are the most effective drying agent to reduce the dissolved water contents in organic solvents.

1.6.3. Isolation, purification, homopolymerization and copolymerization of Aleuritic acid with L-lactic acid: Shellac (Lac) has occupied the most important position among the natural occurring resins. India and Thailand are the only countries where shellac (lac) is cultivated **[105]**. The principal lac hosts in India are Palas and Ber for the Rangini strains and the Kusum for Kusmi strains. The term shellac and lac are often used synonymously. Its industrial applications are many, yet its expansion is limited due to its inferior thermal stability and resistance to moisture **[106]**. The entire field of structure-property relationship of the polymeric material has undergone considerable growth in recent years. The lac (shellac) resin is not a single compound but consists of intimate mixture of several polar and non-polar components in a molecule. The manner in which these molecules are linked together to build up shellac complex has led to intensive chemical research during the last few decades. Shellac is always associated with an odoriferous compound, a wax and a mixture of dyes such as erythrolaccin and desoxyerythrolaccin, which are hydroxyanthraquinone derivatives. Due to the presence of the dyes, shellac gives a characteristic color reaction with alkali. The shellac has been fractioned into three main components namely hard resin, soft resin and wax. Resinous character of shellac is believed to be due to the association of the components through hydrogen bonding. When dewaxed shellac is slowly heated, it softens at 65-70 ^{0}C and melts between 75-80 ^{0}C. Both the resinous constituents of shellac, soft resin and hard resin, contain hydroxy acids **[107-109]**, and their polar groups are present at the interface of the molecule. It is presumed that the ability of shellac to adhere strongly to smooth surfaces is the result of orientation of these polar groups.

1.6.3a. Chemical Structure of Shellac: Shellac in its refined form is a polyester type of resin consisting of inter-and intra esters of polyhydroxy carboxylic acids **[110]**, formed from certain hydroxy acids and sesquiterpene acids. It is believed to have five hydroxyl

[111, 112], groups including vicinal hydroxyl group, one carboxyl group, in free state, three ester groups, one double bond and one partly masked aldehyde group **[113]**, and the probable linkages ester, acyal, acetal and ether in an average molecule. Shellac easily undergoes periodic acid oxidation, which is specific for vicinal hydroxyl groups and also to Tollen's reagent due to the presence of aldehyde group. The hydroxyl groups have been reported to react with various monohydric alcohols viz., ethyl alcohol, butyl alcohol, allyl alcohol and dihydric alcohols **[114]**, to form ethers. This also seems to be the reason for the action of water on shellac molecules, although no chemical reaction takes place on its short contact.

From a study of the composition of total shel1ac acids, Khurana et al **[115]**, concluded that the chief building blocks of shellac are aleuritic acid and Jalaric acid-A (a tricyclic sesquiterpene). The structure of jalaric acid-A as an aldehydic acid has been established by Wadia et al **[116]**. According to them shellolic acid and epishellolic acid are not the primary products of shellac, and these acids together with laksholic acid. Shellac structure, characteristics and modifications and epilaksholic acid, arise from a cannizaro reaction or jalaric acid-A. Sahu and Misra **[117]**, have reported that there is no doubt that the most important components or shellac are aleuritic acid (9, 10, 16 tri-hydroxy palmitic acid) (**Figure 1.2.)** and jalaric acid-A (a tricyclic sesquiterpene). These are connected with lactide through ester linkages.

1.6.3b. *Isolation of different constituent of Shellac*: On hydrolysis **[118]**, the constituent acids of shellac are liberated and consist mainly of hydroxy aliphatic and terpenic acids. The aliphatic acids are almost insoluble in water, whilst the terpenic acids are readily soluble and these are present almost in the proportion of 50: 50. Among aliphatic acids, the main constituent acid is aleuritic (~35%) and amongst terpenic acids the main constituent acid is jalaric (25%). Other acids isolated are butolic acid (8%), shellolicjepishellolic and laccijalaric (8%) acids (Figure.1). Water-soluble jalaric acid and laccijalarie acids have aldehyde functions in the molecule.

1.6.3c. *Isolation of aleuritic acid:* The structures of aleuritic acid and shellolic acid had been established by Sukh Dev **[119]**. He isolated laksholic acid **[120-122]**, epilaksholic acid **[120-122]**, laccishellolic acid, epilaccishellolic and laccijalaric acid. Although it is generally accepted that shellac is a polyester (~35) formed from terpenes possessing the

cadence skeleton and threo-aleuritic acid (9, 10, 16 trihydroxyhexadecanoic acid). The 9- and 10-hydroxy groups of aleuritic acid are involved in alkali-stable linkages, and a large part of the aleuritic acid remains in the combined form in the primary gum obtained after treatment with aqueous 20% sodium hydroxide **[123]**.

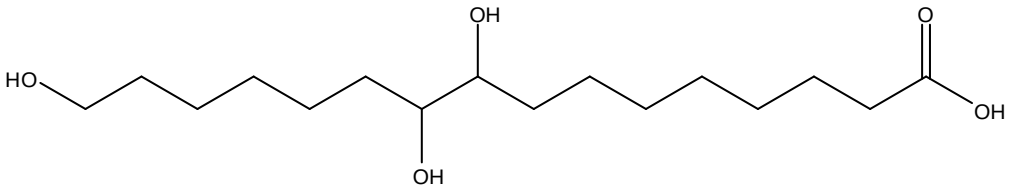

Aleuritic acid

Figure 1.2: Structure of aleuritic acid.

1.6.3d. Physical Properties: Aleuritic acid is a white crystalline solid melting at 101 ^{0}C (Harries and Nagrl) **[121]**; the acid crystallizes from boiling water or aqueous alcohol in the form of a mixture of rhombic plates and elongated parallelograms. Melted aleuritic acid, on cooling, looks like a wax and crystallizes from aqueous alcohol and chloroform in the form of rhombic plates. It is soluble in hot water and in alcohol, acetone and ammonia in the cold. Specific gravity of shellac varies between 1.14 to 1.21. It has an average molecular weight 1006, acid value 65- 75 and saponification value 220-230. Shellac is insoluble in water, glycerol, hydrocarbon solvents and esters but dissolves readily in alcohol, aqueous solution of alkalies, organic acids and ketones. This finding has led to the conclusion that hydroxyl, carboxyl and carbonyl groups are present in shellac **[124]**.

1.6.3e. Isomers of aleuritic acid: Aleuritic acid exists in two isomeric forms namely erythro and threo-aleuritic acid. Erythroform is in most abundant in nature.

Derivative of aleuritic acid: Exaltone was prepared from threo-aleuritic acid by oxidation to the diacids, dehydration to the hexadecenedioic acid, reduction to the hexadecanedioic acid, and cyclization to the ketone via the acid chloride **[125]**. Starting from threo- and erythro-aleuritic acids, the derived terminal dicarboxylic acid monoesters have been subjected to a photochemical decarboxylation-iodination reaction to give some useful iodo esters with chain lengths of 15 C. (Z)-9-Tetradecenyl acetate, the pheromone of the

fall armyworm moth was prepared from erytho-aleuritic acid **[126]**. Aleuritic acid, after acetylating, was oxidatively decarboxylated and then subjected to phase-transfer oxidation of the terminal olefin to give 7,8,14-trihydroxytetradecanoic acid **[127]**. Ferric chloride as a catalyst is used for esterification of aleuritic acid and its derivatives **[128]**. Functional transformation of (±)-threo-aleuritic acid, synthesis of 5-methyltetrazoles **[129],** and synthesis of glyceryl monoaleuritate **[130]** has also been attempted. Allyl aleuritate, aleurityl crotonate and aleurityl cinnamate have been prepared, and their oligomerization has been effected by free-radical initiation. Dimers of the unstable esters of aleuritic acid have been obtained **[131]**. A convenient synthesis of 2-methylheptadecane, the tiger mothpheromone, from aleuritic acid has been carried out **[132]**.

1.6.3f. Homopolymer and copolymer of aleuritic acid: Unstable macrolides (m + n = 10-15), useful for perfumes are prepared by lactonization of aleuritic acid **[133]**. An additional secondary hydroxyl group in the molecular structure further improves the 2D crosslinking as observed for aleuritic acid (9,10,16-trihydroxyhexadecanoic acid). These observations can be extended to the understanding of the short-range structure and the formation mechanism of some biopolymers such as cutin, a natural polyester supporting the lipidic extracellular membrane that have covered the aerial parts of leaves and fruits of plants **[134]**. The polyester resin compound is prepared by mixing aliphatic dicarboxylic acid and aliphatic glycol at a mole ratio of (1.2-1.8):1 for reaction to obtain polyester, adding 0.1-2.0 g tetra basic alcohol, adding 0.0001-0.002 g titanates organic metal catalyst (based on 1 mol aliphatic dicarboxylic acid), adding phosphates stabilizer 0.5-1 wt parts of metal catalyst. Aliphatic dicarboxylic acid includes succinic acid 75-100, and other dicarboxylic acids with C_{2-3} or C_{5-10} alkylene group 0-25. Aliphatic glycol includes 1,4-butylene glycol and/or ethylene glycol 75-100, and other glycols with C2-3 or C5-10 alkylene group 0-25. Tetrabasic alcohol with aliphatic long main chain prepared from aleuritic acid and ethylene glycol is used as organic compound catalyst. The polyester resin compound has good processability, and adjustable mechanical strength, toughness and degradation rate, so as to be used for absorptive suture line, drug delivery carrier, and all kinds of medical materials **[135]**. Direct synthesis of functional polyesters from readily available monomers, ambrettolide epoxide, and

isopropyl aleuriteate has been carried. These monomers allow for an easy and accessible synthesis of a variety of functional polyesters without the need for protection/deprotection strategies. Novozym-435, immobilized CALB on a polyacrylic resin and has been selected as the biocatalyst for the polymerization reactions **[136]**.

1.6.3g. Uses of aleuritic acid: Synthesis of fragrances such as civetone, exaltone, ambrettolide and isoambrettolide and glucose manoaleuritate has been reported. The other suggested applications of aleuritic acid are the following:

1. Glucose manoaleuritate (a non-toxic non-hemolytic water-soluble compound) in medicine as an isocaloric substitute for dietary tripalmitin.
2. Preparation of plastics with good adhesive properties by the condensation of aleurtic acid with pthalic andydride and glycerin, rosin etc.
3. Aleuritic esters for compounding with cellulose esters for the preparation of lacquers, plastics and fibers.

1.6.4. Dehydropolycondensation of L-lactic acid with 12-hydroxy stearic acid: 12-hydroxy stearic acid (12-HSA) or 12-hydroxyoctadecanoinc acids, which is an aliphatic hydroxy-carboxylic acid, has been polymerized into aliphatic polyester by self-condensation. The dehydropolycondensation of 12-HSA has been performed in bulk polymerization at 160 ^{0}C under vacuum, using p-toluene sulphonic acid (PTSA) as a catalyst. A polymer with $\bar{M}_n$ up to 3500 – 4000 was obtained in 5 hours **[137]**. Its structure was confirmed by showing, with the help of titration methods, that equal number of hydroxyl and carboxylic acid end groups were present. The homopolymer of 12-HSA, that is poly (12-HSA) (PHSA), is a colorless, viscous liquid. The presence of n-hexyl pendant (side chain) affects any parallel arrangement of the backbone polymer chains, which is essentially required for crystallization, although a similar polyester, poly (11-hydroxyundecanoate), which does not have such an aliphatic pendant is considerably crystalline even at low number average molecular weight **[137]**.

The low molecular weight homopolymers of 12-HSA ($\bar{M}_n$ 5000 – 50,000) have found application in diverse fields for example, as an adhesion tuner and carrier material in ink-compositions **[138]**, as a softener in styrene-butadiene rubber **[139]**, and as a surface active agent in finished cotton-polyester mixed fabric and leather treatment **[140]**.

1.7. Ring Opening polymerization of lactide: Poly (lactic acid) can be obtained from an entirely different route, that is ring opening polymerization (ROP) of the cyclic dilactone of lactic acid, called dilactide or lactide, in presence of an initiator (also called catalyst). The lactide is prepared from lactic acid oligomers by a thermal depolymerization process using certain catalysts, as discussed elaborately in a previous section.

The lactide is a molecule with two chiral carbon centers, thereby giving rise to three diastereoisomers of LL, DD and LD (meso) configurations respectively. A 50-50 mixture of the LL and DD enantiomers is called the racemic lactide. Therefore depending on the choice of stereo-comonomers in the feed and the initiator, different sequences can result, giving rise to different tacticities of the polymer.

Stereoselective and living ring opening of meso-dilactide with enantiomerically pure aluminum alkoxide initiator has yielded purely syndiotactic poly (lactic acid) with narrow polydispersity and controlled molecular weight **[141]**.

The more straightforward route to isotactic poly (lactides), poly (L-lactide) or poly (D-lactide), undoubtedly involves the enantiomerically pure monomers, provided no epimerization occurs during their polymerization. So far, most of the catalytic systems tested for such a stereo controlled polymerization proceed with retention of configuration. Nevertheless, this strategy is considerably limited by the requirement for enantiopure monomers, and kinetic resolution of *rac*-lactide has been suggested as an alternative route to isotactic poly (lactides). This approach was first investigated with aluminum complexes featuring the chiral SALEN ligand derived from (*R,R*)-binaphthyldiamine **[142, 143]**. The alternating stereochemistry of syndiotactic poly lactides clearly requires the stereocontrolled polymerization of *meso*-lactide. Chain-end stereocontrol was recently investigated by Coates et al. with the bulky beta,-diiminate complex **[144]**.

Preparation of heterotactic poly lactides from racemic lactide results from alternative incorporation of L and D-lactide and thus requires chain-end control. Coates et al. demonstrated that *beta* –diiminate dinuclear complex catalyzed the stereoselective ROP of *rac*-lactide yielding highly heterotactic microstructures, with stereoselectivities of 90 % at room temperature and 94% at 0 ^{0}C **[145, 146]**. The isopropyl groups at the aryl substituents were found to play a key role on the chain-end control, as indicated by the decreased heterotacticities observed with ethyl (79% at room temperature) and *n*-propyl

(76% at room temperature) groups. Comparatively, only modest stereocontrol has been reported for the analogous mononuclear tin initiator **[146]**. This methodology has been successfully extrapolated to complexes featuring SALEN ligands, and the highest selectivity in heterotactic enchainment was obtained for the chlorinated ligands (88% and even 96% in toluene at 70 ^{0}C) **[147]**. Lastly, the yttrium complexes lead to stereoselectivities of 80% in tetrahydrofuran but only of 60% in toluene at room temperature **[97]**. The chain-end control was of similar magnitude for alkyl and amido co-ligands (complexes but significantly lower for the lanthanum derivative **(**64% in tetrahydrofuran). Coates et al. recently demonstrated that regular alternation of L- and D-lactide units could also be achieved from *meso*-lactide and the racemic aluminum catalyst **[148]**.

Stannous Octoate gave a ring opening polymerization of L-lactide resulting high molecular weight and narrow polydispersity, but depolymerization started beyond a conversion of about 80 % that takes 72 hours at 130 ^{0}C in a bulk (solvent less) polymerization. Depolymerization starts sooner if the reaction temperature is higher **[149]**.

A method for evaluation, computation and prediction of favored diastereoisomeric sequence in the ring opening polymerization of racemic dilactide using stannous octoate and Zn metal initiators in absence of transesterification has been discussed on the basis of equivalent reactivity and stereo-dependent reactivity between LL and DD pairs generated from the racemic mixture of DD and LL dilactide diastereoisomers, which indicates that LL/DD heterotactic junctions are formed preferentially **[150]**.

Poly (l-lactide) has been prepared using Zn (II) L-lactate in bulk at 120 ^{0}C or 150 ^{0}C. The highest number average molecular weight ($\bar{M}_{w)}$ ~ 70,000 are formed at [M]/ [I] ratio was 4000 and 100 % optically pure PLA formed even at high reaction temperature **[151]**.

The controlled polymerizations of L-lactide have been carried out using active zinc catalyst. The result showed good control of molecular weight and molecular weight distribution **[152]**.

The thermal stability of PLA has been studied in presence of residual monomer as well as metals. The results showed the thermal stability of PLA is more in presence of tin than

zinc metal. The more selective of the catalyst for PLA polymerization is found the less efficient its depolymerization at high temperature **[153]**.

Ring opening polymerization of L-lactide has been examined in presence of zinc amino acid salt at 150 ^{0}C and reaction time 92 h. PLA obtained using zinc proline as catalyst showed 90 % yield, 97-100 % optical purity and moderate molecular weight have been observed regardless of catalyst and reaction condition **[154]**.

Ring opening polymerization of D, L-lactide with Zn (II) lactate at 150 ^{0}C for 96 hours gave 96.7 % conversion of poly (lactide) having number average molecular weight ~ 100,000 and polydispersity 1.5 **[155]**.

Copolymer of poly (lactide) and PEG have been synthesized by ROP of L-,D-lactide in the presence of mono or dihydroxy PEG using nontoxic Zn (II) lactate as catalyst. The result showed that the properties of polymeric micelle strongly depended on the chain structure and composition of copolymers **[156]**.

Vert et all **[157]**, have studied structural characterization and hydrolytic degradation of Zn metal initiated copolymerization of L-lactide and ε-caprolactone. The copolymer showed the presence of long PLA blocks in comparison with ε-caprolactone blocks. The absence of (ε-caprolactone-lactide-ε-caprolactone) triad signal suggested the absence of transesterification rearrangements **[157]**.

A "coordination insertion" mechanism of Sn (Oct) $_2$ initiated ROP of lactones has been proposed and demonstrated separately by both Penczek et al **[158]**, and Kricheldorf et al **[159]**. The mechanism is generally accepted for all lactones including the lactides and glyolides.

Kricheldorf et al has also shown that Sn $(Oct)_2$ catalyzed ROP of lactones and lactides do not entail transesterification reactions below 120 ^{0}C **[160, 161]**.

Six different acetylacetonato complexes (M $(AcAc)_n$, M = Nd, Y, Zn, Zn, Fe, Co, Ni) as initiators have been found to give ring opening polymerization of D, L-dilactide with close to 99 % conversion in all cases, the conversion for the rare earth metal complexes being higher and decreasing remarkably with increase in reaction temperature and time **[162]**.

Aluminium alkoxides are also another class of ROP catalysts that proceeds through the coordination-insertion mechanism and give living polymerization, controllable molecular wrights and low molecular weight distribution (1.1–1.4) of PLLA **[163, 164]**, and also give rapid polymerization with high conversion, low transesterification and zero racemization, when ROP is carried out below 150 ^{0}C **[165, 166]**. Dubois et al. have carried out thorough studies of the ROP of lactones (especially, lactides) catalyzed by aluminum isopropoxide, $Al(OiPr)_3$, and confirmed the coordination-insertion mechanism, involving three active sites per aluminum atom, no aggregation of catalyst and insertion of the lactide into the aluminum alkoxide bond with lactide acyl-oxygen cleavage, similar to the Sn Octoate mechanism **[167-169]**.

Lanthanum and yttrium based ring-opening catalysts, studied in detail separately by McLain and coworkers **[170-175]**, and Feijan and coworkers **[176, 177]**, also go by similar coordination-insertion mechanism, but they give very fast reactions (100 % conversion in as less as 15 minutes) at room temperature and the turnover frequencies of these catalysts for the ROP of lactides at 25 ^{0}C are more than 30 times as much as the turnover frequency of Al (iso-Pr)$_3$ for the same reaction at 70 ^{0}C.

1.7.1. Coordination-insertion polymerization: The most widely used complex for the industrial the three-step coordination-insertion mechanism for the ROP of cyclic esters was first formulated in 1971 by Dittrich and Schulz **[178]**. The first experimental proof for such a mechanism in the Al (*iso*-Pr)$_3$ (**scheme 1.4**) initiated polymerization of lactide was independently reported in the late 1980s by Kricheldorf **[179]** and Teyssie **[167]**. Recently, further support for such a mechanism has been provided by experimental **[180, 181]** as well as theoretical studies. The living character of the polymerization in toluene at 70 ^{0}C has also been deduced from the linear dependence of the mean DP on the monomer to initiator molar ratio calculated for the actual monomer conversion. **[167]**. The first step of the coordination-insertion mechanism (i) consists of the coordination of the monomer to the Lewis-acidic metal center. The monomer subsequently inserts into one of the aluminum alkoxide bonds via nucleophilic addition of the alkoxy group on the carbonyl carbon. (ii) followed by ring opening via acyl-oxygen cleavage. (iii) hydrolysis of the active metal-alkoxide bond leads to the formation of a hydroxyl end group. The

most widely used complex for the industrial preparation of PLA is undoubtedly tin (II) bis (2-ethylhexanoate) (**scheme 1.5**).

1.7.2. Cationic polymerization: After unsuccessful attempts reported in 1971 by Dittrich and Schulz, **[178]** the feasibility of such a cationic ROP of lactide was demonstrated by Kricheldorf et al. in the late 1980s **[182]**. Among the numerous acidic compounds investigated only trifluoromethanesulfonic acid (HOTf) and methyl trifluoromethanesulfonate (MeOTf) (**scheme 1.6)** proved to be efficient initiators. The polymerization rates were significantly higher in nitrobenzene than in chlorinated solvents, with 50 ^{0}C being found to be the optimum reaction temperature.

1.7.3. Anionic polymerization: Anionic polymerization of lactide has been much less investigated than the coordination insertion approach. Although higher activities might be anticipated for anionic promoters that typically display strong nucleophilic and/or basic character, the deleterious contribution of transesterification and racemization reactions might be expected to be significantly more important when naked or loosely bonded anionic species are involved.

From a mechanistic point of view, anionic ROP of (**scheme 1.7)** lactide has been demonstrated to occur via acyl cleavage, the initiation step being either the deprotonation of the monomer or its ring opening by nucleophilic attack **[183]**. Notably, the two initiation pathways are easily differentiated by end-group analysis, since the deprotonation route is associated with the absence of initiator fragments, whereas the nucleophilic attack route typically results in ester end groups derived from the alkoxide promoters.

1.7.4. Nucleophilic polymerization: Metal-free catalysts are attracting growing interest as more economical and environmentally friendly alternatives for classical organic transformations. To this end, enzymes (such as lipases) as well as organocatalysts (such as amines, phosphines, and N-heterocyclic carbenes) have recently been investigated for transesterification reactions **[184-186]**, including lactide ROP **[187-190]**. These metal-free nucleophilic catalysts (**scheme 1.8)** are particularly attractive for biomedical applications of the resulting polymers, since there is no concern of contamination, waste, and removal of metals.

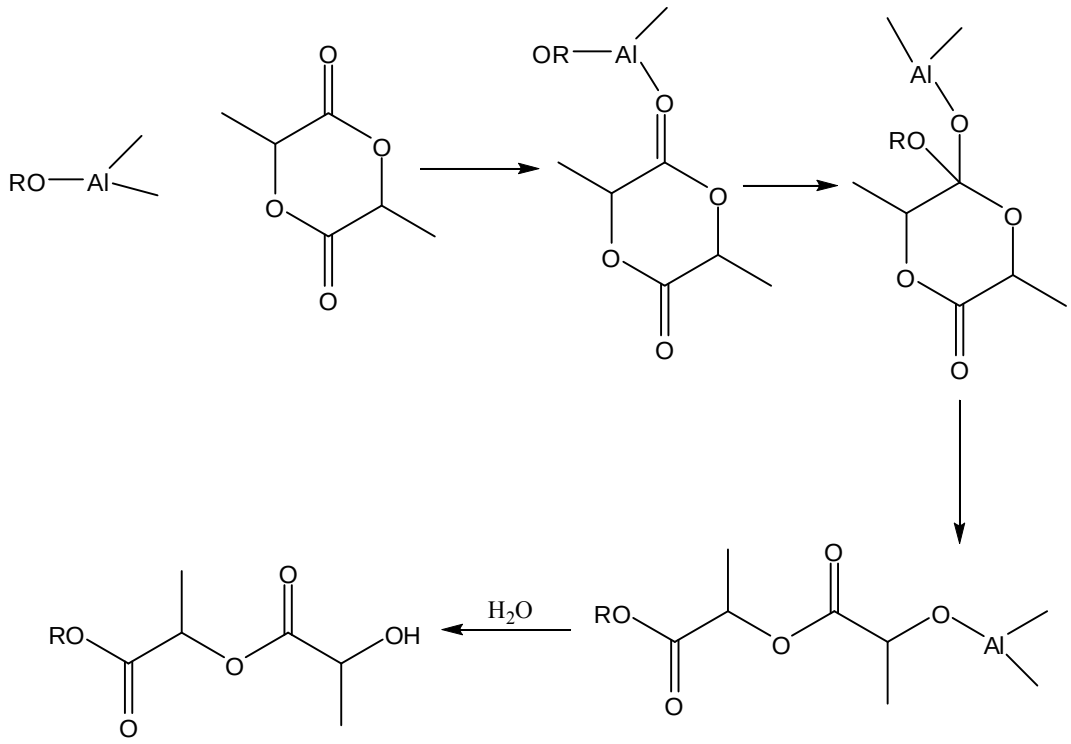

Scheme 1.4: ROP of lactide in presence of Al (*iso*-Pr) $_3$.

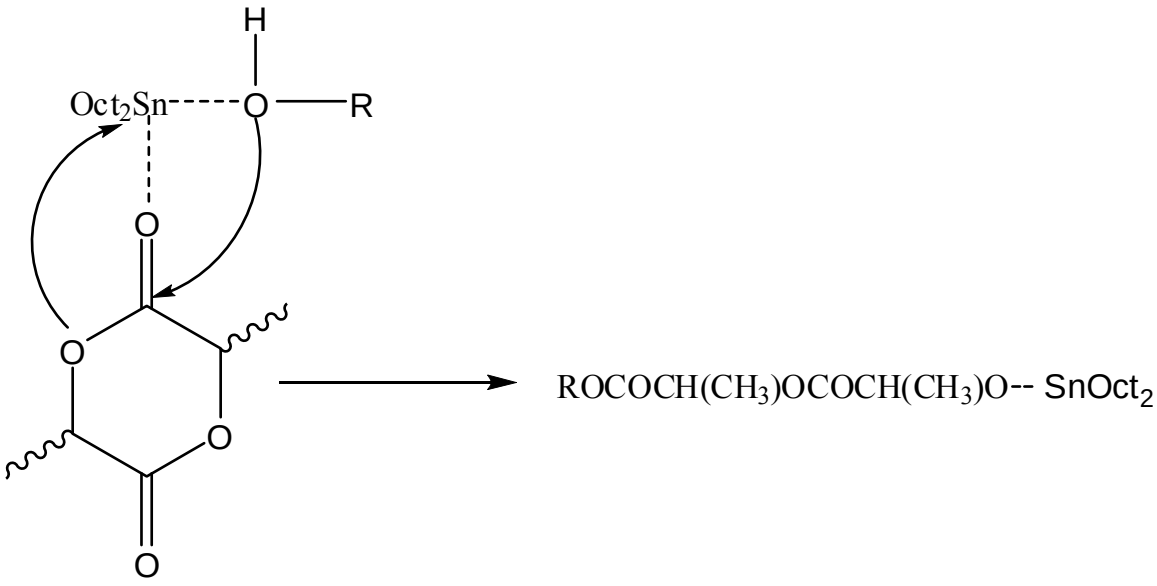

Scheme 1.5: ROP of lactide in presence of tin (II) bis (2-ethylhexanoate).

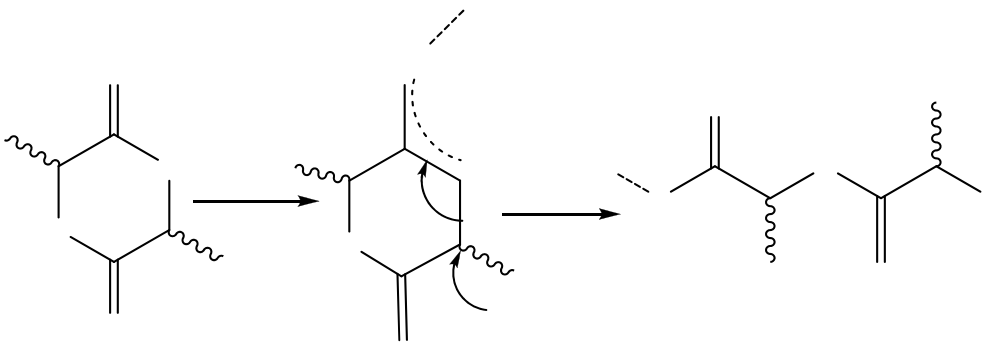

Scheme 1.6: Cationic polymerization of lactide in presence of trifluoromethanesulfonic acid (HOTf) and methyl trifluoromethanesulfonate MeOTf.

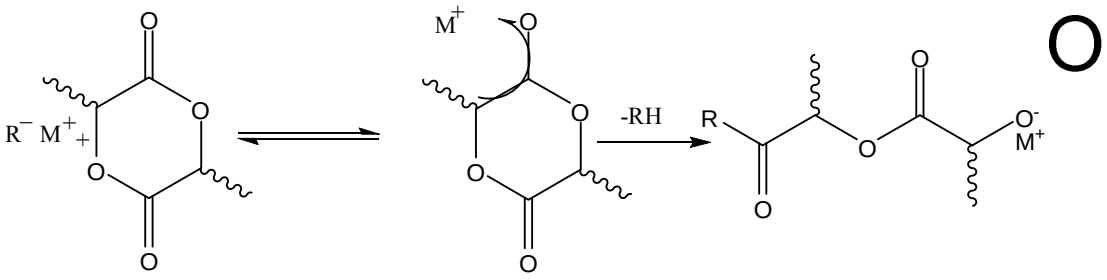

R=alkyl, alkoxy and M = Li, K, Mg

Scheme 1.7: Anionic polymerization of lactide.

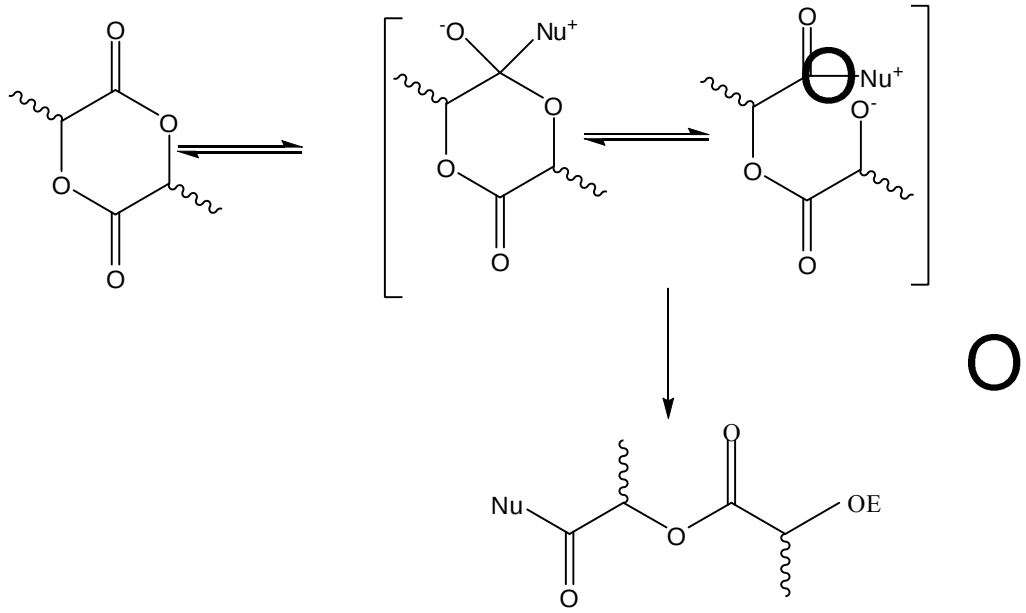

Scheme 1.8: Lactide polymerization via nucleophlic ROP mechanism

1.8. Structure and properties of poly (lactic acid) s:

1.8.1. General structure-property relationships: Pure poly (L-lactic acid) (PLA) and pure poly (D-lactic acid) (PDLA) are semicrystalline, with spherulites composed of crystalline lamellae and amorphous regions located between lamellae and between spherulites **[191-193]**. Within the lamellae the polymer adopts a 10/3 helical structure **[194-196]**. The degree of crystallinity and melting point of PLA are affected by the stereo irregularity in the polymer **[197, 198]**. Incorporation of the other isomer in a primarily stereo pure PLA reduces both the degree of crystallinity and the spherulite size, with a concomitant decrease in the ΔH value of the crystalline melting endotherm related to one another by a best fitting straight-line equation **[198]** of the form.

$$Y = 1.63 + 1.27X,$$

Where Y is % crystallinity and X is ΔH (in J/g) of the crystalline melting at T_m.

While de' Santis and Kovacs **[195]** propose a 10/3 helix, ten Brinke and coworkers **[196]** have shown that another helical structure, a 3/1 helical structure called the beta-structure (the 10/3 helix being called the alpha-structure henceforth) is also possible for PLA isotactic polymers. Only hot drawing of PLA fibers at high temperature and under high stress (high draw ratios) can make an alpha to beta-structure transformation possible. Besides, they have also calculated the relative atomic positions in a chemical unit of PLA. Shikinami and coworkers **[199],** have experimentally validated both the propositions, but held the view that the previous report on the relative positioning of two helical chains were in error. They have determined the correct positions. The second chain rotates by 2.46 degrees with respect to the first chain. Besides, the gyration tensor components of solid PLA fibers along the helical axis was found to be extremely large, which corresponded to a high rotatory power, about two orders of magnitude higher than those of ordinary crystals. This is the first experimental evidence that helical polymers like PLA will produce enormous optical activity in solid state.

Poly (lactide) s can exhibit different microstructures depending both on the monomer involved and on the course of the polymerization reaction **[200]**. Isotactic polylactides, either poly (L-lactide) or poly- (D-lactide), contain sequential stereocenters of the same relative configuration, while syndiotactic polylactides, namely, poly (*meso*-lactide),

contain sequential stereocenters of opposite relative configuration. Regular alternation of L- and D-lactide units leads to another ordered structure, namely, heterotactic polylactides, also described as disyndiotactic polylactides. Last, atactic polylactides are obtained when the polymerization occurs without any stereoregularity. The stereosequence distribution in poly lactide samples (Figure 1.3) is usually determined by NMR spectroscopy through inspection of the methine and/or carbonyl regions (^{13}C NMR and homonuclear decoupled ^{1}H NMR) **[201-203]**. More recently, application of heteronuclear chemical shift correlation (HETCOR) NMR has been proposed by different groups, but the precise assignment of the different signals remains in debate **[204]**. The physical properties of poly lactides are strongly dependent on their stereochemical composition; thus, melting and glass-transition temperatures have been used to characterize the stereoregularity of poly lactides. For instance, when pure isotactic poly (L-lactide), a highly crystalline material with a T_m around 180 ^{0}C, is contaminated with *meso*-lactide, the melting point and the crystallinity both decrease and consistent with an amorphous polymer with a T_m around 130 ^{0}C, when the stereochemical defects reach 15% **[205]**.

Stereo regular crystalline poly (lactides) retains their mechanical properties near their melting points and thus has higher use temperatures than atactic amorphous polymers. High melting poly lactides are thus attractive targets for a wide variety of new applications, provided their preparation is achievable through efficient and inexpensive processes.

The stereochemical composition of the PLA polymer significantly affects the crystallization kinetics, spherulite size and ultimate extent of crystallinity **[206]**. Both spherulitic size and the percentage crystallinity are particularly influential in determining the crystalline melting point of the polymer. A completely pure PLA has a melting point of 180 ^{0}C, which can go down to as low as 130 ^{0}C with increasing stereo-irregularity. Although crystallinity is necessary for certain end application of the PLA polymer, which require properties such as high mechanical strength, high heat resistance, stiffness, high chemical resistance and permeability, a lower crystalline melting point benefits by allowing lower melt-processing temperatures. Reduction in processing temperature in turn reduces hydrolytic and oxidative degradation as well as lactide reformation.

Although essentially structure dependent, crystallinity can be developed in two ways, namely the nucleating agent-driven, solvent-induced, quiescent crystallization, which is but a slow process, and the fast, stress-induced crystallization. The former process gives an opaque material while the latter gives transparent material.

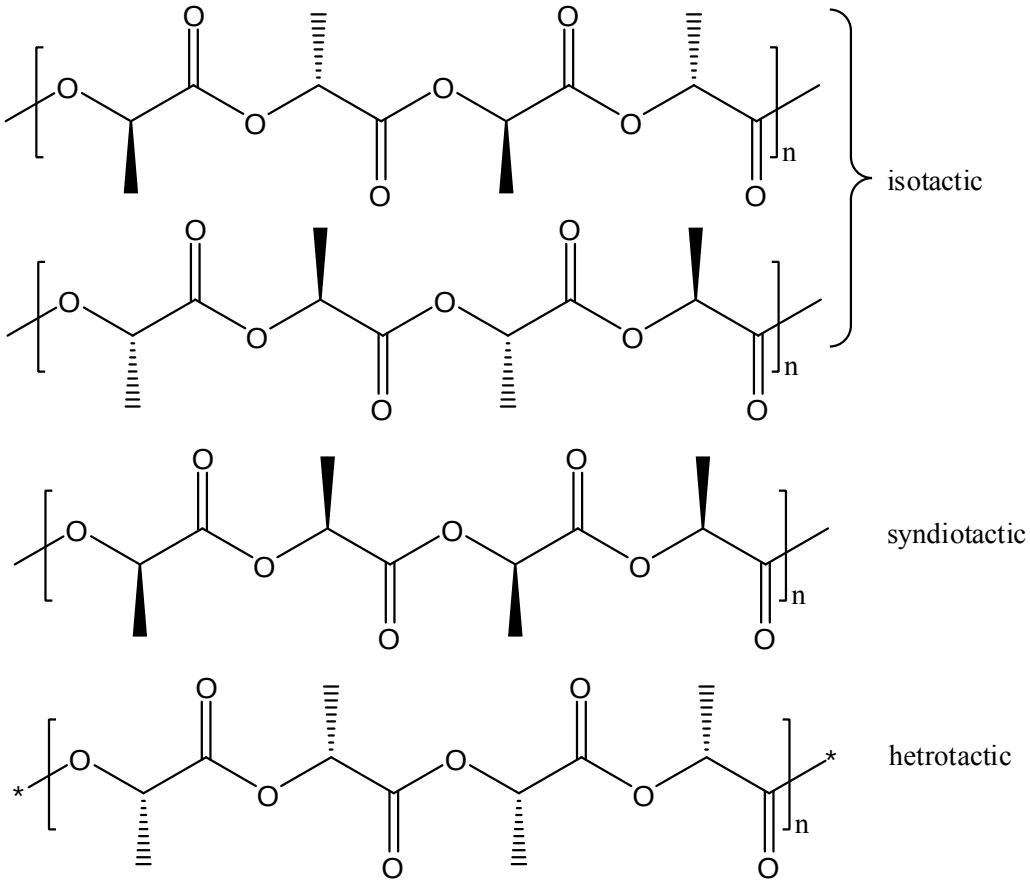

Figure 1.3: Different stereotypes of poly lactides.

In contrast to poly olefins, PLA polymer has relatively poor melt elasticity, thereby leading to problems in extrusion processes typically used for cast film, paper coating and blown film manufacture. The poor melt elasticity results from poor degree of entanglement in linear PLA chains. This problem of low elasticity can be taken care of by introducing a low amount of branching during the polymerization process, which is achieved by utilizing low levels of epoxidized natural oil **[207]**. Another viable alternative for increasing melt elasticity can be introduction of small amount of cross-linking by cross-linkers such as peroxides, though at the cost of a slight increase in melt

viscosity. Essentially any process that increases the polydispersity increases the melt elasticity **[208]**.

Analysis by small and wide angle X-ray scattering together throws some light on the lamellar stack parameters and on the degree of crystallinity during heating of a quenched sample of poly lactic acid up to the melting and subsequent cooling. The two processes differed very significantly as far as crystallization mechanism is concerned. During heating there was a sudden crystallization at around 80 ^{0}C and then there was not much change in the lamellar and amorphous layer thickness till the melting. But while cooling, two different crystallization mechanisms operated, the first one involving lamellar thickening and the second one the formation of new lamellae in the stacks **[209]**.

Effect of structure especially that of the amorphous region related to the deformation behavior of poly (lactic acid) has been study by Raman spectroscopy **[210]**. Ikada and coworkers **[211]** have determined the experimental dependence of both glass transition and melting point of PLA on molecular weight and found that both of them reach a maximum or saturation value at high molecular weights. The maxima of glass transition and melting points were found to be at 58 and 184 ^{0}C respectively, while the heat of fusion at the melting point per mole of repeating unit was found to be 3.5 kcal/mole, which is comparable to the value of 3 kcal/mole for poly (caprolactone) (PCL).

Both crystallinity and molecular weight have considerable impact on the properties of poly (lactic acid). The amorphous polymer is soluble in most common organic solvents such as ketones, THF, benzene, acetonitrile, dioxane and chlorinated solvents, whereas a highly crystalline PLA material will dissolve only in chlorinated solvents or benzene at elevated temperatures. Poly (L-lactic acid) (PLA) showed more interesting mechanical properties than poly (D, L-lactic acid) (PDLA) and its behavior significantly improves with increase in crystallinity. Annealed specimens possess higher values of tensional and flexural modulus of elasticity, Izod impact strength and heat resistance. The plateau region of flexural strength as a function of molecular weight appears around $\bar{M}_v$ = 35,000 for PDLA and amorphous PLA and at higher molecular weight around 55,000 for crystalline PLA **[212]**. Table 1.2 shows comparison of property of PLA with other commercial polymers and Table 1.2 shows somewhat of a correlation of crystallinity with certain mechanical properties.

Melt rheological properties of star polymers of poly (lactic acid) are completely different from those of linear poly (lactic acid). Branch entanglement starts at a much lower molecular weight (around 3500) and zero shear viscosity of the star is also higher than that of linear poly (lactic acid) **[213]**. Zero shear viscosity of the star is a function of the number of arms.

1.8.2. Stereocomplex: Stereo pure PLA polymers show another remarkable property called stereocomplex formation. Polymer-polymer complexation is known, when two different polymers with different chemical structures complex between themselves upon simple mixing because of favorable interactions existing between the different polymer chains.

The well-known inter-polymer complexes include (1) a poly-electrolyte complex between poly-anion and poly-cation **[214]**, (2) a hydrogen-bonding complex between a poly(carboxylic acid) and a polyol or polyether **[215]** and (3) a charge-transfer complex polymeric donor and acceptor **[216]**.

Table-1.2: Effect of stoichiometry and crystallinity on mechanical properties

Properties	PLLA		
	L-PLA	Annealed L-PLA	D,L-PLA
Yield strength (MPa)	70	70	53
Tensile strength (MPa)	59	66	44
Flexural strength (MPa)	106	119	88
Notched Izod impact ($J.m^{-1}$)	26	66	18
Vicat penetration (°C)	59	165	52

But stereocomplexes are complexes between two polymers of same chemical structures but different stereochemical configurations. This is comparable to two enantiomeric compounds forming a racemic crystal if their molecular affinity is sufficiently strong. For example, L,L-dilactide (cyclic monomer of PLA) and D, D-lactide (that of PDLA)

possess a melting point of 97.5 ^{0}C each, while racemic mixture crystallizes differently to give a new crystalline melting point of 124 ^{0}C.

A stereo complex differs from a racemic mixture of the two, stereo pure polymers in the sense that the stereocomplex, unlike a racemic mixture, should have a new crystalline packing pattern. Racemates of optically active D- and L- polymers are well known, but among them only a few are stereocomplexes **[217-219]**.

Stereocomplex between separately prepared, pure poly (L-lactic acid) and poly (D-lactic acid) was first synthesized and reported by Ikada and coworkers **[220]**. They got the stereocomplex by mixing equal moles of the two polymers, both taken as dichloromethane solutions, together and precipitating into methanol and drying under vacuum. While the individual PLAs showed a single crystalline melting point of 180 ^{0}C each, the stereocomplex showed a single, new melting endotherm at 230 ^{0}C. Wide angle X-ray diffraction patterns also showed peaks at completely new positions for the 50-50 mixtures. All physical and material properties of the stereocomplex are different from the individual poly (lactic acid). An interesting property, for example, is that it forms gel in a concentrated solution **[221]**.

Stereocomplexes are generally made from 50-50 mixtures of stereo pure PLAs in solution. But in-situ stereocomplex has also been reported of late. There are mainly two different strategies. One is synthesizing a stereo pure poly (lactic acid) from an enantiopure lactide in presence of poly (lactic acid) of the opposite configuration **[222]**. The other strategy is in-situ stereocomplex formation by polymerizing a racemic lactide in presence of a suitable chiral catalyst **[223]**. The stereocomplex has found use in the industry as a new poly (lactic acid) material because of its high crystallinity, good processability and good moldability **[224]**. Interestingly, high melting temperatures are not restricted to enantiomerically pure poly (L-lactide) or poly (D-lactide) (T_m 170-180 ^{0}C) and are even surpassed (T_m up to 230 ^{0}C) by PLA stereocomplexes **[225]** and PLA stereoblocks (**Figure 1.4.**).

ROP.So far, only a few preliminary results have been reported for the stereochemically controlled polymerization with nucleophilic catalysts: (i) no racemization occurred in the enzyme **[187]**, and DMAP catalyzed **[188]**, polymerization of the enantiomerically pure L-lactide and (ii) no stereosequence enrichment was detected when D,L-lactide was

polymerized with lipase PS **[187a]** or chiral phosphines **[188]**. The latter result has been attributed to the rather drastic conditions required with phosphines as ROP catalysts (bulk, 135 or 180 ^{0}C). However, higher stereocontrol might be anticipated for the much more active N-heterocyclic carbenes since these catalysts efficiently achieve lactide ROP in solution even at room temperature.

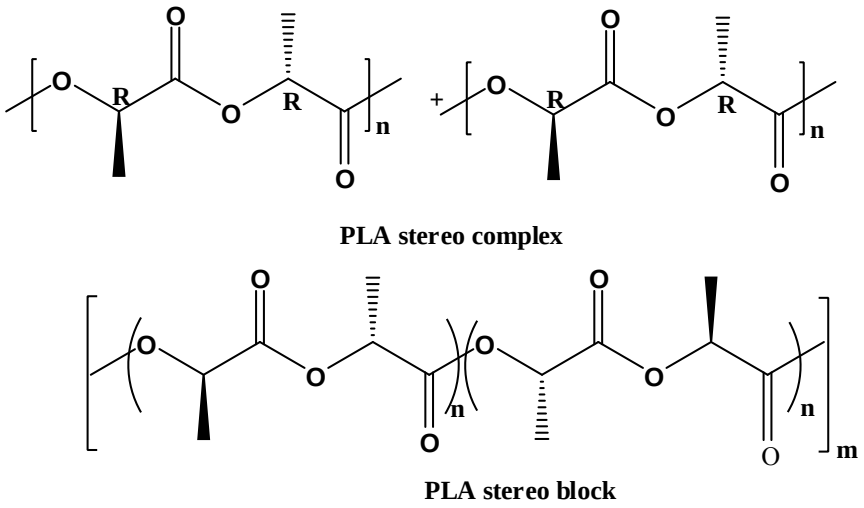

Figure 1.4: PLA stereo complexes and stereo blocks.

1.9. Properties of copolymers:

The ability to make PLA polymers in two different ways, namely polycondensation and ring opening polymerization, leads to a wide variety of copolymers for improving or changing the final properties. The use of direct condensation leaves open the use of any hydroxy-acid, diol, or diacid, with which to form random or nearly random copolymers, mostly with increased flexibility and modified solubility. The use of ROP yields the ability the form random, block, or pseudo block copolymers to produce polymers with a wide range of mechanical properties.

However, beginning of a discussion of properties of poly (lactic acid) copolymers can as well be made with the aliphatic copolyesters of lactic acid, which in many cases have been found to be more processable due to lower glass transition temperatures and more thermally stable.

For example, copolyesters of L-lactic acid/ethylene glycol/adipic acid and L-lactic acid/1,4-butanediol/succinic acid were been prepared by direct dehydropolycondensation, yielding linear polyesters whose molecular weights were less than 30,000, while addition of a polyol such as pentaerythritol produced multibranched with a little higher molecular weights (>50,000) **[226]**. The glass transition temperatures of linear and branched copolyesters were in the ranges form -17 to 43 ^{0}C and from 10 to 23 ^{0}C respectively, both of which are lower than that of linear poly (L-lactic acid), which is close to 60 ^{0}C. Initial thermal decomposition temperatures (T_D) of the linear and branched copolyesters were in the ranges from 205 to 272 from 194 to 228 ^{0}C respectively, both of which are higher than that of linear PLA, which is about 170 ^{0}C.

High molecular weight copolyesters of L-lactic acid and ε-caprolactone were prepared using Sb_2O_3 as catalyst and dipentaerythritol (DIP) as initiator **[227]**. In this process short chain polycaprolactone (PCL) oligomers were produced by ROP, which simultaneously co-polycondensed with the lactic acid, thereby yielding copolyesters that was mostly amorphous. The T_g was in the range of 48 to 43 ^{0}C and decreased with increasing caprolactone content. The initial thermal decomposition temperature (T_D) was in the range of 212 and 289 ^{0}C, while that of PLA homopolymer was 168 ^{0}C.

The most frequently synthesized and most largely exploited copolyesters of lactic acid, as far as material application is concerned, are the copolyesters of lactic and glycolic acid, prepared by both dehydropolycondensation of lactic and glycolic acids as well by ring opening polymerization of the lactides with dilactone of glycolic acid, called glycolide **[228-236]**. The higher (than PLA) melting point of 228 ^{0}C and a lower T_g of 37 ^{0}C for polyglycolic acid leads to a range of amorphous polymers, depending on the sequence of glycolic and lactic blocks in the backbone of the copolymer, with lower glass transition temperature yet more toughness than pure PLA. Increasing glycolic acid content also reduces the hydrophobicity of copolyesters with 30 mol% or more glycolic acid content are insoluble in non-polar aprotic solvents and more easily degradable than pure PLA.

Introduction of mandelic acid comonomer in a poly (lactic acid) synthesized by dehydropolycondensation improved thermal and mechanical properties, in spite of randomness of the incorporation and consequent destruction of crystallinity **[237]**. As amount of comonomer feed increased, the molecular weight of the copolymer decreased

linearly. But the glass transition and decomposition temperature shifted higher, indicating improved thermal stability with increased mandelic acid content. Tensile strength of cast films also improved in copolymers with 5 - 10 wt% of mandelic acid.

Direct dehydropolycondensation of bis-carboxyl-terminated PLA with PEG yielded multiblock copolymers, in which PLA and PEG blocks were phase separated and the properties of one block were affected by the block length of the other **[238]**. The longer the PLA block the lower the crystallinity and melting temperature of the PEG block. These copolymers were having different crystallization behavior in melt and solution casting crystallization process, even though the chemical structures and molecular weights were the same in both cases. The crystallizability of the PLA block was more affected by the crystallization method than that of the PEG block. Such alternating multiblock copolymers formed interesting hydrogels, which are thermoplastic in nature **[239]**. They offer potential for application in drug delivery and various other biomedical projects.

Di- and triblock copolymers of telechelic PEG with aliphatic polyesters like PLA showed thermo-reversible gelation because of the hydrophilicity-hydrophobicity balance between the two block components **[240]**. Such block copolymers formed micelle in water at lower concentrations while at higher concentrations the gel to sol transition was observed as temperature was increased up to a certain temperature beyond which the polymer precipitated. With increasing block length of the hydrophobic aliphatic ester block, the gel to sol transition is observed at lower concentrations and with a broad temperature range from 0 ^{0}C to 90 ^{0}C. Such properties are worth exploitation in the drug delivery industry.

Aqueous solutions of triblock copolymers, poly(ethylene glycol-b-(D, L-lactic acid-co-glycolic acid)-b-ethylene glycol) (PEG-PLGA-PEG), coupled with hexamethylene diisocyanate, have shown even more interesting thermo-reversing gelation, where there is a sol-to-gel transition at lower temperature and a gel-to-sol transition at a higher temperature **[241]**. It is the lower transition, sol-to-gel, which is more important because the polymer will flow as a solution at room temperature while gel inside the body at body temperature. Such polymers are worth exploitation in the drug delivery industry as "injectable gel".

Investigation of surface topography of PLA-PEO diblock copolymer submerged in water by AFM visualized the apices of the PEO chains extending into the aqueous environment from the surface, corresponding to visualization of polymer brushes at molecular level and anticipated resistance to protein interactions **[242]**.

Linear and star stereoblock copolymers (**Scheme 1.20**) of lactic acid are prepared by sequential polymerization of isomeric lactides in presence of diol or polyol. The most important message is that the block copolymers crystallize even at 35 mol % concentration of the D-isomer in a preponderance of the L-units, in contrast to the amorphous nature of random steerocopolymers similar and less incorporation of the stereoisomer **[243]**. The crystallinity of the stereoblock copolymer is a function of annealing temperature and time.

PLA has a very crucial hydrophile-lipophile balance that is severely affected, rather altered, by block-copolymerization with PEO. At the same time, fine-tuning the relative block lengths of PEO and poly lactide, its stability against rupture of microscopic liquid film and nanoemulsions can be controlled **[244]**.

The onset of weight loss during hydrolytic degradation of poly (lactic acid) is generally found to become more rapid when block-copolymerized with PEO, but with time the difference almost vanishes **[245]**. This is explained in terms of initial rapid diffusion of water in to the copolymer due to miscibility of the PLA and PEG blocks and greater water solubility of the PEG-PLA copolymer. But as water intake increases and chain scission of PLA blocks occurs, a gradual phase separation between the PLA and PEG blocks that makes the chain rates of the PLA blocks similar to that in a pure PLA homopolymer.

Copolymers of itaconic anhydride and methacrylate terminated PLA macromonomer was made with 15–85 mol % incorporation of the itaconic anhydride and retention of the cyclic anhydride structure in order to provide a new set of biodegradable polymers prepared from natural resources and with a wide range of properties **[246]**. The copolymers showed a range of glass transition temperatures from 31 to 73 ^{0}C, increasing with increase in the itaconic anhydride incorporation. No residue of crystallinity of the parent PLA is restored in these copolymers.

Comonomers that impart lower glass transition temperatures and flexibility have been increasingly researched in order to improve the low temperature properties and ductility of PLA. The work has been driven mainly by the need for biocompatible ingredients that would that would improve the properties of implantable medical devices and drug delivery systems. Extensive studies have been done on more common and commercial monomers to elucidate reactivity ratios and sequence formation during melt and/ or solution copolymerization.

The ring opening copolymerization of lactide and ε-caprolactone give polymers with wider spectrum of properties than the polymers synthesized by copolycondensation of the corresponding hydroxy acids, which have been discussed earlier. Such ring opened copolymers yield tough polymers with properties ranging from rigid thermoplastics to elastomeric rubbers **[247, 248]**, with tensile strengths ranging from 80 to 7000 psi (0.6 – 48 MPa), and elongations over 400 % **[249]**. The larger reactivity of lactide over ε-caprolactone leads to copolymers that are blocky, where the block lengths depend on the starting comonomer composition, catalyst **[250]** and polymerization temperature. Poly (ε-caprolactone) (PCL) itself has a T_g of –60 ^{0}C with a melting point of 59 – 60 ^{0}C, which when the monomer is ring open polymerized with pure L-lactide yields a copolymer with flexibility because of the caprolactone segment and high crystalline melting points from the L-PLA blocks. These blocks must be sufficiently large to allow rapid crystallization. Grijpma has synthesized a copolymer with 1:1 monomer molar ratio, which crystallized at room temperature very quickly, in contrast to a similar copolymer with average block lengths of 8.5, which exhibited crystallinity only after weeks of annealing at room temperature and the former polymer with longer block lengths had a T_g of –39 ^{0}C, both PLA and PCL block melting points, a tensile strength of 18.2 MPa, and elongation at break of 480 % **[251]**.

Poly (lactic acid) is one of the highest glass transition temperature-possessing polymers among aliphatic polyesters and polyethers. Only a few monomers, including the mandelic as mentioned before, have been found to increase the glass transition temperature of PLA when copolymerized into the backbone. Lactones of salicylic acid are reported to have homopolymer glass transition temperatures of 73 – 110 ^{0}C and

polymerize slowly with lactide to give copolyesters with higher T_g values than PLA homopolymers **[252, 253]**.

The size and chemistry of the rings and the variety of comonomers, which can be ring-open polymerized with lactides to form different block or random block copolymers, is thus largely dependent on their mode of propagation, reactivity and initiation.

Use of functional amino acids in the synthesis of the morpholinedione has thus become an effective way of incorporating functional pendant groups into the polymer. Comb-like graft copolymers of lactic acid, poly(L-lactic acid-co-L-lysine), with L-lysine side chains, of degree of polymerization ranging from 10 to 100, have been reported, with the overall L-lysine content in the copolymer varying from 7 to 72 % **[254]**. L-lysine residues of such poly (L-lactic acid-co-L-lysine) copolymers were further modified with an RGD (arginine-glysine-aspartic acid) cell adhesion promoting peptide, the modified copolymer being useful for tissue engineering **[255]**. Its degradation rate was faster than poly (L-lactic acid) due to disruption of crystallinity by the lysine residues in the copolymers.

Boury and coworkers **[256]**, have investigated the interfacial behavior of PLA in comparison with influence of lactic acid and glycolic acid proportion in copolymers by studying on monolayer spreading at air/water interface, using Langmuir-Blodgett films. The size and chemistry of the rings and the variety of comonomers, which can be ring-open polymerized with lactides to form different block or random block copolymers, is thus largely dependent on their mode of propagation, reactivity and initiation. Figure 1.5 shows some of the monomers (**1.3 – 1.19**) that have been studied extensively with regards to ring opening copolymerization with lactides. Thus, besides lactones and epoxides, morpholinediones are another important class of cyclic compounds that have been copolymerized with the lactides. The pure poly (L-lactide) gave a more rigid film and had higher surface pressure than the film of the copolymer. The extent of orientation decreases with increasing incorporation of the glycolide unit, while the parent pure poly (L-lactide) film is highly oriented, which is the cause of high surface pressure. The high surface area is attributed to strong lateral interaction between lactic groups, which form microdomains in small areas. Glycolic acid units disrupt this interaction and do not allow formation of the microdomains. In condensed state, the major contribution to the surface free energy was non-polar, although small polar component of the force, due to O atoms

was measured. The lactic acid groups, particularly the methyl groups are oriented towards the air phase.

1.10. Stability of polymer: The stability of a polymer has a major impact on all of the different stages of a polymer life cycle. This is especially important for biodegradable polymers, where the biodegradation must proceed in a controlled way, although the appearance and the properties must be comparable to traditional polymers. The degradation of polymers has been defined as the number of chain scissions produced during a known period of time and can be expressed by equation (Reich and Stivala, 1971) **[257]**.

$$1/DP = 1/DP_0 + K_D t$$

Where DP_0 and DP are respectively the initial and final numbers of the average degree of polymerization, K_D is the degradation rate constant, and t is the time. This equation is valid for condensation polymers when the amount of broken bonds are low; i.e. the term $K_D\ t$.

1.11. Depolymerization: Pyridine catalysts such as DMAP and PPY **(scheme 1.9.**) have also been used for the chain scission of poly lactides **[188]**. Low as well as high-molecular-weight polymer samples were depolymerized with primary alcohols either in solution at 38 ^{0}C or in bulk at 185 ^{0}C. The resulting poly lactides have DPs consistent with the alcohol-to-polymer ratio and polydispersity indexes in the same range as the initial polymer. Thus, this transesterification approach allows for the preparation of controlled molecular weight and end group functionalized poly lactides. Promising results were also reported for more complexes macromolecular.

1.12. Degradation Mechanisms and Degradability:

1.12.1. Hydrolytic / Enzymatic: A sort of quantitative correlation can be drawn among the degree of crystallinity, orientation and enzymatic degradability of poly(lactic acid), the rate of enzymatic degradation decreased with increase in crystallinity **[258]**. A threshold was observed when the heat of fusion was less than 20 J/g. Effects of temperature; pH, molecular weight and copolymerization on the hydrolysis rate of poly(lactic acid) have been studied **[259-264]**.

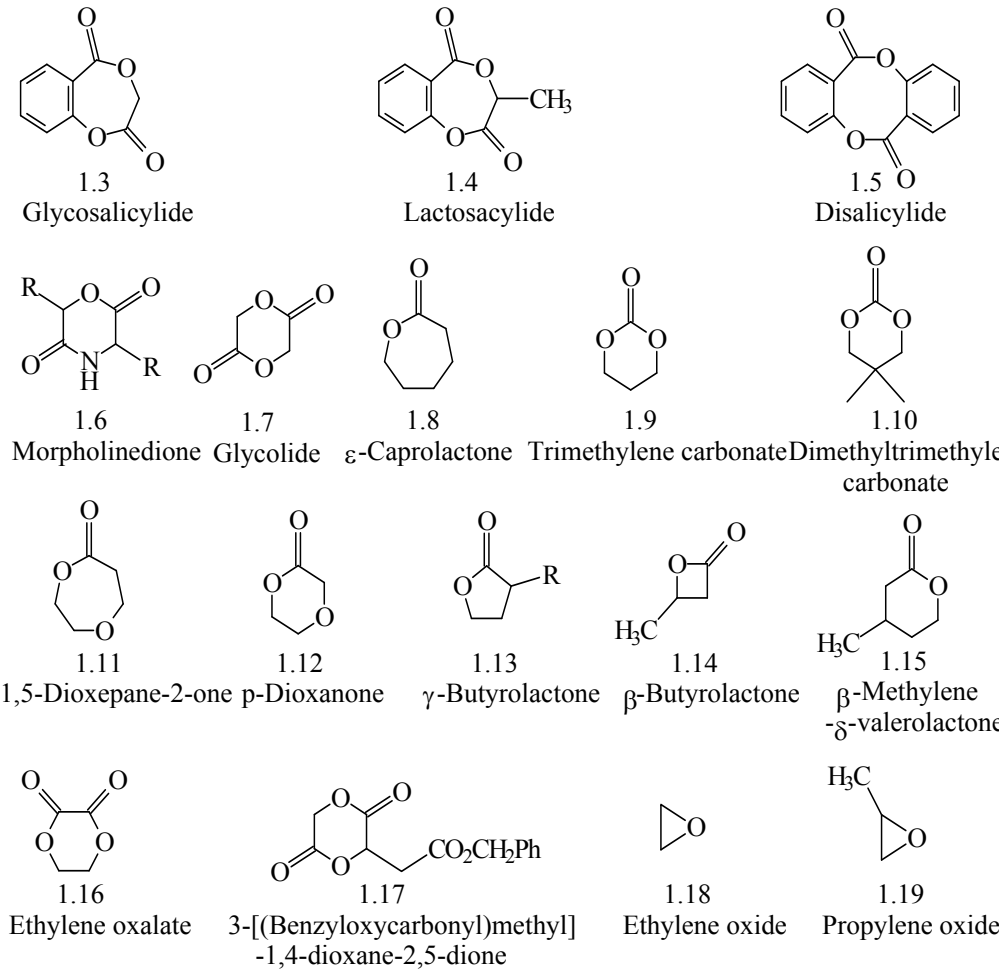

Figure 1.5: A few comonomers that have been polymerized with lactide.

Impurities and residual monomer increase the hydrolysis rate **[265, 266]**. Peroxide modification increases the hydrolysis rate **[267]**. In larger size devices of PLA, the rate of hydrolytic degradation is higher inside than at the surface of the material because of the autocatalyzing effects of the carboxylic acid groups trapped inside the device **[268]**.

Whether there are microorganisms in nature that are able to biodegrade PLA polymers of any molecular weight is still under discussion and investigation.

There have been only a few studies where PLA or its oligomers have been subjected to selected microorganisms. In general, these studies tell us that the molecular weight is initially decreased by abiotic hydrolysis, but after the initial abiotic degradation, the molecular weight of samples aged in a biotic medium goes down faster than samples aged in an abiotic medium **[269]**. Presence of certain enzymes such as pronase,

proteinase K and bromelain decreases the degradation rate of PLA **[270]**, but effect of certain other important and likely enzymes such as esterase and lactate dehydrogenase is yet to be ascertained.

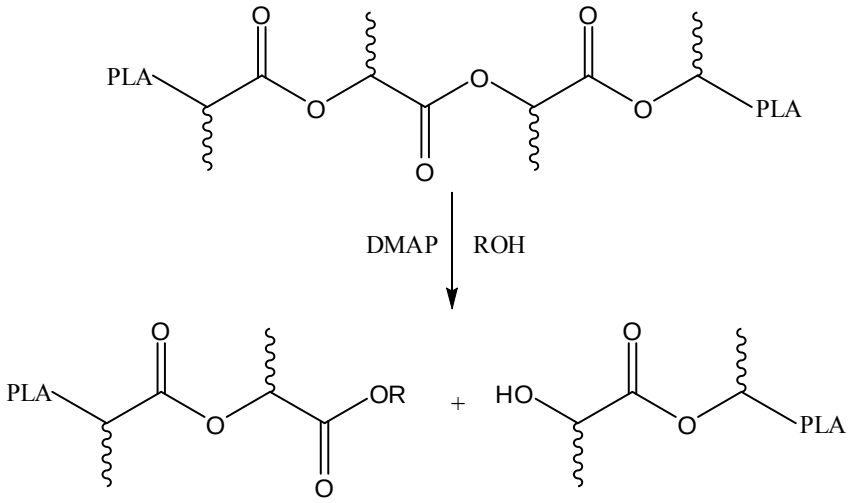

Scheme 1.9: DMAP-catalyzed PLA depolymerization.

Presence of easily assimilated lactic acid and lactoyl lactic acid was not only important for an enhanced degradation of poly (lactic acid) in biotic media, but was also a prerequisite for the initial growth of microorganisms on the surface of the material **[271]**.

The effects of physical aging is profound on crystallinity and consequently on degradation also. The enzymatic degradation rate decreases as a function of physical aging that is excess enthalpy relaxation, the change of which is fast at the beginning of heating and slows down with time **[272]**.

In the acid catalyzed hydrolysis of PLA, the chain end scission is the predominant pathway, in contrast to hydrolysis of poly (ε-caprolactone) (PCL), which occurs predominantly by random scission of backbone ester linkages **[273]**. Blocking the free carboxylic acid function of PLA, for example by esterification, gives good hydrolysis resistance and enhances shelf-life **[274]**.

1.12.2. Thermo-oxidative: When examined by heating under nitrogen within a temperature range of 180 and 240 ^{0}C, PLA showed thermal instability and loss of mass even at temperatures as low as 190 ^{0}C. There may be several reasons for its poor thermal stability: (1) hydrolysis by trace amounts of water catalyzed by hydrolyzed monomer

(lactic acid); (2) depolymerization in unzipping fashion resulting lactide molecules, catalyzed by residual polymerization catalyst; (3) oxidative, random main chain-scission and (4) intermolecular transesterification with monomer and oligomeric esters **[275]**. The dominant reaction pathway is an intramolecular transesterification-giving rise to formation of cyclic oligomers. In addition, acrylic acid from cis-elimination as well as oxides of carbon and acetaldehyde from fragmentation reactions were detected **[276]**.

Thermal degradation of PLA in air involves an initial rapid decrease in molecular weight and high rate of loss of mass, accompanied by an initial decrease of the melting point and then increase with time die to chain stiffening **[277]**. Thermal decomposition of PLA forms cyclic oligomers, which are detected by pyrolysis mass spectroscopy accompanied with positive and negative chemical ionization, but unstable under electron impact ionization method **[278]**.

1.13. Conclusion and future directions:

A number of synthetic approaches such as dehydropolycondensation, post-polymerization, and coupling of low molecular weight chain and ring opening of lactide have been practiced to achieve high molecular weight poly (lactic acid) s from lactic acid. A minimum weight average molecular weight of 50,000 is required for mechanical properties suitable for material application. PLA behaves as stiff thermoplastic like polystyrene because of its high glass transition temperature and also can be enhanced by stereo complex mechanism. Different approaches have been tailor made to modulate the properties of PLA, especially the improvement of flexibility by plasticization (grafting and blending).

Moreover, tremendous enlargement of the available range of properties, form a brittle thermoplastic to a rubbery polymer, has been achieved through random and block copolymerization with a number of monomers in general and with glycolide/ glycolic acid, PEG/ PEO/ epoxides and ε-caprolactone in specific. Lactic acid is a non-toxic constituent of the human metabolic cycle, gives absolute biocompatibility to the PLA polymer, making it a safe polymer for human body-contact applications such as biomedicals and textiles. It is also a truly hydrolysable/ biodegradable polymer, which

can be composted and degraded through the mechanism of ester hydrolysis to return lactic acid, which is naturally consumed to yield carbon dioxide, water and biomass.

However, in spite of the fact that PLA is now in the shape of a technical preparedness to sell as numerous materials such as non-woven fibers, oriented films, extrusion coating, flexible film, cast sheet, injection molding and foam, the prohibitive cost is one factor that has kept its application still mainly confined to the high-value, speciality applications such as nonocomposite such as PLA nanocomposite (grafting and blending) and nano particles in biomedicals application.

References

1. The term "biodegradable" is used here in the broadest sense, meaning that the polymer will eventually disappear following introduction in the body, without reference to the mechanism of degradation, which may or may not be enzymatically assisted.
2. Hayashi, T. *Prog*. *Polym. Sci*. **19**, 663 (1994).
3. Sinclair, R. G. *Pure Appl. Chem*. **A33**, 585 (1996).
4. Chiellini, E.; Solaro, R. *Adv. Mater*. **8**, 305 (1996).
5. Amass, W.; Amass, A.; Tighe, B. *Polym. Int*. **47**, 89. **(**1998).
6. Ikada, Y.; Tsuji, H. *Macromol. Rapid Commun*. **21**, 117 (2000).
7. Middlenton, J. C.; Tipton, A. J. *Biomaterials* **21**, 2335 (2000).
8. Langer, R. *Acc. Chem. Res*. **33**, 94 **(**2000).
9. ASTM Standards on Environmentally Degradable Plastics, ASTM Publication Code Number (DCN): 03-**420093**-19 (1993).
10. CEN TC 261 SC4 W62 draft "Requirements for packaging recoverable in the form of composting and biodegradation. Test scheme for the final acceptance for packaging March 11 (1996).
11. Reeve, M. S.; McCarthy, S. P.; Downey, M. J.; Gross, R. A. *Macromolecules* **27**, 825 (1994).
12. MacDonald, R. T.; McCarthy, S. P.; Gross, R. A. *Macromolecules* **29**, 7356 (1996).
13. Li, S.; McCarthy, S. *Macromolecules* **32**, 4454 (1999).

14. Li, S.; Tenon, M.; Garreau, H.; Braud, C.; Vert, M. *Polym. Degrad. Stab*. **67**, 85 (2000).
15. Tsuji, H.; Miyauchi, S. *Polym. Degrad. Stab*. **71**, 415 (2001).
16. Tsuji, H.; Miyauchi, S. *Polymer* **42**, 4465 (2001).
17. US Industry Study with Forecasts for 2012 & 2017 Biodegradable Plastic Study **2387**, 199 (2008).
18. Holten, C. H. "Lactic Acid Properties and Chemistry of Lactic Acid and Derivatives" Verlag Chemie, Germany (1971).
19. Bogaert, J-C.; Coszach, P. *Macromol. Symp*. **153**, 287 (2000).
20. Hofvendahl, K.; Hahn-Hagerdahl, B. *Enzyme Microb. Technol*. **20,** 301 (1997).
21. Hofvendahl, K.; van Niel, E. W. J.; Hahn-Hagerdahl, B. *Appl. Microbiol. Biotechnol*. **51**, 669 (1999).
22. Akerberg, C.; Hofvendahl, K.; Zacchi, G.; Hahn-Hagerdahl, B. *Appl. Microbiol. Biotechnol*. **49,** 682 (1998).
23. Qian, N.; Stanley, G. A.; Hahn-Hagerdahl, B.; Radstrom, P. *J. Bacteriol.* **176**, 5304 (1994).
24. Lohmeier-Vogel, E. M.; Hahn-Hagerdahl, B.; Vogel, H. J. *Appl. Microbiol. Biotechnol.* **25**, 43 (1986).
25. Garrigues, C.; Loubiere, P.; Lindley, N. D.; Cocaign-Bousquet, M. *J. Bacteriol.* **179**, 5282 (1997).
26. Thomas, T. D.; Turner, K. W.; Crow, V. L. *J. Bacteriol.* **144**, 672 (1980).
27. Cheng, P.; Mueller, R. E.; Jaeger, S.; Bajpai, R.; Eannoti, E. L. *J. Ind. Microbiol.* **7**, 27 (1971).
28. Wood, B. J. B.; Holzapfel, W. H. eds. "The Genera of Lactic Acid Bacteria" 1st edition, Glasgow, UK, Blackie Academic and Professional (1995).
29. Dicks, L. M. T.; Dellaglio, F.; Collis, M. D. *Int. J. Syst. Bacteriol.,* **45**, 395 (1995).
30. Viniegra-Gonzalez, G.; Gomez, J. "Lactic acid production by pure and mixed bacterial cultures" in: Wise, D. L. ed. Bioconversion Systems. Boca Raton, FL: CRC Press, Inc., 17 - 39 (1984).
31. Thomas, T. D.; Ellwood, D. C.; Longyear, M. C. *J. Bacteriol.* **138**, 109 (1979).

32. Hofvendahl, K.; "Fermentation of wheat starch hydrolysate by *Lactococcus lactis* factors affecting product formation", Lund, Sweden: Lund University, PhD Thesis (1998).
33. Kandler, O. *A van Leeuw*. **49**, 209 (1983).
34. Nolasco-Hipolito C, Matsunaka T, Kobayashi G, Sonomoto K, Ishizaki A .J Biosci Bioeng. **93**,28 (2002
35. Inskeep, G. C.; Taylor, G. G.; Breitzke, W. C. *Ind. Eng. Chem.* **44**, 1955 (1952).
36. Kulozik, U.; Wilde, J. *Enzyme Microb. Technol.* **24**, 297 (1999).
37. Prescott, S. C.; Dun, C. G. Industrial Microbiology, 3rd ed. New York: Mcgraw-Hill, (1959).
38. Moat, A. G., "Biology of lactic, acetic and propionic acid bacteria" in Demain, A. L. and Solomon, N. A. eds. Biology of Industrial Microorganisms. Boston: Butterworths, p. 174 (1985).
39. Aeschlimann, A. A.; von Stockar, U. *Appl. Microbiol. Biotechnol.* **32**, 398 (1990).
40. Payot, T.; Chemaly, Z.; Fick, M. *Enzyme Microl, Techno.* **24**, 191 (1999).
41. Mulligan, C. N.; Safi, B. F.; Groleau, D. *Biotechnol. Bioeng.* **38**, 1173 (191).
42. Tejayadi, S.; Cheryan, M. *Appl. Microbiol. Biotechnol.* **43**, 242 (1995).
43. Chiarini, L.; Mara, L.; Tabacchioni, D. *Appl. Microbiol. Biotechnol.* **36**, 461 (1992).
44. Lund, B.; Norddahl, B.; Ahring, B. *Biotechnol. Lett.* **14**, 851 (1992).
45. Hujanen, M.; Linko, Y.-Y. *Appl. Microbiol. Bitechnol.* **45**, 307 (1996).
46. Borgardts, P.; Krischke, W.; Trosch, W.; Brunner, H. *Bioprocess Eng.* **19**, 321 (1998).
47. Kwon, S.; Lee, P. C.; Lee, E. G.; Keun Chang, Y.; Chang, N. *Enzyme Microb. Technol.* **26**, 209 (2000).
48. Rojan PJ, Nampoothiri KM, Nair AS, Pandey A . Biotechnol Lett. **27**,1685(2005).
49. Sentisiran, A.; Arasaratnam, V.; Balasubramaniam, K. *J. Natl. Sci. Found. Sri Lanka* **27**, 107 (1999).
50. Soccol C, Marin B, Raimbault M, Lebeault JM Appl Microbiol Biotechnol. **41**,286 (1994).
51. Wee Y-J, Kim J-N, Ryu H-W .Technol Biotechnol. **44**,163 (2006).

52. Jarvinen, M.; Myllykoski, L.; Keiski, R.; Sohlo, J. *Bioseparation* **9**, 163 (2000).
53. Hong, Y. K.; Hong, W. H. *Biotechnol. Tech.* **13**, 915 (1999).
54. Zhou, K.; Fan, X.; Su, Y. *Huadong Huagong Xueyuan Xuebao.* **18**, 560 (1992).
55. Suga, K. I.; Omasa, T.; Katakura, Y.; Kishimoto, M. *Biotechnol. Sustainable Util. 66. Biol. Resour. Trop.* **13**, 134 (1999).
56. Kashket, E. R. *FEMS Microbiol. Rev.* **46**, 233 (1987).
57. Ohta, M.; Obuchi, S.; Yoshida, Y. *US 5512653* (1996).
58. llmans Encyklopadie der Tochischen Chemie, Verlag Chemie GmbH, 4th Edition, Volume **17**, 1 (1979).
59. Lenninga, H. "History of Lactic Acid Making", Kluwer Academic Publications (1990).
60. Holten, C. H. "Lactic Acid: Properties and Chemistry of Lactic Acid and Derivatives", Verlag Chemie GmbH (1971).
61. Veldhuis-Stribos, B. I.; Breugel, J. V.; Groot, W. J.; Dierdrop, B. M. *NL001013265* (1999).
62. Winkellar, H. M.; Breugel, J. V.; Vila, M. C.; Lancis, J. M. V. *NL001013682* (1999).
63. Lockwood, D. E.; Yoder, D. E.; Zienty, M. *Ann. N. Y. Acad. Sci.* **119**, 854 (1965).
64. (a) Breugel, J. V.; Krieken, J. V.; Baro, B. C.; Lancis, J. M. V.; Vila, M. C. *WO056693* (2000). (b). Borsook, H.; Huffman, H. M.; Liu, Y.-P., *J. Biol. Chem.* **102**, 449 (1993).(b) Buszko, M. L.; Andrew, E. R. *Mol. Phys.* **76**, 83 (1992).
65. Ing, T. S.; Yu, A. W.; Nagraja, V.; Amin, N. A.; Ayache, S.; Gandhi, V. C.; Daugirdas, J. T. *Int. J. Artif. Organs*. **17**, 70 (1994).
66. Velthuijsen, J. V.; Krieken, J. V. *EP0563455* (1992).
67. Kanters, J. A.; Krieken, J. V. *J. Mol. Struct.* **323**, 165 (1994).
68. Amiel, C.; Mariey, L.; Curk-Daubie, Marie-C.; Pichon, P.; Travert, J. *Lait.* **80**, 445 (2000).
69. Czarnecka, M.; Czarnecki, Z.; Roszyk, H. *Zywnosc* **7**, 92 (2000).
70. Jing, L.; Wang, S.; Qiu, J.; Li, J. *Huanjing Gongcheng* **18**, 46 (2000).
71. Qing, X.; Liu, H.; Zhang, B. *Fenxi Huaxue* **28**, 842 (2000).

72. Kulaeva, L. T.; Sirko, V. N.; Makarova, L. M. *Izv. Vyssh. Uchebn. Zaved., Pishch. Tekhno.* 86 (1999).
73. Ishikuro, E.; Hibino, H.; Soga, T.; Yanai, H.; Swada, H. *Shokuhin Eiseigaku Zasshi* **41**, 261 (2000).
74. (a) Kodama, S.; Yamamoto, A.; Soga, T.; Minoura, K. *J. Chromatogr. A.* **875**, 371 (2000). (b) Kodama, S.; Yamamoto, A.; Soga, T.; Minoura, K.; Minoura, K.; Matsui, K.; Nakagomi, K.; Tanimura, T.; Hayakawa, K. *Chromatography* **20**, 154 (1999).
75. Tejeda, A.; Oliva, A. I.; Simon, L.; Grande, M.; Caballero, M. C.; Moran, J. R. *Tetrahedron Lett.* **41**, 4563 (2000).
76. Szakacs-Schmidt, A.; Albert, L.; Kelemen-Horvath, I. *Biomed. Chromatogr.* **13**, 252 (1999).
77. Ohara, Hitomi; Ito, Masahiro; Sawa, Seiji PCT Int. Appl. WO 2002060891 A1 8 , 37 (2002).
78. Lou, Ling; Yin, Jing-bo; Liang, Qi-zhi; Gao, Zhan-tuan; Dong, Li-song; Chen, Xue-si; Jing, Xia-bin . Gaofenzi Cailiao Kexue Yu Gongcheng **19**, 72 (Chinese) (2003).
79. Shvets, V. F.; Kozlovskii, R. A.; Schastlivaya, S. V.; Varlamova, E. S.; Makarov, M. G.; Staroverov, D. V.; Suchkov, Yu. P. (Rossiyskii Khimiko-Tekhno. Univ. im. D. I. Mendeleeva, Russia). Russ. *RU 2301230 C2, 6* (2007).
80. Hiltunen, K; Seppala, J. V.; Harkonen, M. *Macromolecules* **30**, 373 (1997).
81. Gruter, R.; Pohl, H. *US1095205* (1914).
82. deProspero, D. A.; Schmitt, E. E. *US3597449* (1967).
83. Bellis, H. E. *US4727163* (1986).
84. Paul, D. *US5089632* (1992).
85. Bhatia, K. K.; Lin, K.; Nash, R. S.; Stambaugh, T. W. *WO9302075* (1993).
86. Okada, Y.; Shirasawa, S.; Ogata, F. *JP06065230* (1994).
87. Noda, Masaki.; Okuyama, Hisashi. Chem. Pharm. Bull. **47**, 467 (1999).
88. Takeshi, Akio. *JP 07339757 **A2*** (1995).
89. Jiang, Xin.; Chen, Lianxi.; He, Jianhua.; *Li Shipu. Wuhan Ligong Daxue Xuebao* **24**, (Chinese) (2002).

90. Kawanabe, Takashi.; Horibe, Taisei.; Takahashi, Masatoshi.; Okuyama, Hisatsugu *JP 10168077* ***A2*** (1998).
91. Sawa, seiji.; Kawamoto, Tatsuji.; Horibe,Yasumasa.; Obara, Hitormi. *JP 07138253* ***A2*** (1995).
92. Tsuda, Atsushi. *JP.06031175 A2* (1994).
93. Mueller, M. *DE3632103* (1988).
94. Mueller, M. *EP261572A1* (1988).
95. Bhatia, K. K.; Lin, K.; Nash, R. S.; Stambaugh, T. W. *WO9302075* (1993).
96. Drysdale, N. E.; Lin, K.; Stambaugh, T. W. *WO9318021* (1993).
97. Ajioka, M.; Enomoto, K.; Suzuki, K.; Yamaguchi, A. *Bull. Chem. Soc. Jpn.* **68**, 2125 (1995).
98. Kim, Soo Hyun; Kim, Young Ha Recent Advances in Environmentally Compatible Polymers, International Cellucon Conference, 11th, Tsukuba, Japan, Mar. 24-26, 1999, Meeting Date 1999, 217-226. Edited by: Kennedy, John F. Woodhead Publishing Ltd.: Cambridge, UK. ISBN: 1-85573-545 (2001).
99. Bing; Zhao, Yaoming; Mai, Hangzhen; Wang, Zhaoyang; He, *Yifan Hecheng Xianwei Gongye*. **25**, 19 (2002).
100. Kim, Ki Woong; Woo, Seong Ihl *Macromolecular Chemistry and Physics* **203**, 2245 (2002)
101. Fukushima, Kazuki; Kimura. *Polymer Preprints* **46**, 250 (2005).
102. Kobayashi, Mineo; Ito, Hiroyuki; Oogami, Kuninobu; Jinno, Yoshitsugu *JP 06298913 A2* 25 Oct Heisei, 4 pp (1994).
103. Enomoto, K.; Ajioka, M.; Yamaguchi, A. *USP, 5,310,865* (1994).
104. Kim, K.W.; Woo, S.I. *Macromol. Chem. Phys.* **203**, 2245 (2002).
105. Bose, P. K.; Sankara:narayanan, Y.;Sengllpta, S. C. *Chemistry of Lac.* 1 (1963).
106. Khanna, B. B.; Tripathi, S. K. M. *Chemicals and Petrochemicals J,* 1 (1979).
107. Tschirch, A.; Farner, A., *Arch Pharm*. **237**, 36 (1899).
108. Verman, L. C.; Bhattacharya, R., London *Sheliac Res. Bur. Tech. Paper* No.1 (1934).
109. Palit, S. R. *J. Indian Chem, Soc*. **5**, 25 (1942).
110. Trjpathi, S. K. M.; Misra. G. S., *Res. and Ind.* **13**, 129 (1968).

111. Bose, P. K.; Sankaranarayanan, Y.; Sengupta, S. C., .*Chemistry of Lac* 43 (1963).
112. Sengupta, S. C.; Ghosh, D.; Das, R. K.; Sinha, A. R. *J. Oil Col. Chem. Assoc*, 63 (1980),
113. Sengupta, S. C.; Agarwal, S. C.; Prasad, N. *J. Oil Col. Chem, Assoc*. **62**, 85 (1979).
114. Gupta, P. C.; Mukherjee, M.; Sankaranarayanan. Y. *Paint India* **19**, 26 (1969),.
115. Khurana, R. G.; Wadia, M. S.; Mhaskar, V. V.; Sukh Dev. *Tetrahedron Letters* 1537 (1964).
116. Wadia, M. S.; Mhaskar, V. V.; Sukh Dev. *Tetrahedron Letters* 513 (1963).
117. Sahu, T.; Misra, G. S. *Paint India* 22 (May 1970).
118. Prasad, R.; Sengupta, S. C., *J. Oil. Chem. Assoc*. **61**, 49 (1978).
119. Sukh, Dev. *J. Indian Chem. Soc*. **51**, 149 (1974).
120. Hussain, M. G.; Ali, M. H.; Ali, M. M.; Chowdhury, F. Khan Nun. *J. Bangladesh Acad. Sci*. **11**, 231 (1987).
121. Harries, C. D.; Nagel, *W. Ber*, **50B**, 3833 (1922).
122. Wadia, M. S.; Mhaskar, V. V.; Sukh Dev. *Tetrahedron Letters* 513 (1963).
123. Wadia, M. S.; Khurana, R. G.; Mh~skar, V. V.; Sukb Dev. *Tetrahedron* **25**, 3841 (1969).
124. Gardner, W. H.; Whitmore, W. F. *Ind, Eng. Chem.* **21**, 226 (1929).
125. Majee, R. N.; Agarwal, S. O.; Sengupta, S. C.; Mukherjee, S. N.; Chatterje, *J. N. Indian Perfum*., **33**, 156 (1989).
126. Subramanian, G. B. V.; Malathi, N. Indian *J. Chem., Sect*. B, **28B**, 806 (1989).
127. Subramanian, G. B. V.; Sharma, Rajiv *Synth. Commun*. **19**, 1197 (1989).
128. Majee, R. N.; Saha, S. K.; Agarwal, S. C,.*J. Inst. Chem*. **69**, 137 (1997).
129. Sarkar, P. C.; Agarwal, S. C. *J. Org. Chem. Incl. Med. Chem*. **34B**, 1080 (1995).
130. Mukherjee, M.; Majee, R. N.; Kumar, S.; Mukherjee, S. N. *J. Oil Colour Chem. Assoc*. **68**, 46 (1985).
131. Mishra, Mahendra. Kumar *J. Macromol. Sci., Chem*. **A20**, 619 (1983).
132. Subramanian, G. B. V.; Mehrotra, Kalpana. *Indian J. Chem., Sect*. B, **23B**, 665 (1984).
133. Shiina, Isamu. *JP 063247* (2007).

134. Benitez, Jose J.; Heredia-Guerrero, Jose A.; Heredia. Journal of Physical Chemistry C, 111, 9465 (2007).
135. Lee, Su.; Yeong; Kim.; Nam Tae. *KR 001053 A 3* (2008).
136. Martijn A. J.; Veld, Anja R.; Palmans, E.; Meijer, W. *Journal of Polymer Science: Part A: Polymer Chemistry* **45**, 5968 (2007).
137. Brawn, C. E. H.; Huglin, M. B. *Polymer* **3**, 257 (1962).
138. Zahora, E. P.; Murphy, E. J.; Szum, D. M. *WO 9857209 A1* (1998).
139. Yamaoka, K. *JP 11199746 A2* (1999).
140. Ranka, A. *WO 9911693 A1* (1999).
141. Ovitt, T. M.; Coates, G. W. *Polym. Prepr.* **41**, 385 (2000).
142. Spassky, N.; Wisniewski, M.; Pluta, C.; Le Borgne, A. *Macromol. Chem. Phys.* **197**, 2627 (1996).
143. Ovitt, T. M.; Coates, G. W. *J. Polym. Sci., Part A: Polym. Chem.* **38**, 4686 **(2000).**
144. Chamberlain, B. M.; Cheng, M.; Moore, D. R.; Ovitt, T. M.; Lobkovsky, E. B.; Coates, G. W. *J. Am. Chem. Soc.* **123**, 3229 (2001).
145. Cheng, M.; Attygalle, A. B.; Lobkovsky, E. B.; Coates, G. W. *J. Am. Chem. Soc.* **121**, (1999).
146. Dove, A. P.; Gibson, V. C.; Marshall, E. L.; White, A. J. P.; Williams, D. J. *Chem. Commun.* **283**.11583 (2001).
147. Hormnirun, P.; Marshall, E.; Gibson, V. C.; White, A. J. P.; Williams, D. J. *J. Am. Chem. Soc.* **126**, 2688 (2004).
148. Ovitt, T. M.; Coates, G. W. *J. Am. Chem. Soc.* **124**, 1316 (2002).
149. Hyon, S.-H.; Jamshidi, K.; Ikada, Y. *Biomaterials* **18**, 1503 (1997).
150. Coudane, J.; Ustariz-Peyret, C.; Schwach, G.; Vert, M.*J. Polym. Sci., Part A: Polym. Chem.* **35**, 1651 (1997).
151. Kricheldorf, Hans R.; Damrau, Dirk-Olaf. *Macromol. Chem. Phys.* **198**, 1753 (1997).
152. Williams, Charlotte K.; Breyfogle, Laurie E.; Choi, Sun Kyung; Nam, Wonwoo; Young, Victor G., Jr.; Hillmyer, Marc A.; Tolman, William B. *J. A. Che. Soc.* **125**, 11350 (2003).

153. Cam, D.; Marucci, M. *Polymer* **38**, 1879 (1997).

154. Kricheldorf, Hans R.; Damrau, Dirk-Olaf. *Macromol. Chem. Phys.* **199**, 1797 (1998).

155. Vert, Michel.; Coudane, Jean.; Schwach, Gregoire.; Huet, Olivier Jacqueline. *FR 2745005 A1* 16 pp (1997).

156. Yang, Liu.; Zhao, Zhenxian.; Wei, Jia.; El Ghzaoui, Abdelslam.; Li, Suming. *Journal of Colloid and Interface Science* **314**, 470 (2007).

157. Li, S. M.; Espartero, J. L.; Foch, P.; Vert, M. *J. Biomater. Sci., Polym. Ed.* **8**, 165 (1996).

158. (a) Kowalski, A.; Duda, A. and Penczek, S. *Macromol. Rapid Commun.* **19**, 567 (1998). (b) Kowalski, A.; Duda, A. and Penczek, S. *Macromolecules* **33**, 689 (2000). (c) Duda, A.; Penczek, S.; Kkowalski, A and Libiszowski, J. *Macrmol. Symp.* **153**, 41 (2000).

159. Kricheldorf, H. R.; Krieiser-Saunders, I. And Stricekr, A. *Macromolecules* **33**, 702 (2000).

160. Kricheldorf, H. R.; Boetcher, C.and Tonnes, K. U. *Polymer* **33**, 2817 (1992).

161. Kricheldorf, H. R.; Krieiser-Saunders, I. And Boettcher, C. *Polymer* **36**, 1253 (1995).

162. Sun, J.; Cui, L.; Wu, L. *Gongneng Gaofenzi Xuebao* **9**, 252 (1996).

163. Trofimoff, L.; Alida, T.; Inoue, S. *Chem. Lett.* 991 (1987).

164. Song, C, X.; Feng, X. D. *Macromolecules* **17**, 2764 (1984).

165. Bero, M.; Kasperczyk, J.; Jedlinski, Z. J. *Makromol. Chem.* **191**, 2287 (1990).

166. Kricheldorf, H. R.; Berl, M.; Scharnagl, N. *Macromolecules* **21**, 286 (1988).

167. Dubois, Ph.; Jacobs, C.; Jerome, R.; Teyssie, Ph. *Macromolecules* **24**, 2266 (1991).

168. Jacobs, C.; Dubois, Ph.; Jerome, R.; Teyssie, Ph. *Macromolecules* **24**, 3027 (1991).

169. Dubois, Ph.; Jerome, R.; Teyssie, Ph. *Makromol. Chem., Macromol. Symp.* **42/ 43**, 103 (1991).

170. McLain, S. J.; Ford, T. M.; Drysdale, N. E. *Polym. Prepr.* **33**, 463 (1992).

171. McLain, S. J.; Drysdale, N. E. *US 5028667* (1991).

172. McLain, S. J.; Drysdale, N. E. *US 5095098* (1992).

173. Ford, T. M.; McLain, S. J. *US 5208297* (1993).

174. Drysdale, N. E.; Ford, T. M.; McLain, S. J. *US 5235031* (1993).

175. Ford, T. M.; McLain, S. J. *US 5292859* (1994).

176. Stebels, W. M.; Ankone, M. J. K.; Dijkstra, P. J.; Feijan, J. *Macromolecules* **29**, 3332 (1996).

177. Stebels, W. M.; Ankone, M. J. K.; Dijkstra, P. J.; Feijan, J. *Polym. Prepr.* **37**, 190 (1996).

178. Dittrich, W.; Schulz, R. C. *Angew. Makromol. Chem.* **15**,109 (1971).

179. Kricheldorf, H. R.; Berl, M.; Scharnagl, N. *Macromolecules* **21**, 286 (1988).

180. Degee, P.; Dubois, P.; Jeroˆme, R.; Jacobsen, S.; Fritz, H.-G. *Macromol. Symp.* **144**, 289 (1999).

181. (a) Dege´e, P.; Dubois, P.; Jeroˆme, R. *Macromol. Symp.* **1997**, *123*, 67. (b) Dege´e, P.; Dubois, P.; Je´roˆme, R. *Macromol. Chem. Phys.* **1997**, *198*, 1973.

182. Bhaw-Luximon, A.; Jhurry, D.;Spassky, N.; Pensec, S.; Belleney, J. *Polymer* **42**, 9651 (2001).

183. Gutman, A. L.; Zuobi, K.; Bravdo, T. *J. Org. Chem.* **55**, 3546 (1990).

184. Hofle, G.; Steglich, W.; Vorbru¨ ggen, H. *Angew. Chem., Int. Ed. Engl.* **17**, 569 (1978).

185. a) Vedejs, E.; Bennett, N. S.; Conn, L. M.; Diver, S. T.; Gingras, M.; Lin, S.; Oliver, P. A.; Peterson, M. J. *J. Org. Chem.* **58**, 7286 (1993). (b) Vedejs, E.; Diver, S. T. *J. Am. Chem. Soc.* **115**, 3358 (1993).

186. (a) Grasa, G. A.; Kissling, R. M.; Nolan, S. P. *Org. Lett.* **4**, 3583 (2002). (b) Nyce, G. W.; Lamboy, J. A.; Connor, E. F.; Waymouth, R. M.; Hedrick, J. L. *Org. Lett.* **4**, 3587 (2002). (c) Grasa, G. A.; Gu¨ veli, T.; Singh, R.; Nolan, S. P. *J. Org. Chem.* **68**, 2812 (2003). (d) Singh, R.; Kissling, R. M.; Letellier, M.-A.; Nolan, S. P. *J. Org. Chem.* **69**, 209 (2004).

187. (a) Matsumura, S.; Mabuchi, K.; Toshima, K. *Macromol. RapidCommun.*, **18**, 477 (1997). (b) Matsumura, S.; Mabuchi, K.;Toshima, K. *Macromol. Symp.* **130**, 285 (1998). (c) Matsumura,S.; Tsukada, K.; Toshima, K. *Int. J. Biol. Macromol.* **25**,161 (1999).

188. Nederberg, F.; Connor, E. F.; Mo¨ller, M.; Glauser, T.; Hedrick, J. L. *Angew. Chem., Int. Ed.* **40**, 2712 (2001).

189. Myers, M.; Connor, E. F.; Glauser, T.; Mo¨ck, A.; Nyce, G.;Hedrick, J. L. *J. Polym. Sci., Part A: Polym. Chem.* **40**,844 (2002).

190. Connor, E. F.; Nyce, G. W.; Myers, M.; Mo¨ck, A.; Hedrick, J.L. *J. Am. Chem. Soc.* **124**, 914 (**2002).** (b) Nyce, G. W.; Glauser, T.; Connor, E. F.; Mo¨ck, A.; Waymouth, R. M.; Hedrick, J. L. *J. Am. Chem. Soc.* **125**, 3046 (2003).

191. Tsuji, H.; Ikada, H. *Polymer* **36**, 2709 (1995).

192. Tsuji, H.; Ikada, H. *J. Appl. Polym. Sci.* **58**, 1793 (1995).

193. Bruchu, S.; Prudhomme, R. E.; Barakat, I.; Jerome, R. *Macromolecules* **28**, 5230 (1995).

194. Okihara, T.; Tsuji, H.; Kawaguchi, A.; Katayama, K. *J. Macromol. Sci.-Phys.* **B30**, 119 (1991).

195. de' Santis, P.; Kovacs, P. J. *Biopolymers*. **6**, 229 (1968).

196. Hoogstein, W.; Postema, A. R.; Pennings, A. J.; ten Brinke, G. *Macromolecules* **23**, 634 (1990).

197. Thakur, K. A. M.; Kean, R. T.; Zupfer, J. M.; Buehler, N. U.; Doscotch, M. A.; Moonson, E. J. *Macromolecules* **29**, 8844 (1996).

198. Huang, J.; Lisowoski, M. S.; Runt, J.; Hall, E. S.; Kien, R. T.; Buehler, N.; Lin, J. S. *Macromolecules* **31**, 2593 (1998).

199. Kobayashi, J.; Asahi, T.; Ichiki, M.; Oikawa, A.; Suzuki, H.; Watanabe, T.; Fukada, E.; Shikinami, Y. *J. Appl. Phys.* **77**, 2957 (1995).

200. (a) Coates, G. W. *J. Chem. Soc., Dalton Trans.* **2002**, 467. (b) Nakano, K.; Kosaka, N.; Hiyama, T.; Nozaki, K. *Dalton Trans.* **2003**, 4039.

201. (a) Thakur, K. A. M.; Kean, R. T.; Hall, E. S.; Kolstad, J. J.; Lindgren, T. A.; Doscotch, M. A.; Siepmann, J. I.; Munson, E. J. *Macromolecules* **30**, 2422. (b) Thakur, K. A. M.; Kean, R. T.; Hall, E. S.; Kolstad, J. J.; Munson, E. J. *Macromolecules* **31**, 1487 (1998).

202. Kasperczyk, J. E. *Macromolecules* **28**, 3937 (1995).

203. Kasperczyk, J. E. *Polymer* **37**, 201 (1996).

204. (a) Thakur, K. A. M.; Kean, R. T.; Zell, M. T.; Padden, B. E.; Munson, E. J. *Chem. Commun.*, 1913 (1998). (b) Kasperczyk, J. E. *Polymer* **40**, 5455(1999). (c) Chisholm, M. H.; Iyer, S. S.;Matison, M. E.; McCollum, D. G.; Pagel, M. *Chem. Commun.* **37**, 2450 (1997).
205. Drumright, R. E.; Gruber, P. R.; Henton, D. E. *Adv. Mater.* **12,** 1841 (2000).
206. Kolstad, J. *J. Appl. Polym. Sci.* **62**, 1079 (1996).
207.Gruber, P. R.; Kolstad, J. J.; Witzke, D. R. *US 5539026* (1994).
208. Lunt, J. *Polym. Degrad. Stab.* **59**, 145 (1998).
209. Marigo, A.; Marega, C.; Zanneti, R.; Fichera, A. M. *Mater. Eng.* **9**, 215 (1998).
210. Kang, S.; Hsu, L. S. *Polym. Mater. Sci. Eng.* **82**, 367 (2000).
211. Jamshidi, K.; Hyon, S.-H.; Ikada, Y. *Polymer* **29**, 2229 (1988).
212. Perego, G.; Cella, G. D.; Bastioli, C. *J. Appl. Polym. Sci.* **59**, 37 (1996).
213. Dorgan, J. R.; Williams, J. S.; Lewis, D. N. *J. Rheol.* **43**, 1141 (1999)
214. Michaels, A. S. *Ind. Eng. Chem.* **57**, 32 (1965).
215. Ohrimenko, I. S.; Efremov, I. F.; Diakonova, E. B.; Miroshenko, G. V. *Vysokomol. Soedin.* **8**, 1707 (1966).
216. Panarin, E. F.; Sveltova, I. N. *Vysokomol. Soedin.* **15**, 522 (1973).
217. Dumas, P.; Spassky, N.; Sigwalt, P. *Makromol. Chem.* **156**, 55 (1972).
218. Matsubayashi, H.; Chatani, Y.; Tadokoro, H.; Dumas, P.; Spassky, N.; Sigwalt, P. *Macromolecules* **10**, 996 (1977).
219. Grenier, D.; Prudhomme, R. E. *J. Polym. Sci., Polym. Phys. Ed.* **22**, 577 (1984).
220. Ikada, Y.; Jamshidi, K.; Tsuji, H.; Hyon, S.-H. *Macromolecules* **20**, 904 (1987).
221. Tsuji, H.; Horii, F.; Hyon, S. H.; Ikada, Y. *Macromolecules* **24**, 2719 (1991).
222. Spinu, M.; Gardner, K. H. *Polym. Mater. Sci. Eng.* **71**, 19 (1994).
223. Radano, C. P.; Baker, G. L.; Smith, M. R. *J. Am. Chem. Soc.* **122**, 1552 (2000).
224. Fuji, Y.; Ohara, M. *JP 98201173* (1998).
225. Ohara, H.; Fuji, Y. *JP 98201174* (198).
226. Cho, J. H.; Chang, Y.; Noh, I.; Kim, C.; Soo, H.; Kim, Y. H. *Pollimo*. **21**, 879 (1997).
227. Park, S.; Chang, Y.; Cho, J. H.; Noh, I.; Kim, C; Kim, S. H.; Kim, Y. H. *Polymer* **22**, 1 (1998).

228. Reed, A. M.; Gliding, D. K. *Polymer* **22**, 494 (1981).

229. Cohn, D.; Younes, H.; Marom, G. *Polymer* **28**, 2018 (1987).

230. Shen, Z.; Zhu, J.; Ma, Z. *Makromol. Chem., rapid Commun.* **14**, 457 (1993).

231. Ferruti, P.; Penco, M.; D'Addato, P.; Ranucci, E.; Deghenghi, R. *Biomaterials* **16**, 1423 (1995).

232. Mooney, D. J.; Baldwin, D. F.; Suh, N. P.; Vacanti, J. P.; Langer, R. *Biomaterials* **17**, 1417 (1996).

233. Agrawal, C. M.; Huang, D.; Schmitz, J. P.; Athanasiou, K. A. *Tissue Eng.* **3**, 345 (1997).

234. King, E.; Cameron, R. E. *Polym. Int.* **45**, 313 (1998).

235. Farnia, S. M. F.; Mohammadi-Rovshandeh, J.; Sarbolouki, M. N. *J. Appl. Polym. Sci.* **73**, 633 (1999).

236. Penco, M.; Bignotti, F.; Sartore, L.; D'Antone, S.; D'Amore, A. *J. Appl. Polym. Sci.* **78**, 1721 (2000).

237. Kim, W. J.; Kim, J.-H.; Kim, S. H.; Kim, Y. H. *Polymer (Korea)* **24**, 431 (2000).

238. Lee, S.-Y.; Chin, I.-J.; Jung, J.-S. *Eur. Polym. J.* **35**, 2147 (1999).

239. Huh, K. M.; Bae, Y. H. *Polymer* **40**, 6147 (1999).

240. (a) Jeung, B.; Lee, D. S.; Shon, J.-I.; Bae, Y. H.; Kim, S. W. *J. Polym. Sci., Part A: Polym. Chem.* **37**, 751 (1999). (b) Choi, S. W.; Si, Y. C.; Jeong, B.; Kim, S. W.; Lee, D. S. *J. Polym. Sci,. Part A: Polym. Chem*. **37**, 2207 (1999).

241. Jeong, B.; Bae, Y. H.; Kim, S. W. *Macromolecules* **32**, 7064 (1999).

242. McGurk, S. L.; Sanders, G. H. W.; Davies, M. C.; Davis, S. S.; Illum, L.; Roberts, C. J.; Stolnik, S.; Tendler, S. J. B.; Williams, P. M. *Polym. J. (Tokyo)* **32**, 444 (2000).

243. Lee, S. Y; Kim, J.-H. *Polymer (Korea)* **24**, 638 (2000).

244. Babak, V. G.; Gref, R.; Dellacherie, E. *Mendeleev Commun.* **3**, 105 (1998).

245. Shah, S. S.; Zhu, K. J.; Pitt, C. G. *J. Biomater. Sci., Polym. Ed.* **5**, 421 (1994).

246. Wallach, J. A.; Huang, S. J. *Biomacromolecules* **1**, 174 (2000).

247. Sinclair, R. G. *US 4045418* (1977).

248. Sinclair, R. G. *US 4057537* (1977).

249. Wehrenberg, R. H. *ME* **9**, 63 (1981).

250. Vion, J. M.; Jerome, R.; Teyssie, P.; Aubin, M.; Prudhomme, R. E. *Macromolecules* **19**, 1828 (1986).
251. Kricheldorf, H. R.; Jonte, J. M.; Berl, M. *Makromol. Chem., Suppl.* **12**, 25 (1985).
252. Super, H.; Grijpma, D. W.; Pennings, A. J. *Polym. Bullet.* **32**, 509 (1994).
253. Shalaby, S. W.; Koelmel, D. F.; Arnold, S. *US 5082925* (1992).
254. Harkach, J.S.; Ou, J.; Lotan, N.; Langer, R. *Macromolecules* **28**, 4736 (1995).
255. Barrera, D. A.; Zylstra, E.; Lansbury, P. T.; Langer, R. *Macromolecules* **28**, 425 (1995).
256. Boury, F.; Olivier, E.; Proust, J. E.; Benoit, J. P. *J. Collid Interface Sci.* **160**, 1 (1993).
257. Reich, L.; Stivala, S. S. *Elements of Polymer Degradation*; McGraw- Hill: New York, (1971).
258. Cai, H.; Dave, V.; Gross, R. A.; McCarthy, S. P. *Annu. Tech. Conf. - Soc. Plast. Eng.* **2**, 2046 (1995).
259. Grijpma, D. W.; Nijenhuis, A. J.; Pennings, A. J. *Polymer* **31**, 2201 (1990).
260. Grijpma, D. W.; Pennings, A. J. *J. Macromol. Chem. Phys.* **195**, 1633 (1994).
261. Li, S. M.; Garreau, H.; Vert, M. *J. Mater. Sci. Mater. Med.* **1**, 131 (1990).
262. Cam, D.; Hyon, S.-H.; Ikada, Y. *Biomaterials* **16**, 833 (1995).
263. Hakkarainen, M.; Albertsson, A.-C.; Karlsson, S. *Polym. Degrad. Stab.* **52**, 283 (1996).
264. Albertsson, A.-C.; Lofgren, A. *J. Appl. Polym. Sci.* **52**, 1327 (1994).
265. Hyon, S.-H.; Jamshidi, K.; Ikada, Y. *Polym. Int.* **46**, 196 (1998).
266. Zhang, S.; Wyss, U. P.; Pichora, D.; Goosen, M. F. A. *J. Bioactive Compat. Polym.* **9**, 80 (1994).
267. Sodergard, A.; Selin, J. F.; Nassman, J. H. *Polym. Degrad. Stab.* **51**, 351 (1996).
268. (a) Li, S. M.; Garreau, H.; Vert, M. *J. Mater. Sci. Mater. Med.* **1**, 123 (1990). (b) Li, S. M.; Garreau, H.; Vert, M. *J. Mater. Sci. Mater. Med.* **1**, 198 (1990). (c) Grizzi, I.; Garreau, H.; Li, S. M.; Vert, M. *Biomaterials* **16**, 305 (1995).
269. (a) Torres, A.; Li, S. M.; Roussos, S.; Vert, M. *J. Appl. Polym. Sci.* **62**, 2295 (1996). (b) Torres, A.; Li, S. M.; Roussos, S.; Vert, M. *J. Environ. Polym. degrad.*

4, 213 (1996). (c) Pranamuda, H.; Tokiwa, Y.; Tanaka, H. *Appl. Environ. Microbiol.* **63**, 1637 (1997). (d) MacDonald, R. T.; McCarthy, S. P.; Gross, R. A. *Macromolecules* **29**, 7356 (1996).

270. Williams, D. F. *Eng. Med.* **10**, 5 (1981).
271. Cai, H.; Dave, V.; Gross, R. A.; McCarthy, S. P. *J. Polym. Sci., Part B: Polym. Phys.* **34**, 2701 (1996).
272. Hakkarainen, M.; Karlsson, S.; Albertsson, A.-C. *J. Appl. Polym. Sci.* **76**, 228 (2000).
273. Shin, C. *J. Controlled Release*. **34**, 9 (1995).
274. Kimura, K.; uno, K.; Aoyama, T.; Ito, T.; Juchi, M.; Hotsuta, S, *JP 07316273* (1995).
275. Jamshidi, K.; Hyon, S.-H.; Ikada, Y. *Polymer* **29**, 2229 (1988).
276. Kopinke, F.-D.; Remmler, M.; Mackenzie, K.; Moeder, M.; Wachsen, O. *Polym. Degrad. Stab.* **53**, 329, (1996).
277. Gupta, M. C.; Deshmukh, V. G. *Colloid Polym. Sci.* **260**, 514 (1982).
278. Garozzo, D.; Montaudo, G; Giuffrida, M. *Polym. Degrad. Stab.* **15**, 143 (1986).

———

Table: Synthesis of Aliphatic Poly (ester) s, Summery of Patent literature

Patent no	C.A.N	Substrate	Product	Key process	Highlights
Dehydropolycondensation					
KR 022160 A	142:135164	Lactic Acid	Poly (lactic acid)	Polycondensation of L-lactic acid in presence of Sn and $SnCl_2$, and the protic acid was p-toluenesulfonic acid.	The method prepares a high molecular weight poly (L-lactic acid) by direct melt polycondensation of L-lactic acid in the absence of a solvent. The oligomers (L-lactic acid) was synthesized in the absence of a catalyst; direct melt polycondensation in presence of the Sn compound like $SnCl_2$ and the protic acid is p-toluenesulfonic acid.
KR 190230 B1	142:38725	Lactic Acid	Poly (lactic acid)	Polycondensation followed by ring opening polymerization.	The condensation of lactic acid, the obtained lactic acid oligomer of a molecular weight wt. >3000, preferably >5000, was dissolved in chloroform or methylene chloride and subjected to be impregnated in methanol, or was purified by iso-propyl ether to remove sufficiently unreacted lactic acid and water so that the uncreated lactic acid does not exceed 0.5%, then, the resultant lactic acid oligomer was again used for polycondensation.

JP 22163	139:7666	Lactic Acid	Poly (Lactic acid)	Synthesis of Poly (hydroxy carboxylic acids) by polycondensation, polymers with Mw 20,000.	The 90% aqueous L-lactic acid solution was dehydrated with Sn, evacuated at 150 ^{0}C while removing condensed H_2O, and heated to 200° to give a molten poly(lactic acid) with Mw 30,000, which was absorbed with N_2 and polycondensed at 200 ^{0}C for 13 hr to show Mw 190,000 and dilactic acid content 0.02%?
JP 335850 A2	139:381922	Lactic Acid	Poly (lactic acid)	Synthesis of poly (lactic acid) from lactic acid (by passing lactide) by polycondensation of lactic acid in the presence of metal catalysts.	Polycondensation of lactic acid was carried out in the presence of metal catalysts under high temperature. and reduced pressure conditions.
JP 224392 A2	135:179808	D,L-lactic acid	Poly(lactic acid)	Dehydropolycondensation with enzyme catalysis.	Poly(lactic acid) was manufactured. by reacting lactic acid with hydrolases. DL-lactic acid was treated with Pseudomonas cepacia lipase at 130 ^{0}C for 4 days to give poly (lactic acid).
JP 213949 A2	135:137866	Lactic acid	High-molecular-weight Poly (lactic acid)	Reactor design for lactic acid dehydropolycondensation.	The polymer was manufactured. by feeding a solution containing lactic acid monomer, corn starch, and monobutyltin oxide and stirring the soln. at 160-220 ^{0}C under 0.01-9 kPa in the absence of solvents. Byproduct lactide and other low-mol.-wt oligomers were refluxed with the cylinder at 30-80 ^{0}C under 0.01-9 kPa,

					while byproduct H_2O is discharged to atm. Poly(lactic acid) with
JP 031746 A2	134:131985	Lactic acid	High-molecular-weight poly(lactic acid)	Reactor design for lactic acid dehydropolycondensation.	The height of the gas-liq. countercurrent phase was formed between the tower and the reactor was regulated by the flow rate so that evaporation of water and reflux of lactide were appropriately performed for polycondensation of lactic acid.
JP 297145 A2	133:296893	Lactic acid	Oligomer of PLA	Poly(hydroxycarboxylic acids) (Mw 2000-20,000) were prepared by dehydration polycondensation.	Dehydration polycondensation the oligomers of PLA at 50-140 ^{0}C, resulted oligomers (Mw 750-5000) at 130-170 ^{0}C. Thus, L-lactic acid (D-form content 0.40%) was heated in the presence of Sn at 120 ^{0}C under 10 mmHg for 3 h and then at 160 ^{0}C for 10 h to give poly(lactic acid) (D-form content 0.65%, Mw 13,000) in 95% yield.
JP 273164 A2	133:252906	Lactic acid	Poly(hydroxy-carboxylic acid)	Dehydro-polycondensation of L-lactic acid with instrumentation to recycle the vaporized lactide back to the reaction.	Lactic acid was polymd. in the presence of Sn powder at 160 ^{0}C and 30 mmHg for 10 h in o-dichlorobenzene with removing H_2O and recycling the dimer and the solvent to give PLA with Mw 10,000 containing <300 ppm residual solvent.

JP 204144 A2	133:105501	Lactic acid	Poly(lactic acid)	Dehydro-polycondensation of L-lactic acid with instrumentation to recycle the vaporized lactide back to the reaction.	Polycondensation of lactic acid under reduced pressure with removal of water, wherein produced lactide was refluxed with water with reflux appropriate and flow rate of gaseous lactide in the reflux app. is adjusted by detecting height of gas-liquid countercurrent contact layer.
CN1208740A1	132:335039	Lactic acid	Poly(lactic acid)	By heating lactic acid in the presence of 0.02-0.2 mol% catalysts contg. monobutyltin trioxide (sic) or dialkyltin oxides at 150-220 ^{0}C.	Diethyltin oxide, dipropyltin oxide, dibutyltin oxide, dipentyltin oxide, dihexyltin oxide, diheptyltin oxide, dioctyltin oxide, dinonyltin oxide, didecyltin oxide, diundecyltin oxide, didodecyltin oxide and ditetradecyltin oxide were used for preparation of poly (lactic acid)
JP11255877A2	131:229188	Lactide	Poly (lactic acid)	Dehydro-polycondensation of L-lactic acid with instrumentation to recycle the vaporized lactide back to the reaction.	The method improves polymn. efficiency. Thus, poly (lactic acid) with wt.-av. mol. wt. 145,000 was manufactured in 20 h with 98% yield.

JP09165441A2	127:66320	L-lactic acid	Poly (lactic acid)	One-pot preparation of biodegradable poly (hydroxy-carboxylic acids) by using water-stable distannoxane catalysts and silane couplers.	L-lactic acid was mixed with 1,3-dichloro-1,1,3,3-tetrabutyl-distannoxane in a glass tube oven, the inner pressure reduced to 1 mmHg to remove H_2O, and the mixture was treated at 190 ^{0}C for 20 h to give poly (L-lactic acid) with Mw 22,000, which was treated with $Si(OBu)_4$ at 150 ^{0}C for 8 h to show mol. wt. 30,000.
JP09031182 A2	126:238819	L-lactic acid	Poly (lactic acid)	Dehydro-polycondensation using distannoxane catalyst.	100 mmol I was polymerized at 200 ^{0}C for 20 h in the presence of 0.01 mmol 1,3-dichloro1,1,3,3tetrabutyldistannoxaneto to give a polymer with Mw 12,000.
WO9528432A1	124:57097	L-lacctic acid	Poly (lactic acid)	Dehydropolycondensation using synthetic alumino silicate.	Poly (L-lactic acid) with wt.-av. mol. wt. 98,000 was prepd. by heating 150 g a 90% aqueous solution of L-lactic acid at 120 ^{0}C for 5 h while stirring under vacuum, adding 2.1 g a synthetic Al silicate contg. 17 % Al oxide, heating to 220 ^{0}C evacuating to 20 mm-Hg over 30 min, and mixing for 30 min at 220 ^{0}C

JP07173264A2	123:341384	Methyl lactate	Poly (lactic acid)	Dehydro-polycondensation in presence of Sn powder catalyst.	Heating 37.4 g Me lactate with 0.125 g Sn at 140-160 ^{0}C for 12 h with distn. of MeOH and further treatment with 53.9 g Ph_2O at 165 ^{0}C for 3 h in a vessel equipped with Dean-Stark trap and with a mol. sieve in a reflux condenser at 160 ^{0}C/20 mm for 36 h gave a polyester with Mw 61,000.
JP07173265A2	123:314950	L-lactic acid	Poly (lactic acid)	Dehydro-polycondensation with Sn powder catalyst, with solubilization of Sn in lactic acid and removal of insoluble Sn prior to condensation.	0.5 g Sn was dissolved in 100 g 90% L-lactic acid at 80° for 3 h under N_2 and then insoluble Sn was removed by filtration to obtain a solution containing 3000 ppm Sn. It (36.0 g) was treated in 75.6 g Ph_2O at 130-140 ^{0}C under reduced pressure in a vessel equipped with Dean Stark trap, and then with mol. sieve in a reflux condenser at 130 ^{0}C/15 mmHg for 20 h to give 83% poly (lactic acid) with Mw 200,000.
JP07102053A2	123:257882	Poly(lactic acid)with more than 500 ppm Sn	Poly (lactic acid) with less than 5 ppm Sn	Removal of Sn catalyst from poly (lactic acid) synthesized by dehydro polycondensation by contacting with mineral acid.	Thus, poly (L-lactic acid) with logarithmic viscosity 1.50 dL/g containing 560 ppm Sn (catalyst) was stirred with 0.5 N HCl/EtOH at 35 ^{0}C to give polymer with 4 ppm Sn, which showed 5% wt. loss temp. 320 ^{0}C and retention of tensile strength (as film) ^{3}95% after 400-h weathering test.

JP 06306149 A2	122:214894	L-lactic acid	Poly (lactic acid)	Melt dehydro-polycondensation using membrane type evaporator for removal of by product, $SnCl_2$ catalyst.	Thus, 100 parts 90% L-lactic acid was stirred at 130 ^{0}C/50 mm for 3 h with removal of H_2O and then stirred with 0.8 part $SnCl_2$ at 130 ^{0}C/15 mm for 5 h to obtain medium-mol. wt. poly-L-lactic acid (I; wt.-av. mol. wt. (Mw) ~40,000), which was heated to 100 ^{0}C and passed through a membrane-type evaporator at 170 ^{0}C/15 mm and 30 min retention with H_2O separation to obtain PLA (Mw 150,000).
JP 06298913 A2	122:161781	L-lactic acid	Poly (lactic acid)	Dehydro-polycondensation in an azeotroping solvent, with reactor design to recycle the solvent after drying to reaction, Sn powder catalyst.	90% L-lactic acid (I) 112.5, powd. Sn 0.405, and di-Ph ether (II) 236 kg were stirred at 130 ^{0}C and 160-130 mmHg for 6 h to remove H_2O, I was oligomerized at 140 ^{0}C and 110-100 mmHg for 25 h then polycondensed at 130 ^{0}C and 20-15 mm Hg for 30 h to obtain a ~25% solution of poly (L-lactic acid) (av. mol. wt. 126,000) in II, wherein II was recovered by cooling the distg. azeotropic mixture containing H_2O, dried through a mol. sieve-filled tower, vaporized through a heat exchanger, and returned into the reaction system.

JP 93-89676	122:161782	L-lactic acid	Poly (lactic acid)	Melt dehydro-polycondensation with reactor design for high viscosity, $SnCl_2$ catalyst.	100 parts 90% L-lactic acid was stirred at 130 ^{0}C and 50 mmHg for 3 h with removal of H_2O and then stirred with 0.8 part stannous chloride at 130 ^{0}C and 15 mmHg for 5 h to obtain poly (L-lactic acid) [I; wt.-av. mol. wt. (Mw) ~40,000], which was heated to 100 ^{0}C and fed into a twin horizontal high-viscosity reactor at 170 ^{0}C and 15 mmHg at 60 min retention time while removing H_2O to obtain white powder I (Mw 280,000).
JP 06279577 A2	122:134232	L-lactic acid	Poly (lactic acid)	Dehydro-polycondensation in azeotroping solvent in presence of acetaldehyde, Sn powder catalyst.	L-lactic acid contg. 0.05 mol % AcO in Ph_2O in the presence of Sn and mol. sieve 3A^0 at 130 ^{0}C /15 mm gave 96.1% poly (lactic acid) with specific viscosity 1.18.
US 5357034 A1	122:11005	Lactic acid	High molecular weight poly(lactic acid)	Depolymerization of poly (lactic acid) prepolymer into lactide followed by purification by means of melt crystallization and ROP of lactide in melt condition or in solution.	Process for poly (lactic acid) preparation and avoids problems associated with equilibrium between lactic acid, low and high molecular weight PLA, lactide and water.

JP 1638	120:9195	L-lactic acid	Poly (lactic acid)	Dehydro-polycondensation in an azeotroping solvent, Sn powder catalyst.	A mixture of 40.2 g 90% L-lactic acid and 0.5 g Sn in 85 mL anisole was heated at 154 ^{0}C for 2 h with removal of water by azeotropic distillation then further heated at 154 ^{0}C for 45 h with removal of water by azeotropic distn., while the distillate was passed through a 40-g Mol. Sieve 3A^0 tube to remove water to residual water content 1 ppm and returned to the reaction mixture The reaction mixture was then concd., taken up in 300 mL methylene chloride, filtered, and washed with MeOH to give 24.4 g polymer with inherent viscosity 0.84 and mol. wt. 100,000.
CN 1070905 A 14	120:173470	Shellac	Aleuritic acid	Soponification of shellac	The aleuritic acid (I) was prepared with high yield from shellac by saponification with NaOH; salting out with NaCl; acidification with H_2SO_4; washing, decoloration, and purifn. with EtOH and activated Char coal. The I was high in purity, and the method is low in cost.

IN 157851 A 5	106:20293	9, 10,16-Trihydroxypalmitic acid.	9, 10,16-Trihydroxypalmitic acid.	The title compound (I) is manufactured from raw shellac in 2.5-5% yield	Treating the shellac with aq. $Ca(OH)_2$ at 90-100°, filtering the reaction mixt., and acidifying and air-blowing the filtrate, to ppt. crude I. Crude I was dissolved in 5N NaOH at 80-95 ^{0}C, and the resulting alk. slurry kept two days, until I Na salt ppts. The Na salt is squeezed at high pressure, to remove liq. contaminants, and I regenerated from aq. soln. by repptn. with HCl or H_2SO_4

Patent no	CAN	Substrate	Product	Key process	Highlights
Lactide formation and ring opening polymerization					
US 246108	145:478002	L, Lactic acid, D, Lactic acid	Lactide	Depolymerization of oligomer gives lactide ratio which consists of a 25/25/50 blend of L-lactide, D-lactide, and meso-D,L-lactide.	L-lactic acid 125 g, D-lactic acid 125 g, and zinc oxide 5 g was added to 3-necked 500 mL flask, equipped with argon purge, vacuum line, short-path distillation head, and mech. stirrer. A vacuum of 100 mm Hg was applied, and the solution was heated with stirring at 140 ^{0}C for about 8 h. The pressure was lowered to 2 mm Hg, and

					the solution temperature rose to about 210 °C to distill off the lactide formed by depolymerization which consists of a 25/25/.50.
FI 105185 B1	142:336769	Lactide	Poly (Lactide)	Zinc stearate, titanium (IV) butylate, and/or metallic iron powder used as catalyst for lactide production.	A procedure as described above, characterized by the catalyst content in the reaction mixture being 5 -0.0001 wt.%, preferably 0.5 - 0.001 wt.%. A procedure as described above, characterized by the lactic acid being dried before use, at a pressure of 500 - 10 mbar and at a temp. of 50 - 200 °C, preferably 90 - 120 °C. A procedure as described above, characterized by the lactic acid being pre-polymerized before the oligomerization.
U.S. 5,247,073	136:20374	Lactic acid and ester of Lactic acid	Lactide	Lactide polymer was prepared from a purified lactide mixt. of 80% L- and 20% D,L-lactide.	Poly lactic acid, preferably in the presence of a catalyst means in the case of the ester of lactic acid, to form a condensation reaction by product and poly lactic acid, and depolymerizing the poly lactic acid in a lactide reactor to form crude lactide, followed by subsequent purification of the crude lactide in a distillation system. Thus, lactide polymer was prepared from a purified lactide mixture of 80% L- and 20% D, L-lactide in THF in presence of tin(II) 2-ethylhexanoate catalyst wherein the mol. wt. of the polymer was controlled by impurity level and

					was independent of temperature or catalyst concentration.
JP 11035663 A2	130:168818	L-lactide or D-lactide	Racemized lactic acid-based polyesters.	ROP of L-lactide or D-lactide (and optional other monomers) in the presence of (A) polymerization catalysts and (B) 0.005-0.2 mol% alkali metal compds. and/ alk. earth metal compds. as racemizing agents	10.0 g L-lactide was polymerized in the presence of 3 mg Sn octylate and 24 mg Ca acetylacetonate under N at 190 ^{0}C for 2 h to give poly (lactic acid) having |L - D| = 78%, hsp/C = 0.446 dL/g, and av. mol.-wt. 42,000.
JP 10120772 A2	129:5010	Lactide	Poly lactic acid.	ROP of lactide with total catalyst content per the monomers is controlled in £50 ppm and (ii) the catalysts are intermittently or continuously added in reactors little by little while making the stirring power higher in stages or continuously as the thickness of the reaction liquids increases.	Thus, PLA with av. mol. wt 235,000 was prepared by ring-opening polymn. of 10-kg/h lactide at 180-200 ^{0}C in the presence of 0.1 g/h (10 ppm) Sn octylate by using 3 polymerization reactors and an extruder. The resulting poly (lactic acid) had catalyst content £50 ppm.

FR 2745005 A1	127:331916	Lactide	Poly (lactide)	Heating DL-lactide with Zn lactate (ratio 1800:1) at 150° for 96 h gave a 96.7% conversion to polylactide having no.-av. mol. wt. 100,000 and polydispersity 1.5.	The title catalysts have the formula AnMBm(H_2O)p [M = metal having free p, d, or f orbitals; A = -OCOZOH (Z = C1-18 alkyl group); B = hydroxyl acid or OR (R = H, alkyl, cycloalkyl, aryl); n + m + p £ valence of M]. Heating D, L-lactide with Zn lactate (ratio 1800:1) at 150 ^{0}C for 96 h gave a 96.7% conversion to poly (lactide) having no.-av. mol. wt. 100,000 and polydispersity 1.5.
JP 08311176 A2	126:118359	Lactide	Poly lactic acid.	ROP of lactide.	1.0 g L-lactide (optical purity 99.0%) was polymd. at 140 ^{0}C for 1 h and crystallized at 120 ^{0}C for 9 h in the presence of Sn octylate to give 98% poly(lactic acid) having wt.-av. mol. wt. 149,000.
JP 08259676 A2	126:31856	Lactide	Poly lactic acid.	ROP of lactide with special reactor design.	L-Lactide was polymerized as above to give a polymer with low residual monomer content.
JP 08193127 A2	125:222817	Lactide	Lactic acid-based polymers.	ROP of lactides in the presence of catalysts comprising (A) thermal condensates of Al alkoxides, Si halides, and phosphate esters. (B) C 1-4 tri alkyl aluminium and/or dialkyl aluminium	5 g 30% L-lactide CH_2CL_2 solution was treated at 60 ^{0}C for 8 days in a sealed ample in the presence of 38 mg 3%-$AlEt_3$ solution in hexane and 38 mg. Condensate obtained from Al is appropriates $SiCl_4$ and Ba_3PO_4 to give a polymer with sp viscosity 0.42 dl/g

				chloride with the ratio of Al in B based on that in A 0.02-0.35.	
JP 07053684 A2	123:170656	L-lactide	Poly (lactic acid)	ROP of lactide with instrumentation for continuous feed of substrate and continuous removal of the polymer.	Thus, 120 g/min cyclic dimer of lactic acid and 0.036 g/min a 3% Sn octoate (PhMe solution) were continuously supplied with stirring under N_2 in autoclave at 200° and 20 min (av.) retention time with taking out the product [melt viscosity 250 P, reduced viscosity (h) 0.78] at a rate of 120 g/min from the bottom of the autoclave into a twin-kneader and polymerizing the product at 20 min (av.) retention time to obtain PLA (100% recovery).

Patent no	CAN	Substrate	Product	Key process	Highlights
Copolymers prepared by dehydropolycondensation and ring opening polymerization					
JP 34793	147:301923	Lactic acid and poly ethylene	Copolymer	Lactic acid polymer-polyether glycol blocks copolymers, showing good Compatibility.	Poly ethylene glycol was polymerized with D-lactide and L-lactide in the presence of tin octanoate at 160 ^{0}C for 3 h, mixed

		gylycol			with H_3PO_4 crystals, and further polymerized to give a plasticizer, showing good Compatibility with D-lactic acid homopolymer.
EP 778306 A2	127:82591	Aliphatic polyester, especially poly (lactic acid)	Poly(lactic acid)-co-polycarbonate block copolyester	Transesterification between polyester and polycarbonate polymers.	The copolymer was prepared reacting an inert atmosphere, polycarbonate with aliphatic polyester in the presence of a catalyst. The copolymer films had better degradability than aromatic. Polycarbonate, transparency equal to polycarbonate, better thermal resistance than aliphatic polyester, and melt flowability superior to aromatic polycarbonates.
EP 796881A1	127:278615	Lactide	Poly lactic acid	Heating a lactide, a cyclic imide compound e.g. succinimide, and a polymerization catalyst, e.g. Sn octylate at 100-190 ^{0}C with stirring under N_2 flow.	The cyclic imide compound is (1-35 mol. %) based on the lactide was taken. The amount of the polymerization catalyst was small, e.g. 0.00001-0.1 mol.%, based on the lactide, poly(l-lactic acid) could be efficiently prepared. It was possible to avoid remains of the catalyst in the polymer and coloring of the polymer.
EP 96-114321	126:268544	Lactide	Triblock copolymer	Sequential ROP of dimeric lactones of lactic acid and glycolic acid and of ε-caprolactone.	Bioabsorbable, ternary block copolymer consisting of (A) poly lactic acid segment, (B) poly (ε-caprolactone) segment and (C) poly glycolide segment, useful for biomedical.

JP 09031179 A2	126:238836	Lactide	Lactic acid-based polyester-polyether resins	ROP of lactide with a polyether macro-initiator.	A linear ethylene oxide-propylene oxide block copolymer (wt.-av. mol. wt. 4050) 20, L-lactide 76, and D-lactide 4 g were polymerized to give a polymer with no.-av. mol. wt. 25,000, wt.-av. mol. wt. 35,000, Tg 53 ^{0}C m.p. 153 ^{0}C, and tensile strength 290 kg/cm^{2}.
EP 712880 A2	125:88094	Poly(lactic acid)+ poly(butylene succinate)	Degradable block copolyester	Copolymerization by mutual transesterification.	Poly lactic acid and poly(butylenes succinate) were refluxed together in a solvent with b.p. higher than 180 ^{0}C and with capacity of water removal by azeotroping (ethers, alkylaryl ethers, and di-Ph ether), using metals of group II, III, IV, and V and oxides or salts thereof as catalysts, singly or as a mixture, to give co-polymer with high transparency in addition to strength and elongation as well as very good heat resistance.

Patent no	CAN	Substrate	Product	Key process	Highlights
Nanocomposite and grafting of polymers on the carbon nanotube					
US 276077 A1	148:12260	CNT, Polymer	Polymer nanocomposite	The materials implies improved mechanical properties of both clay and carbon nanotube (CNT)-reinforced polymer matrix nanocomposites.	The nanocomposites were obtained by mainly treating Nan particles and polymer pellets prior to a melt compounding process. The nanoparticles are coated onto the surface of the polymer pellets by a ball-milling process The nanoparticles thin film was formed onto the surface of the polymer pellets after the mixture was ground for a certain time
JP 162497	148:102776	CNT, Polymer	polymer nanocomposites	Polyurethane or cellulose fiber CNT nanocomposites.	The material were polyurethane, cellulose fiber, or latex Particles/plastics. The specified dispersant such as N,N-bis(3-D-gluconamido-propyl)-CNT-amide gave nanocarbon evenly dispersed in the polymer materials
KR 071960 A	148:169824	CNT, Polymer	polymer nanocomposites	Poly (1-butene) CNT nanocomposites.	The polymer poly (1-butene); and the carbon nanotube (about 0.1-10 wt%) was a multi-walled carbon nanotube or a single-walled carbon nanotubes were mixed. The method comprises the steps of treating a carbon nanotube by ultrasonication in an apolar organic

					solvent; and mixing it with the polymer dissolved in an apolar solvent. Preferably the apolar organic solvent was toluene
US 600389P	146:275122	CNT, Polymer	Polymer nanocomposites	Coating of PET, glass and fluoropolymer on CNT.	A fluoropolymer containing. binder, which was a solution of one fluoropolymer or a blend of fluoropolymers, which may be formulated with additives, was applied onto a carbon nanotube-based transparent conductive coating at nanometer level of thickness on a clear substrate such as PET and glass. The fluoropolymers or blend could be either semi-crystalline. (with low level of crystallinity) or amorphous, preferably to be amorphous with low refraction index.
JP 070593 A	146:339159	CNT, Polymer	Polymer nanocomposites	Polymer nanocomposites shows tensile strength 1440 MPa, flexural modulus 77.2 GPa,	A epoxy resin 100, dicyandiamide 4.5, and imidazole 0.5 part into films, and thermally laminating the fiber body with the films gave a preparing showing tensile strength 1440 MPa, flexural modulus 77.2 GPa, and compressive strength 635 MPa, and uniform dispersion of CNT among the fibers in the cross-section (electron microscope).

WO 116547 A1	145:455661	CNT, Polymer	CNT/polymer composites.	Grafting of polymer by free radical polymerization.	The interfacial covalent bonding was provided by a free radical reaction initiated during processing. This free radical initiation could be provided by benzoyl peroxide.
WO 085130A2	143:250571	Functionalized CNTs, polymer-matrix	Polymer on CNT nanocomposites	Single walled and multi walled CNT / polymer matrix.	The carbon source could be CO, methane, ethane, propane, acetylene, ethylene, benzene, toluene, o-xylene, p-xylene,1,2,4-trimethylbenzene, 1,2,3-trimethylbenzene, $C_{15}H_{32}$, $C_{16}H_{34}$, $C_{17}H_{36}$,$C_{18}H_{38}$, methanol, ethanol, propanol, butanol, pentanol, hexanol,heptanol, octanol, acetone, Me Et ketone, formic acid or acetic acid. The application includes at least one CNT reactor allowing continuous or batch production of CNT's, doped CNT's, or composites. The method could be used in manufacturing fuel cell or battery electrodes, heat sinks, heat spreaders, or metal-matrix composites or polymer-matrix composites in a printed circuit or electron emitter in a field emission display.

JP 151867	139:396532	CNT, nylon 6-poly butylene terephthalat e blend	Polymer nanocoposite	Nylon 6 polybutylene terephthalate nanocomposites.	The composite contain 0.01-10% fibrous carbon (diam. £1 mm) dispersed in 2 thermoplastic resins (e.g., nylon 6-polybutylene terephthalate blend). The fibrous carbon was selected from vapor phase grown carbon fibers (VGCF) or multilayer carbon nanotubes (CNT) such as multi-walled carbon nanotubes (MWNT).

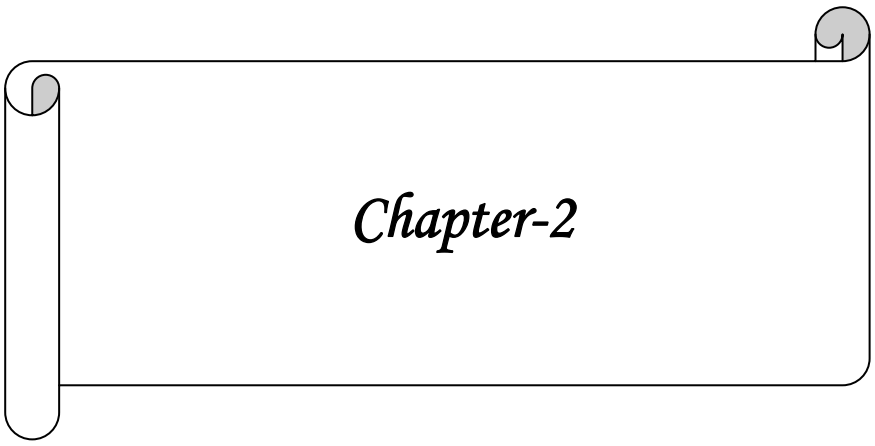
Chapter-2

CHAPTER – 2: SCOPE AND OBJECTIVE OF THE PRESENT WORK

2.1. Objectives of the present thesis:

The present investigation concerns dehydropolycondensation followed by post polymerization of L-lactic acid into a final poly (L-lactic acid) s polymer (PLA). Considerable amount of research work has been carried out in the field of dehydropolycondensation. They focus on molecular weight, yield, and racemization and lactide formation using various catalysts **[1-4]**. The removal of byproduct water has been realized because of equilibrium between free acid, water and polymers cause difficulty in removing water as by product **[5]**. A modified direct dehydropolycondensation has been attempted in presence of various catalysts and molecular sieve ($3A^0$) as desiccating agent **[6]**. The result deals with marginal enhancement of molecular weight slow ever, a depth of study dehydropolycondensation in presence of various catalysts, solvents (polar and nonpolar) and influence of desiccating agent (various type of zeolites) has generally been lacking. The end group and sequence analysis have also been lacking. For any successful post polymerization of lactic acid oligomers, existence of appropriate end groups is a key requirement. The end groups change because of side reaction, for example cyclization, or dehydration of the hydroxyl terminal giving rise to olefinic double bonds. The trace amount of impurities in the monomer which can derivatize the end groups and consequently stop further condensation. These possibilities have not so far studied thoroughly.

Aleuritic acid (9, 10, 16-trihydroxy palmitic acid) has been obtained from renewable recourses (Lac) by hydrolysis **[7]**. Few literature reports are available so far regarding polymerization of aleuritic acid. Haque, M.et. al **[8]**, obtained insoluble and infusible materials, which has been formed due to cross linking reaction of several functional groups. Polymerization of isopropyl aleuriteate using Novozym 435 was feasible and resultant polymer with moderate molecular weight ($\bar{M}_n$ 5.6 kg/mol, PDI 3.2) was isolated in moderate yield (43%) **[9]**. The poly (aleuritic acid) by chemical synthetic method, characterization and application have been lacking. An aggregation behavior study of polystyrene polypropylene imine dendrimer having hydrophilic and hydrophobic

groups has been observed **[10]**. The aggregation behavior in poly (aleuritic acid) has also been lacking.

Much effort has been carried out at fabrication of carbon nanotube (CNT) s/ polymer composite and the characterization of their physical properties. The nanocomposite of CNT/biocompatible polymers has been attracted much attention because of their potential biomedical application. The enhancement of mechanical, thermal and electrical properties has been observed by several authors **[11, 12]**. The biocompatibility evaluation results of PLA/MWCNTs composite have shown that the presence of MWCNTs in composite inhibits the growth of the fibroblast cells **[13]**. Extensive research has been carried out in the fields of surface modification of CNT to enhance their chemical compatibility and dissolution properties. The esterification and amidation reaction on the surface of CNT have been accomplished by the 'grafting to' technique **[14]**. Grafting of L-lactic acid, L-lactic acid oligomers and L-lactic acid-12-hydroxy stearic acid copolymer on the surface of MWCNTs using dehydropolycondensation technique have also not been studied.

Ring opening polymerization of lactides using several zinc catalysts have been carried out **[15-17]**, they have dealt with control molecular weight and molecular weight distribution and stereochemistry of the polymer using various types of organo zinc (changing ligands), however these catalysts are not FDA approved. Zinc prolinate has been used for ROP of lactide (Kricheldorf et al) **[18]**, and it is FDA approved catalyst. The detailed study of PLA homopolymer and copolymer of lactide-ε-caprolactone by using ROP technique zinc prolinate as a catalyst have not been studied in details.

2.2. Approaches:

2.2.1a. Synthesis of L-lactic acid oligomers and sequence determination by ^{13}C quantitative NMR: L-lactic acid oligomers would be synthesized by dehydro-polycondensation using Lewis acid catalysts, their carboxylic end groups would be determined. The validity of the NMR technique for determination of carboxylic acid end groups would be established by preparing model L-lactic acid oligomers having known number average molecular weight through controlled ring opening polymerization of L-lactide. The existence of carboxylic acid and hydroxyl end groups as such would also be

checked using MALDI-ToF, which would also show derivatization, if any, of the end groups due to either side reactions or impurities.

2.2.1b. *Post polycondensation of poly (L-lactic acid) oligomers by dehydropolycondensation in presence of various zeolites (ZSM-5, ZSM-12, β-zeolite) and Lewis acid catalysts:* Zeolites having various pore sizes would be selected, which would be inert in the dehydropolycondensation system. Dehydropolycondensation reaction would be performed in presence of various Lewis acid catalysts. The effect of various solvents (polar and nonpolar), reaction time and reaction temperature would be studied. The sequence analysis of the resultant PLA could be carried out by using quantitative ^{13}C NMR analysis.

2.2.2. Synthesis of new homopolyester and copolyester materials: Aleuritic acid was chosen as the monomer and could be polycondensed, in order to synthesize a homopolymer. The homopolymer (PAA) protected at 9, 10 position would be used as a modifier for rheological properties. The deprotected homopolymer (deprotection at 9, 10 positions) would be prepared and their aggregation behavior will be studied as micelle in various solvents (polar and non-polar).

Aleuritic acid was also chosen as the co-monomer and would be co-polycondensed with L-lactic acid in order to synthesize copolyester of lactic acid having long aliphatic aleuritic moieties at various places of the backbone. At the same time each repeating unit due to the co-monomer would contribute 9, 10 carbons having protected pendent groups that were expected to internally plasticize the resultant polyester. The resultant copolyester after deprotection at 9, 10 positions, and the hydroxyl pendent groups were expected to form aggregation that was expected to increase the T_g of the copolyester.

2.2.3. Detailed study of grafting of L-lactic acid, L-lactic acid oligomers and copolymer of L-lactic acid and 12-hydroxy stearic acid on the surface of MWCNTs by" grafting to" technique: MWCNTs was chosen as the grafting surface, because MWCNTs can be oxidized by strong acid to produce carboxylic functional groups on its surface. The grafting reaction would be carried out by using" grafting to" technique. The mechanical properties, thermal stability and electrical properties would be studied in case of grafted L-lactic acid, L-lactic acid oligomers and copolymer of L-lactic acid-12-hydroxy stearic

acid. An additional property for example internal plasticization would be expected along with mechanical, thermal and electrical properties.

2.2.4. Ring opening polymerization (ROP) of lactones by using zinc prolinate: Zinc prolinate was selected as a catalyst for ROP of lactone homopolymerization and copolymerization, because it is FDA approved catalyst. Homopolymer of L, L-lactide and D, L-lactide would be attempted in presence of zinc prolinate as a catalyst using ROP technique. Copolymerization of L, L-lactide with ε-caprolactone at various co-monomer compositions would also be studied in details.

References

1. Ajioka, M.; Enomoto, K.; Suzuki, K.; Yamaguchi, A. *Bull. Chem. Soc. Jpn.* **68**, 2125 (1995).
2. Hiltunen, K.; Seppala, J. V.; Haerkoenen, M. *Macromolecules* **30**, 373 (1997).
3. Nagahata, Ritsuko.; Sano, Daisuke.; Sugiyama, Junichi.; Takeuchi. *JP 119597 A* 17 (2007).
4. Moon, S. I.; Lee, C.-W.; Taniguchi, I.; Miyamoto, M.; Kimura, Y. *Polymer* **42**, 5059 (2001).
5. Ohara, Hitomi.; Sawa, Seiji.; Fujii, Yasuhiro.; Ito, Masahiro.; Oota, Masaaki. *US 5880254 A* (1999).
6. K. W. Kim.; S.I. Woo. *Macromol. Chem. Phys.* **203**, 2245 (2002).
7. Hussain, M. G.; Ali, M. H.; Ali, M. M.; Chowdhury, F. Khan. Nun. J. *Bangladesh Acad. Sci.* **11**, 231 (1987).
8. Haque, M. Zahurul.; Faruq, M. Omar.; Ali, M. Umar. *Journal of Bangladesh Academy of Sciences* **24**, 171 (2000).
9. Veld, Martijn A. J.; Palmans, Anja R. A.; Meijer, E. W. *Journal of Polymer Science, Part A: Polymer Chemistry* **45**, 5968 (2007).
10. van, Hest J.C.M. *Science* **268**, 1592 (1995).
11. Krul, L. P.; Volozhyn, A. I.; Belov, D. A.; Poloiko, N. A.; Artushkevich, A. S.; Zhdanok, S. A.; Solntsev, A. P.; Krauklis, A. V.; Zhukova, I. A. *Biomolecular Engineering* **24**, 93 (2007).

12. Kim, Hun-Sik; Park.; Byung Hyun; Yoon, Jin-San.; Jin, Hyoung-Joon. *European Polymer Journal* **43**, 1729 (2007).
13. Zhang, Donghui.; Kandadai, Madhuvanthi A.; Cech, Jiri; Roth, Siegmar.; Curran, Seamus. A. *Journal of Physical Chemistry B* **110**, 12910 (2006).
14. Baskaran. D.; Mays J. W.; Bratcher M. S. *Angew. Chem, Int. Ed*. **43**, 2138 (2004).
15. Dove, A. P.; Gibson, V. C.; Marshall, E. L.; White, A. J. P.; Williams, D. J. *Chem. Commun.* **283**. 11583 (2001).
16. Coudane, J.; Ustariz-Peyret, C.; Schwach, G.; Vert, M. *J. Polym. Sci., Part A: Polym. Chem*. **35**, 1651 (1997).
17. Williams, Charlotte. K.; Breyfogle, Laurie. E.; Choi, Sun. Kyung; Nam, Wonwoo; Young, Victor. G. Jr.; Hillmyer, Marc. A.; Tolman, William. B . *J. A. Chem. Soc*. **125**, 11350 (2003).
18. Kricheldorf, Hans. R.; Damrau, Dirk-Olaf. *Macromol. Chem. Phys*. **199**, 1797 (1998).

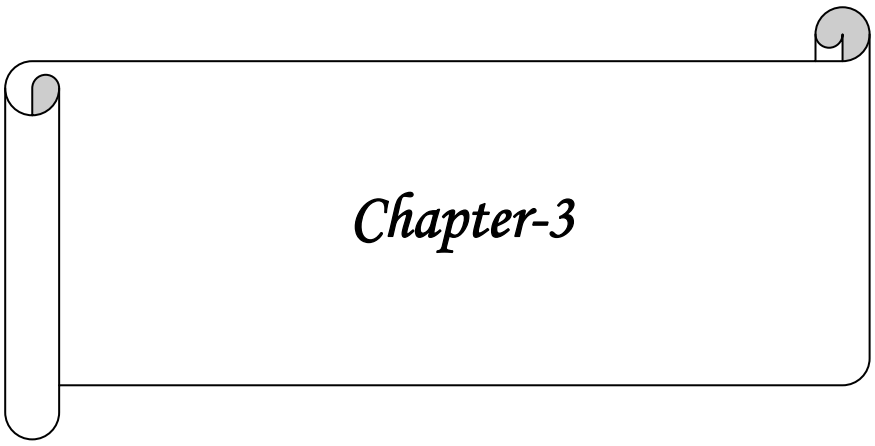
Chapter-3

CHAPTER 3: ANALYSIS OF L-LACTIC ACID AND POLY (L-LACTIC ACID)

3.1. Introduction:

In the dehydropolycondensation of L-lactic acid (L-LA) to poly (L-lactic acid) (PLA), small amounts of impurities are expected to play a major detrimental role. L-LA prepared by fermentation of biomass may contain impurities derived either from the fermentation step itself or from the separation and purification steps after fermentation. Several impurities, for example, methanol, ethanol, acetic acid, pyruvic acid, some dicarboxylic acids like oxalic, fumaric and succinic acids etc, have been reported to occur in the fermentation derived L-lactic acid **[1]**. The level as well as nature of impurities in the polymerization is believed to have a large effect on the final molecular weight by end capping either the hydroxyl or the carboxylic acid terminal of the growing polymer chain and thereby limiting the chain growth. It has been found that total level of interfering impurities should be less than 100 ppm in order to achieve high molecular weight PLA polymer **[2]**.

This chapter describes the effort to analytically detect and quantitate the level of impurities in the L-LA to be used for all polymerization reactions in the subsequent chapters. The L-LA obtained as an aqueous solution was esterified with ethyl alcohol to form ethyl L-lactate. Both the L-LA aqueous solution and the ethyl lactate were analyzed by gas liquid chromatography (GC), High Performance Liquid Chromatograph (HPLC), LC-MS.

Controlled ring opening polymerization (ROP) of L,L-dilactide (the dilactone of L-LA, alternatively called L-lactide) was also performed with stannous 2-ethylhexanoate (stannous octoate, Sn $(Oct)_2$) catalyst and measured amount of water as co-initiator, to produce linear PLA oligomers of well-defined number average molecular weight with carboxylic acid and hydroxyl end groups. These polymers were desired as model PLA oligomers for any L-LA that would be prepared in the work described in subsequent chapters. The carboxylic end groups were also quantitatively determined using ^{13}C NMR spectroscopic technique, which, in turn, was used to calculate the number average molecular weight.

3.2. Materials and methods:

3.2.1. Materials: L-lactic acid (L-LA) was obtained from PURAC chemical company, Holland, in the form of 88 % aqueous solution and was used as such, without any purification. Ethanol and benzene were both obtained from S. D. Fine Chemicals, India. Ethanol was purified by distillation and dried on fused calcium chloride followed by magnesium ethoxide before use. Benzene was purified (freed of thiophene) by stirring with 98 % H_2SO_4, washed with sodium bicarbonate and water, followed by drying first over fused calcium chloride and then over sodium metal. THF was dried over fused calcium chloride followed by calcium hydride (CaH_2). Trimethylsilyl chloride (TMSCl), acetone, 98 % H_2SO_4, sodium carbonate, fused calcium chloride and sodium metal were all obtained from S. D. Fine Chemicals, India, and used without purification. CaH_2 was procured from Aldrich Chemicals and was also used without any purification. L,L-dilactide was procured from Aldrich Chemicals and was used after recrystallization from dry THF. Doubled distilled and de-ionized water was used as co-initiator of ROP reactions. Sn $(Oct)_2$ catalyst was procured from Aldrich Chemicals and was freshly distilled before use.

3.2.2. Preparation of ethyl lactate from L-lactic acid: L-lactic acid was azeotropically dried with benzene (thiophene-free) without any catalyst, followed by removal of benzene under reduced pressure of 0.1 mbar at 60 ^{0}C (5 h). The dry, waxy L-lactic acid (10 g) was esterified by refluxing in dry ethanol (50 mol/ mol of L-LA) with a few drops of 98 % H_2SO_4 as catalyst for 20 hours, with intermittent (azeotropic) distilling out of ethanol and by-product water at every 4 hours. After 20 hr the whole reaction mixture was distilled up to dryness, so that all ethanol together. Further fractional distillation at the boiling point of ethanol and under atmospheric pressure removed ethanol and yielded 9.87 g (86 %) pure ethyl lactate.

3.2.3. General procedure for ROP of L-lactide: To 2.20 g (0.015 mol) L-lactide (recrystallized and dried) taken in single-neck, 250 mL volume round bottomed flask, previously passivated with 30 % acetonic solution of TMSCl followed by drying, maintained under inert (argon) atmosphere and fitted with standard joints and, was added Sn $(Oct)_2$ catalyst 0.1214g, 2 mol % of lactide and required amount of deionized water (0.008mL, 0.03 mol/ mol of lactide) was added subsequently using a hypodermic syringe.

The mixture was stirred at room temperature for 5 h, followed by evacuating and sealing under vacuum and then heating at 120 ^{0}C for 12 h.

3.3. Analysis:

3.3.1. Gas liquid chromatography (GC): GC-analysis of L-lactic acid was done on Perkin Elmer GC Auto System XL-200 by injecting 0.1, 1 and 10 microliter injection volumes of the L-LA 88 % aqueous solution as such to a Perkin-Elmer BP-20 (polyethylene oxide, terephthalic acid treated) capillary column of 25 meter length by means of on-column injection procedure and comparing with the chromatograms of aqueous solutions of 4, 9 and 19 ppm (that is below 5, 10 and 20 ppm, respectively) concentrations each of methanol, ethanol, acetic acid, and pyruvic acid. The split ratio was 1:60, the detector was FID, the carrier gas was nitrogen with a pressure of 7 psi and the fuel for FID was hydrogen. Oven was isothermal at 50 ^{0}C for 30 min, followed by heating with a ramp rate of 5 ^{0}C/ min from 50 ^{0}C till another 30 min. The injector and detector were kept at 250 and 280 ^{0}C, respectively. Dicarboxylic acids, namely oxalic, fumaric and succinic acid, did not elute through this column.

Ethyl lactate was analyzed under the same conditions, except that the column was Perkin-Elmer BP-21 (polysiloxane) and the injection was done in normal injection mode, where the sample evaporated inside the injector and went into the column in a gaseous form. Ethyl lactate chromatograms (corresponding to 0.1, 1 and 10 micro liter injection volumes) were compared with chromatograms of ethanolic solutions of 4, 9 and 19 ppm (that is below 5, 10 and 20 ppm, respectively) concentrations each of diethyl oxalate and diethyl succinate.

3.3.2. High Performance Liquid Chromatography: Quantification of impurities by HPLC is the process of determining the unknown concentration of a compound in a known solution. It involves injecting a series of known concentrations of the standard compound solution onto the HPLC for detection. The chromatograph of these known concentrations will give a series of peaks that correlate to the concentration of the compound injected.

The HPLC system employed for this work consisted of modular HPLC of WATERS make consisting of: Pumps 3 x 515 HPLC High pressure pumps, Injector: 717-Autosampler, Detectors: 996 PDA [Photodiode Array Detector] 410 RI [Refractive

Index Detector] and Millennium Software. The column used for impurity analysis was YMC (polar embedded, C_{18}). The chirality. of 88 % L-LA aqueous solution was determined using MN-chiral 1 column. The chiral purity of 88 % L-LA aqueous solution was obtained as 99, 9 %.

3.3.3. LC-MS: The LC-MS of L-lactic acid was analyzed in methanol solution using API Qstar Pulse.

3.3.4. Molecular weights: Molecular weights (relative, $\bar{M}_n$ and $\bar{M}_w$) and polydispersity ($\bar{M}_w/\ \bar{M}_n$) were determined with respect to polystyrene standards by size exclusion chromatography on a Thermo Finnigan Spectra Series AS300 machine at 25 ^{0}C by eluting PLA solutions of 10 mg/ mL concentration in $CHCl_3$, with toluene as internal standard, through a series of five μ-Styragel columns of pore sizes 10^5, 10^4, 10^3, 500, and 100 A^0 respectively, and length 30 cm each. $CHCl_3$ was used as the mobile phase (flow rate 1 mL/ min) and a refractive index detector (Spectra Series RI-150) was used for detection of different molecular weight fractions. Molecular weights were calculated with respect to polystyrene calibration. Number average molecular weights and intrinsic viscosities were determined with the help of a KNAUER K-7000 Vapor Pressure Osmometer (25 ^{0}C) and a 3-arm Ubbelohde viscometer (SCHOTT GERATE) at 30 ^{0}C in chloroform.

3.3.5. Quantitative ^{13}C-NMR spectroscopic analysis: For NMR measurements, the samples were dissolved in Chloroform-d in 5 mm dia. NMR tubes at room temperature. The chemical shifts in parts per million (ppm) were reported up field with reference to internal standard chloroform-d at 7.25 ppm. The sample concentration for ^{13}C NMR measurements was 10 % by weight. Proton decoupled ^{13}C NMR spectra with NOE were recorded on a Bruker DRX 500 MHz NMR spectrometer working at 125.577 MHz for carbon-13. $CDCl_3$ served as solvent and TMS as internal standard for all ^{13}C-NMR measurements. Relative peak areas were proportional to the number of carbon atoms. Peak areas were calculated by deconvolution method using WIN-NMR software.

3.3.6. Thermal analysis: Differential scanning calorimetric (DSC) measurements were made on a Perkin-Elmer thermal analyzer model DSC-7 in a nitrogen atmosphere. The measurements were run from –40 to 200 ^{0}C at a heating rate of 10 ^{0}C/ min and a cooling

rate of 100 ^{0}C/ min. The glass transition temperature (T_g) and the crystallinity data were recorded from the second and first heating curves, respectively. Crystallinity values for different polymers were calculated from the heat of fusion. By integrating the normalized area of the melting endotherm, determining the heat involved, and rating it to the reference 100 % crystalline polymer (93.6 J/ g) **[3]**, the relative crystallinity of the polymer was assessed. In the present work, the relative degree of crystallinity is referred to as crystallinity, and T_m is the melting temperature.

3.3.7. X-ray analysis: Wide-angle X-ray scattering (WAXS) pattern of the samples was obtained in reflection mode using a Rigaku Dmax 2500 diffractometer and Ni filtered copper radiation. The sample was scanned in the range $2\theta = 10 - 35^0$ and the generator was operated at 40 kV and 150 mA. The FWHM of the 110 peak was determined by peak fitting software available with the Rigaku diffractometer.

3.4. Results and discussion:

3.4.1. Impurity detection and analysis in the L-lactic acid and ethyl L-lactate:

3.4.1a. L-lactic acid: The total level of impurities in the L-lactic acid 88 % aqueous solution was less than 30 ppm. Only methanol (< 5 ppm), ethanol (< 10 ppm) and acetic acid (< 10 ppm) were found to be present as impurities. Presence of L-lactide was also detected, but its quantification was not attempted because its formation inside the GC column was also possible, since L-LA is a thermally labile material. Some peaks, though with much tailing and disturbed baseline, which eluted after the L-LA remained unidentified. Although pyruvic acid was not found at all in the L-LA sample when injected, it was individually detectable up to the 4-ppm level from its own aqueous solution. So it was thus concluded that pyruvic acid was present in less than 5 ppm level in the L-LA sample and oxalic acid, fumaric acid and succinic acid were found < 5ppm.

HPLC result shows the quantitative estimation of acid impurities present in L-LA 88 % aqueous solution. The quantitative results showed the presence of oxalic acid (28 ppm), pyruvic acid (174 ppm), acetic acid (1717 ppm) and succinic acid (388 ppm). The other acids for example, citric acid, itaconic acid, acotinic acid, propeonic acid, citraconic acid and buatyric acid are observed below the detection limit. The presence of fumaric acid was 0.6 ppm and other impurity is 6.6 ppm. Methanol and ethanol are observed below

the detection limit. The purity (percentage) of L-lactic acid is 97.7 %. The chiral purity of L-lactic acid was examined in 1.5 molar solution of sodium hydroxide using at 20 ^{0}C. The specific rotation was obtained as -14.6.

The LC-MS result showed the presence of CH_3COOH---K^+ (100 Da), Lactoyl lactic acid---Na^+ (185 Da), trimers of lactic acid--- Na^+ (257 Da), trimer of lactic acid---K^+ (257 Da), tetramer of lactic acid--- Na^+ (329 Da), pentamer of lactic acid---Na^+ (401), hexamer of lactic acid---Na^+ (473 Da), heptamer of lactic acid---Na^+ (563) and cyclic octameer of lactic acid---Na^+ (597 Da).

3.4.1b. Ethyl lactate: No impurities peaks were found in the ethyl lactate sample when injected (cut off time of 4 min given for ethanol) and there was only a single peak of ethyl lactate in the chromatogram. Impurities with boiling points less than that of ethanol had presumably been removed at the time of removal of ethanol. However, any impurity with a boiling point higher than ethanol should remain in the sample after esterification. But the fact that no impurities were found implied that the peaks found after the L-LA peak during elution of the L-LA aqueous solution sample might be due to small oligomers of L-LA. The detection level of diethyl oxalate, diethyl fumarate and diethyl succinate was about 4 ppm, under the specified condition of analysis. Thus it can be inferred that these impurities were present in less than 5 ppm concentration in the ethyl lactate sample.

The GC analysis thus could detect only three impurities, namely methanol, ethanol and acetic acid. Traces of L-lactide that was found could be either due to its presence as an impurity in the sample or its formation during the elution through the heated GC column, or both.

3.4.2. Synthesis and characterization of linear PLA oligomers of controlled number average molecular weight and with both carboxylic and hydroxyl end groups: Synthesis, by ROP of L-lactide: Sn $(Oct)_2$-catalyzed (or, -initiated) ring opening polymerization (ROP) of lactonic monomers, including L-lactide, in presence of alcoholic co-initiators proceeds via a coordination-insertion mechanism of initiation and propagation **[4-6]**, (Scheme-3.1).

In the present work, L-lactide was thoroughly dried under vacuum and all precautions were taken to avoid in traces of moisture during the reactions. Water was used as the co-initiator, so that carboxylic acid end groups instead of ester end groups as found in the Scheme-3.1 could be generated at the terminal of each PLLA oligomer chain. The number average molecular weight and degree of polymerization, $\bar{M}_n$ and $\bar{D}P_n$, respectively, of PLA oligomers thus prepared were calculated as:

$$\bar{M}_{n,} = ([M] / [I]) \text{ x } M_L \text{ x conversion \%}$$

$$\text{and } \bar{D}P_n = ([M] / [I]) \text{ x conversion \%}$$

Where [M] = moles of monomer, [I] = moles of co-initiator (water) and M_L = molecular weight of L-lactide. Conversion was determined from yield of PLLA oligomer.

3.4.3. Determination of molecular weights of oligomers: The achieved degree of polymerization and number average molecular weight was determined from the ratio of integral of the ester carbonyl carbon to that of the carboxylic acid carbonyl carbon in the ^{13}C-NMR spectrum, as shown in Figure. 3.2.

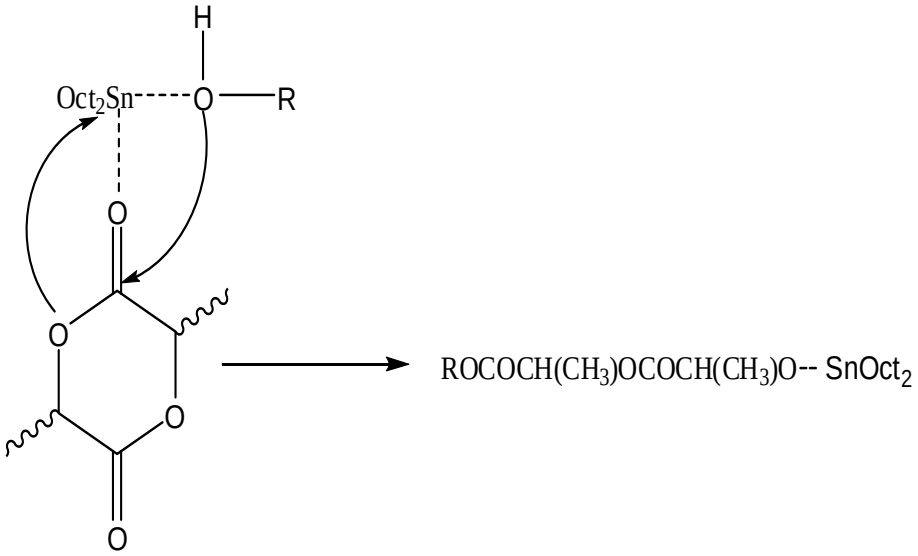

Figure 3.1: Coordination-insertion mechanism of ROP of L-lactide

Both theoretically calculated and experimentally obtained values of these parameters are organized in the data shown in Table-3.1, where samples 3.1 and 3.2 are the two PLA oligomers synthesized in this procedure with different [M]/[I] ratios and different Sn $(Oct)_2$ concentrations in proportion to the lactide monomer, to obtain oligomers of

different degrees of polymerization and hence different number average molecular weights.

The theoretically calculated and experimentally obtained values of these parameters were found to be in very good agreement, thereby indicating successful use of water as a co-initiator in the ROP of L-lactide.

3.4.4. Thermal characterization (DSC) and powder XRD of oligomers: The thermal characterization data (melting point, T_m, and glass transition temperature, T_g) of the two oligomer samples 3.1 and 3.2 are shown in Table-3.2 as well as in Figure. 3.3. Both oligomers had similar values of T_m and T_g. Effect of $\bar{D}P_n$ on T_m is also evident from the result. The powder XRD patterns of the two oligomers are shown in Figure. 3.4, where it can be found that the two polymers showed almost identical patterns, as expected. The crystallinity values of the oligomers calculated from these XRD patterns are shown in Table-3.2 and they were also found to be similar.

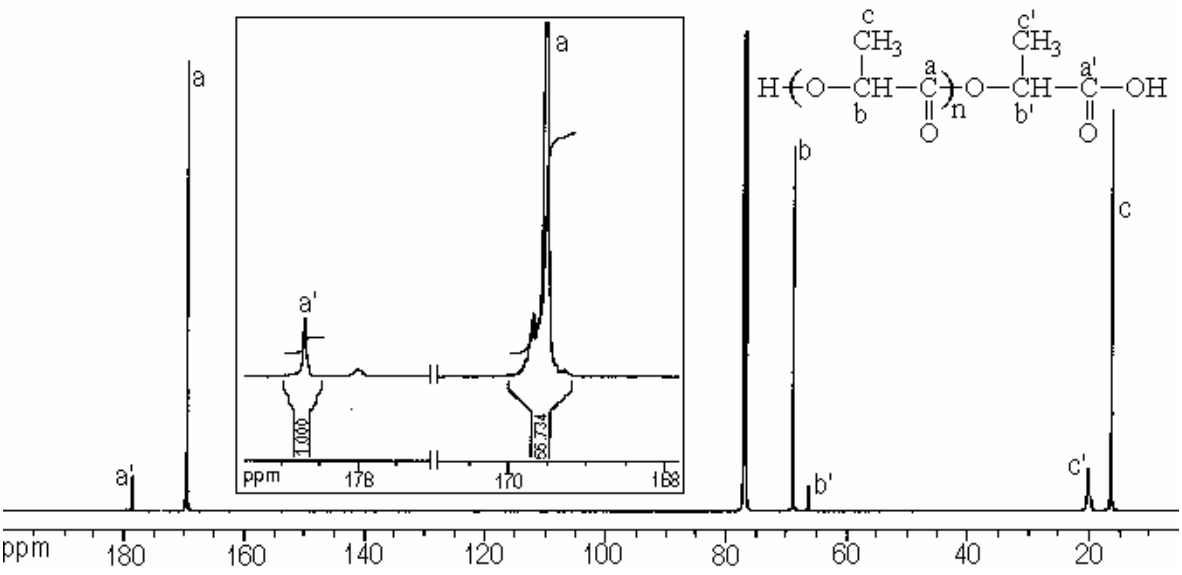

Figure. 3.2: ^{13}C-NMR spectrum of PLA oligomer 3.1 synthesized by ROP of L-lactide: inset showing ester carbonyl region (ester as well as carboxylic acid) as enlarged.

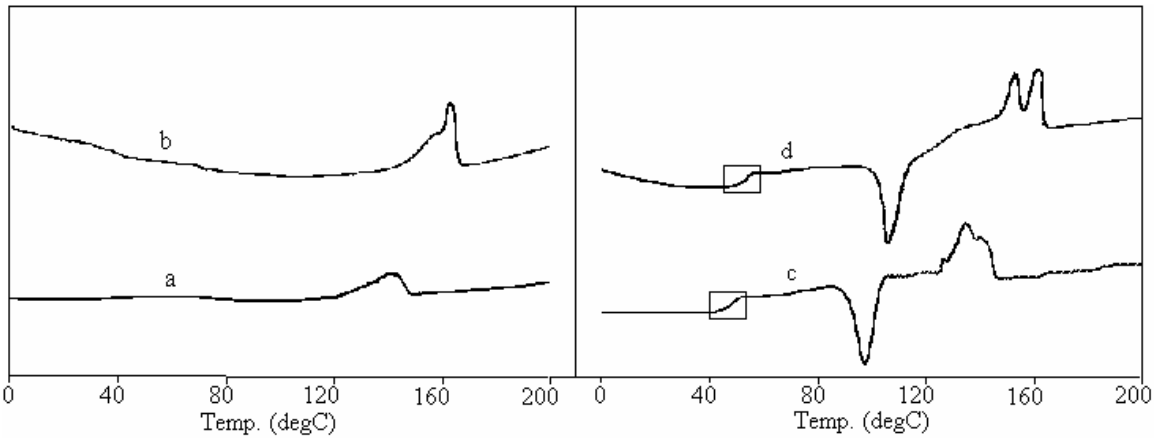

Figure. 3.3: Thermal characterization (DSC) first and second heating showing T_m and T_g, respectively of PLA oligomers: (a) 3.1, first heating; (b) 3.2, first heating; (c) 3.1, second heating and (d) 3.2, second heating.

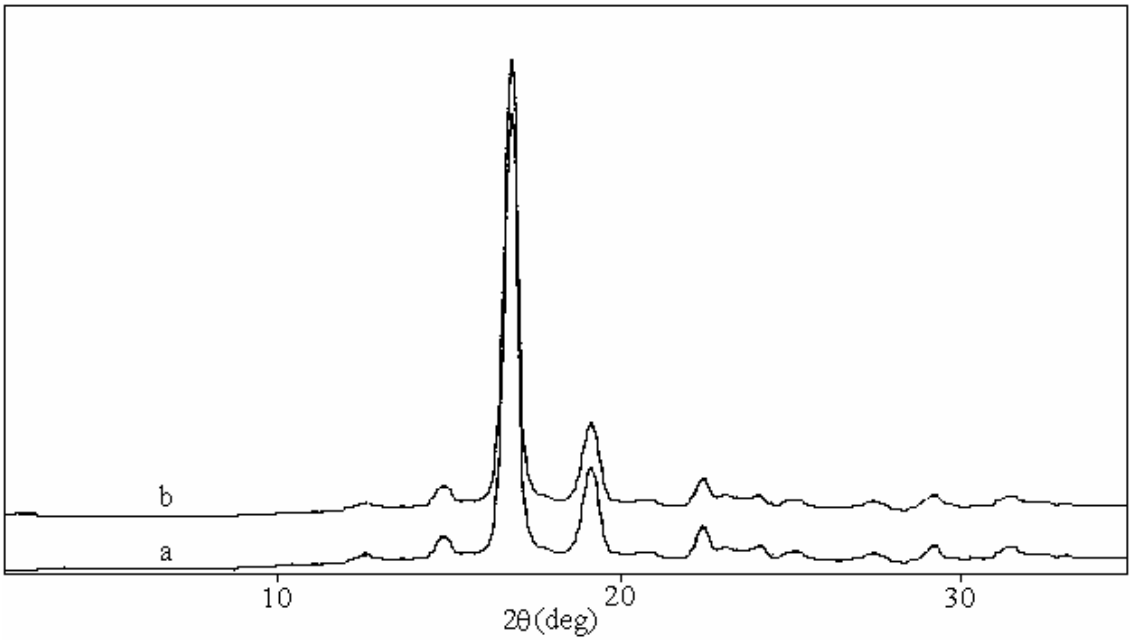

Figure. 3.4: Powder XRD patterns of PLA oligomers: (a) 3.1 and (b) 3.2.

Table-3.1: Number average molecular weights of the PLA oligomers synthesized by ROP of L-lactide with water as co-initiator and Sn $(Oct)_2$ as initiator

PLA sample	[Lactide]/ [Sn$(Oct)_2$]	[Lactide]/ [H_2O]	Yield (%)	$\bar{D}P_{n,\ Calc}$	$\bar{D}P_{n,\ NMR}$	$\bar{M}_{n,\ NMR}$	$\bar{M}_{n,\ VPO}$
3.1	200	32	86	55	60	4320	4400
3.2	400	45	87	79	77	5544	5692

Table-3.2: Thermal characterization and crystallinity values of PLA oligomers synthesized by ROP of L-lactide

PLA samples	T_g (°C)	T_m (°C)	$\Delta H_{melting}$ ($J.g^{-1}$)	% Crystallinity from powder XRD
3.1	48	141	53.4	85.52
3.2	51	162	59.7	85.73

3.5. Conclusion:

Impurities present in L-LA 88 % aqueous solution, the presence of oxalic acid (28 ppm), pyruvic acid (174 ppm), acetic acid (1717 ppm) and succinic acid (388 ppm). The other acids for example, citric acid, itaconic acid, acotinic acid, propeonic acid, citraconic acid and buatyric acid are observed below the detection limit. The presence of fumaric acid was 0.6 ppm and other impurities are 6.6 ppm. Methanol and ethanol are observed below the detection limit. The purity (percentage) of L-lactic acid is 97.7 %.

Linear PLA oligomers of controlled molecular weight were successfully prepared for the first time using ring opening polymerization (ROP) of the L-lactide. These polymers were terminated by carboxylic acid at one end and hydroxyl at the other. The molecular weights ($\bar{M}_n$) were determined by ^{13}C-NMR technique.

References

1. Hartmann, M. H. in: Kaplan, D. L. (Ed.) *Biopolymers from Renewable Resources* Springer, Chapter 15, p. 357 (1998).
2. Ohta, M.; Obuchi, S.; Yoshida, Y. *USP 5512653* (1996).
3. Leensing, J. W.; Gogolewski, S.; Pennings, A. J. *J. Appl. Polym. Sci.* **29**, 2829 (1984).

4. Duda, A.; Penczek, S.; Kkowalski, A.; Libiszowski, J. *Macrmol. Symp.* **153**, 41 (2000).
5. Kricheldorf, H. R.; Krieiser-Saunders, I.; Stricekr, A. *Macromolecules* **33**, 702 (2000).
6. Kowalski, A.; Duda, A.; Penczek, S. *Macromolecules* **33**, 689 (2000).

Chapter-4

CHAPTER-4: SYNTHESIS OF POLY (L-LACTIC ACID) BY DEHYDROPOLYCONDENSATION USING VARIOUS PORE SIZES OF ZEOLITES AND DETERMINATION OF SEQUENCE BY ^{13}C NMR METHOD

4.1. Introduction:

In recent years, poly (L-lactic acid) (PLA) has attracted tremendous attention among commonly used commodity plastic as an environmentally friendly biodegradable polymer suitable for large-scale application due to its good transparency, mechanical strength and safety **[1-2]**. PLA is not only used in medical applications but also in packaging, consumer goods and many other article of short-term use **[3]**. For fiber application, the molecular weight of poly (L-lactic acid) needs to be relatively high in order to the mechanical properties to be acceptable. Among all biodegradable polymers reported in the literature, poly (lactic acid) (PLA) has been acknowledged for the use of packaging material and commodity because of its excellent properties.

The high molecular weight PLA is achieved through the ring opening polymerization of lactide. Several steps are included the production and isolation of intermediate lactide which results high process costs of synthesizing and purifying lactide. However lactide production is relatively complicated and expensive. PLA has been restricted to medical applications such as suture materials. Therefore, alternate polymerization routes for lactic acid are thus of considerable interest.

The main focus of the work is to remove by-product water efficiently and synthesize high-molecular-weight PLA by direct polycondensation to find its better applicability in packaging and commodity. However, it was reported that it was very difficult to obtain high-molecular-weight PLA by direct polycondensation because of equilibrium between free acids, water and polyesters causing difficulty in removing water as a by-product **[4]**. The breakthrough for direct process is attributed to overcome the three subjects, i.e. kinetic control, suppression of depolymerization and efficient removal of water.

Poly (hydroxyl carboxylic acid) has been prepared by ring opening polymerization of lactide in presence of aluminum silicate **[5]**. Transesterification of aromatic diesters forming derivatives with glycols in the presence of metal catalysts have been reported and synthetic zeolites have been used for removal of metal catalysts. Finally the product has been further polymerized in presence of Me_3PO_4 and Sb_2O_3. There are few literature

reports where molecular sieves of various pore sizes have been used in dehydropolycondensation reactions by raising temperature as well as vacuum **[6]**. The polymer yield varied from 70 to 78 %. Woo et al **[7]**, have studied the effect of desiccating agents i.e. molecular sieves $3A^0$ using various catalyst systems such as $SnCl_2.2H_2O$, SnO, tin powder , trifluoro methanesulphonate and found that $\bar{M}_v$ of PLA synthesized with molecular sieves is little bit higher than that of PLA synthesized in solution. The other catalysts such as SnO, Sn powder and trifluoro methanesulphonate did not show any increase in $\bar{M}_v$ of PLA with $3A^0$ molecular sieves because it is an irreversible process where molecular sieve will get saturated as polymerization proceeds even though molecular sieves are the most effective drying agent to reduce the dissolved water contents in organic solvents. Therefore, solution polymerization of L-lactic acid to PLA is an inefficient route. Zeolites like ZSM-5, ZSM-12 and β-zeolite are generally used as a Lewis acid catalyst as well as better desiccating agents in presence of minimum amount of water. There is no literature report available so far regarding the use of zeolites as desiccating agents like ZSM-5, ZSM-12 and β-zeolite.

Lactic acid possesses one asymmetric carbon and exists in two configurations R and S. The lactic acid with S configuration is referred to as L-lactic acid in comparison with L-glyceraldehyde. Poly (lactide) polymer is formed by ring opening polymerization of lactic acid cyclic dimers (lactide), which exist as the RR, SS or RS configuration. High purity RR and SS lactide are known to polymerize to stereoregular (isotactic), poly (D, L-lactide) and poly (L-lactide) respectively.

A number of physical properties of PLA are linked to its stereosequence distribution. Pure isotactic poly (L-lactide) crystallizes at a faster rate and to a larger extent than when L-lactide is polymerized with small amounts of either D-lactide or meso-lactide. Hence the isotactic S-length distribution may be linked to the crystallization properties. Poly (lactide) with equal amount of R and S stereogenic centers which has not undergone any transesterification or racemization reaction. All the stereosequence pairs of R and S stereo configuration e.g. –RRSSSS, -RSSRR, -RRRSSS etc. and an unpaired sequence like –SSSSRS, -SSRSSR have been observed. If the polymerization process is truly random, the stereoseqence distribution will be predicted by pair wise Bernoullian statistics. The fraction of R configuration in PLA can be determined by saponification

followed by separation. The quantity of R-lactic acid can be obtained by HPLC or measurements of optical activity. Recently, Kasperczyk **[8]** could quantify the syndiotactic preference for solution polymerization of D.L-lactide with lithium tert.-butoxide by using ^{13}C-NMR and determined the coefficient of probability of isotactic addition is equal to 0.24 and coefficient of probability for syndiotactic addition is equal to 0.76.

In this Chapter, The proposed work was undertaken to synthesize high molecular weight PLA by direct polycondensation to find its better applicability in fiber application, packaging material and commodity. However, it was reported that it was very difficult to obtain high molecular weight PLA by direct polycondensation because of equilibrium between free acids, water and polyesters causing difficulty in removing water as a by-product. To overcome these problems, the polymerization conditions were optimized by screening various catalysts such as $SnCl_2.2H_2O$, 1, 3- dicloro-1, 1, 3, 3 -tetra (n-butyl) distannoxane and tetraphenyltin. These reactions were carried out in presence of various zeolites such as ZSM-5, ZSM-12 and β-zeolite. Because the surface area of ZSM-5, ZSM-12 and β-zeolite are 300, 392 and 435 m^2/g respectively and the zeolite having high surface area absorb more water, well documented in the literature. The effect of various solvents (polar and non polar) and reaction temperatures were also investigated. In this contribution, the influence of process variables on the molecular weight of PLA synthesized by direct polycondensation will be highlighted. We report the use of high-resolution ^{13}C-NMR (125 MHz) spectroscopy to identify the sterosequence distribution and determine stereo specific preference for L-lactic acid addition during tin chloride dihydrate ($SnCl_2.2H_2O$) catalyzed polymerization, and effect of various specific polymerization conditions such as temperature, duration of reaction and the nature of solvents used and type of desiccating agent.

4.2. Experimental part:

L-lactic acid was obtained from Purac (United States) as an 88 % aqueous solution and was used without further purification. 1, 3-dicloro-1, 1, 3, 3-tetra (n-butyl) distannoxane catalyst was prepared through the condensation of equimolecular amounts of di (n-butyl) tin dichloride and di (n-butyl) tin dioxide in toluene for 10 h. The crude product was obtained through the evaporation of toluene. It was purified by crystallization from

minimum amount of hot n-hexane. The yield of pure product (dichloro distannoxane) was 88 %, mp 109-111 ^{0}C (reported 110-112 ^{0}C) Analytical Calculation for $C_{16}H_{36}Sn_2OCl_2$ (552.42): C, 34.75; H, 6.52: Sn, 42.98, found. C, 33.62; H, 6.93; Sn, 43.47. Tin chloride dehydrates ($SnCl_2.2H_2O$) and tetraphenyltin (Ph_4Sn) from Aldrich (United States) were used as such without any further purification. The structures of catalyst were shown in Figure 4.1.

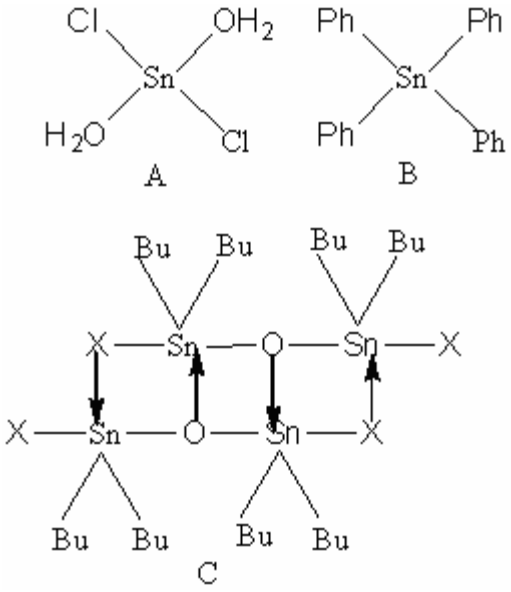

Figure 4.1: Structure of catalysts (A) tin chloridedihydrate, (B) tetraphenyl tin and (C) dichloro distannoxane.

4.2.1. Synthesis of distannoxane catalysts: Catalyst C was prepared by condensing 1.5192 g (0.5 mmol) n-butyltin dichloride and 1.2446 g (0.5 mmol) di-n-butyltin dioxide in toluene for 10 h. Crude product was obtained by evaporating toluene and purified by crystallization form a minimum amount of hot n-hexane. Pure catalysts were identified by melting points and gravimetric analysis.

4.2.2. Passivation of glass surface: Inner surface of glass reactors whenever required were passivated by treating with trimethyl silyl chloride (30 % w/v acetone solution), washed with methanol, dried at 150 ^{0}C in an oven and cooled immediately before polymerization reaction.

With a quartz reactor vessel equipped with a Dean-Stark-type condenser, the solution polymerization was carried out by varying the polymerization time, the amount of catalyst and kind of catalyst including stannous compounds, $SnCl_2.2H_2O$, Ph_4Sn and

dichloro distannoxane catalyst in argon atmosphere. An aqueous solution of L-Lactic acid (88 %) was azeotropically dehydrated with xylene for 5 h at reflux temperature without any catalyst. After the removal of water in the trap of the Dean-Stark condenser, the reaction vessel was cooled to 50 ^{0}C, the required amount of catalyst was added and this was followed by slow heating of the reaction mixture to the refluxing temperature of the solvent under mild stirring with the help of magnetic stirring bar. The reaction time was 5h. The reaction mixture was cooled to room temperature, and 50 mL of chloroform was added to dissolve the resultant mixture. The resultant solution was poured into 200 mL of n-hexane for the precipitation of the polymer. The polymer was collected by filtration and further purified repeated dissolution and precipitation. PLA oligomer was prepared, fully characterized and was used as a starting material for post polymerization. The post polymerization was carried out using prepolymer, catalyst and desiccating agents (ZSM-5, ZSM-12 and β−zeolite) to remove traces amount of by-product water. A tube packed with activated zeolite was mounted on the reaction flask in the place of the Dean-Stark trap so as to recycle the distilled azeotropic mixture through desiccating agents. The resultant mixture containing prepolymer, catalyst and solvent was polymerized at different temperature 145, 155, 165 and 190 ^{0}C for different time 1-5, 15, 30, 45 h using the Dean-Stark trap and a tube packed zeolite under inert atmosphere. After the required polymerization time, the following steps were the same as for the above-mentioned method.

4.3. Characterization:

4.3.1. Molecular weights: As in chapter 3.

4.3.2. Nuclear Magnetic Resonance; As in chapter 3.

4.3.3. Thermal Analysis: As in chapter 3.

4.3.4. X-ray Analysis As in chapter 3.

4.3.5. MALDI-ToF MS Analysis: MALDI-ToF MS analysis was performed on a Kratos Kompact MALDI IV spectrometer equipped with 0.7-m linear and 1.4 m reflection flight tubes as well as a 337 nm nitrogen laser with pulse width of 3 ns. All experiments were carried out at an accelerating potential of 20 kV. In general mass spectra from 200 shots were accumulated to produce a final spectrum. The obtained data were smoothened to reduce the spikiness by the average method; the smoothening filter moved along the

collected data channels, adding together a number of channels and dividing by that number to give an average signal. This smoothening, however, did not eliminate or hide minor signals distinct from the baseline noise. The samples were dissolved in $CHCl_3$ (1 mg/ mL) and mixed with matrix (15 mg/mL of tetrahydrofuran) before being dried on the sample plate. 4-hynohyroxy cinnamic acid (CHCA) was used as the matrix. The sample plate was inserted in to the apparatus under a high vacuum (10^{-5} Pa).

4.4. Result and Discussion:

The prepolymer was prepared by dehydropolycondensation using xylene as a diluent and tin chloride dehydrate ($SnCl_2.2H_2O$) as a catalyst. With a quartz reactor vessel equipped Dean-Stark-type condenser, 20 gm of 88 % L-LA was azeotropically dehydrated with 40 mL of xylene for 5h at the reflux temperature. Thereafter, the polymerization was carried out at 145 ^{0}C for another 5h, where the concentration of monomer 20gm/40mL and the amount of catalyst was 0.2%. The weight average molecular weight ($\bar{M}_w$) was found to be 3500 and used as starting material for post polymerization.

4.4.1. Solution post polymerization with zeolites: Table 4.1 shows the effect of reaction time with different zeolites keeping all other parameters are constant. It was observed that there is an increase of molecular weight trend up to 30 h in presence of ZSM-5, ZSM-12 and β-zeolite. The molecular weight remains constant even after further increase in reaction time except β-zeolite. β-zeolite is a high-silica large-pore zeolite consisting of unidimentional channels with 12-membered ring pore-openings. The polycondensation system of PLA oligomer involves two thermodynamic equilibria, the dedydration/hydration equilibrium of ester formation and ring/chain equilibrium of lactide. The absorbed water may be leached out because of large-pore of zeolites and cause degradation of the polymer chain.

4.4.2. Molecular weight determination: Table 4.2 shows the effect of catalyst concentration ($SnCl_2.2H_2O$) on conversion and molecular weight of PLA. The polymerization was carried out at 145 ^{0}C for 30 h where the concentration of PLA oligomers was 4g/10mL and length to diameter ratio of each bed is fixed irrespective zeolites such as ZSM-5, ZSM-12 and β-zeolite in all reactions. The catalyst

concentration of $SnCl_2.2H_2O$ was varied keeping all other parameters constant. The maximum values of $\bar{M}_n$ and $\bar{M}_w$ are obtained as 20,500 and 30,200 respectively and PDI=1.4. Thereafter the trend leveled off after 0.2 wt %. Similar kind of trend was observed in presence of ZSM-12 and β-zeolite.

Table-4.1: Effect of L-lactic acid polymerization time on various type zeolites

Polymer samples	Time (h)	ZSM-12 (II) ($\bar{M}_w$) (GPC)	ZSM-5 (I) ($\bar{M}_w$) (GPC)	β-Zeolite (III) ($\bar{M}_w$) GPC)
PLA-0	0	3,500	3,500	3,500
PLA-1	15	17,000	29,000	29,000
PLA-2	30	30,000	30,000	34,000
PLA-3	45	22,000	30,500	34,500

Xylene as solvent and temperature of the polymerization reaction was 145^0C

The maximum $\bar{M}_n$ and $\bar{M}_w$ was observed 21,000 and 34,000 in case of β-zeolite using 0.2 wt % of catalyst concentration. The catalyst $SnCl_2.2H_2O$ had a better activity than any other catalysts and the molecular weight of PLA was about 30,000.

Table 4.3 shows the effect of various the natures of catalysts, the catalyst tetraphenyltin showed about 29,000 Da, whereas dichloro distannoxane was 11,000 Da. Similarly the catalyst $SnCl_2.2H_2O$ had better activity than other two catalysts in presence of ZSM-12 system. The weight average molecular weight ($\bar{M}_w$) were 30,000, 27,000 and 24,000 Da respectively due to the corresponding catalyst such as $SnCl_2.2H_2O$, tetraphenyltin and dichlorodistannoxanes. Tin chloride dihydrate undergoes self-condensation reaction to form an activated hydrate and hydrochloric acid. .

Table 4.2: Dehydropolycondensation of L- lactic acid prepolymer using various catalyst concentrations

Polymer samples	Zeolites	Catalyst Canc^{an} (wt %)	Conv. (%)	$\bar{M}_{an}$ (NMR)	$\bar{M}_n$ (GPC)	$\bar{M}_w$ (GPC)	% cryst powder (XRD)	T_m (^{0}C)	T_g (^{0}C)
PLA-4	Blank	A (0.2)	99.1	3,570	5300	11,000	nd	160.6	38.9
PLA-5	I	A (0.05)	99.2	nd	17,900	27,000	nd	162.3	39.2
PLA-6	I	A (0.1)	99.0	nd	19,400	29,000	nd	165.4	38.1
PLA-7	I	A (0.2)	99.2	5,200	20,500	30,200	82.5	167.7	38.2
PLA-8	I	A (0.3)	99.3	nd	19,400	29,000	nd	165.2	37.9
PLA-9	II	A (0.05)	98.9	nd	16,400	25,000	nd	161.6	35.6
PLA-10	II	A (0.1)	99.0	nd	17,400	28000	nd	164.5	37.8
PLA-11	II	A (0.2)	98.7	9,500	18,200	30,000	83.0	163.7	49.6
PLA-12	II	A (0.3)	98.6	nd	17,500	26,000	nd	161.8	43.0
PLA-13	III	A (0.05)	99.3	nd	16,000	24,000	nd	164.8	41.9
PLA-14	III	A (0.1)	99.4	nd	18,500	28,000	nd	163.3	41.0
PLA-15	III	A (0.2)	99.6	18,200	21,000	34,000	84.0	167.7	52.7
PLA-16	III	A (0.3)	98.5	nd	19,000	29,000	nd	169.5	40.5

I: ZSM-5, II: ZSM-12, III: β-zeolite and A: $SnCl_2.2H_2O$. Xylene as solvent and temperature of the polymerization was 145 ^{0}C.

The terminal carboxylic group of the L-lactic acid oligomers reacts with hydroxyl group of activated hydrate to produce water and the product. The hydroxyl terminal group of L-

lactic acid oligomers should be coordinated towards the reaction center to show that condensation may be induced around the metal such as tin to form polymer having ester-linkage and activated hydrate form. It can be thought that the dehydropolycondensation proceeds via such a cycle.

The dehydropolycondensation reaction was carried out in presence of ZSM-5 with variation of $SnCl_2.2H_2O$ catalyst. The remarkable increase in the molecular weight was observed in comparison with PLA synthesized in solution polymerization without using zeolite. The $\bar{M}_w$ value of PLA increased from 27,000 to 30,200 with increase in $SnCl_2.2H_2O$ concentration, from 0.05 to 0.2 wt % and thereafter decreases. Two diffraction maxima, characteristic of the α-crystal cell of PLA, were observed at 2θ angles of 16.8 and 19.2^0. The degree of crystallinity calculated from XRD was 80 %. Similarly in the presence of ZSM-12, the $\bar{M}_w$ of PLA increased from 25,000 to 30,000 with increase in $SnCl_2.2H_2O$ concentration from 0.05 to 0.2 wt % and decreases further increase of catalyst concentration. The degree of crystallinity calculated from XRD was 79 %. PLA obtained using β-zeolite showed an increase of $\bar{M}_w$ from 24,000 to 34,000 with increase in catalyst concentration and decreases further increment of catalyst. ZSM-5, ZSM-12 and β-zeolite have pore size as ZSM-5 (5.6 x 5.3 A^0) ⇔(5.5 x 5.1 A^0), ZSM-12 (5.6 x 6.0 A^0) and β-zeolite (7.6 X 6.4 A^0 ⇔ 5.5 X 5.5 A^0), ZSM-5 (Si/Al = 100), ZSM-12 (Si/Al = 60) and β-zeolite (Si/Al=25). The amount of acid site is greater in β-zeolite in comparison with ZSM-5 and ZSM-12. ZSM-5 is considered that 10-oxygen–member-ring medium pore channels get saturated as polymerization proceeds even though zeolites is the most effective drying agent to reduce the by product water. On the other hand, in case of ZSM-12 having 12-oxygen member-ring large-pore structures showed the similar kind of trend as ZSM-5. The highest molecular weight obtained using β-zeolite must be ascribed to its three dimensional large-pore (12-oxygen-member-ring) channels without super cages. It is obvious that the pore structure like β-zeolite and the amount of acid site is necessary effective polymerization of PLA oligomers to high molecular weight PLA.

Table 4.4 showed the effect of solvents i.e. polar and nonpolar solvents. The solvent decaline at 190 ^{0}C showed the high molecular weight $\bar{M}_n$ 18,000 and $\bar{M}_w$ 35,000 (PLA-15). In presence of diphenyl ether (polar solvent) in 2 h the molecular weight was

obtained $\bar{M}_n$ 4000 and $\bar{M}_w$ 14,000. After 2 h polymerization in diphenyl ether gives colored polymer. The solvent mesitylene at 165 ^{0}C, showed the molecular weight $\bar{M}_n$ 11,000 and $\bar{M}_w$ 35000 and the PDI was 3.0 and anisole shows the number average molecular weight 4,500 and weight average molecular weight 8,000 at 155 ^{0}C.

Table 4.3: Effect of catalyst concentration on the dehydropolycondensation of L-lactic acid

Polymer samples	Zeolites	Catalyst and concentration variation (wt %)	Conv. (%)	$\bar{M}_n$ (NMR)	$\bar{M}_n$ (GPC)	$\bar{M}_w$ (GPC)	Cryst. powder (XRD)	T_m (^{0}C)	T_g (^{0}C)
PLA-5	I	A (0.2)	99.2	nod	20,500	30,200	83.0	167.7	nd
PLA-17	I	B (0.2)	98.3	9,330	19,700	29,000	nd	165.5	53.9
PLA-18	I	C (0.2)	98.3	nd	9,700	11,000	nd	163.8	53.2
PLA-11	II	A (0.2)	98.7	nd	18,200	30,000	83.0	163.7	49.6
PLA-19	II	B (0.2)	98.2	6,300	16,700	27,000	nd	161.2	51.6
PLA-20	II	C (0.2)	98.5	19,500	16,700	24,000	nd	163.2	51.3
PLA-15	III	A (0.2)	99.6	nd	21,000	35,000	83.0	167.7	52.7
PLA-21	III	B (0.2)	98.5	6,100	20,000	30,000	nd	165.7	54.3
PLA-22	III	C (0.2)	99.4	5,000	19,500	28,000	nd	165.3	55.0

I:ZSM-5, II: ZSM-12, III: β-zeolite, A: $SnCl_2.2H_2O$, B: dichloro distannoxane and C: tetraphenyltin. Xylene as solvent and temperature of the polymerization was 145^{0}C.

The reaction time for PLA-23 to PLA-26 was 15 h. Table 4.5 shows the effect of time in a solvent (decaline) at very high temperature 190 ^{0}C. The high molecular weight i.e. $\bar{M}_n$=24,000 and $\bar{M}_w$=42,000 were obtained in case of PLA-33. The molecular weight

increased from PLA-29 to PLA-33 and decreased thereafter in PLA-34 due to backbiting reaction. The GPC curve of PLA-29 to PLA30 and PLA-31, PLA-32, PLA-33 and PLA-34 was shown in Figure 3.2.

Table 4.4: Effect of solvent (polar and nonpolar) on the dehydropolycondensation of L- lactic acid

Polymer samples	Solvent	Temperature (^{0}C)	Time (h)	Conv. (%)	$\bar{M}_n$ (NMR)	$\bar{M}_n$ (GPC)	$\bar{M}_w$ (GPC)	T_m (^{0}C)	Tg (^{0}C)
PAL-23	E	145	15	98.5	nd	17,000	29,000	144.5	48.4
PAL-24	F	154	15	99.0	3,800	4,500	8,000	164.2	51.0
PAL-25	G	165	15	99.4	25,000	11,000	34,000	151.7	43.3
PAL-26	H	190	15	99.2	nd	18,000	35,000	nd	45.3
PAL-27	I	190	2	99.4	9,600	4,000	14,000	115.2	37.7
PAL-28	I	190	1	99.1	nd	2,400	8,200	137.5	33.0

E-xylene, F- anisole, G- mesitylene, H-decaline, I-diphenyl ether and nd- not detected.

4.4.3. Thermal characterization: Result of thermal characterizations is shown in Table 4.2 to Table 4.5. The values of T_g and $T_{m\ followed}$ the similar trend like molecular weight. The maximum values of T_g and T_m are 55.5 and 169.7 ^{0}C respectively (Table 4.2). Table 4.3 showed the maximum values of T_g and T_m are 55.0 and 167.7 ^{0}C respectively. Table 4.4 shows the maximum T_g and T_m values are 51.0 and 164.2 ^{0}C (PLA-24). The glass transition temperature (T_g) of the polymers varied from 54.3 to 42.2 ^{0}C (Table 4.5). The melting temperature (T_m) of the polymers varied from 139.7 to 159.8 ^{0}C, and thermograms are all shown in Figure 4.3 and 4.4.

The degree of crystallinity was calculated from powder XRD patterns and is shown in Figures 4.5 to 4.7 and the values are tabulated in Table 4.2, Table 4.3 and Table 4.5. Typically, the degree of crystallinity was found between 83% to 78 % except in case of PLA-33 and PLA-34, which were abnormally low. These could be due to racemization of L-LA to D-LA and its copolymerization.

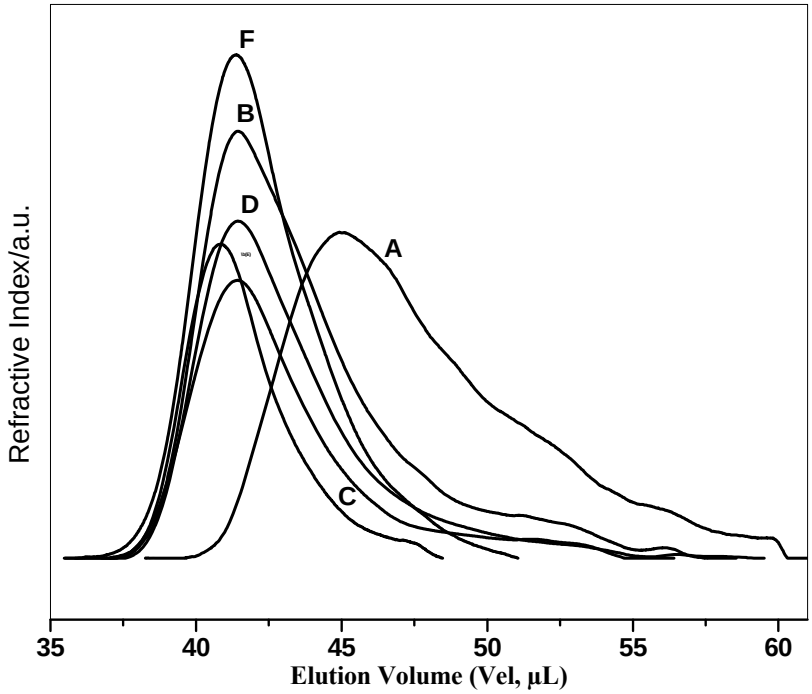

Figure 4.2: SEC elugrams of PLA oligomers (a) PLA-29, (b) PLA-30, (c) PLA-31, (d) PLA-32, (e) PLA-33 and (f) PLA-34.

4.4.4. End group analysis by ^{13}C NMR: ^{13}C NMR has been utilized as a useful tool for determining the number average molecular weight, $\bar{M}_n$ quantitatively. Besides end group determination, this technique has also been used for the determination of residual L, L-lactic acid, lactide formed due to unzipping of chain ends **[9, 10]**, and the optical purity of the polymer. In the present study, NMR was used to determine end groups, residual lactic acid, lactide and stereosequence of poly (lactic acid) in PLA samples. For this purpose the PLAs were prepared by using various parameters such as catalyst concentration, reaction time, reaction temperature variation are shown in Table 4.2, Table 4.3, Table 4.4 and Table 4.5.

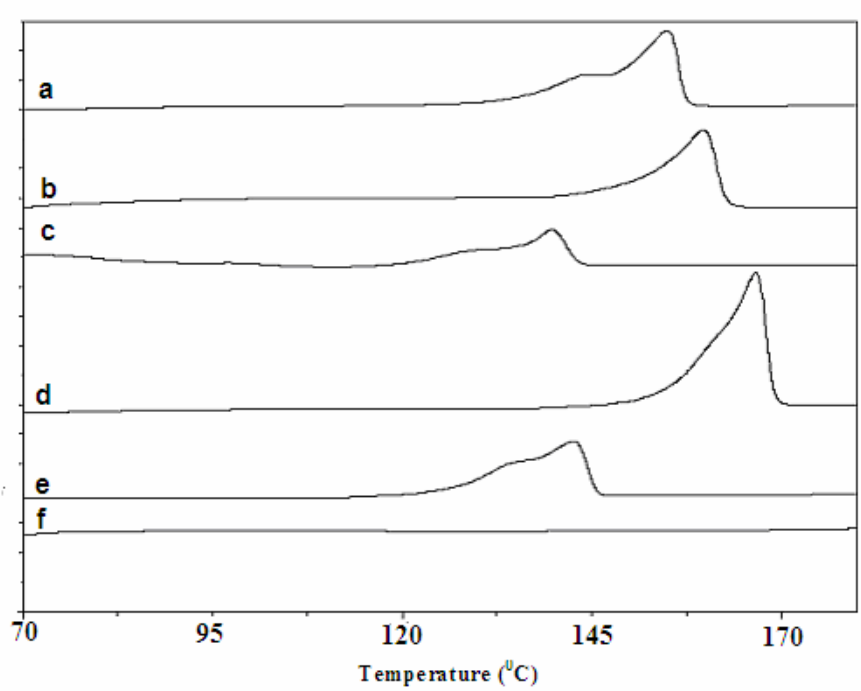

Figure 4.3: DSC thermograph showing melting temperature of PLA oligomers (a) PLA-29, (b) PLA-30, (c) PLA-31, (d) PLA-32, (e) PLA-33 and (f) PLA-34.

The spectra of oligomers, PLA-4, PLA-1 and PLA-15 are shown in Figure 4.8. The peaks appearing from 169.23 to 169.70 ppm are due to ester carbonyl groups and peaks arising from 172.9 to 173.4 ppm are due to carboxylic acid end functional groups. The accuracy of degree of polymerization (DPn) estimate, which was same in two consecutive NMR measurements. There are no peaks due to lactide in these polymers. In the spectrum of PLA-29, PLA-30, PLA-31, PLA-32, PLA-33 and PLA-34 (Figure 4.9), the peaks for ester carbonyl groups and the carboxylic acid end groups were assigned 169.13 to169.72 ppm and 172.9 to 173.5 ppm respectively. The DPn and $\bar{M}_n$ were calculated in same way by taking the ratio of these two signals and the values were depicted in Table 4.5. In the Figure 4.10, ^{13}C NMR spectra of PLA-24 and PLA-25 showed the effect of solvents (polar and nonpolar solvent) presented in Table 4.4. PLA-24 was prepared in anisole at 15 h and the polymerization temperature was 154 ^0C. The spectrum showed the NMR assignments ranges from 169.07 to 169.55 ppm for ester carbonyl groups.

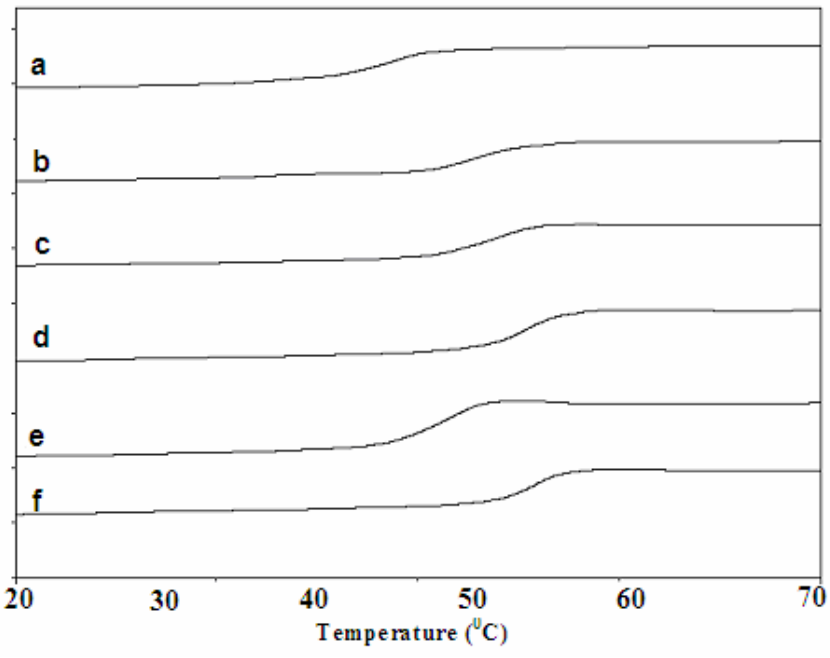

Figure 4.4: DSC thermogram showing glass temperature of PLA oligomers (a) PLA-29, (b) PLA-30, (c) PLA-31, (d) PLA-32, (e) PLA-33 and (f) PLA-34.

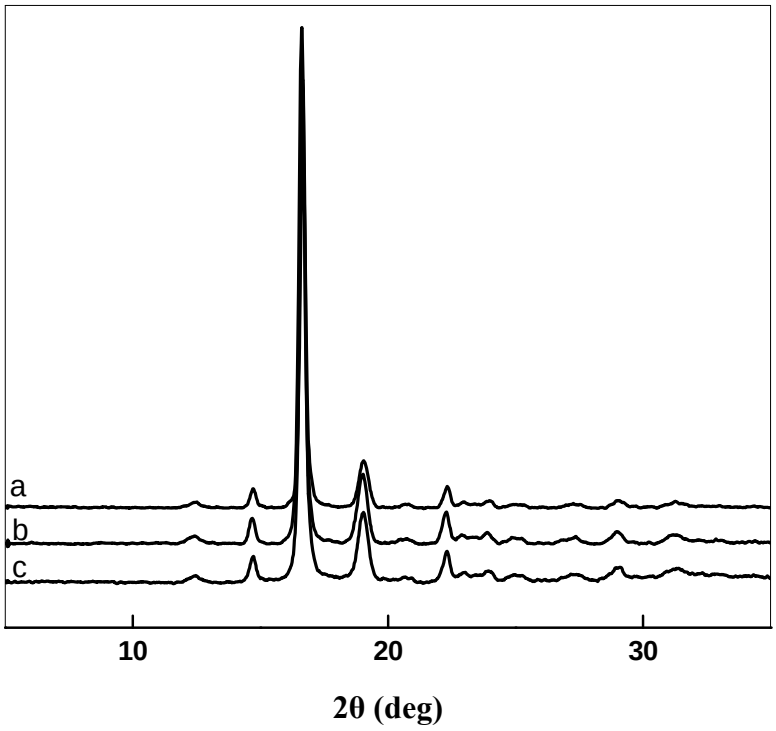

Figure 4.5: XRD pattern of PLA oligomers (a) PLA-15, (b) PLA-19 and (c) PLA-20.

Table 4.5: Effect of reaction time on the dehydropolycondensation of L-lactic acid in decaline

Polymer samples	Time (h)	Conv. (%)	$\bar{M}_n$ (NMR)	$\bar{M}_n$ (GPC)	$\bar{M}_w$ (GPC)	% cryst. powder (XRD)	T_m (°C)	T_c (°C)
PAL-29	1	98.8	3,900	1,700	2,900	83.0	155.0	42.2
PAL-30	2	99.0	4,770	4,500	8,000	78.0	159.8	48.5
PAL-31	3	99.1	nd	11,000	34,000	nd	139.7	49.1
PAL-32	4	99.3	4,900	18,000	35,000	76.5	152.2	54.3
PAL-33	5	99.2	nd	24,000	42,000	48.2	143.2	46.3
PAL-34	15	98.3	14,000	18,000	35,000	5.0	nd	45.3

nd- not detected and polymerization reaction temperature 190 ^{0}C.

The peak value for carboxylic acid was appeared at 172.8 ppm. The number average molecular weight ($\bar{M}_n$) of the polymer sample was 3,800. The PLA-25 was synthesized in mesitylene, polymerization temperature was 165 ^{0}C and reaction time was same as PLA-24. The peaks for ester carbonyl group and carboxylic end group were assigned at 169.24 to 169.57 ppm and 172.9 ppm respectively, the calculated $\bar{M}_n$ was 10,500. The proportion of formed lactide in PLA-24 was determined by calculating the integral ratio of peaks for lactone carbonyl and ester carbonyl, and the value was found 0.5 mol %. In the spectrum (Figure 4.11), PLA-27 and PLA-28 were synthesized in diphenyl ether and reaction temperature was 190 ^{0}C. The polymerization time was 1 h and 2 h respectively. Assignments for ester carbonyl ranges from 169.12 to 169.67 pmm were depicted in Table 4.4 and carboxylic end groups were appeared at 173.1 ppm. The calculated $\bar{M}_n$ was 2,200 and 9,600 respectively.

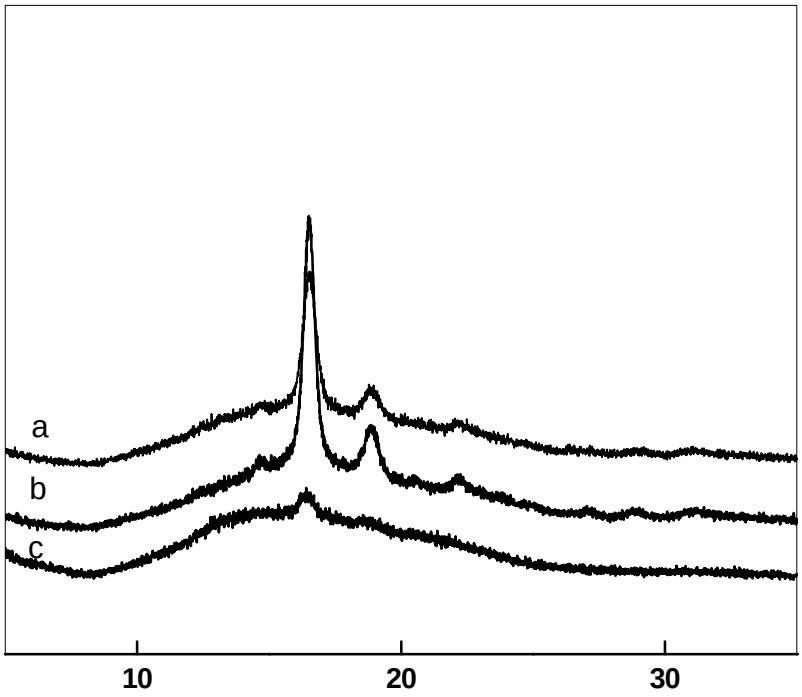

Figure 4.6: XRD pattern of PLA oligomers (a) PLA-30, (b) PLA-33 and (c) PLA-34.

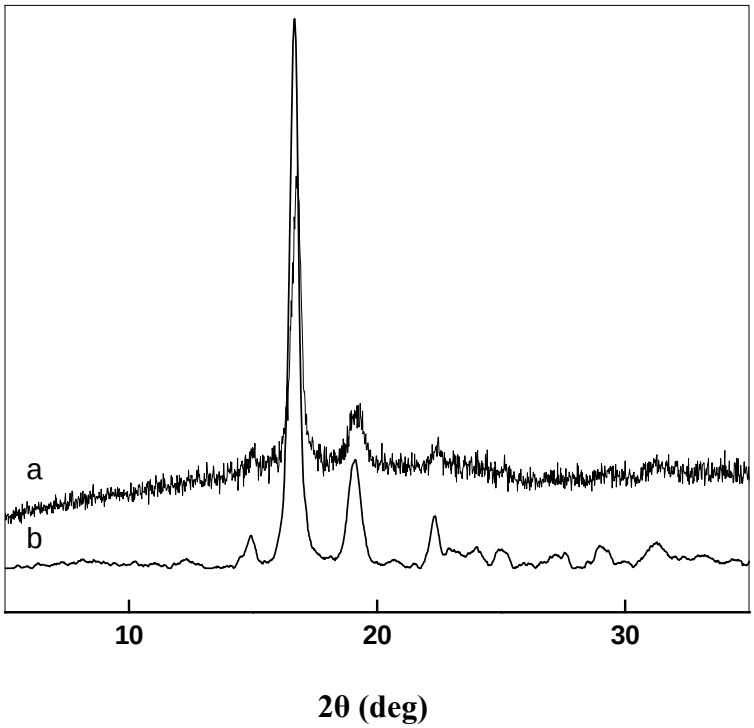

Figure 4.7: XRD pattern of PLA oligomers (a) PLA-27 and (b) PLA- 28.

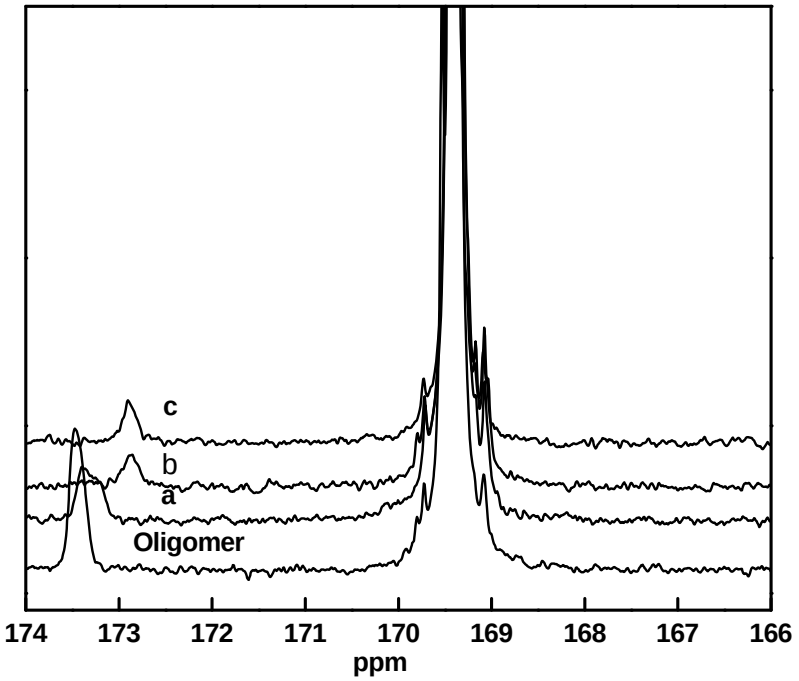

Figure 4.8: ^{13}C NMR spectra (500 MHz) around carbonyl (ester), carbonyl (acid) and carbonyl (lactide) areas of PLA oligomers (a) PLA-4, (b) PLA-1 and (c) PLA-15.

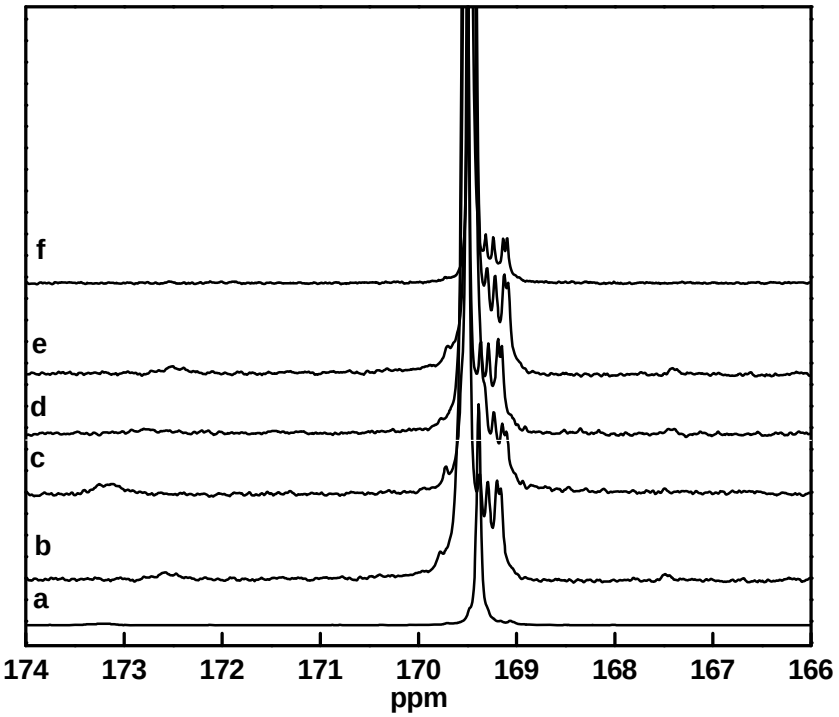

Figure 4.9: ^{13}C NMR spectra (500 MHz) around carbonyl (ester), carbonyl (acid) and carbonyl (lactide) areas of PLA oligomers (a) PLA-29, (b) PLA-30, (c) PLA-31, (d) PLA-32 (e) PLA-33 and (f) PLA-34.

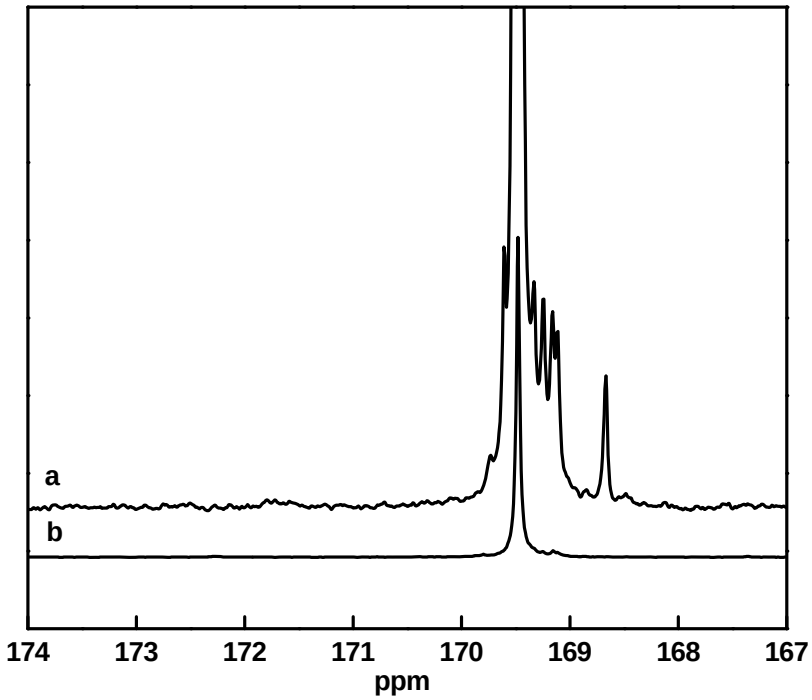

Figure 4.10: ^{13}C NMR spectra (500 MHz) around carbonyl (ester), carbonyl (acid) and carbonyl (lactide) areas of PLA oligomers (a) PLA-24 and (b) PLA- 25.

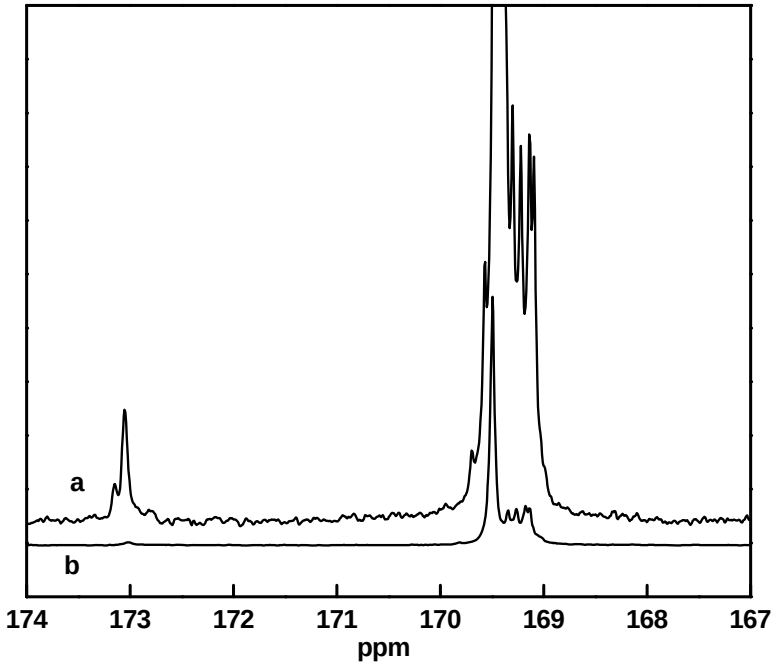

Figure 4.11: ^{13}C NMR spectra (500 MHz) around carbonyl (ester), carbonyl (acid) and carbonyl (lactide) areas of PLA oligomers (a) PLA-27 and (b) PLA- 28.

4.4.5. Stereosequence determination of poly (L-lactic acid) by ^{13}C NMR: The ^{13} C spectra of four representatives PLA samples are PLA-0 PLA-4, PLA-1 and PLA-15 used, and is also shown in Figure 4.12 and 4.13. The ^{13}C NMR spectra of the polymer are shown in Figure 4.14 to 4.18. The carbonyl region exhibited several lines, which correspond to hexads resulting addition of enantiomers of L-lactic acid molecule.

In the NMR spectra of PLA, the observed resonance can be assigned to stereosequence combinations in the polymer. The assignments are designated as various combinations of "i" isotactic pairwise relationships (-RR and -SS) and "s" syndiotactic pairwise relation ships (-RS and-SR). In the NMR spectra, the diads -RR- and –SS- are indistinguishable and would have identical chemical shifts as–RS- and –SR. For stereosequence sensitivity of length n, there is $(n-1)^2$ possible combination of pair wise relationship that can be observed in the NMR spectra. For example there are 2^2 =4 possible combination for triads, 2^3 =8 possible combination for tetrads, and 25 = 32 possible combination for hexads and so on. Often, due to either insufficient resolution, overlap of chemical shifts, or probability of stereo sequence formation, not all the possible streosequence combination is observed in the NMR spectra.

In the case of the carbonyl resonance, Kasperczyk **[8]** has reported hexads stereo sequence assignments for poly (D, L-lactide). The carbonyl resonance in ^{13}C spectrum indicates more than five distinct peaks. For poly (D, L-lactic acid) only five out of eight possible peaks (stereo sequences) are expected for tetrad sensitivity, seven out of 16 for pentad sensitivity, eleven out of 32 for hexads sensitivity, fifteen out of 64 for heptads sensitivity and twenty three out of 128 possible peaks for octads sensitivity. Hence, there are more than three distinct regions is shown in Figure 4.12 and Figure 4.13, which imply same as hexad labeled as A, B and C with the low field that peak A and the high field peak C. A is a single peak which corresponds to siiii and also predominantly isotactic (iiiii), which appear in the region from 169.48- 169.58 ppm. The peak B of PLA appeared from 169.22-169.48 ppm, which may be attributed due to (iiisi, iisii+ sisii+ sisis and isiii). The peak of PLA appeared from 199.04-169.20 ppm, which may be attributed due to isisi. The carbonyl resonance of poly (L-lactic acid) implies that the stereosensitivity is greater than pentads and is most likely to be hexads. However, due to larger number peaks observed, many of them with significant overlap, conclusive

assignments of the peaks to hexad stereosequences were difficult. The experimental value of carbonyl regions is somewhat closely matched to the theoretical values of hexad sequences.

Table 4.6: ^{13} C NMR carbonyl assignments of poly (L-lactic acid) prepared from L-lactic acid in xylene

PLA-0		PLA-4		PLA-1		PLA-15	
Carbonyls regions (ppm)	Observed value	Carbonyls regions (ppm)	Observed value	Carbonyls regions (ppm)	Observed value	Carbonyls regions (ppm)	Observed value
169.33	0.034	169.23	0.009	169.25	0.012	169.24	0.014
169.57	0.932	169.56	0.990	169.58	0.987	169.41	0.023
169.70	0.033	nd	nd	nd	nd	169.57	0.963

nd: not detected

The theoretical values calculated according to Bernoullian pair-addition statistics somewhat slightly closer with experimental values rather than to Bernoullian single-addition statistics. The chemical shifts are concentration-dependent and also configuration-dependent. The patterns of carbonyl groups for lactic acid stereocopolymer (PLA) show similarity with predominantly isotactic PLA.

The area percentage of PLA polymers (PLA-0, PLA-4 PLA-1 and PLA -15), which were deconvoluted and calculated quantitatively by using WIN NMR software was shown in Table 4.6. The stereosequence of PLA-1 is rich in isotactic hexads. The stereosequence of PLA-4 increased the isotactic hexads in comparison with PLA-0. However, in presence of β-zeolite (PLA-1), the molecular weight increased ten folds but the stereosequences remained as such. As the reaction time increased from 15 h to 30 h, the molecular weight increased further ($\overline{M}_w$ = 34000) and the stereosequence of isotactic hexads decreased subsequently. There are no patterns for syndiotactic and atactic stereosequences. Some peaks appeared at the lower field, which may be attributed due to

some incorporation of syndiotactic groups (s) in the isotactic hexad sequences. The increase in the dehydropolycondensation polymerization reaction time affects the stereosequences of PLA polymer.

It is necessary to derive the equations, which describe such processes. In the studied polymerizations of L-lactic acid is used. It is possible to assume that the probabilities of enantiomers addition to the growing chain terminated with the same enatiomer are equal $P_{LL/LL}=P_{DD/DD}$ = pi, Because $P_{DD/DD}+P_{LL/PDD}=1$ and $P_{LL/LL}+P_{DD/LL}=1$, the probabilities of the enantiomer addition to the growing chain terminated with opposite enantiomers are equal too, e.g. $P_{LL/DD}=P_{DD/LL}= P_2$.

Diads: (i) $= p_1^3 + 2.5\ p_1^2p_2 + 2\ p_1p_2^2 + 0.5p_2^3$ (1)

(s) $= 0.5\ p_1^2p_2 + p_1p_2^2 + 0.5p_2^3$ (2)

triads: (ii) $= p_1^3 + 2p_1^2p_2 + p_1p_2^2$ (3)

(is)= (si) $= 0.5\ p_1^2p_2 + p_1p_2^2 + 0.5p_2^3$ (4)

tetrads: (iii) $= p_1^3 + 1.5p_1^2p_2 + 0.5p_1p_2^2$ (5)

(iis) = (sii) $= 0.5\ p_1^2p_2 + 0.5p_1p_2^2$ (6)

(isi) $= 0.5p_1^2p_2 + p_1p_2^2 + 0.5p_2^3$ (7)

(sis) $= 0.5p_1p_2^2 + 0.5p_2^3$ (8)

pentads: (iiii) $= p_1^3 + p_1^2p_2$ (9)

(iiis) = (iisi) = (isii) = (siii) $= 0.5p_1^2p_2 + 0.5p_1p_2^2$ (10)

hexads: (iiiii) $= p_1^3 + 0.5p_1^2p_2$ (11)

(iiiis) = (siiii) = (iisii) $= 0.5p_1^2p_2$ (12)

(iiisi) = (isiii) $= 0.5p_1^2p_2 + 0.5p_1p_2^2$ (13)

(iisis) = (siiis) = (sisii) $= 0.5\ p_1p_2^2$ (14)

(isisi) $= 0.5p_1p_2^2 + 0.5p_2^3$ (15)

(sisis) $= 0.5p_2^3$ (16)

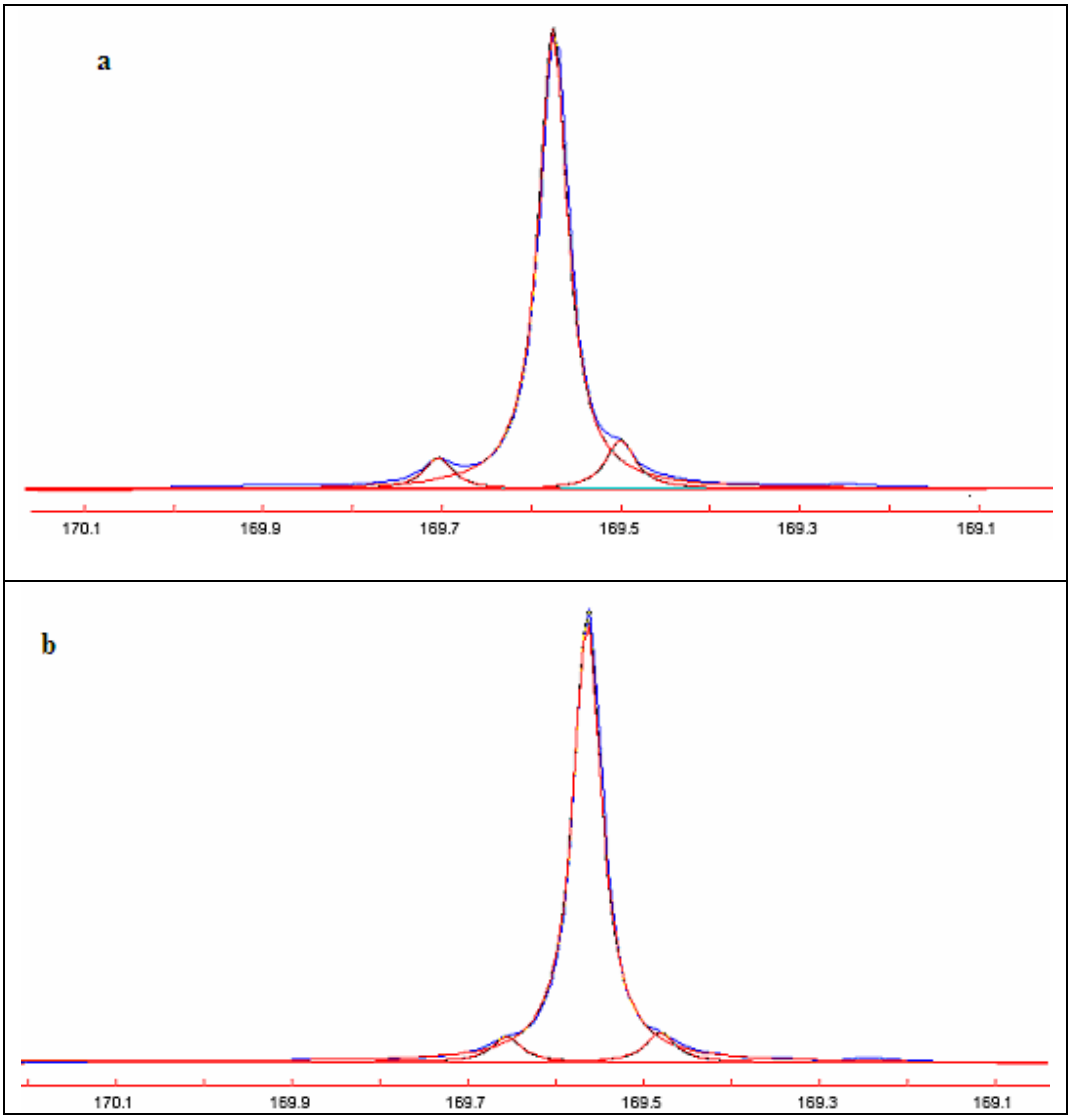

Figure 4.12: ^{13}C NMR spectra (500 MHz) around carbonyl (ester), carbonyl (acid) and carbonyl (lactide) areas of PLA oligomers (a) PLA-0 and (b) PLA- 4.

From the equations presented above using intensities of signals in the ^{13}C NMR spectrum, the coefficient probabilities p_1 and p_2 were calculated. The structures of the polymer chain resulting from extreme p values are shown in scheme 1. In the previous work, the equation describing intensity values of the individual sequences obey pair-addition Bernoullian statistics and various ratios of enantiomers were presenting in non

typical appearance of the peaks in the carbonyl regions of the ^{13}C NMR spectra shown in Figure 4.14 to Figure 4.16.

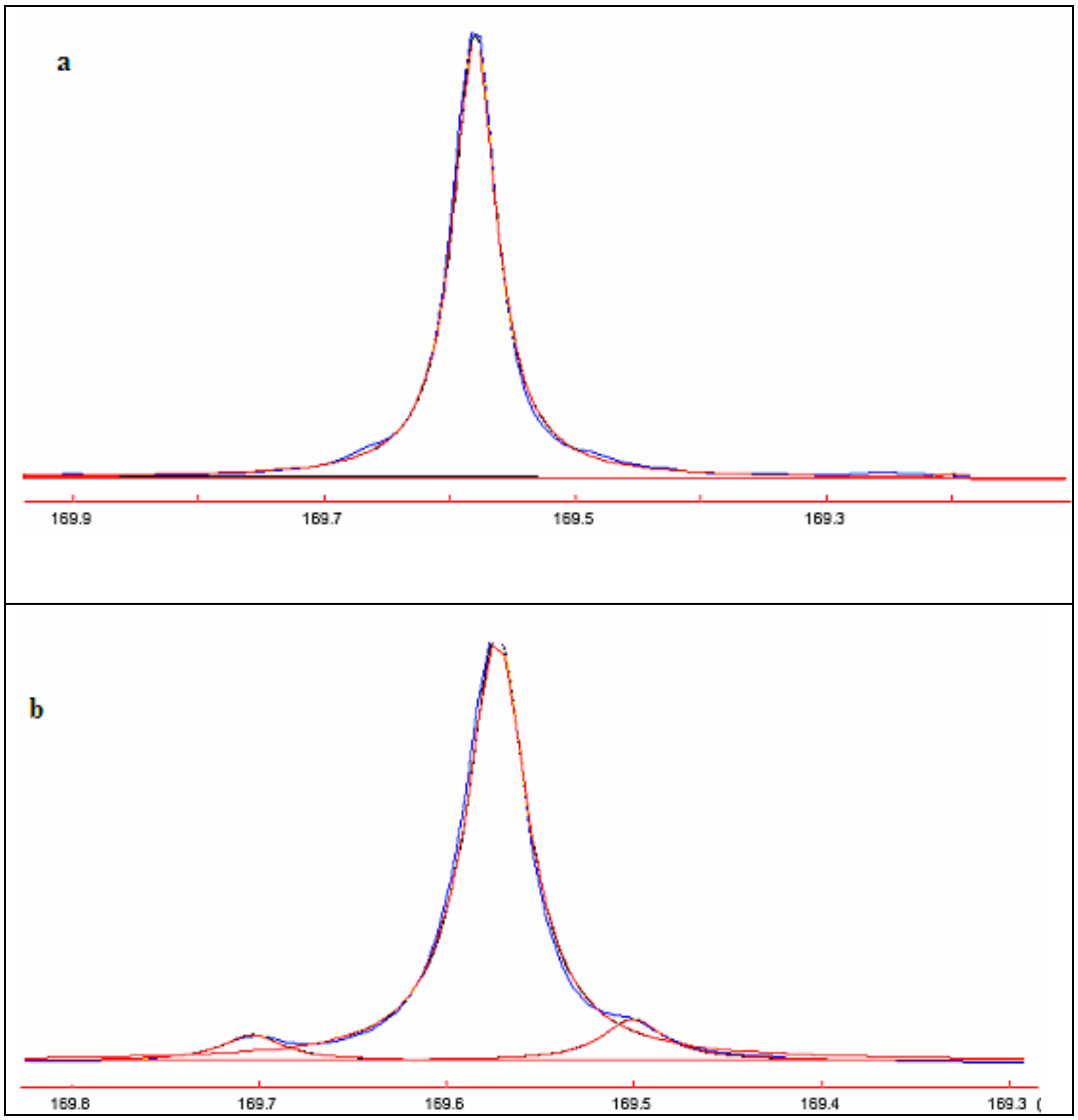

Figure 4.13: ^{13}C NMR spectra (500 MHz) around carbonyl (ester), carbonyl (acid) and carbonyl (lactide) areas of PLA oligomers (a) PLA-1 and (b) PLA-15.

The results suggested a possibility of non Bernoullian statistics and stereoselection during the dehydropolycondensation polymerization of L-lactic acid in presence of tinchloride dihydrate ($SnCl_2$. $2H_2O$) using β-zeolite as desiccating agent.

Assuming these carbonyl carbon atoms are sensitive to hexad as suggested by Bero et al **[11]**, the three broad bands received the following assignments (Figure 4.15 to Figure 4.17) and (Table 4.7 and, 4.8), (band B and A) covering the 169.5-169.7 ppm range

included iiiii, iiiis, siiii, siiis, iisis, isiii hexads, (A and B) covering the 169.1-169.2 ppm range corresponded to isisi hexads. (band B and C) covering the range 169.2-169.4 ppm included iiiss, iisii, sisii, sisis, iisis, isiii hexads.

D,D + L,L (p1 =1, p2 = 0) ⟶ .....LLLLLL… + ….DDDDD….

isotactic

D,D + L,L (p1= p2 = 0.5) ⟶ …….LLLDDLLLLDDD….

"Predominantly isotactic"

D,D + L,L (p1 = 0, P2 = 1) ⟶ ……LLDDLLDDLLDD…

disyndiotactic

Scheme 4.1

In the ^{13}C NMR spectra of PLA shown in Table 4.6, the appearance of 169.3 ppm may be attributed due to hexads, the calculated coefficients of probability count to be p_1 varies from 0.48-0.58 where as p_2 varies from 0.42-0.52. The obtained results are due to variation of reaction time keeping all other reaction parameter unaltered. This indicates that the preference in incorporation of D and L, L-enantiomers addition to the growing chain and leading to an enhanced contribution of disyndiotactic segments in poly lactic acid molecules.

4.5.5a. Effect of reaction time at higher temperature: When the solvent was changed from xylene to decaline, the molecular weight increased from 29,000 to 35,000 at the same polymerization time (15 h) as shown in Table 4.6. Figure 4.14 and Table 4.7 showed the dehydropolycondensation of L-lactic acid prepolymer using β-zeolite as a desiccating agent and decaline as a solvent using at various reaction times. The maximum molecular weights i.e. $\bar{M}_n$, $\bar{M}_w$ and molecular weight distributions were obtained by GPC measurement. The values of $\bar{M}_n$, $\bar{M}_w$ and PDI are 24,000, 42,000 and 1.75 respectively in case of PLA-33. The A part was obtained by deconvolution and the calculated value was 0.88 instead of 0.38 for Bernollian pair-addition and A/C parts does not match with Bernoullian pair-addition. The isotactic sequences decreased as the reaction time increased. As the reaction time varied to 1–2 h, the syndiotactic groups

were incorporated in isotactic hexads and also some syndiotactic sequences were preferred. The isotactic sequence values were changed from 0.978 to 0.880. The sequence values are also supported by degree of crystallinity measured by XRD, melting point T_m values as shown in Table 4.7 the maximum molecular weight (42,000 i.e. PLA-33) as the reaction progresses up to 5 h.

4.5.5b. Effect of solvents: Table 4.8 depicts the dehydropolycondensation of L-lactic acid in presence of β-zeolite at various solvents. When the reaction was carried out in presence of diphenyl ether at 1 h, the isotactic hexad values decreased dramatically in comparison with PLA-29. As the reaction time increased from 1h to 2h, the isotactic hexads decreased further. The effect of solvents (polar and non polar) has played an important role during polymerization process in non polar solvents, the probability of higher isotactic hexad sequences were predominant over polar solvents. The polymerization reactions were further carried out for longer reaction period and found out that color of the polymeric mass changed from brown to dark brown in color. The sequences of these materials have not studied.

The polymerization reaction was carried in anisole (at 154 ^{0}C for 15 h i.e. PLA-24), the isotactic hexad sequence value was reasonably better along with some syndiotactic sequences. Similar polymerization was carried out in mesitylene (at 165 ^{0}C for 15 h, i.e. PLA-25), showed mostly isotactic hexad addition and absence of syndiotactic and atactic sequences. The results focused that even at low reaction temperature (165 ^{0}C and 145 ^{0}C), non-polar solvents preferred isotactic addition than the polar solvents. However, more and more syndiotactic groups incorporated in to the isotactic sequences therefore; there are various kind of isotactic hexads along with syndiotactic hexads. The discrepancies were regarded as evidences for deviation from the pair addition Bernoullian statistics. In this case, the best fit was obtained for p_i = 0.72 in agreement with the steroselectivity in favor of isotactic enchainment of L-lactic acid units were observed.

Further, it was observed that transesterification reaction occurred after 5 h reaction time and there was no substantial transesterification below 5 h reaction time even if the reaction temperature was 180 ^{0}C. Figure 4.17 and Table 4.8 showed the ^{13}C-NMR spectra of PLA-27 and PLA-28 in presence of diphenyl ether prepared at 180 ^{0}C. Transesterification facilitated at faster rate and results were tabulated in Table 4.8.

Figure 4.18 showed the ^{13}C NMR spectra of PLA-24 and PLA-25 at two different solvents i.e. polar solvent (anisole) and non-polar solvent (mesitylene) using same catalyst and reaction temperature. Transesterification in a polar solvent (anisole) is faster than that of nonpolar solvent (mesitylene).

In case of methine resonance, higher degree of overlaps of the peaks made conclusive assignments difficult but hexads stereosensitvity is probable. In some instances, however depending on the experimental condition new lines were found to broaden the fine structure in the methine resonances, whose stereo dependence were shown in Figure 4.19 in terms of hexads, on the basis of Bero's assignments **[11]**. The new lines observed at 69.95 ppm, 68.95 and 68.86 ppm were respectively assigned to iss, sss, ssi tetrads, where one can find successive syndiotactic ('s") diads, a feature could not result from the pair addition mechanism only. The theoretically forbidden "SS" sequences reported earlier and ascribed to intermolecular transesterification occurring during the polymerization **[12]**. A significantly higher level of noise is apparent in the spectrum, and this makes quantification somewhat difficult. The racemization reactions are mostly due to dynamic equilibrium of ester interchange reactions occurring between the polymer chains. During the ester interchange reactions, there are two ways in which the ester linkages between successive lactic acid units can cleave and reform. One is acyl-oxygen cleavage, which does not involve the chiral carbon in question. The other is alkyl-oxygen cleavage, in which the covalent bond between oxygen and the chiral carbon breaks and subsequently reforms; this results in an inversion of the configuration. The change from L-LA (the L- form) to the D, L form in presence of the catalyst partially through racemization has been observed with DSC and XRD. The strong proton acid assists with the breaking of ester bond through typical carbon-oxygen bond breaking.

The results of PLA-33 and PLA-34 in Table 4.9 indicate that reaction time increased at same reaction temperature (195 ^{0}C), the probability of alkyl-oxygen cleavage increased, and this resulted in the formation of inverted configuration. PLA-24 showed less probability of alkyl-oxygen bond cleavage in comparison with PLA-26 irrespective of same reaction time (15 h).

Table 4.7: ^{13} C NMR carbonyl assignments of poly (L-lactic acid) prepared from L-lactic acid in decaline

PLA-29		PLA-30		PLA-31		PLA-32		PLA-33		PLA-34	
Carbonyls regions (ppm)	Observed value	Carbonyls regions (ppm)	Observed value	Carbonyls regions (ppm)	Observed value	Carbonyls regions (ppm)	Observed value	Carbonyls regions (ppm)	Observed value	Carbonyls regions (ppm)	Observed value
169.23	0.022	169.14	0.054	169.14	0.012	169.13	0.079	169.15	0.060	169.15	0.198
169.56	0.978	169.17	0.001	169.18	0.124	169.17	0.024	169.20	0.032	169.19	0.140
nd	nd	169.26	0.037	169.28	0.074	169.26	0.049	169.29	0.055	169.21	0.040
nd	nd	169.49	0.880	169.36	0.077	169.35	0.011	169.38	0.077	169.29	0.097
nd	nd	169.72	0.029	169.52	0.712	169.49	0.798	169.52	0.775	169.43	0.524

nd: not detected

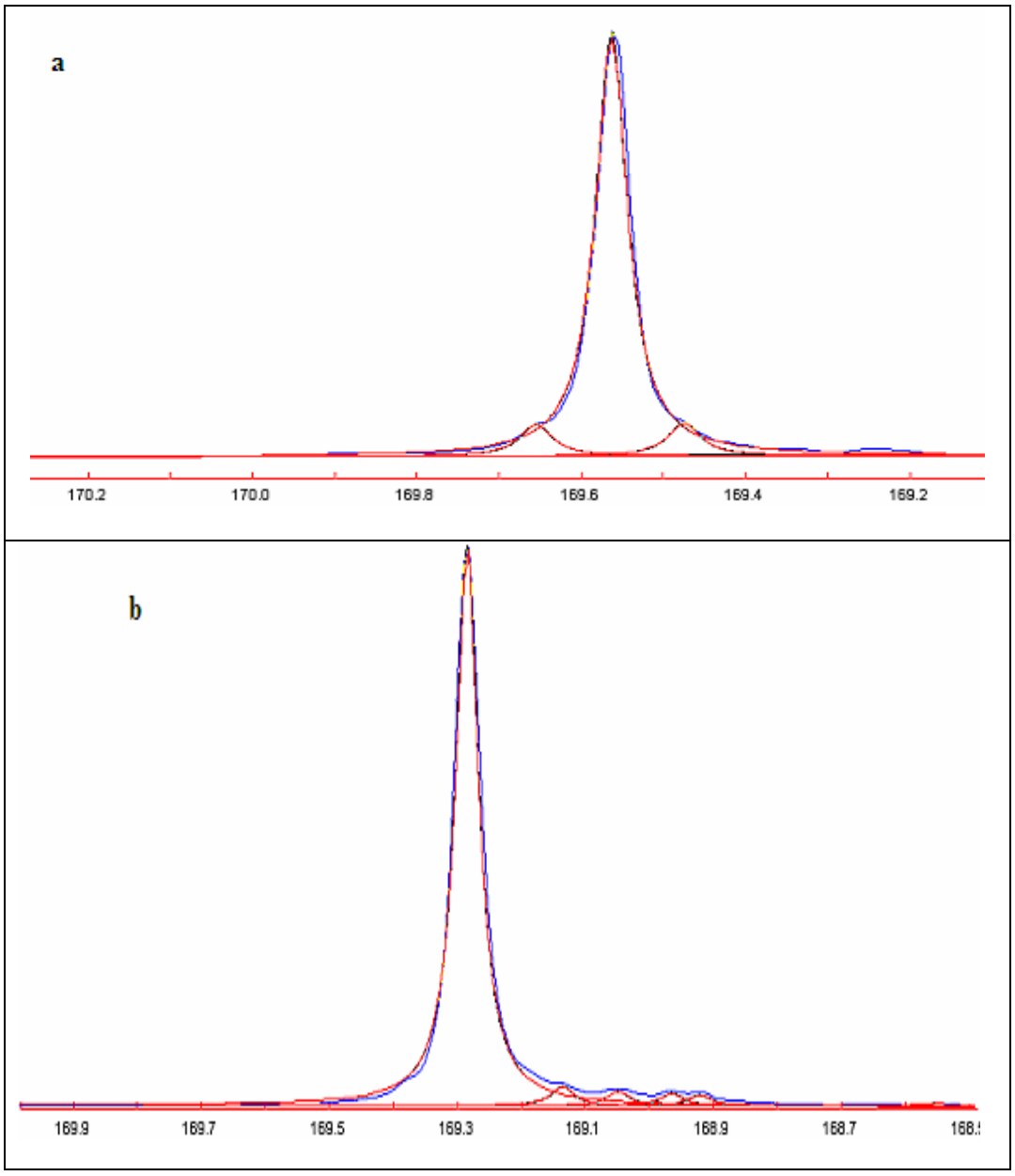

Figure 4.14: ^{13}C NMR spectra (500 MHz) around carbonyl (ester), carbonyl (acid) and carbonyl (lactide) areas of PLA oligomers (a) PLA-29 and (b) PLA-30.

These results indicate that as the temperature increased, the probability of alkyl-oxygen cleavage increased and resulted in the formation of inverted configuration. When the results of PLA-24 were compared with PLA-27, the results showed more alkyl-oxygen

bond cleavage in case of PLA-27 even if at lower dehydropolycondensation reaction time (2h).

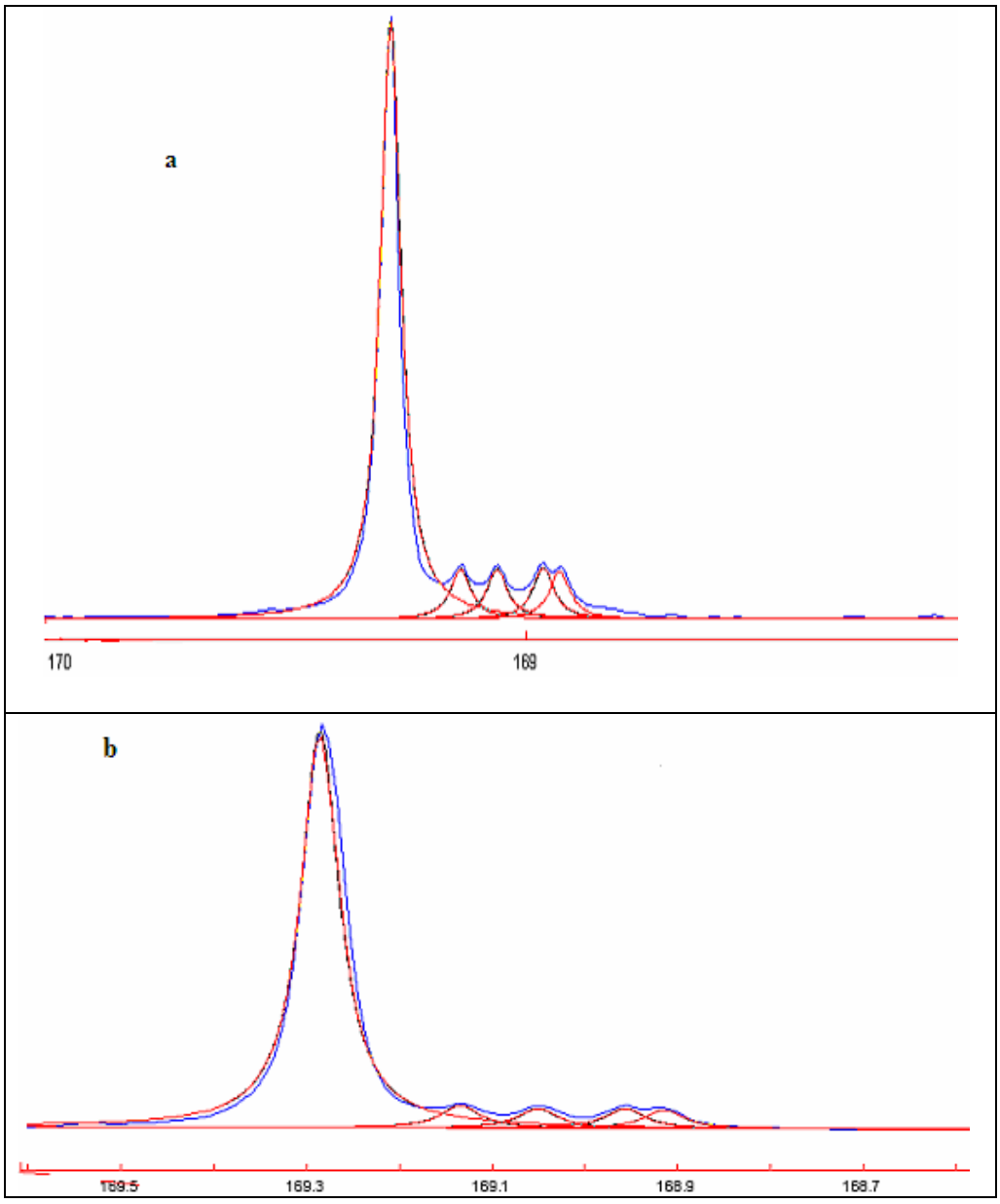

Figure 4.15: ^{13}C NMR spectra (500 MHz) around carbonyl (ester), carbonyl (acid) and carbonyl (lactide) areas of PLA oligomers (a) PLA-31 and (b) PLA-32.

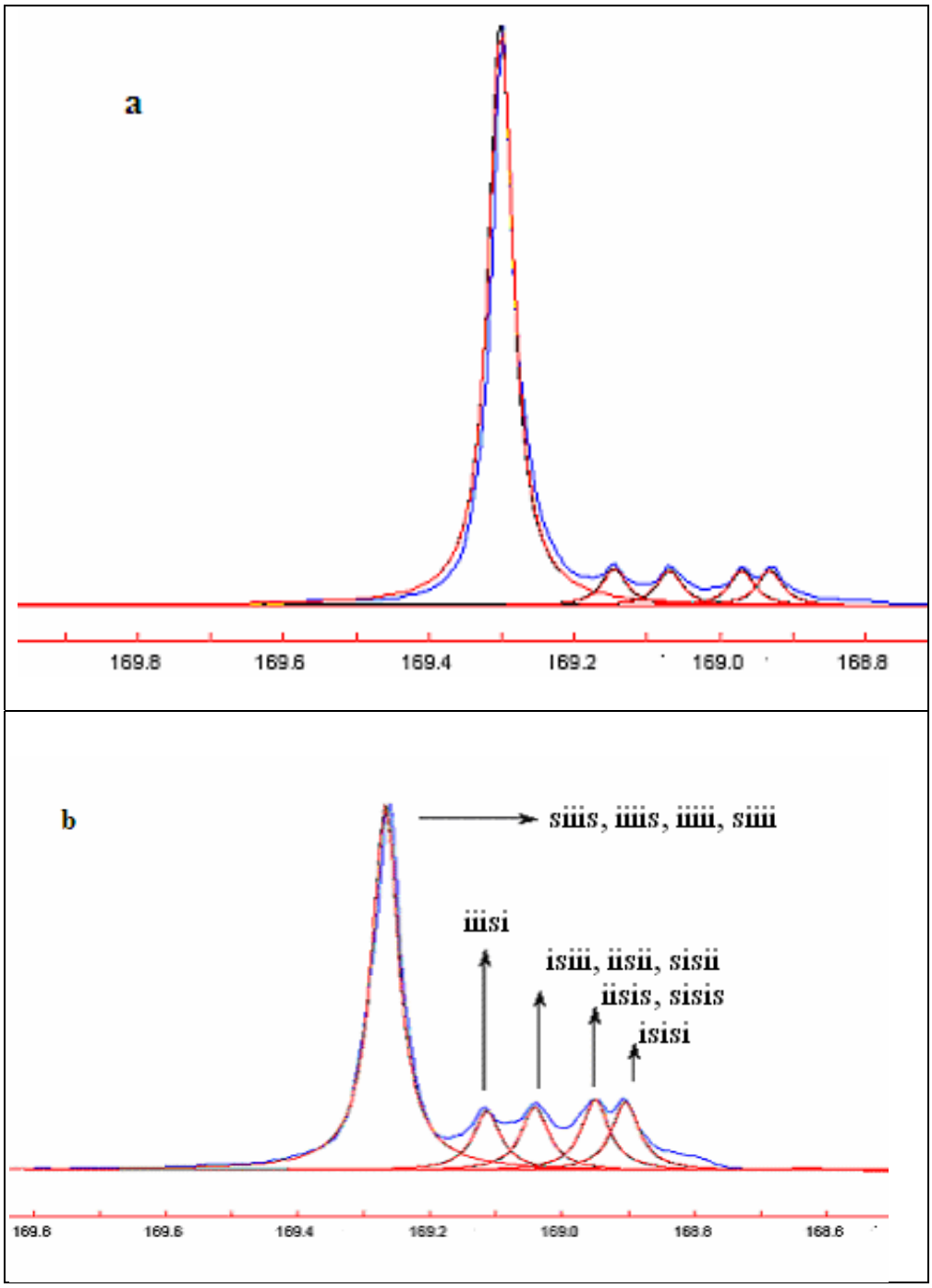

Figure 4.16: ^{13}C NMR spectra (500 MHz) around carbonyl (ester), carbonyl (acid) and carbonyl (lactide) areas of PLA oligomers (a) PLA-33 and (b) PLA-34.

Table 4. 8: ^{13} C NMR carbonyls assignments of poly (L-lactic acid) prepared from L-lactic acid using various solvents

PLA-27		PLA-28		PLA-24		PLA-25	
Carbonyls regions (ppm)	Observed value	Carbonyls regions (ppm)	Observed value	Carbonyls regions (ppm)	Observed value	Carbonyls regions (ppm)	Observed value
169.21	0.012	169.12	0.087	169..07	0.025	169.24	0.025
169.24	0.198	169.19	0.116	169.12	0.027	169.42	0.046
169.34	0.058	169.22	0.032	169.20	0.028	169.57	0.929
169.42	0.074	169.30	0.067	169.29	0.067	nd	nd
169.57	0.657	169.43	0.661	169.43	0.774	nd	nd
nd	nd	169.56	0.032	169.55	0.076	nd	nd
nd	nd	169.69	0.003	nd	nd	nd	nd

Table 4.9: Percentage of transesterification in polymer samples

Sr. No.	Percentage of transesterification
PLA-33	4.32
PLA-26	7.04
PLA-28	3.18
PLA-24	2.55

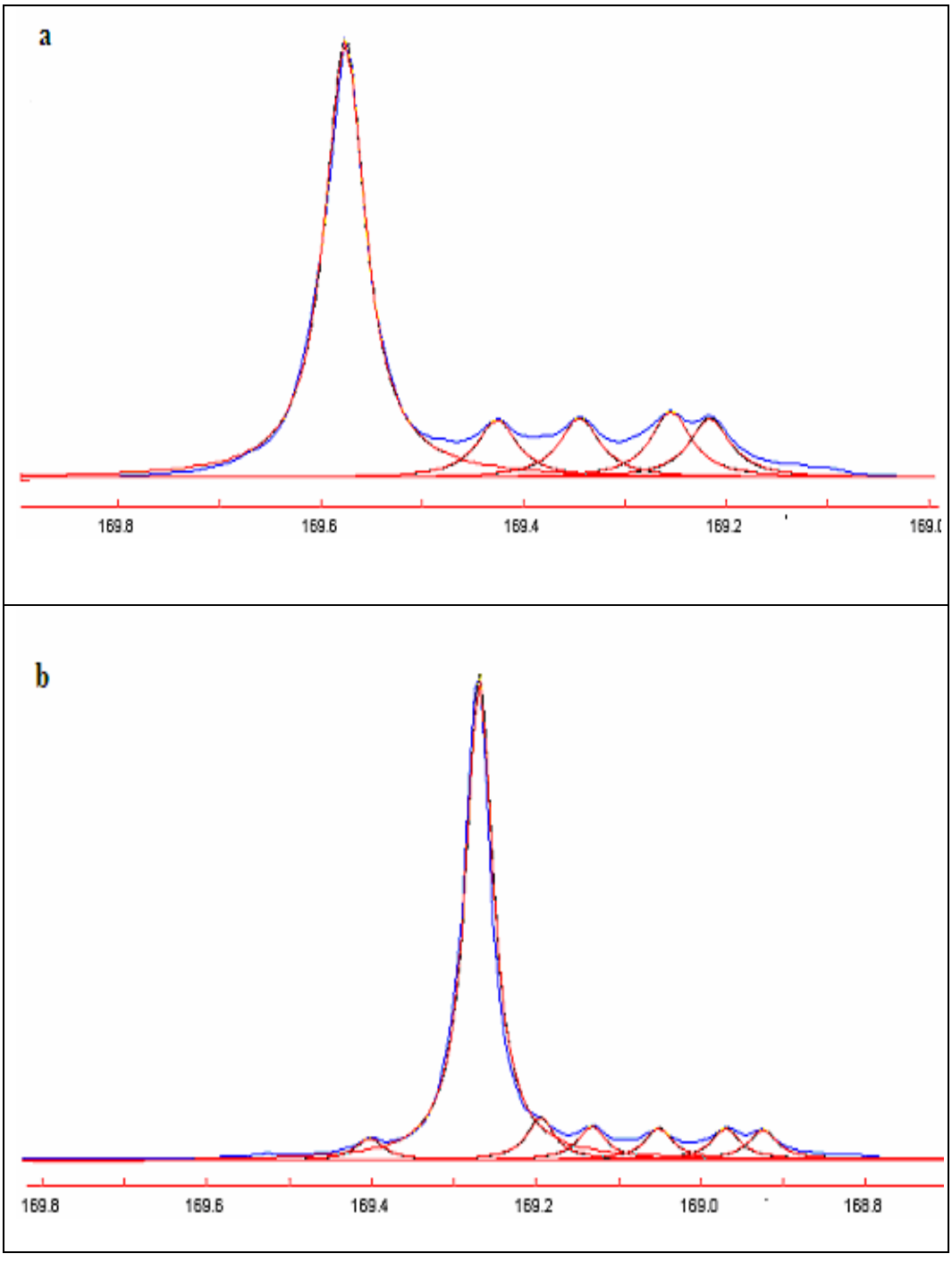

Figure 4.17: ^{13}C NMR spectra (500 MHz) around carbonyl (ester), carbonyl (acid) and carbonyl (lactide) areas of PLA oligomers (a) PLA-28 and (b) PLA- 27.

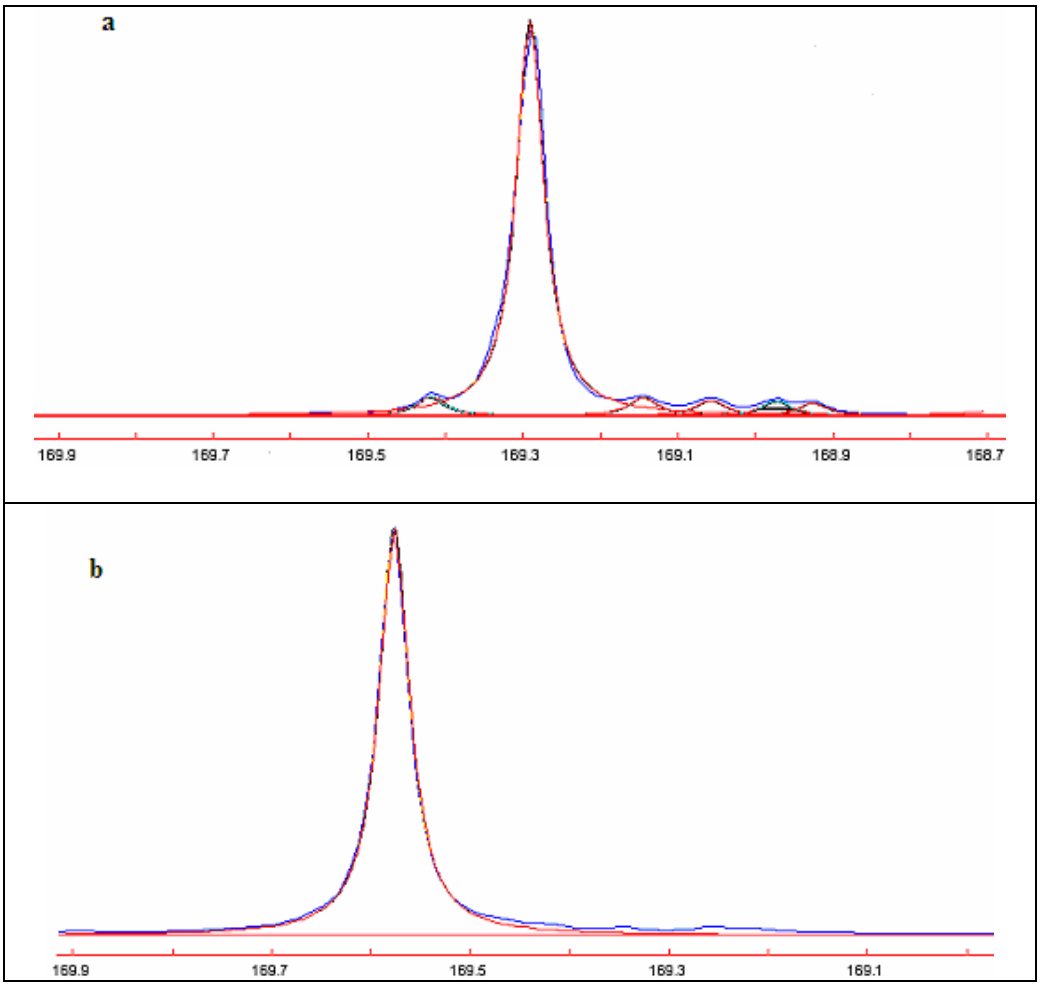

Figure 4.18: ^{13}C NMR spectra (500 MHz) around carbonyl (ester), carbonyl (acid) and carbonyl (lactide) areas of PLA oligomers (a) PLA-24 and (b) PLA- 25.

4.5.6. MALDI-TOF MS Analysis: MALDI-ToF MS technique has employed for the determination of molecular weight of synthetic polymer chains as well as determination of their end groups.

Low molecular weight polymers (oligomers) are amenable to analysis by MALDI-ToF. The identification and quantification of end groups becomes very important if the polymer have very high molecular weight. There are several analytical tools for end group determination techniques such as NMR, titration method etc. NMR is an accurate as well as quantitative technique.

However, it has detector sensitivity limitation. Titration (for carboxylic acid end groups) is not feasible for aliphatic polyester, which undergoes main chain hydrolysis under this condition. MALDI-ToF MS can detect all end groups and impurities with a high level of sensitivity. However, quantification is difficult by using this technique.

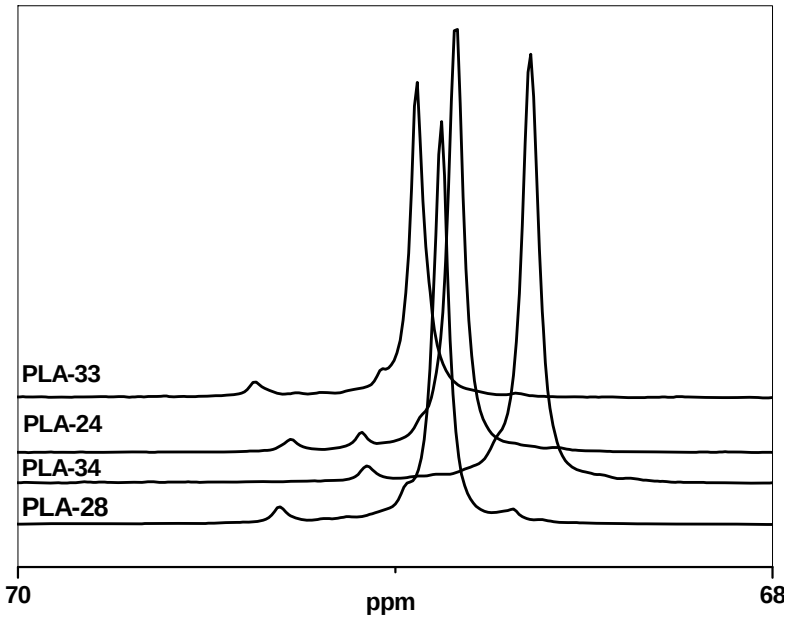

Figure 4.19: ^{13}C NMR spectra (500 MHz) methine areas of PLA oligomers PLA-33, PLA-24, PLA-34 and (b) PLA- 28.

The result of the analysis is shown in Figure 4.20 reports the MALDI-ToF mass spectrum of PLA. The oligomer was found to contain chain terminated by –OH on one side and –COOH on the other. The MALDI-ToF spectrum is dominated by series of intense peaks ranging from mass 617.23 to 1769.62 Da, corresponding to sodiated adduct molecular ion of type H- $[-O-CH(CH_3)CO]_n$-OH-----Na^+, (mass.72.on+18+23), where n is found to be ranging from 7 to 24 being the mass number of sodium (Na) ion that formed the adduct molecular ion. The spectrum shows other peaks of lower intensities, which described as potassiated ions (K^+ adduct molecular ions, mass = 72.0n+ 18+ 39, see peaks at 849, 921 and 1137 Da respectively.

Figure 4.21 shows the MALDI ToF spectrum of PLA-4. The most intense peak belonging to this series corresponding to oligomers with n = 11 to 20 in the spectrum.

Table 4.10: Experimental relative intensities of various regions in the C=O ^{13}C pattern of PLA stereocopolymers shown in Figure 4.14 to Figure 4.18

Polymer samples	169.04-169.2 Observed value (syndiotactic)	169.22-169.48 Observed value (heterotactic)	169.48-169.70 Observed value (isotactic)
oligomers	nd	0.034	0.965
PLA-4	nd	0.009	0.990
PLA-1	nd	0.012	0.987
PLA-15	nd	0.037	0.963
PLA-29	nd	0.022	0.978
PLA-30	0.055	0.037	0.909
PLA-31	0.136	0.151	0.712
PLA-32	0.078	0.159	0.798
PLA-33	0.092	0.132	0.775
PLA-34	0.338	0.661	nd
PLA-27	0.012	0.330	0.657
PLA-28	0.235	0.727	0.032
PLA-24	0.080	0.841	0.076
PLA-25	nd	0.071	0.929

nd-not detected.

The spectrum also shows the potassiated ions (mass = 72.0n + 39+18). see peaks from 1064 to 1279 Da). Figure 4.22 shows MALDI ToF spectrum of PLA-24 as expected and the spectrum shows a series of intense peak ranging from 832 to 1479 Da corresponds to sodiated adduct molecular ions (mass = 72.0n+ 18+ 23), where n is found to ranging from

11 to 20. The spectrum also shows the potassiated ions (mass=72.0n+39=18, see peaks from 832.40 to 1493.0). The spectrum shows some other mass series of lower intensity.

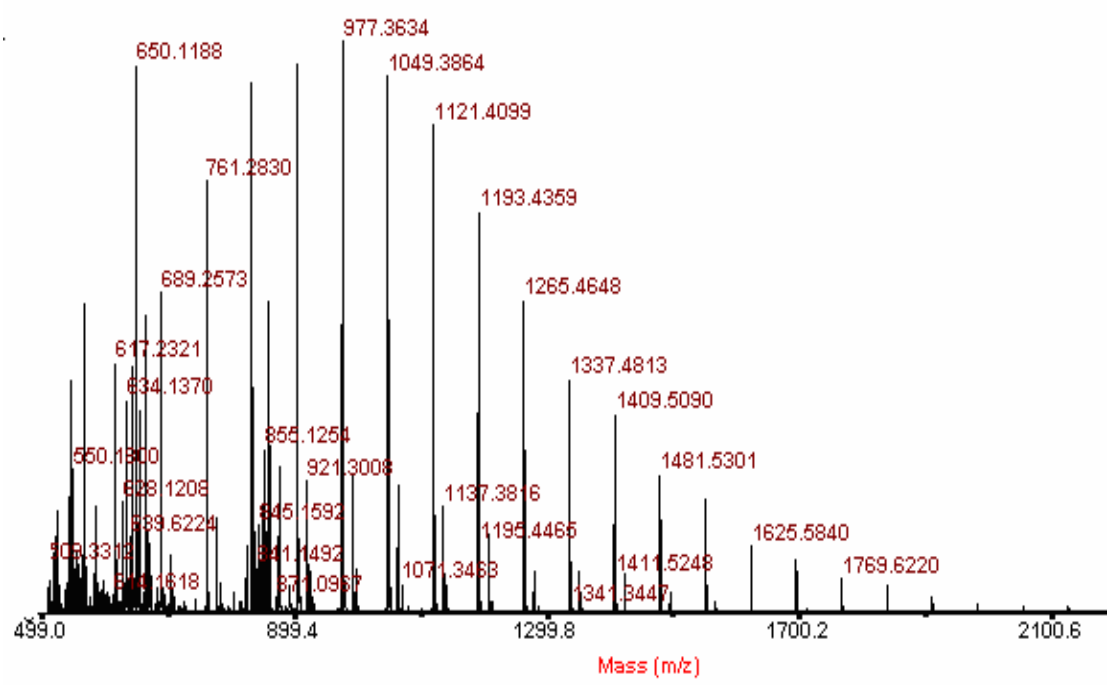

Figure 4.20: MALDI ToF spectrum of PLA prepolymer.

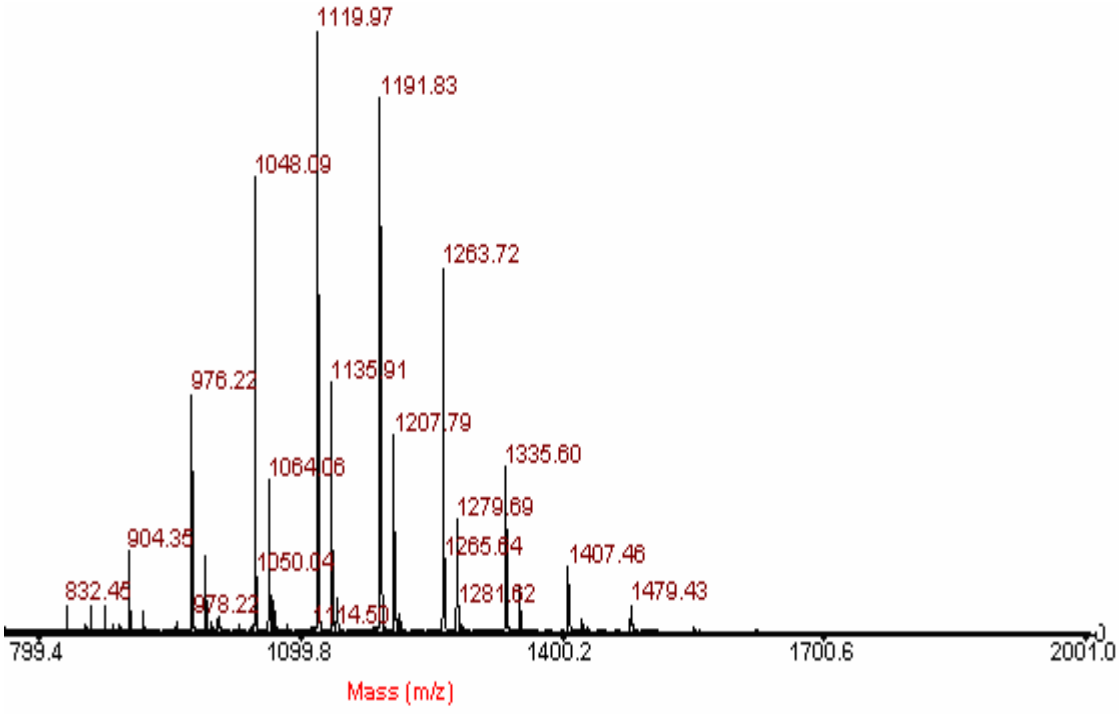

Figure 4.21: MALDI ToF spectrum of PLA-4.

Figure 4.23 shows MALDI ToF spectrum of PLA-25. The most intense peaks ranging from 526 to 1102 Da correspond to sodiated cyclic oligomer molecular ions where n range 7 to 15. The potassiated ions that appear in the region from 687 to 1263 Da are also of the cyclic oligomers present in this sample.

MALDI ToF mass spectrum shows a series of peaks ranging from 687 to1335 Da correspond to sodiated adduct molecular ions (72n+18+ 23), where n is found to ranging from 9 to 18. Some other peaks of lower intensity show the impurity profile of lactic acid present in end groups. The MALDI ToF spectrum of PLA-26 (Figure 4.24) shows the intense inset ranging from 527 to1246 Da corresponds to macrocyclic end group with sodiated molecular ions having masses (72,0n +23) and (72.0n+39), respectively.

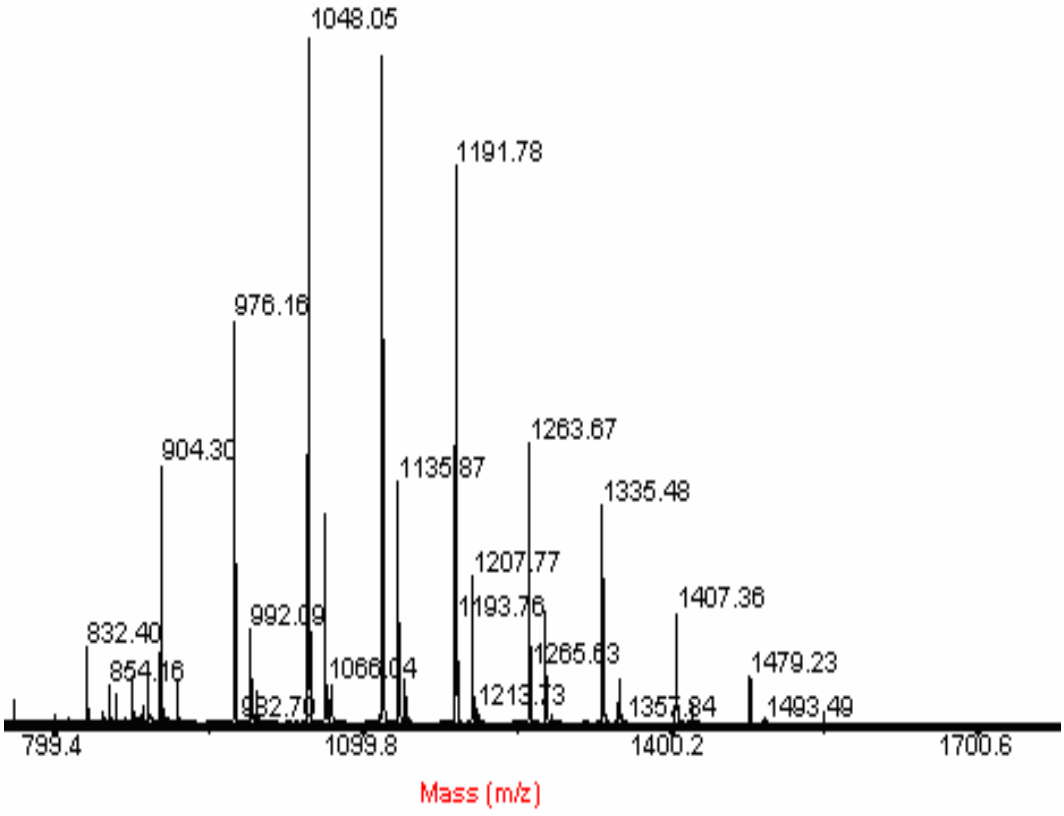

Figure 4.22: MALDI ToF spectrum of PLA-24.

The intensity of peaks due to cyclic compound falls sharply at higher molecular masses. The peaks ranging form 545 to 1121 are arising from sodiated molecular ions of linear

polymer chains. The sample expected to be formed by oligomers bearing $–COCH_3$ and –OH as terminal groups, corresponding to a general formula CH3-CO-[-O-CH(CH3)-CO]-OH----Na+, shows peak in this region have molecular mass (72.0n+60+23).

MALDI-TOF spectrum of PLLA oligomer (PLA-27) is shown in Figure 4.25. The mass spectrum of PLA-27 has both cyclic and linear polymer molecular ions with Na+ adduct and K+ adduct.

MALDI-TOF spectrum of PLLA oligomer (PLA-33) is shown in Figure 4.26. The spectrum shows both linear and cyclic polymer chains with sodiated and potassiated molecular ions having masses (72.0n+23 and 72.0n +39). The sample expected to be formed by oligomers bearing $–COCH_3$ and –OH as terminal groups, corresponding to a general formula CH3-CO-[-O-CH(CH3)-CO]-OH----Na+, shows peak in this region have molecular mass (72.0n+60+23).

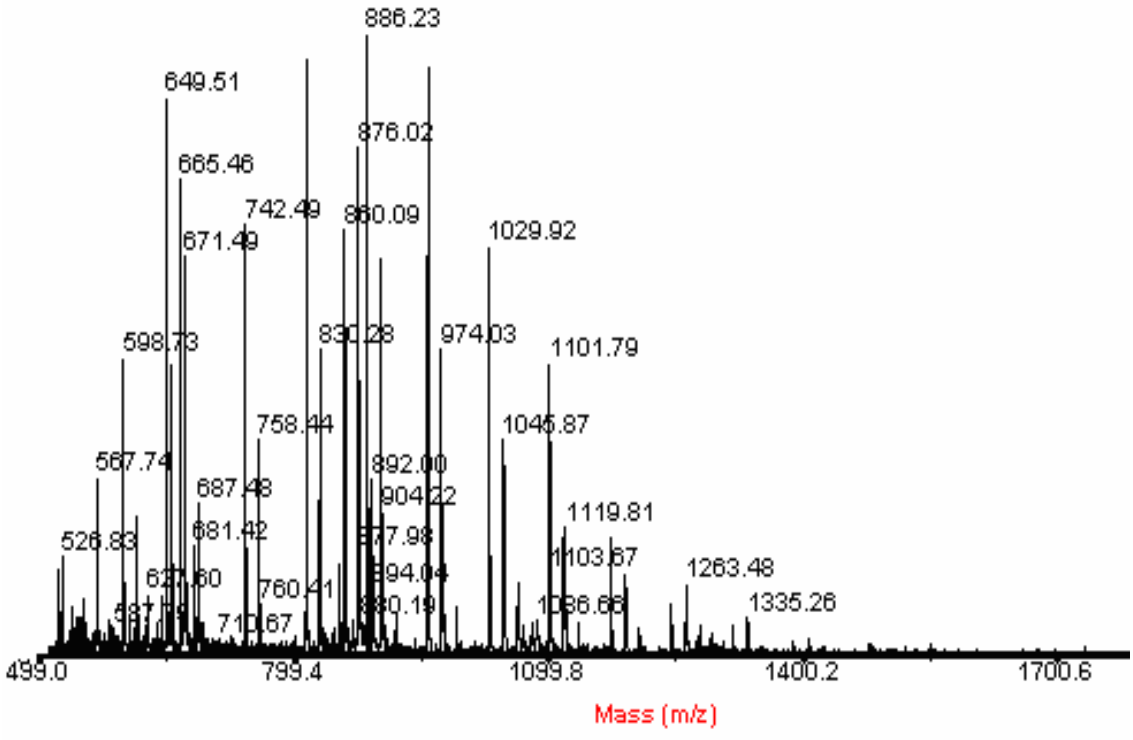

Figure 4.23: MALDI ToF spectrum of PLA-25.

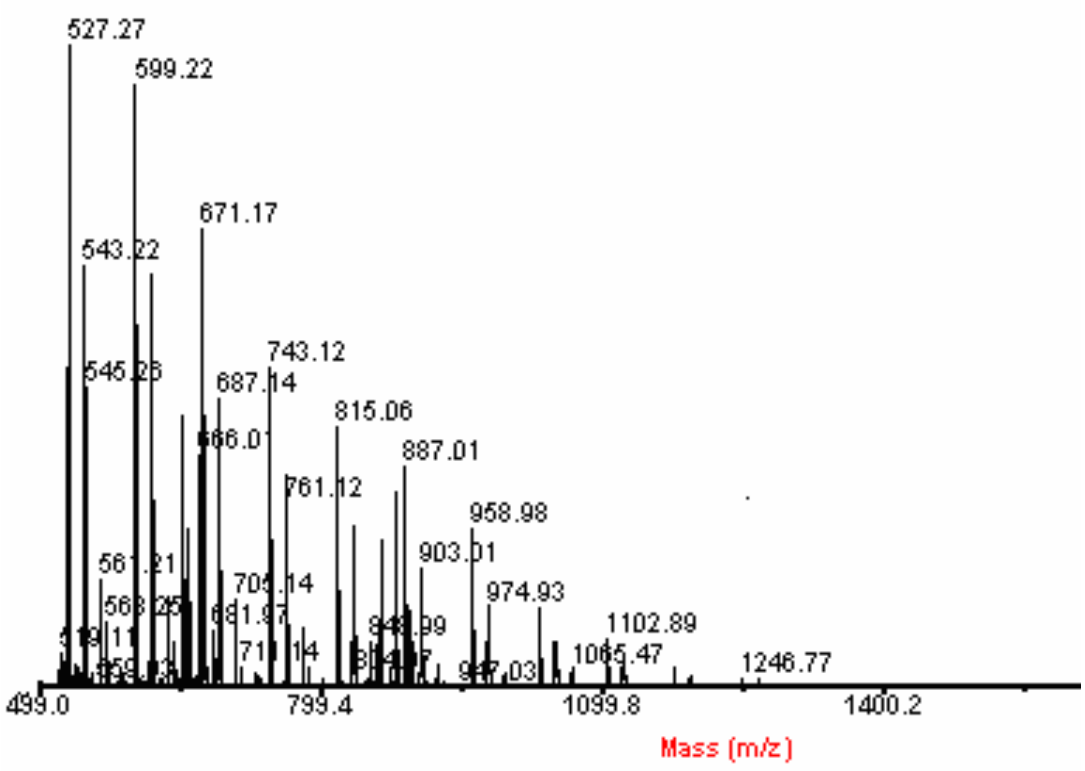

Figure 4.24: MALDI ToF spectrum of PLA-34.

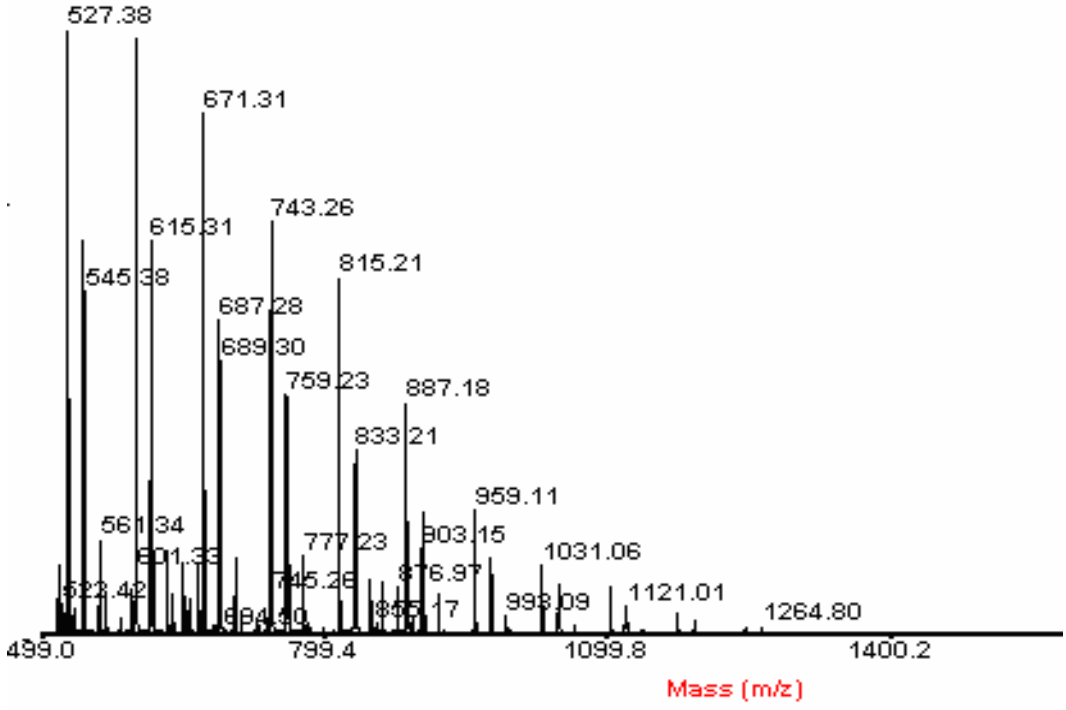

Figure 4.25: MALDI ToF spectrum of PLA-27.

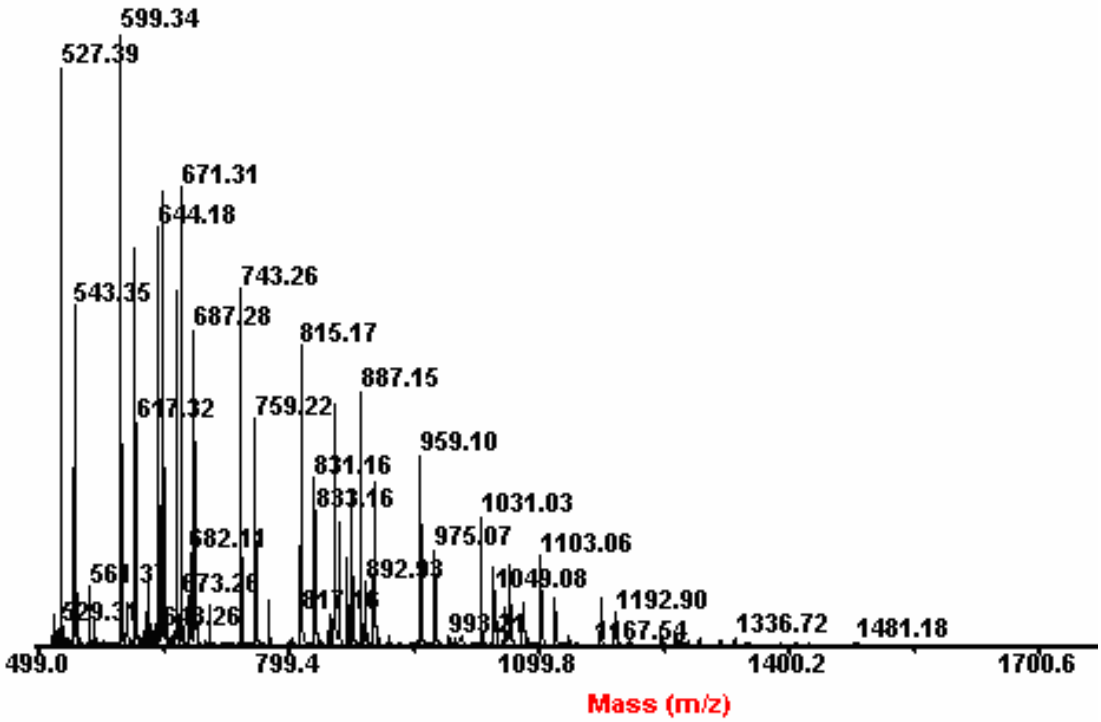

Figure 4.26: MALDI ToF spectrum of PLA-33.

4.6. Conclusion:

PLA prepolymers were synthesized by direct dehydropolycondensation using quartz reactor with Dean-Stark trap. Various types of zeolites such as ZSM-5, ZSM-12 and β-zeolite were used to reduce the small amount of water in ppm level from the reaction system (organic solvent). The longer the polymerization time (30 h), the higher the molecular weight of PLA became, because of the higher activation energy of the polycondensation. However, the highest molecular weight was about 42,000 ($\bar{M}_w$) was obtained when $SnCl_2.2H_2O$ was used as catalyst, β-zeolite as desiccating agent, reaction time (5 h) and reaction temperature (190 ^{0}C). NMR has confirmed the absence of L-lactic acid and lactide except PLA prepared by using anisole as solvent. MALDI-TOF also confirmed the presence of linear oligomer at 143 ^{0}C, mixture of linear and cyclic oligomer at 165 ^{0}C and predominantly cyclic oligomer at 190 ^{0}C. The carbonyl carbon atoms of L-lactic acid stereo polymers are sensitive to hexads at 125 MHz, when the resolution enhancement techniques were used. It was confirmed that the mechanism of dehydropolycondensation polymerization of L-lactic acid consists primarily addition of repeating units. PLA prepared at various conditions such as using β-zeolite as a desiccant, did not change the stereroesequence. However, we have shown that the

configurational structure of the polymers prepared at higher temperature are more complicated because of transesterification and redistribution at the ester bond under the experimental conditions. Other chemical reactions, such as the attack of polymer chain ester bond by active centers, might contribute to the configurational rearrangement and might be configuration dependent too. The more transesterification was observed in polar solvents in comparison to non-polar solvents. Polymer PLA prepared with $SnCl_2.2H_2O$ exhibits lower transesterification values in comparison with other reported catalysts in the literature. A stereospecificity favoring long isotactic block was detected. Increasing temperature and reaction time favors transesterification and thus, randomization of stereosequences. The maximum transesterification value was obtained in case of PLA-34. The structure property relationship of PLA can be tailor-made by choosing different dehydropolycondensation reaction parameters even if using L-lactic acid as starting materials.

References

1. Liggat, J. J. PCT Int. *Appl. WO 942870* (1994).
2. Shymroy, S.; Garnaik, B.; Sivaram, S. *Journal of polymer Science Part-A* **43**, 2164 (2004).
3. Vert, M.; Sehwarch, G.; Coudane. *J. Macromol. Sci. Pure Appl. Chem.* **A32**, 787 (1995).
4. Mitsui Toatsu Chemicals, Inc.; Enomoto, K.; Ajioka, M.; Yamaguchi. *A.USP 5310865* (1994).
5. Norio, Y.; Toshikazu, M.; Nobuko, T.; Yoruzu, Y. PCT Int. *Appl. WO 9712926* (1997).
6. Enomoto, K.; Ajioka. M.; Yamaguchi, A. *USP. 5310,865* (1994).
7. Kim, K.W.; Woo, S. I. *Macromol. Chem. Phys.* **203**, 2245 (2002).
8. Kasperszyk, J.E. *Macromolecule* **28**, 3937 (1995).
9. Espartero, J. L.; Rashkov, I.; Li, S.M.; Manolova, N.; Vert, M. *Macromolecules* **29**, 3535 (1996).
10. Hiltunen, K.; Harkonen, M.; Seppala, J. V.; Vaananen, T. *Macromolecules* **29**, (1996).
11. Bero, M.; Kasperszyk, J.E.; Jedlinsky, Z. *J. Makromol. Chem.* **191**, 2287 (1990).
12. Chabot, F.; Vert, M.; Chapelle, S.; Granger. P. *Polymer* **24**, 53 (1983).

Chapter-5

CHAPTER 5: HOMO AND COPLYMERIZATION OF ALEURITIC ACID WITH L-LACTIC ACID AND STUDY THE AGGREGATION BEHAVIOR IN DIFFERENT SOLVENTS

5.1. Introduction:

Aliphatic polyesters constitute an important class of polymers because of their biodegradability **[1]**, and biocompability **[2a, b]**, that enable their use in drug delivery systems, artificial tissues **[3a, b]**, and commodity materials. Polyesters are commonly produced through either condensation or ring opening polymerization using various catalysts **[4-6]**. Self-organization of condensation polymer is rare in the literature. Particularly, self-organization of amphiphilic polymers has resulted in assemblies such as micelle, vesicles, fibers, helical, superstructures and macroscopic tubes. These materials have potential application in areas ranging from material science to biological science. Thermo or pH sensitive polymer micelles **[7a, b]**, and vesicles **[7c]**, have been reported in which the nature of the functionality at the corona changes in response to the stimulus. A little attention has been paid to realize an environment-dependent switch from a micelle-type assembly with a lipophilic corona **[8]**. Here, we report a new class of aliphatic polyester superstructures that exhibit such properties.

Shellac is the only known commercial resin of animal origin. It is an important natural resinous product secreted by an insect (Laccifer lacca), which lives on the sap of some host trees. India is the major shellac producing country in the world. Shellac (Lac) is known to comprise of several hydroxyl acid unit, aleuritic acid and its esters have great importance in industrial domain. It is a valuable starting material for preparation of transparent water-clear adhesive, plasticizers **[9]**. Aleuritic acid has been used as a raw material for the synthesis of macrocyclic musk like lactones such as ambrettolide, civetone and exaltone. There is only one literature report of poly aleuritic acid, where aleuritic acid has been polymerized thermally and resulted insoluble product **[10]**. We demonstrate for the first time that the linear homopolymer of aleuritic acid (PAA) is obtained from aleuritic acid (Figure 5.1). The change in the surface of the assembly is the amplified consequence of change in molecular level conformation with each polymer chain due to the presence of 9, 10-hydroxy group in each monomeric unit. These

polymers with such properties could find use in the applications such as carriers for trafficking drugs and as components of smart adhesives. PAA is biocompatible and biodegradable polymer, which could find potential use in biological system.

Block copolymers are often used for a variety of supramolecular assemblies, in which the driving force involves the mutual immiscibility of the block and/or the immiscibility of one of the blocks in the bulk solvent. In case of poly (styrene-co-acrylic acid) block copolymers exhibit several interesting amphiphilic assemblies **[11-12]**. We aimed to synthesize aliphatic polyester by polycondensation. The hydrophilic 9, 10-hydroxy functionality, the hydrophobic methylene moiety are stitched in the same polymer backbone. The methylene group's greater than five units in a polymeric chain show zigzag conformation in the polymer molecule **[13]**.

The thermal polymerization of Aleuritic acid leads to insoluble product because both intra and intermolecular condensation are possible leading fast to the formation of fusible ethers, anhydrides, lactones and esters which ultimately become infusible and insoluble three dimensional network structures.

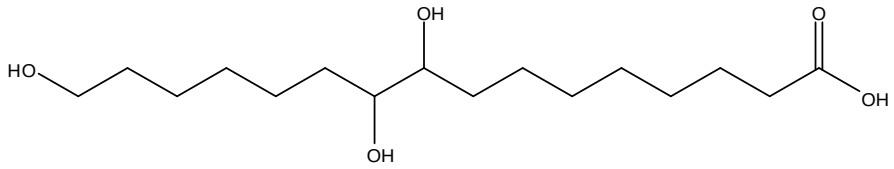

Aleuritic acid

Figure 5.1: 9, 10, 16-trihydroxy, palmitic acid (aleuritic acid).

These functional polymers can be post modified to crosslink the polymer, or to attach bioactive molecules such as peptides or drugs and have shown potential application in drug delivery systems and scaffold materials. The functional polyesters have tunable mechanical properties with in vivo degradability **[14]**. Polyesters syntheses have been explored by both chemical synthesis and enzymatic approaches. Several hydroxyl functional polyesters **[15-21]**, and poly (carbonate esters) **[22]**, have been synthesized. Polymers with vicinal diols were prepared by chemical polymerization of L-lactide with protected sugars **[23, 24]**, followed by deprotection **[25-27]**. Use of monomers, initiators with unsaturated bond enabled the introduction of epoxide groups by post modification reaction with m-chloroperbenzoic acid (m-CPBA), while treatment of allylic side chains

with NMO/OsO_4 resulted in dihydroxylation of side chains **[28]**. Chemical polymerization of unprotected hydroxyl functional caprolactones **[29]**, and hydroxymethyl substituted 1, 4-dioxan-2-ones **[30, 31]**, resulted in hyper branched structures with comparable molecular weights and degree of branching.

The biodegradable polymers are intensively aliphatic polyester of both natural and synthetic origin. Polyesters can be synthesized by polycondensation of hydroxyl acids or by ring-opening polymerization of cyclic esters (lactones), grafting, chain extension, or transesterification **[32]**. A wide range of monomers has been used to produce biodegradable polyesters. Their polymerizations can be carried out either in the bulk or in solution. The most useful monomers used for polycondensation are lactic, glycolic, hydroxybutyric acid and hydroxycaproic acids. Polyesters of glycolic and lactic acids are the main group of interest due to their long history of safety.

Lactic acid can be condensed with other hydroxyl acids such as 6-hydroxycaproic acid, glycolic acid, and hydroxybutyric acid or in the presence of diols, diacids, and diamines. Direct condensation usually resulted in low molecular weight copolymers that can then be further linked to yield high-molecular-weight polymers. In the second step, linking molecules such as diisocyanates, bis (amino-ethers), phosgene, phosphate, and anhydrides takes place **[33-35]**.

There is no report available so far, where the 9, 10 secondary vicinal diol is protected and the hydroxy and carboxylic acid groups are free to undergo dehydropolycondensation reaction to produce a linear high molecular weight homopolymer.

Fatty acids are suitable candidates for the preparation of biodegradable polymers **[36, 37]**, as they are natural body components and they are hydrophobic, and thus they may retain an encapsulated drug for longer time periods when used as drug carriers. Aleuritic acid (9, 10, 16-trihydroxy palmitic acid) is common C16 fatty acids with two secondary hydroxyl groups at 9, 10 positions and a primary hydroxyl group in the 16th position. It is produced from resin (Shellac).

The objective of this study is to incorporate aleuritic acid in lactic acid based polymers for the purpose of altering its physical properties. The trifunctionality of aleuritic acid (9, 10, 16-trihydroxy palmitic acid) does not allow forming the linear polymer. Previous study in our laboratory focused on the synthesis aleuritic acid (9, 10, 16-trihydroxy

palmitic acid) homopolymer. The homopolymer synthesized from aleuritic acid by protecting the 9, 10 hydroxyl groups with dimethoxy propane (DMP) to make –COOH and 16th position –OH group free for reaction to make linear polyester **[38]**. These copolymers have pendent hydroxyl groups for aggregation to form micro scale morphologies. Molecular self-assembly of organic molecules has generated a wide variety of objects with nanoscale or micrometer-scale morphologies including micelles **[39, 40]**, vesicles **[41, 42]**, ribbons **[43]**, films **[44]**, fibers **[45, 46]**, and tubules **[47-48].**

In this present work, we highlight the copolymerization of L-lactic acid (L-LA with protected aleuritic acid in presence of Lewis acid catalyst using dehyropolycondensation method. The resulted copolymers are pliable, soft, waxy or even viscous liquid copolymers influenced by the aleuritic acid content. The purpose of this study is to investigate the physical properties. In addition, deprotected copolymers focus micelle-like aggregates in various organic solvents and mixed organic solvent at various proportions.

5.2. Experimental:

5.2.1. Materials and Method: L-lactic acid was obtained from Purac as a 88% (w/w) aqueous solution with impurity , aleuritic acid, tetraphenyltin (Aldrich, USA), p-toluene sulfonic acid (PTSA) (Aldrich, USA), Xylene (S.D Fine Chemicals, India), anisole (Aldrich, USA), sodium sulphate, chloroform and methanol (S.D Fine Chemicals, India), mesitylene (Aldrich, USA), decaline (Aldrich, USA), and diphenyl ether (Fluka, Germany). All solvents were dried by using standard procedures for example toluene by distilling over metallic sodium. .All liquids were transferred by syringe under dry argon atmosphere.

5.2.2. Synthesis of methyl ester of aleuritic acid: Crude aleuritic acid was converted to methyl ester by using tetraphenyltin (TPT) as a catalyst in dry methanol solution at reflux temperature. The reaction mixture was refluxed for 9 h, during which reaction was monitored using TLC (solvent system; chloroform/ methanol 9/1). The ester was dried using rotavapour and further purified by column chromatography (chloroform/ methanol 9/1). The impurity profile was checked by gas chromatography (Figure 5.2 A and Figure 5.2 B). The ester was recrystallized using ethyl acetate, the crystal was dried under vacuum and the yield was calculated as 90 %, m.p : 71-72 ^{0}C , FT-IR (KBr) ν_{cm-1} : 1740-

1720 cm^{-1} ($\underline{COO}CH_3$). ^1H NMR (500 MHz): δ 3.66 (s, 3H, $COOC\underline{H_3}$), 3.64 (t, j = 5.24, 2H, $C\underline{H_2}OH$, 3.39 (bs, 2H –C<u>H</u>(OH)-C<u>H</u>(OH)), 2.30(t, j = 7.44,2H,-$C\underline{H_2}$-$COOCH_3$), 1.61-1.31(s, 22H, -$C\underline{H_2}$-).

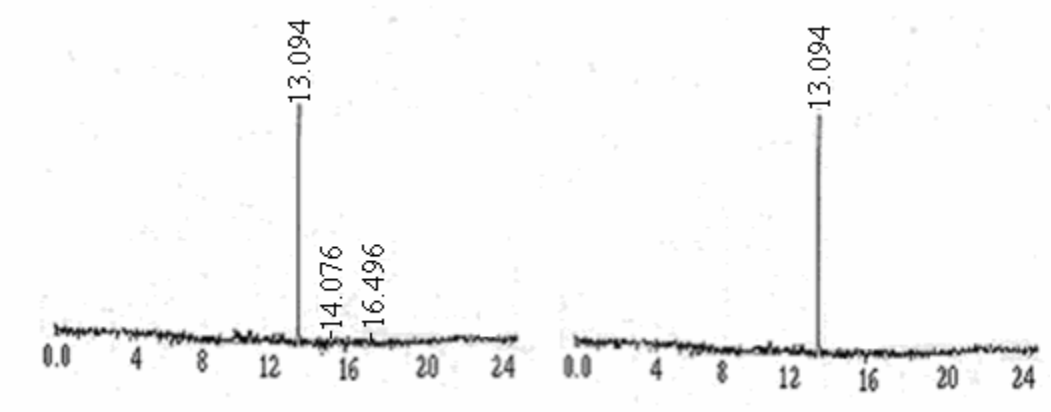

Figure 5.2A: GC of methyl ester of aleuritic acid before purification.

Figure. 5.2B: GC of methyl ester of aleuritic acid after purification.

5.2.3. Synthesis of protected aleuritic acid: Pure methyl ester of aleuritic acid (9, 10, 16 tri hydroxy hexadecanoate) (9 gm, 0.028M) was taken in a two-neck flask and equimolar quantity of dimethoxy propane was added, p-toluene sulfonic acid (PTSA) and the toluene were used as catalyst and solvent respectively. The reaction mixture was refluxed under the blanket of inert atmosphere (argon) for 6 h. After the completion of the reaction, the toluene was removed using rotavapour. The reaction mixture was washed several times with deionized water and extracted with chloroform. The chloroform layer was dried over Na_2SO_4 and finally stripped off. Finally, it was vacuum dried to give 8.2 gm (yield- 82%). The structure of protected methyl ester of aleuritic acid (ProAL) (monomer) FT-IR (KBr) ν $_{cm-1:}$ 1740.17cm^{-1}(-$\underline{COO}CH_3$), 1377.55 cm^{-1} and 1368.73 cm^{-1} (-O-$C(CH_3)_2$-O-). ^1H NMR (500 MHz) : δ 3.66 (s, 3H, -$COOC\underline{H_3}$), 3.64 (t, j = 5.64, 2H, $C\underline{H_2}OH$), 3.56 (bs,2H –C<u>H</u>-(O)-C<u>H</u>(O)-), 2.17 (t, j =7.44,2H, -$C\underline{H_2}$-$COOCH_3$), 1.38,(s, 6H, -C-$(CH_3)_2$-) , 1.50-1.31 (s, 22H, -CH_2-). 1.31 (s, 22H, -CH_2-).

5.2.4. Homo polymerization of ProAL: The monomer (ProAL) was taken in three-neck flask and equipped with Dean Stark apparatus, the requisite amount of TPT catalyst was used for the polymerization using various solvents. The characterization of these polymers (PALs) were carried by SEC, DSC, SEM and ^{13}C NMR.

5.2.5. Deprotection of homopolymer: The homopolymers were dissolved in chloroform in a single neck flask and equal amount of methanol, catalytic amount of PTSA was added into it. The reaction mixture was stirred at room temperature (25 ^{0}C) under inert atmosphere (argon) for 6 h. The resultant polymer was washed with methanol several times and GC confirmed the absence of dimethoxy propane. ^{13}C CP/MAS NMR, DSC, and TEM confirmed the structure of PAA.

5.3. Characterizations:

5.3.1. FT-IR: IR spectra were recorded as KBr pellets, on Perkin-Elmer Infrared Spectrometer Model 16PC FT-IR, using sodium chloride optics. IR bands are expressed in frequency (cm^{-1}).

5.3.2. Size Exclusion Chromatography Molecular weight (SEC): As discussed in Chapter 3

5.3.3. Differential Scanning Calorimetry (DSC): Differential scanning calorimetry (DSC) measurements were performed on a thermal analyzer in nitrogen atmosphere. The measurements were run from –90 to 200 ^{0}C at a heating rate of 10 ^{0}C / min and at a cooling rate of 100 ^{0}C/min. The glass- transition temperature (T_g) and the crystallinity data were recorded from the second and first heating curves, respectively.

5.3.4. Nuclear Magnetic Resonance Spectroscopy (NMR): For NMR measurements, the polymer samples were dissolved in chloroform–d in 5mm diameter. NMR tubes at room temperature.^{1}H NMR spectra were recorded on Bruker DRX 500 MHz with 4 % w/v concentration of solution. The chemical shifts in parts per million (ppm) are reported up field with reference to internal standard chloroform-d at 7.25 ppm. The sample concentration for ^{13}C NMR measurements was 10 % by weight. Proton decoupled ^{13}C NMR spectra with NOE were recorded on Bruker DRX 500 MHz spectrometer working at 125.577 MHz for carbon-13. A digital resolution of 32 K data points/ 18,000 Hz spectral width was used a pulse angle of about 30 along with a relaxation delay of 2s and 10^3–10^4 transients were accumulated. $CDCl_3$ served as solvent and TMS as internal standard for all ^{13}C- NMR measurements. Relative peak areas were proportional to the number of carbon atoms. Peak areas were calculated by deconvolution method using XWIN-PLOT software.

5.3.5. ^{13}C *Cross Polarization /Magic Angle Spinning (*^{13}C *CP/MAS):* ^{13}C CP/MAS NMR spectra were measured with Bruker MSL-300 NMR Spectrometer (75.5 MHz) with CP/MAS accessory at room temperature (25 ^{0}C). The sample powder (ca. 200 mg) was placed in a cylindrical ceramic rotor and spun at 3 KHz. Contact time and repetition time were 2ms and 5s respectively. Spectral width and data points were 27KHz and 8 K respectively. The ^{1}H field strength was 2mT for both the CP and decoupling processes. The number of accumulations were 160-200, ^{13}C Chemical shifts were calibrated indirectly with reference to the higher field adamantane peak (29.5 ppm relative to tetramethlysilane ($(CH_3)_4Si$). The Hartmann-Hann condition was matched using adamantane in each case. The experimental errors for the chemical shifts were within ± 0.1 ppm for broad peaks as described.

5.3.6. Transmission Electron Microscopy (TEM):

5.3.6a. Sample preparation: The sample was dissolved in solvents and mixture of solvents to understand the aggregation behavior. The solutions were collected on 300 mesh carbon coated copper grids. The copper grids were kept overnight on filter paper for drying. TEM imaging was performed using a JEOL 1200EX electron microscope operating at an accelerating voltage of 80 kV. Images were captured using charged couple detector camera and viewed using Gatan Digital Micrograph software.

5.4. Result and Discussion:

Synthesis of poly (aleuritic acid) from aleuritic acid is depicted in Figure 5.3. At the outset, methyl ester of Aleuritic acid was prepared and the hydroxyl groups at 9, 10 position were protected by dimethoxy propane. Protected poly (aleuritic acid) (ProAL) was prepared from protected methyl ester of aleuritic acid by polycondensation method using tetraphenyltin and xylene as catalyst and solvent respectively.

5.4.1. Molecular weight determination: Poly (aleuritic acid) was obtained from protected poly (aleuritic acid) by simple deprotection. At the out set, the effect of polymerization reaction time (5 to 20 h) was studied and shown in Table 5.1. The number average molecular weight ($\bar{M}_n$) and weight average molecular weight ($\bar{M}_w$) increased with reaction time to a certain extent (15h) and thereafter declined. The obtained homopolymer in all the cases were soluble in various solvents such as dioxane and dimethylformamide etc. It was observed that at low molecular weight range up to

15,500 Da, the distribution is comparable with the high molecular weight ($\bar{M}_w$=120, 000 Da).

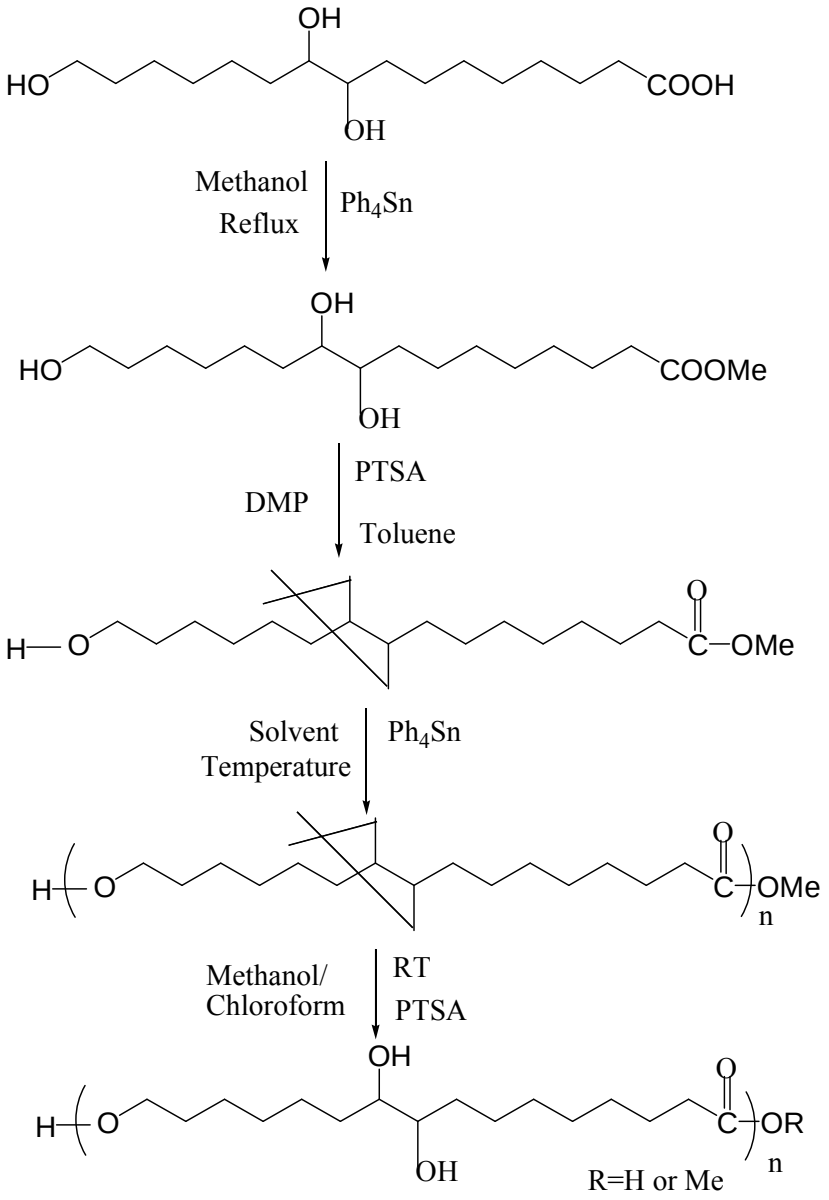

Figure 5.3: Scheme of polymerization of monomer.

The molecular weights were cross checked with light scattering experiments. The highest molecular weight (Mw) was calculated as 98,000. The hike in molecular weight observed may be attributed due to hydrolysis of some protected groups. The hydrolysis of small amount of protected groups do not affects the solubility but micelle structures may be formed which affects the hydrodynamic volume and ultimate high molecular

weights were observed. The low molecular model ester polymer will be prepared and affect of deprotected group on molecular weights will be examined.

5.4.2. Thermal analysis: DSC data of PAL-3 in Figure 5.4A showed two melting points (T_m) at -39.0 and –17.0 ^{0}C respectively. The T_m value of poly (12-hydroxy stearic acid) has also been observed as –20 ^{0}C **[49]**. These two different melting temperatures of PAL-3 may be due to different crystalline structure in the polymer molecule. DSC analysis of deprotected sample (PAA) in Figure 5.4B showed the values of glass transition T_g and melting transition T_m are -15.50 and 75.07 ^{0}C respectively.

The second DSC heating curve showed two distinctly difference peaks (melting transitions), of almost similar intensity (T_{m1}= 43.73 ^{0}C / ΔH_f =14.24 J/g and T_{m2} = 70.0 ^{0}C / ΔH_f =29.90 J/g). These two different melting temperatures of PAA may be attributed due to the indication of disturbances in the crystalline growth of the PAA phase. The T_g of PAA was observed in second DSC curve as –29.3 ^{0}C.

5.4.3. ^{13}C Nuclear Magnetic Resonance Spectroscopy: The ^{13}C NMR spectra of PAL are shown in (Figure 5.5 A) and dept in (Figure 5.5 B). The ^{13}C NMR spectra show a resonance peak at 173.81 ppm that corresponds to carbonyl carbon. The peak at 107.76 ppm is due to the quaternary carbon atom of the protecting group. The peak at 80.97 ppm is attributed due to 9 and 10 methine groups linked covalently to the oxygen atom of protecting groups. The peak shown at 64.27 ppm is appeared due to primary alcohol group (-$\underline{C}H_2OH$), which is attached to the end groups of the polymer.

Table 5.1: Effect of reaction time on polymerization reactions of proAL

Polymer samples	Time (h)	Yield (%)	$\bar{M}_n$ (GPC)	$\bar{M}_w$ (GPC)	PDI (GPC)	$\bar{M}^w$ (LS)	T_{m1} (^{0}C)	T_{m2} (^{0}C)	ΔH_1 (J/g)	ΔH_2 (J/g)
PAL-1	5	99.2	2,800	6,400	2.2	nd	-47.0	-3.6	3.2	0.85
PAL-2	10	99.0	34,100	82,000	2.4	75,400	-41.2	-14.2	2.9	0.52
PAL-3	15	98.0	46,100	120,000	2.6	98,000	-34.7	-18.7	1.6	6.93
PAL-4	20	98.0	5500	15,500	2.8	nd	-42.1	-13.2	2.9	0.53

Xylene as a solvent, nd –not determined and temperature of polymerization 145 ^{0}C

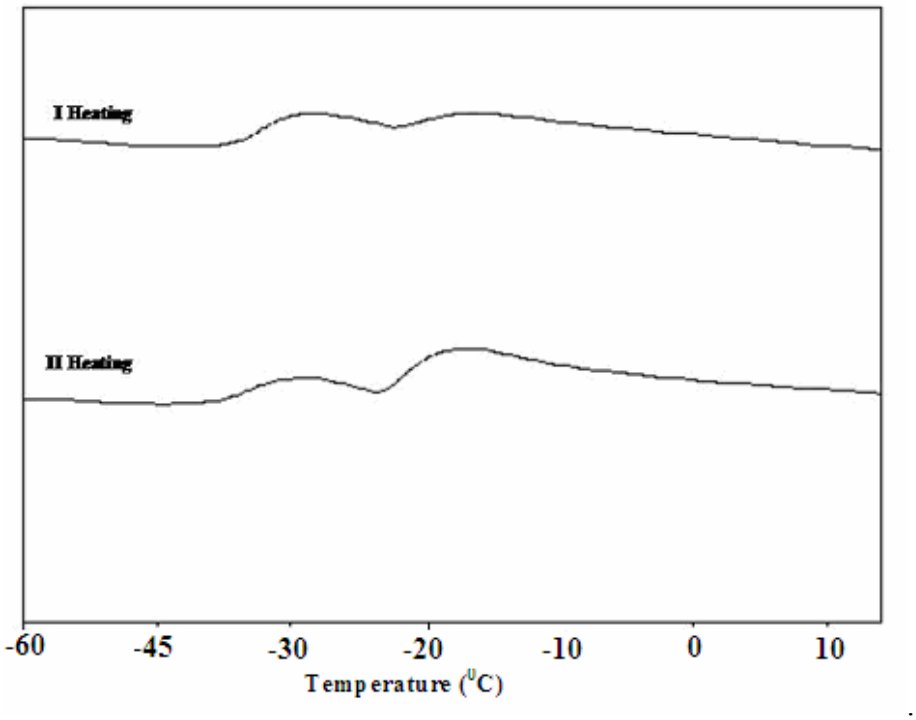

Figure 5.4A: Differential scanning calorimetry (DSC) first and second heating, thermograms showing melting points (PAL).

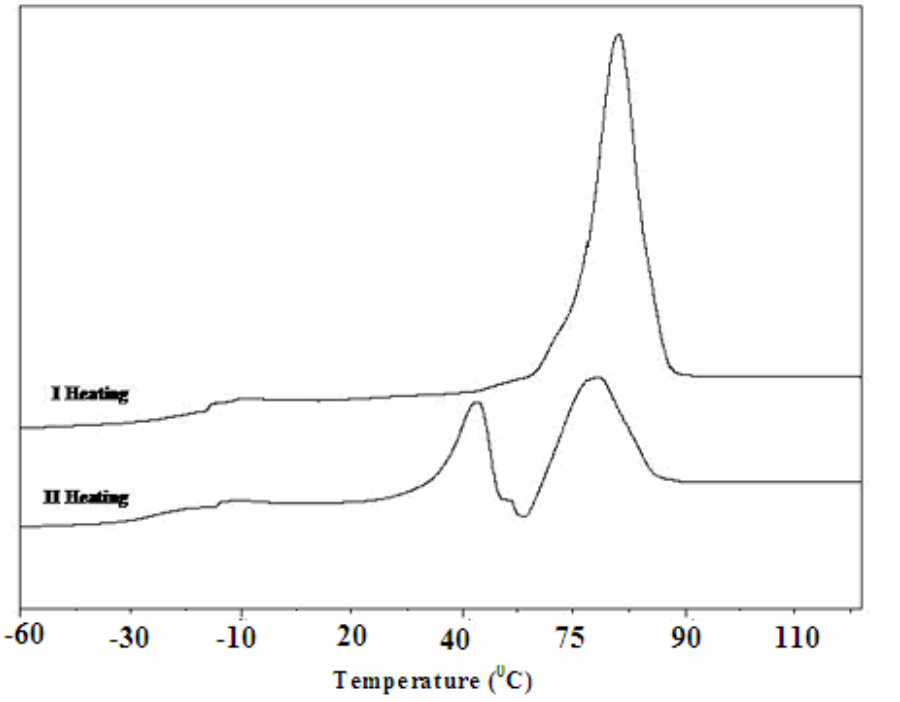

Figure 5.4B: Differential Scanning Calorimetry (DSC) first and second heating thermograms showing melting points and glass transition points respectively (PAA).

The peaks at 34.30 ppm, 32,93 ppm, 29.11ppm, 26.03 ppm and 24.93 ppm are due to the methylene groups present in the polymer backbone. The peak at 27.31 ppm is attributed due to methyl group of the protecting group. The peak at 51.43 ppm (-COO$\underline{C}H_3$) is appeared due to CH_3 group attached to ester linkage. The $\bar{M}_n$ calculated from ^{13}C NMR (quantitative) spectra is 15600 Da. All the assignments confirmed the structure of PAL-3. The end groups of the homopolymers were -$COOCH_3$ and -CH_2OH.

The ^{13}C NMR spectrum of PAA is shown in Figure 5.6 A. ^{13}C CP/MAS NMR spectrum shows the resonance, which corresponds to various groups such as 27.30-34.07 ppm (-$\underline{C}H_2$ group), 65.11 ppm (-COO$\underline{C}H_2$) and 75.47 ppm (-$\underline{C}$HOH—$\underline{C}$HOH-) and 174.75 ppm (-$\underline{C}$OO-) respectively. The linear structure of PAA was confirmed by NMR.

5.4.4. Effect of catalyst concentration on polymerization reaction: Table 5.2 shows the effect of catalyst concentration on polymerization reaction. The catalyst concentration was varied from 0.1- 0.4 wt %. The molecular weight and molecular weight distribution increased up to 0.3 wt % as the catalyst concentration increased and thereafter decreased irrespective of yield. The result shows that the reaction proceeds linearly up to 0.3 wt % catalyst. Lewis acid-catalyzed polycondensation is a reversible equilibrium reaction and aliphatic polyester is known to undergo an irreversible, thermal unzipping, back-biting side reaction, which is also Lewis acid catalyzed, giving rise to reduction of moleculer weight and simultaneous formation of cyclic compound, the amount of catalyst used, therefore play a critical role. The mechanism of esterification by tin and tin derivative catalysts in general is well discussed in the literature **[50]**, while the reaction pathway of tetraphenyltin is yet unknown. There is a possibility of alcoholysis one, two, three or all four of the Sn-C linkages of tetraphenyltin in presence of alcohol and protected ester of poly (aleuritic acid) in the reaction system leading to alkoxy-tin or tin carboxylate covalent linkage **[51]**.

Table 5.3 illustrates the effect of reaction temperature on polymerization reaction. The polymerization reactions were carried out in various sets of nonpolar solvents starting from xylene (145 ^{0}C), mesitylene (165 ^{0}C) to decaline (190 ^{0}C). Similarly the reaction was carried out in polar solvents namely anisole (154 ^{0}C) and diphenylether (190 ^{0}C). The yield of the polymer was comparable either in nonpolar solvent or polar solvents.

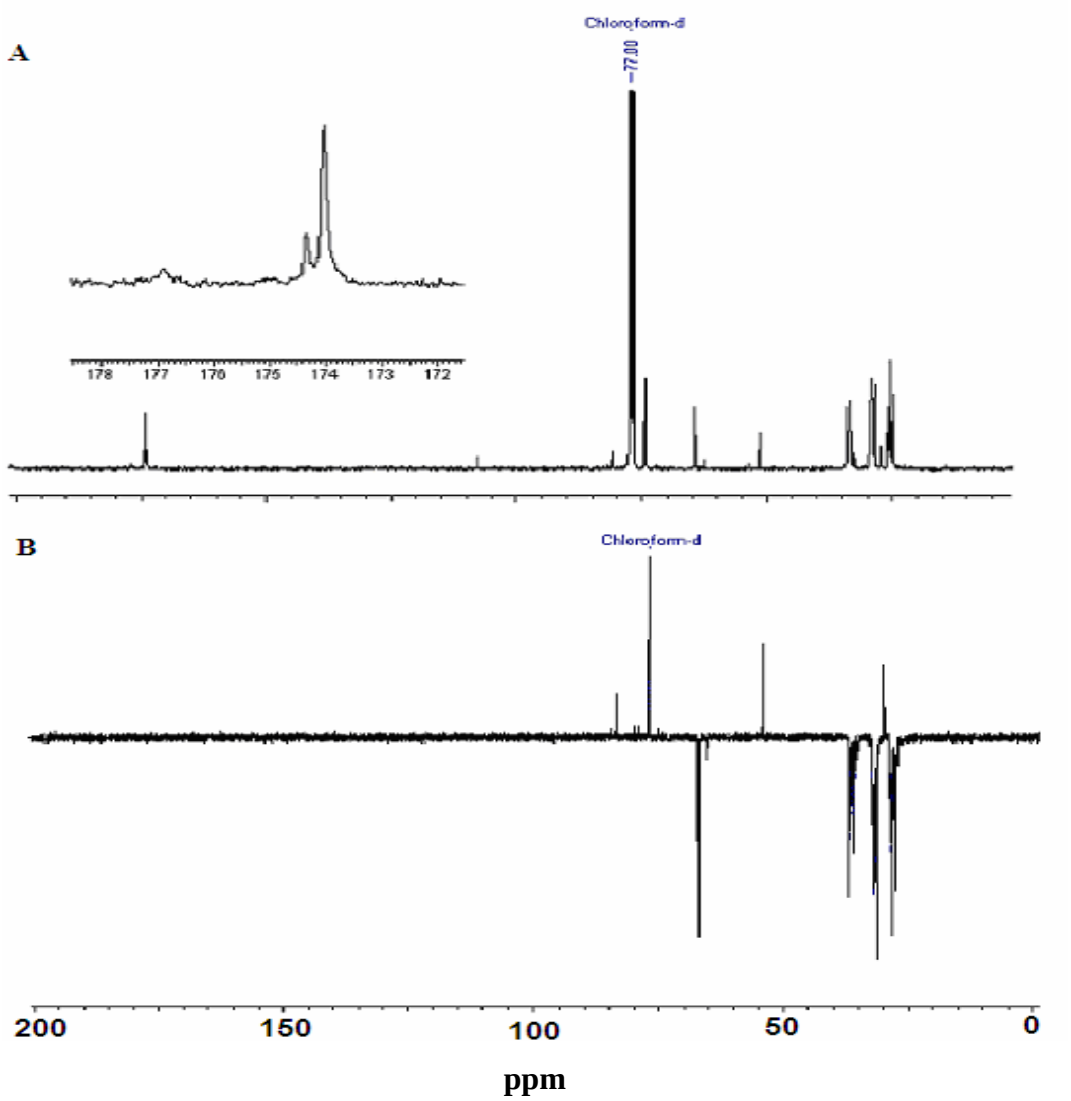

Figure 5. 5: (A) ^{13}C NMR (500 MHz) of protected poly (aleuritic acid) and (B) DEPT of PAL-3.

5.4.5. Effect of reaction temperature on polymerization reaction: It is important to note that the molecular weight increased with increased in reaction temperature (reflux temperature) of the solvent. DSC data showed two melting temperatures, which increased with increase in reaction temperature. The reaction was carried out at 190 ^{0}C (decaline reflux temperature) and yellow hard soluble material was observed. The ^{13}C CP/MAS NMR of the cross linked polymer is shown Figure 5.6.B which showed resonance at various positions. There are number of reactions occurred in cross linking reaction i.e. etherification as well as small esterification.

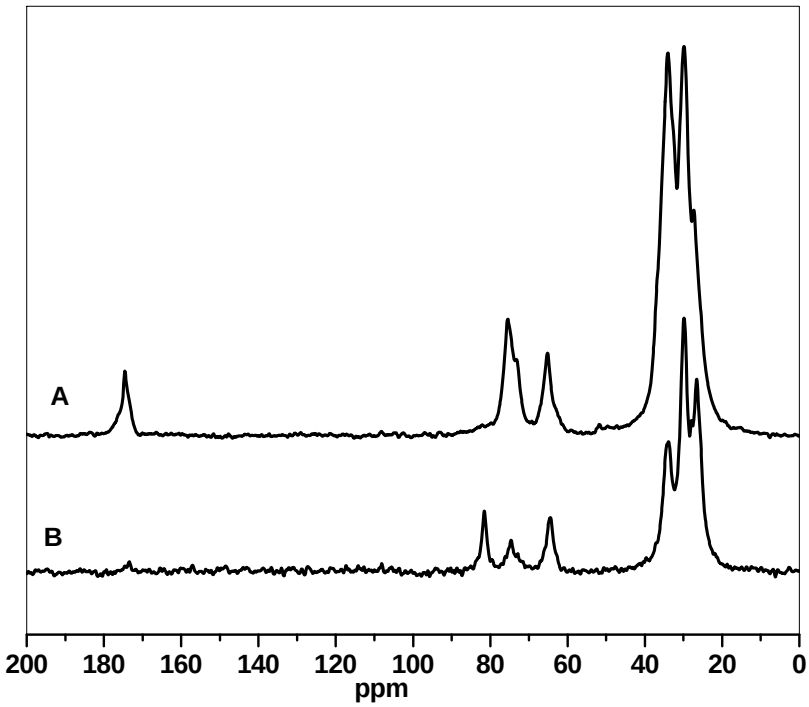

Figure 5.6: (A) ^{13}C CP/MAS (Cross Polarization/ Magic Angle Spinning) N.M.R. (500 MHz) of poly (aleuritic acid) and (B) ^{13}C CP/MAS of polymer PLA-10.

Table 5.2: Effect of catalyst concentrations on polymerization reactions of proAL

Polymer samples	Cat. conc. (wt.%)	Yield (%)	$\bar{M}_n$ (GPC)	$\bar{M}_w$ (GPC)	PDI	$\bar{M}_w$ (LS)	T_{m1} (^{0}C)	T_{m2} (^{0}C)	ΔH_1 (J/g)	ΔH_2 (J/g)
PAL-5	0.1	99.2	2,500	5,000	2.0	nd	-38.2	-18.1	2.4	0.36
PAL-6	0.2	99.0	3,100	6,900	2.2	nd	-38.4	-17.9	2.3	0.29
PAL-3	0.3	98.0	46,100	120,000	2.6	98,000	-39.0	-17.0	2.2	0.34
PAL-7	0.4	98.0	8200	24,000	2.9	21,200	-39.4	-16.9	2.1	0.32

Xylene as a solvent, nd –not determined and temperature of reaction 145 ^{0}C.

The products formed were fusible ethers, lactones and small amount of ester group, insoluble product of three-dimensional structures, which were confirmed by solid-state ^{13}C CP/MAS NMR spectroscopy. The peaks correspond to 81.59 ppm is due to intermolecular reaction result (-CH-O<u>C</u>H-). The peak for two carbons involved in the

intramolecular ether groups appeared at 67.08 ppm. Both the carbons in CH-O-CH structure have the same environment. The peak at 65.93 ppm is due to (-CH-O-CH-) group.

The peak region from 26.5 to 37.2 ppm corresponds to methylene region. All the three hydroxyl and one-carboxylic groups of aleuritic acid capable of entering into reactions both in the form of inter and intra-molecular condensation. Many broad peaks were observed, indicating the absence of selectivevely in the chemical polymerization. GPC analysis of this polymer was difficult due to its low solubility. DSC analysis of the polymers did not show a melting transition. The polymer obtained in anisole showed $\bar{M}_n$ = 821, $\bar{M}_w$ =2100 and dispersity 2.6 respectively. The two observed T_ms are –40.6 and –14.7 ^{0}C. Similar reaction was carried out in diphenylether at 190 ^{0}C and low molecular weight polymer was observed.

Table 5.4 showed the comparison results of PAL-3 and PAA. The number average molecular weight ($\bar{M}_n$), weight average molecular weight ($\bar{M}_w$) and distribution of PAL-3 are shown in Table 5.4. The melting temperatures T_{m1}= -39.0 and T_{m2}= -17. 0^{0}C were observed in PAL-3. T_g of PAL-3 was not observed until -90 ^{0}C. T_g may be lower than –90 ^{0}C, which is beyond our instrument limitation. PAL-3 was deprotected with mild experimental condition. DSC data showed a single melting temperature at 75.07 ^{0}C, which may be attributed due to aggregation of pendent hydroxyl groups and similar crystallite structure. The glass transition temperature (T_g) was determined as –29.3 ^{0}C. The increase in Tg and Tm may be attributed due to –OH group interference.

The $\bar{M}_w$ =120,000, $\bar{M}_n$= 46,100, PDI = 2.6 and average DP were determined by size exclusion chromatography (SEC) against polystyrene standards. Hydrolysis of protected poly (aleuritic acid) afforded free hydroxyl groups at, 9 and 10 position of each monomeric unit of the polymer. The homopolymers are linear and soluble in various solvents such as N, N-dimethyl formamide (DMF) and dioxane etc.

5.4.6. TEM analysis: The consequences of 9, 10 hydroxyl groups and aliphatic methylene groups in the main chain of the polymer, the key hydrophilic and hydrophobic functionalities in PAA polymer, within the same monomer of homopolymer should be interesting from an intermolecular phase separation perspective **[52]**.

Table 5.3: Effect of temperature on polymerization reactions of proAL

Polymer samples	Solvent	Yield (%)	Temp. (^{0}C)	$\bar{M}_n$ (GPC)	$\bar{M}_w$ (GPC)	PDI	$\bar{M}_w$ (LS)	Tm_1 (^{0}C)	Tm_2 (^{0}C)	ΔH_1 (J/g)	ΔH_2 (J/g)
PAL-8	A	99.2	145	2,800	6,400	2.2	nd	-47.0	13.6	3.2	0.85
PAL-9	B	98.0	165	17,600	46,000	2.6	44,000	-38.2	17.8	1.6	0.3
PAL-10	C	-	190	-	-	-	nd	-	-	-	-
PAL-11	D	99.0	154	821	2,100	2.6	nd	-40.6	14.7	1.2	0.5
PAL-12	E	-	190	-	-	-	nd	-	-	-	-

Reaction time 5 h, nd-not determined and A= Xylene, B= mesitylene, C=decaline, D= anisole and E= diphenyl ether

Table 5.4: Comparison results of PAA and PAL polymers

Polymer	$\bar{M}_n$ (GPC)	$\bar{M}_w$ (GPC)	$\bar{M}_w$ (LS)	T_g (^{0}C)	ΔC_p (j/g*^{0}C)	T_{m1} (^{0}C)	T_{m2} (^{0}C)	ΔH_{f1} (J/gm)	ΔH_{f1} (J/g)
PAL-3	46,100	120,000	98,000	>100	nd	-34.7	-18.77	1.67	6.93
PAA	nd	Nd	nd	-29.3	0.075	75.07	nd	61.72	nd

nd- not determined

The hydrophilic hydroxyl unit and methylene moiety will be placed on the opposite sides of the polymer backbone in solvents of different polarity. The hydrophobic and the hydrophilic functionalities are stitched together within the same monomer in polymers. Therefore, it may be expected that the spatial distribution of the interior groups of the assembly closely followed the distribution of the functionalities in the corona. Close examination of the normal structure is shown in (Figure 5.7). The core part of the new structure is folded methylene groups, which are dark, and hydroxyl pendant groups are in the periphery. Multiple morphologies of PAA in various solvents such as polar solvents

and nonpolar solvents and structure property relationship through morphologies were obtained by using TEM.

The polymeric solution in polar solvents was optically clear. Typical TEM photographs for the poly (aleuritic Acid) are displayed in Figure 5.7 and explained the structure of the assemblies. The images obtained from PAA polymer in dioxane and N,N-dimethyl formamide (DMF) are shown in Figure 5.7 (A and B) respectively. The observed solubility characteristic may be attributed to the formation of micelle like structure in dioxane, N, N-dimethyl formamide (DMF), in which the hydrophilic hydroxyl groups are exposed to the bulk solvent and the hydrophobic methylene groups are tucked in the interior of an assembly (Figure 5.7 A and B). Similarly, an inverted micelle-like structure would be expected in a nonpolar solvent, in which the functional group placements are, reversed (Figure 5.7 C). The structural hypothesis also suggests that the hydrophilic hydroxyl groups and hydrophobic methylene moiety will be placed on the opposite sides of the polymer backbone in the solvents of different polarity. The image obtained from polymer exhibit darker core compared to the corona. The darker contrast provided by methylene chains of backbone of PAA are shown in TEM images (Figure 5.7 A and B). For the interaction of the electron beam with material of the polymer, carbon forms a decisive amongst majority of the elements. Further the density of backbone carbon is slightly greater than that of hydroxyl group and hence we except PAA having higher density to appear dark in the TEM image. The TEM picture of pure PAA reflected this in explanation. The image obtained in Figure 5.7 C from toluene solution of polymers was consistent with the expected features. However, nonspherical micelles in solution have been observed only rarely and mostly indirectly.

5.5. Copolymerization of L-lactic acid with aleuritic acid: The homopolymer of protected aleuritic acid was found to be transparent, viscous liquid, which showed a low crystalline melting point and glass transition temperature. By virtue of its low glass transition protected poly (aleuritic acid) could be expected to impart some flexibility to poly (L-lactic acid) (PLA) as a plasticizer. The processing of PLA addresses lot of problems. The copolymers containing protected aleuritic acid is expected to behave as a plasticizer whereas the same copolymer after deprotection might improve the rheological properties due to occurrence of small branching on the PLA chain. Copolymerization of protected

aleuritic acid with L-lactic acid was attempted to improve structure property relation during processing.

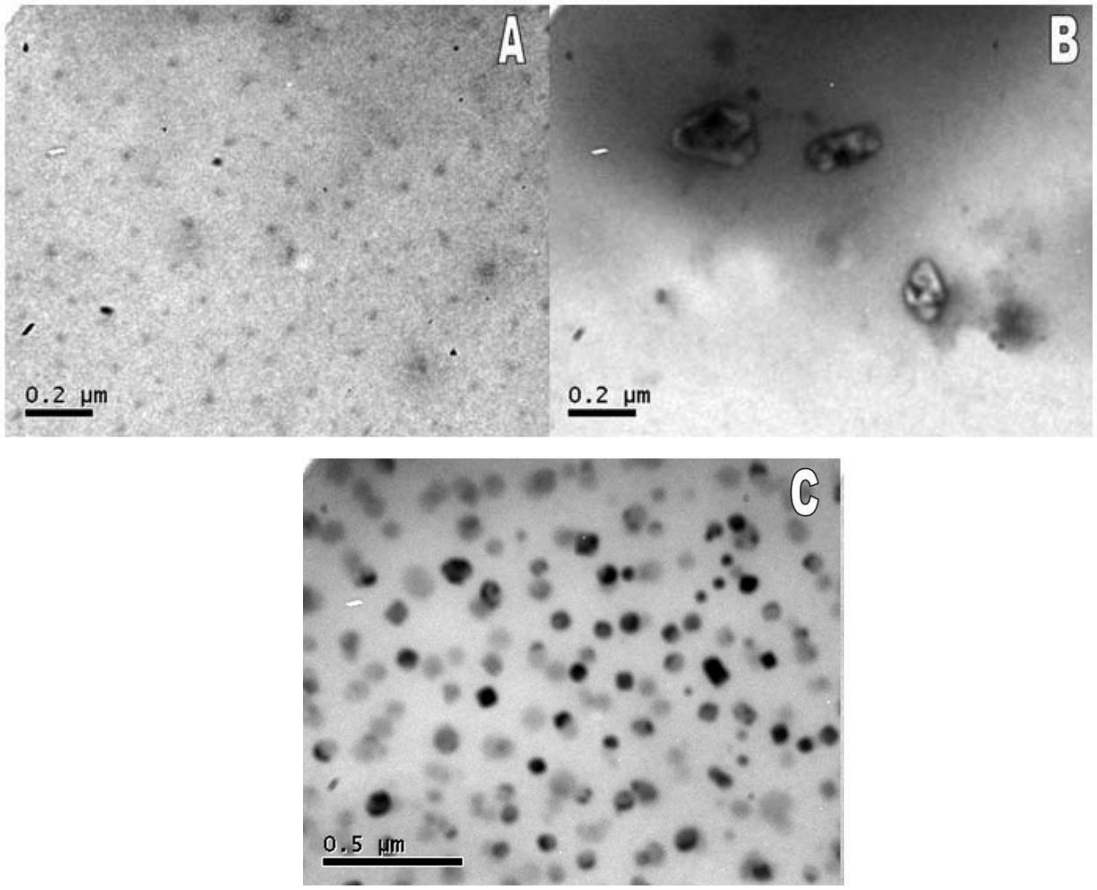

Figure 5.7: TEM images of the micelle-like and inverted micelle-like structures formed by PAA polymer (A) Image of normal micelle-like particle from dioxane, (B) Image of micelle-like particle from DMF and(C) Image of inverted micelle-like particle formed by a toluene solution of PAA.

The synthesis of protected aleuritic acid was carried out and characterized. The synthesis of L-lactic acid- protected aleuritic acid copolymers was accomplished by dehydropolycondensation using Lewis acid (tetraphenyltin) as a catalyst and shown in Figure 5.8. 5 mL of L-lactic acid (88% aqueous solution) was taken a in three neck flask and xylene was added (1:1 v/v) proportion The reactant was refluxed for 6h using Dean Stark apparatus to remove water as an azeotrope and requisite amount of protected aleuritic acid was added into the reaction flask. The reaction mixture was further continued up to 15h. The reaction mixture was cooled and the extra xylene was removed by vacuum distillation. The copolymer of various compositions ranging from 90:10 to

50:50 ratios was prepared accordingly. Reaction scheme for copolymerization is shown in Figure 5.8. The resulting copolymer was dissolved in chloroform in a single neck flask and equal amount of methanol, catalytic amount of PTSA was added into it. The reaction mixture was stirred at room temperature (25 ^{0}C) under inert atmosphere (Argon) for 6 h. The deprotected copolymer was dissolved in chilled methanol and filtered using Whatman filter paper. The resulting copolymer was characterized by ^{1}H NMR, GPC, DSC and aggregation behavior in different solvent was observed by TEM.

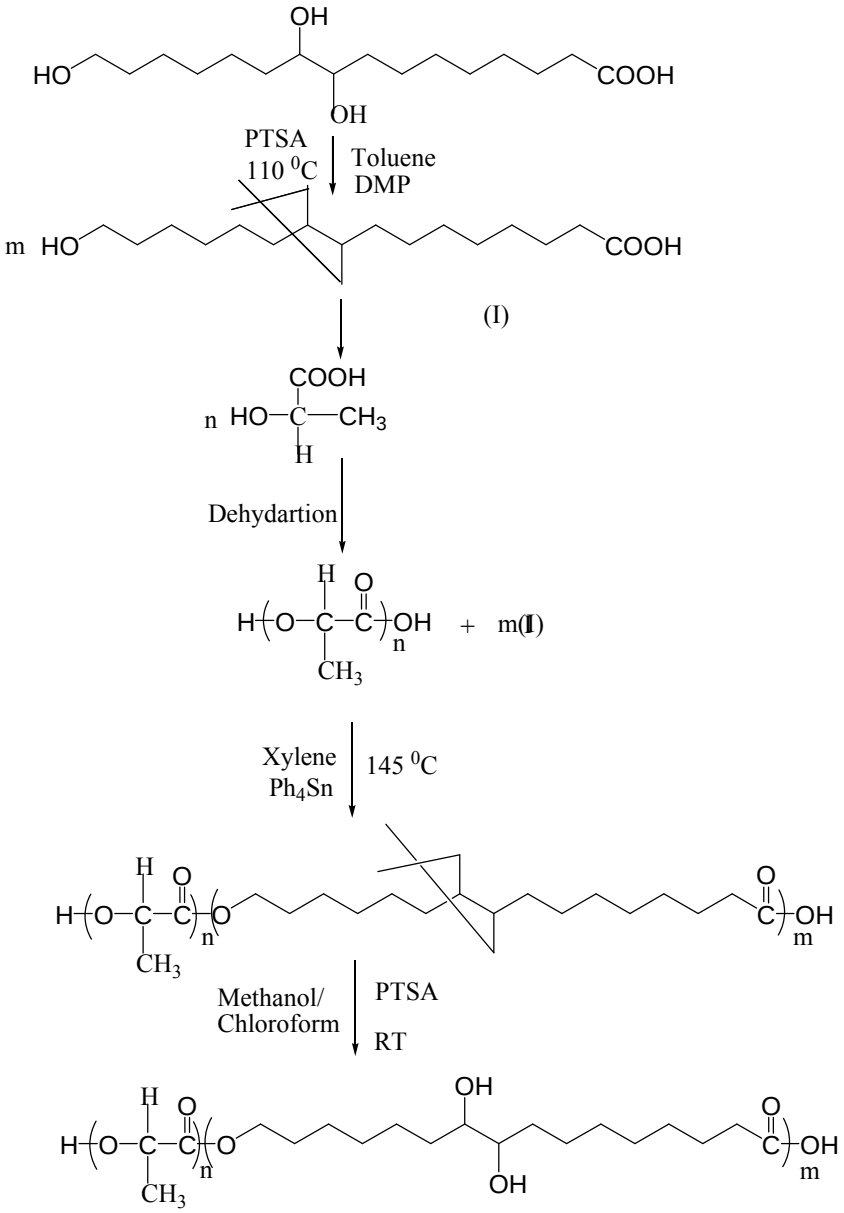

Figure 5.8: Reaction scheme of copolymerization.

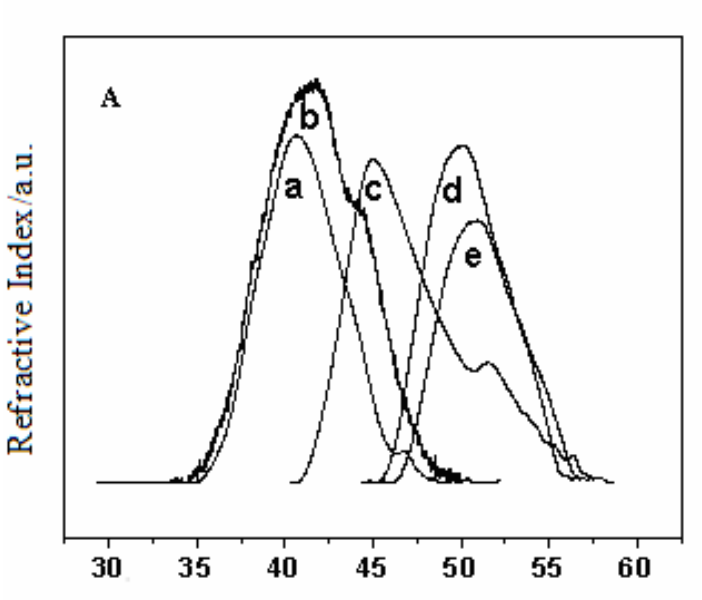

Elution Volume (Vel, µL)

Figure 5.9A: Size Exclusion Chromatography (SEC) of protected copolymers (a) COP-1, (b) COP-2, (c) COP-3, (d) COP-4 and (e) COP-5.

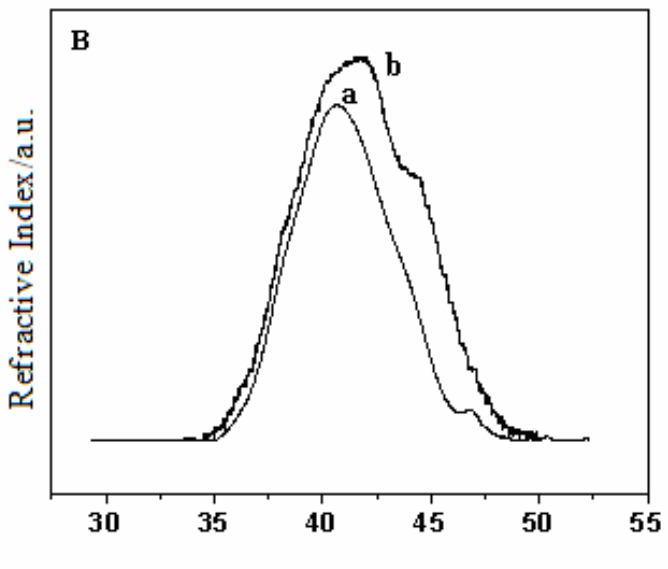

Elution Volume (Vel, µL)

Figure 5.9B: Size Exclusion Chromatography (SEC) of deprotected copolymers (a) DCP 1 and (b) DCP-2.

5.5.1. SEC Analysis: The SEC thermograms of protected copolymer samples are all shown in Figure 9A. The copolymers and homopolymers were prepared by

dehydropolycondensation method using tetraphenyltin as a catalyst and p-xylene as a solvent. Copolymers (COP-1 to COP-5) showed a single peak (Figure 5.9A) whereas COP-2 and COP-3 showed a shoulder peak on them. These results are attributed due to very low molecular weight oligomeric species in equilibrium with each other. The copolymer COP-1 showed $\bar{M}_n$, $\bar{M}_w$ and molecular weight distribution as 7,500, 13,200 and 2.2 respectively.

Table 5.5: Properties of L-lactic acid protected aleuritic acid copolymers

Copolymer samples	Feed ratio	Copolymer (comp.)	$\bar{M}_n$ (GPC)	$\bar{M}_w$ (GPC)	PDI	T_m (^{0}C)	ΔH_f (J/g)	T_g (^{0}C)	ΔC_p (j/g*^{0}C)
PLA	100:0	100:0	900	2,100	2.3	146.0	42.0	44.5	0.46
COP-1	90:10	85:15	7,500	13,200	1.7	161.4	4.1	10.62	0.50
COP-2	80:20	75:25	5,700	12,700	2.2	175.5	0.80	-11.5	0.33
COP-3	70:30	70:30	2,100	6,400	3.0	127.3	5.7	-22.0	0.37
COP-4	60:40	60:40	1,250	1,750	1.4	148.7	0.41	-30.2	0.44
COP-5	50:50	50:50	800	2,000	2.5	138.8	1.2	-31.5	0.41

Temperature of polymerization 195 ^{0}C and time for polymerization 8 hr.

Table 5.6: Properties of L-lactic acid- protected and deprotected aleuritic acid copolymers

Copolymer sample.	Feed ratio	$\bar{M}_n$ (GPC)	$\bar{M}_w$ (GPC)	PDI	T_m (^{0}C)	ΔH_f (J/g)	T_g (^{0}C)	ΔC_p (j/g*^{0}C)
COP-1	90:10	7,500	13,200	1.7	161.4	4.1	10.62	0.50
COP-2	80:20	5,700	12,700	2.2	175.5	0.80	-11.5	0.33
DCP-1	90:10	7,500	13,000	1.7	135.6	5.2	34.7	0.43
DCP-2	80:20	5,700	12,700	2.2	140.0	5.5	40.5	0.27

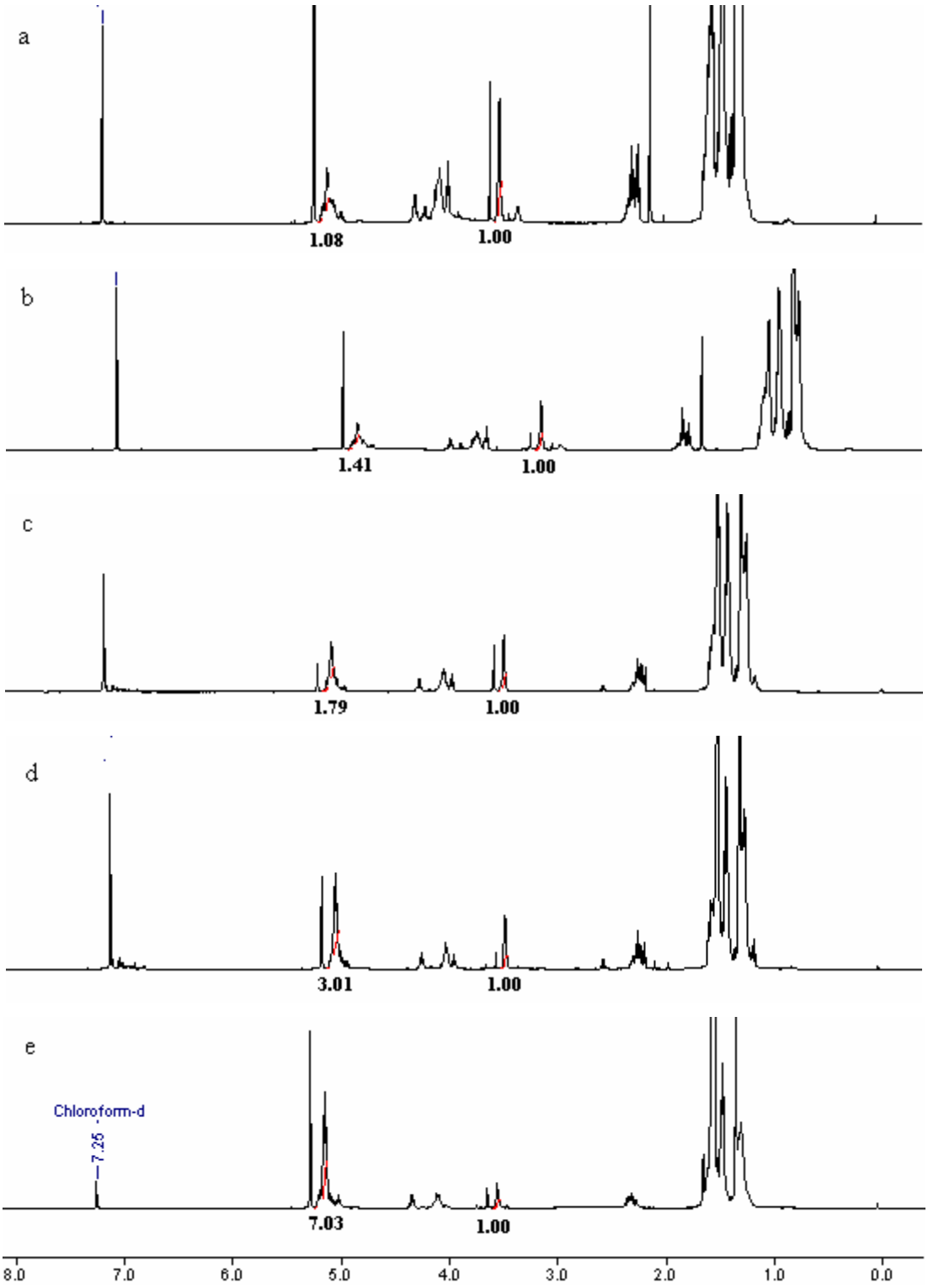

Figure 5.10: ^{1}H NMR spectra of copolymers (a) COP-5, (b) COP-4, (c) COP-3, (d) COP-2 and (e) COP-1.

COP-2 showed $\bar{M}_n$, $\bar{M}_w$ and molecular weight distribution as 5,700, 12,700 and 2.2 respectively with a small shoulder peak. Similar observation was obtained in case of COP-3. COP-4 which showed a single peak and the calculated $\bar{M}_n$, $\bar{M}_w$ and molecular weight distribution are 1250, 1750 and 1.4 respectively.

The copolymer COP-5 also showed a single peak and the calculated $\bar{M}_n$, $\bar{M}_w$ and molecular weight distribution are 800, 2000 and 2.5 respectively. The SEC elugrams of deprotected copolymer samples (DCP-1 and DCP-2) are all shown in Figure 5.9B.

5.5.2. Nuclear Magnetic Resonance: The copolymer compositions were determined from peak area in ^{1}H NMR spectra and shown in Figure 5.10. Comparison of the peak area in the region δ=3.56 pap due to disubstituated proton contributed by aleuritic acid (9, 10 position) with the area of the proton at δ= 5.15 pap due to methane group of the L-lactic acid enables the estimation of the copolymer composition. Samples obtained from mole ratios of protected aleuritic acid: L-lactic acid = 10: 90 to 50: 50 were soluble in $CDCl_3$. The results of COP-1 to COP-5 along with PLA and protected poly aleuritic acid are shown in Table 5.5. The results of protected copolymers (CAP-1, CAP-2) and deprotected copolymers (DCP-1, DCP-2) are shown in Table 4.6.

5.5.3. Thermal properties: Results of thermal characterization are shown in Table- 5.5 and thermograms are shown in Figure 5.11 A**.** The glass transition temperature, T_g, of the copolymers varied from 31.46 to 10.62 ^{0}C. A gradual reduction in the Tg was observed with increase in comonomer incorporation as shown in Table 5.5 and Figure 5.11A thereby indicating increased mobility of the amorphous phase. The crystalline melting point, T_m of PLA phase was also found to be disturbed. The depression of the glass transition temperature was more prominent than T_m of PLA.

Although the absence of Tg characteristic of protected PAA could not be ascertained, yet the absence of a glass transition characteristic of pure homopolymer PLA was, however, sufficient proof of plasticization. Therefore, the lowering of glass transition temperature of PLA by a statistical copolymerization with molar proportions of protected PAA can indeed be called a case of "internal plasticization".

The copolymers (COP-1 and COP-2) were dissolved in chloroform, equal amount of methanol and catalytic amount of p- toluene sulphonic acid (PTSA) was added into it.

The reaction mixture was stirred at room temperature (25 ^{0}C) under inert atmosphere (argon) for 6 h. The resultant copolymer was washed with methanol several times and G.C analysis result confirmed the absence of dimethoxy propane. The structures of DCP-1 and DCP-2 were confirmed by ^{1}H NMR. Results of thermal characterization of DCP-1 and DCP-2 are shown in Table 5.6 and thermograms are shown in Figure 5.11 B. The protected copolymer COP-1 (waxy mass) and deprotected copolymer DCP-1 (solid powdery mass) showed dramatic increase of T_g values from 10.62 (COP-1) to 34.7 ^{0}C (DCP-1) and also affected T_m value. The increase in T_g value may be attributed due to aggregation of hydroxyl groups present at 9 and 10 position of aleuritic acid unit in the copolymer chain. Similarly copolymer COP-2 (highly viscous mass) and after deprotection (DCP-2) also showed increase of T_g value from -11.5 to 40.5 ^{0}C and also affected T_m value.

5.5.4. Transmission Electron Microscopy (TEM): The thermal characteristic result showed the aggregation behavior, which was further examined by TEM. Functionalized interfacial organic and polymer layers fabricated from molecular segments with different amphiphilicity can be designed to act as a smart or switchable surface. These surfaces are capable of responding to very suitable changes in the surrounding environment such as pH, surface pressure and temperature, light and solvent quality. In the present system, these deprotected copolymer DCP-1 and DCP-2 aggregate in various solvents and their structures are slightly different from each other. These structures are responsible for controlling physical properties in term of application such as drug delivery and biomimetic materials. The copolymer DCP-1 and DCP-2 used in this study is L-lactic acid and protected aleuritic acid, which was synthesized by dehydropolycondensation and followed deprotection. The polydispersity indices of the copolymers, estimated by gel permeation chromatography were 1.7 and 2.2 respectively.

The consequences of 9, 10 hydroxyl groups of aleuritic acid unit and methylene groups of aleuritic acid and L-lactic acid unit in the main chain of the copolymer, the key hydrophilic and hydrophobic functionalities in copolymer, within the different monomers of copolymers should be interesting from an intermolecular phase separation perspective. The hydrophilic and the hydrophobic will be placed on the opposite sides of the copolymer backbone in solvents of different polarity. The hydrophobic and hydrophilic

functionalities are stitched together within different monomers in copolymers. Figures 5.12A and 5.12 A' showed the morphologies of the aggregates of DCP-1 and DCP-2 copolymers in N, N-dimethylformamide (DMF). DCP-1 gives micelles of low polydispersity whereas DCP-2 shows slightly elongated form. They consist of a hydrophobic units core covered with hydrophilic units forming the corona. Similar observation has been made by Lifeng Zhang et al **[39]**. Figures 5.13 B and 5.13 B' showed the morphologies of the aggregates from DCP-1 and DCP-2 copolymers in tetrahydrofuran (THF). DCP-1 formed micelles of low polydispersity whereas DCP-2 showed polydispersity. The hydrophobic units' core are covered with hydrophilic units forming the corona. Figures 5.14 C and 5.14 C' showed the morphologies of the aggregates from DCP-1 and DCP-2 copolymers in dioxane. DCP-1 and DCP-2 give spherical micelles of low polydispersity.

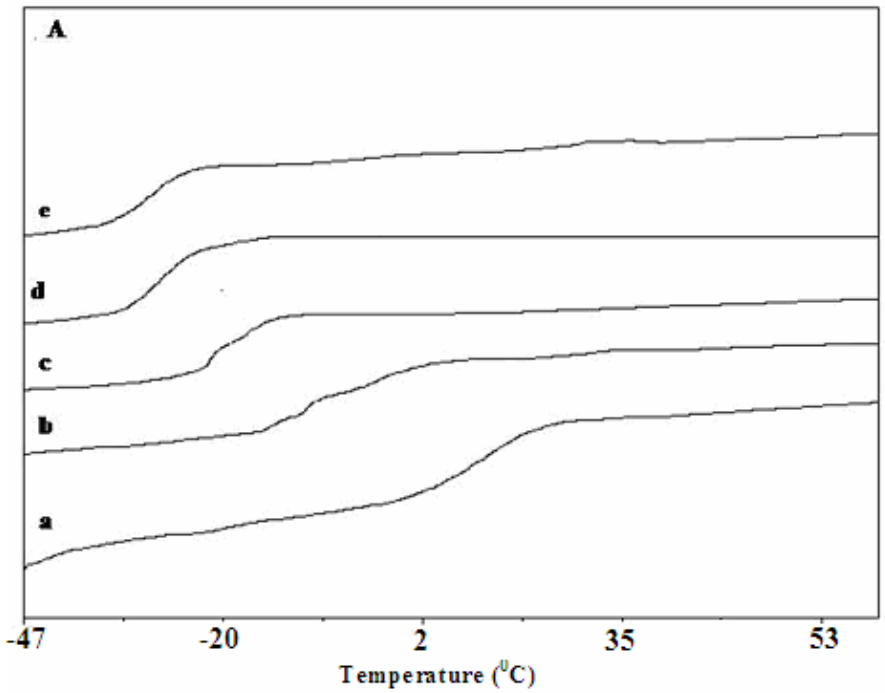

Figure 5.11 A: Differential Scanning Calorimetry (DSC) second heating thermograms (a) COP-1, (b) COP-2, (c) COP-3, (d) COP-4 and (e) COP-5.

In fact, DCP-2 gives better size of spherical micelles with low polydispersity. These copolymers are not soluble in toluene, whereas PLA is soluble in chloroform. Therefore mixed solvents of toluene and chloroform at various proportions (50:50 and 60:40) were taken and morphologies of these two copolymers (DCP-1 and DCP-2) are shown by

TEM. Figures 5.15 D and 5.15 D' shows the morphologies of the aggregates in mixed solvents (50:50 ratio of toluene: chloroform). DCP-1 and DCP-2 showed narrow distribution.

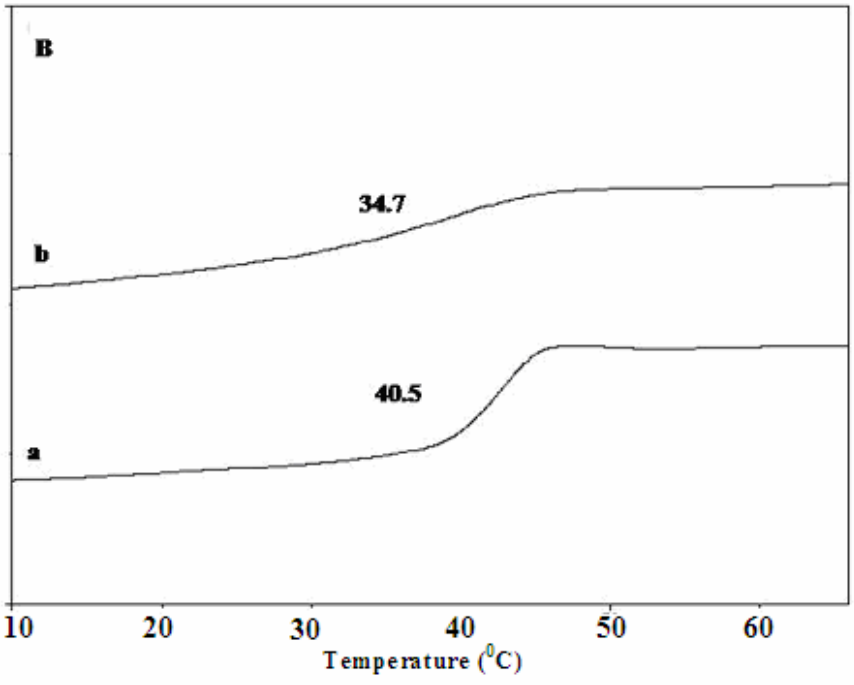

Figure 5.11B: Differential Scanning Calorimetry (DSC) of second heating thermograms (a) DCP-1 and (b) DCP-2.

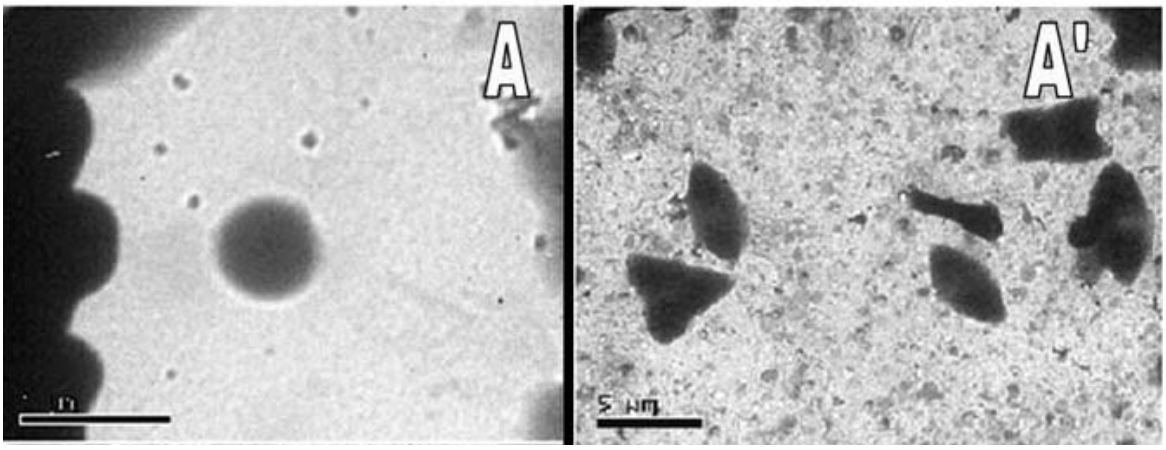

Figure 5.12: TEM images of the micelle-like aggregates in DMF (A) DCP-1 and (A') DCP-2.

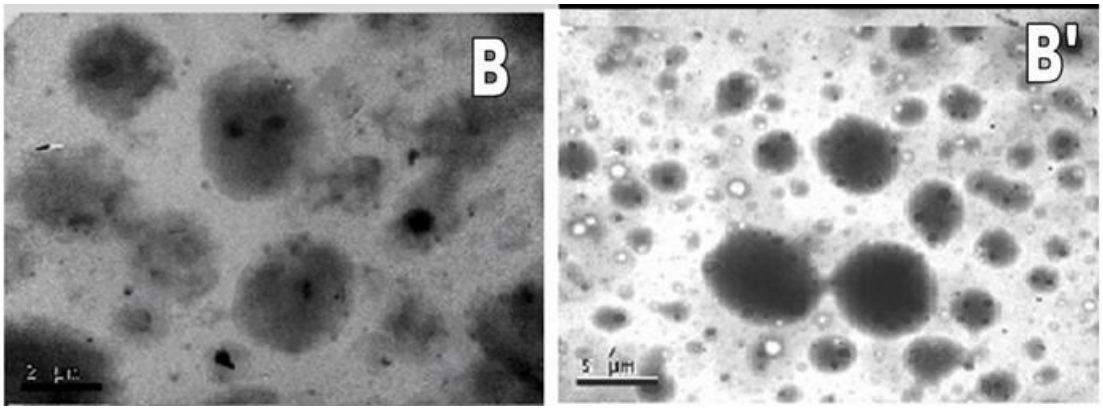

Figure 5.13: TEM images of the micelle-like aggregates in THF (B) DCP-1 and (B') DCP-1 .

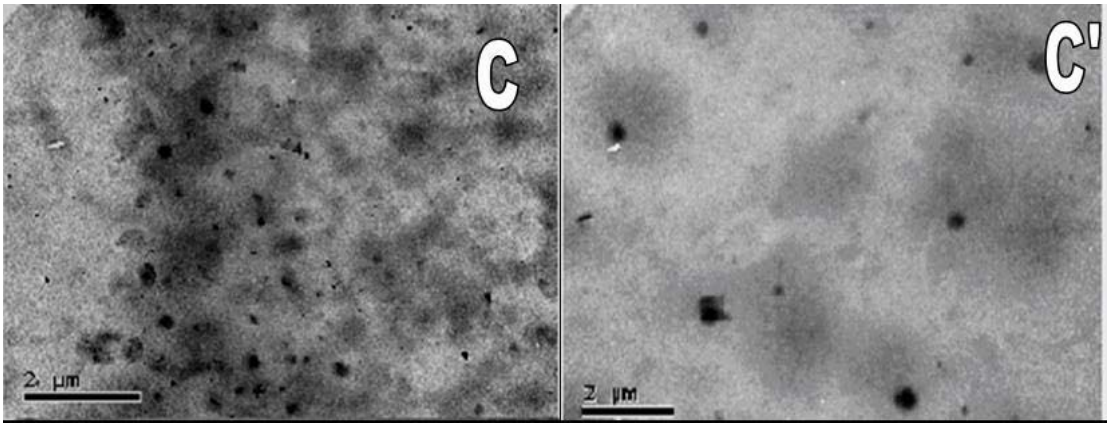

Figure 5.14: TEM images of the micelle-like aggregates in dioxane (C) DCP-1 and (C') DCP-2.

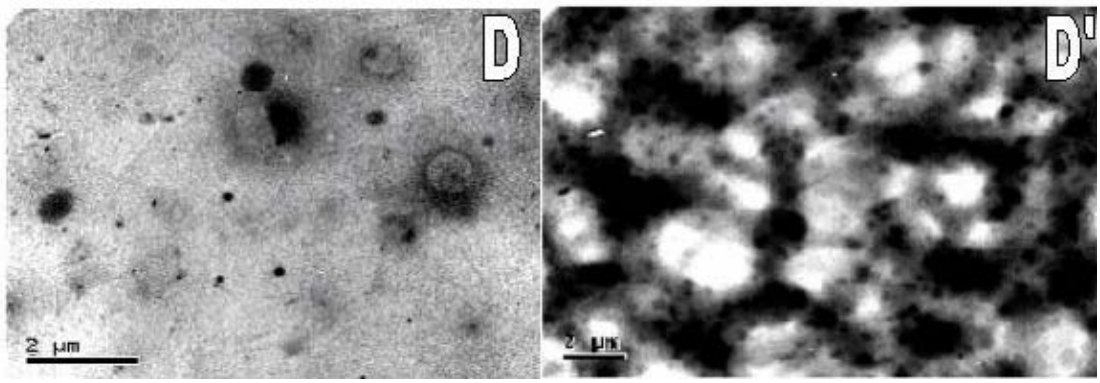

Figure 5.15: TEM images of the micelle-like aggregates in (50:50) toluene: chloroform (D) DCP-1 and (D') DCP-2.

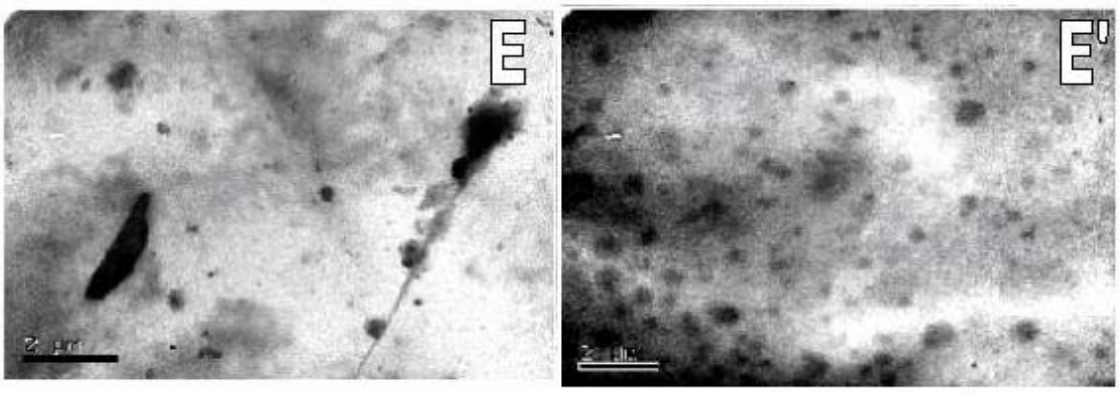

.

Figure 5.16: TEM images of the micelle-like (E) DCP-1 and (E') DCP-2 in toluene-chloroform mixtures (60:40).

The hydrophilic groups (hydroxyl groups) are present in core and hydrophobic groups are covered as corona of the spherical micelle. Similar observations were observed in case of mixed solvents (60:40 ratio of toluene: chloroform) at room temperature. The Figures 5.16 E and 5.16 E' shows precised narrow distribution of micelles-like aggregates in mixed organic solvents. The hydrophilic moieties are directed towards the interior and hydrophobic groups are directed towards the exterior in the micelle-aggregates. Similar observation has also been reported **[12]**.

5.6. Conclusion:

In summery, a new class of value added biodegradable poly (aleuritic acid) from renewable resources (Shellac) are produced by polycondensation. Results show that linear PAA polymer with $\bar{M}_w$~120,000 can be prepared with organotin catalyst. The structure and properties of PAA polymers are determined. Poly (aleuritic acid) s amphiphilic linear homopolymers containing both hydrophilic (hydroxyl pendant groups) and lipophilic functionalities (backbone) in each repeats unit have been synthesized where all the hydroxyl pendant groups aggregate and form new structures. Amphiphilic functions reported here are likely to form the basis for new nanoscale aggregates in solution which could be implications in a broad range of application. A new class of copolymers showed internal plasticization effect when protected aleuritic acid was incorporated in the PLA backbone chain at different molar compositions. These copolymers behaved differently after deprotection of aleuritic acid at 9 and 10 positions. Amphiphilic copolymers containing both hydrophilic and hydrophobic functionalities in

repeat units have been synthesized. These amphiphilic copolymers are soluble in organic and mixed organic solvents and assemble into micelle-like structures. Amphiphilic functions reported here is likely to form the basis for micro scales assembles in solution, which could also have implications in a broad range of applications.

References

1. Konkani, R. K.; Moore, E. G.; Hegel, A. F.; Leonard, F. *J. Boomed. Mater. Res*. **5**, 169 (1971).

2. (a) Van, Siderite. A.; De, Grout, K.; Van, Blitterswijk. C. A. J. *Mater. Science. Med.* **4**, 213 (1993). (b) Nakamura. T.; Hitomi. S.; Watanabe, S.; Shimizu Y.; Jamshidi, K.; Hyon, S.-H.; Ikoda, *Y. J. Biomed. Mater. Res.* **23**, 1115 (1989).

3. (a) Domb, A .J.; Amselem, S.; Maniar, M. *Polym. Biomater*. **33**, 399 (1994). (b) Domb, A. J.; Nudelman, R. *J. Polym. Sci. ; Polym. Chem*. **33**, 717 (1995).

4. Marks, T. A.; Schlinder, A. In Biodegradable drug delivery systems Based on Aliphatic Polyesters: Application of contraceptives and Nacrotic Antagonists. Controlled Release of Bioactive Materials, Baker,R.Ed.; Academic: New York (1980).

5. (a) Shyamroy, S.; Garnaik, B.; Sivaram, S. *J. Polym. Sci. Part-A. Polym Chem*. **43**, 2164 (2005). (b) Moon, S.; Lee, W.; Miyamoto, T. M.; Kimura, Y. *Polymer* **42**, 5059 (2001).

6. Charlotte, K. Williams.; Laurie, E. Breyfogle.; Sun, Kyung.; Choi, Wonwoo. Nam.; Victor, G.; Young, Jr.; Mare, A.; Hillmyer.; William , B.; Tolman *J. Am. Chem*. *Soc.* **125**,11350 (2003).

7. (a)Liu, S.; Armes, S. P. *Angew. Chem., Int. Ed.* **41**, 1413 (2002). (b) Arotcare´na, M.; Heise, B.; Ishaya, S.; Laschewsky, A. *J. Am. Chem .Soc.* **124**, 3787 (2002). (c) Liu, F.; Eisenberg, A. *J. Am. Chem. Soc.* **125**, 15059 (2003).

8. For block copolymers on surfaces that exhibit switching behavior, see Julthongpiput, D.; Lin, Y.-H.; Teng, J.; Zubarev, E. R.; Tsukruk, V. V. *J. Am. Chem. Soc*. **125**, 15912 (2003).

9. Sen, H. K.; Vennugopalan, M. Practical Application of Recent Lac Research Orient Longmans Ltd. Bombay P114 (1948).

10. Haque, M. Zahurul.; Faruq, M. Omar.; Ali, M. Umar. *Journal of Bangladesh Academy of Sciences* **24**, 171 (2000).

11. (a) Terreau, O.; Bartels, C.; Eisenberg, A. *Langmuir* **20**, 637 (2004). (b) Zhang, L.; Eisenberg, A. *Macromolecules* **32**, 2239 (1999). (c) Ma, Q.; Remsen, E. E.; Clark, Jr. C. G.; Kowalewski, T.; Wooley, K. J. *Proc. Nat. Acad. Sci.* U.S.A. **99**, 5058 (2002).

12. Basu S.; Vutukuri D.R.; Shyamroy, S.; Sandanaraj, B. S.; Thayumanvan, S. *J. Am. Chem. Soc*. **126**, 9890 (2004).

13. Finkleman, H.; Koldehoff, J.; Ringsdorf, H. *Angew. Chem. Int. Ed. Engl*. **19**, 935 (1978).

14. Vert, M. *Biomacromolecules* **6**, 538 (2005).

15. Tian, D.; Dubois, P.; Grandls, C.; Jerome, R. *Macromolecules* **30**, 406(1997).

16. Trollsas, M.; Lee, V.Y.; Mecerreyes, D.; Lo¨wenhielm, P.; Moller, M.; Miller, R. D.; Hedrick, J. L. *Macromolecules* **33**, 4619 (2000).

17. Tian, D.; Dubois, P.; Jerome, R. *Macromolecules* **30**, 1947 (1997).

18. Tian, D.; Dubois, P.; Jerome, R. *Macromolecules* **30**, 2575 (1997).

19. Leemhuis, M.; van Nostrum, C. F.; Kruijtzer, J. A. W.; Zhong, Z. Y.; Ten Breteler, M.R.; Dijkstra, P. J.; Feijen, J.; Hennink, W. E. *Macromolecules* **39**, 3500 (2006).

20. Mecerreyes, D.; Atthoff, B.; Boduch, K. A.; Trollsas, M.; Hedrick, J. L. *Macromolecules* **32**, 5175 (1999).

21. Marcincinova-Benabdillah, K.; Boustta, M.; Coudane, J.; Vert, M. *Biomacromolecules* **2**, 1279 (2001).

22. Ray, W. C.; Grinstaff, M. W. *Macromolecules* **36**, 3557 (2003).

23. Chen, X. H.; Gross, R. A. *Macromolecules* **32**, 308 (1999).

24. Kumar, R.; Gao, W.; Gross, R. A. *Macromolecules* **35**, 6835 (2002).

25. Olson, D. A.; Sheares, V. V. *Macromolecules* **39**, 2808 (2006).

26. Mecerreyes, D.; Miller, R. D.; Hedrick, J. L.;Detrembleur, C.; Jerome, R. *J Polym. Sci. Part. A: Polym. Chem.* **38**, 870 (2000).

27. Finne, A.; Albertsson, A. C. *J Polym Sci Part A:Polym Chem*. **42**, 444 (2004).

28. Parrish, B.; Quansah, J. K.; Emrick, T. *J Polym Sci Part A: Polym Chem* . **40**, 1983 (2002).

29. Liu, M.; Vladimirov, N.; Frechet, J.M. J. *Macromolecules* **32**, 6881 (1999).

30. Parzuchowski, P. G.; Grabowska, M.; Tryznowski, M.; Rokicki, G. *Macromolecules* 39, 7181 (2006).

31. Yu, X.-H.; Feng, J.; Zhuo, R.-X. *Macromolecules* **38**, 6244 (2005).

32. Sodergard, A.; Stolt, M. *Prog. Polym. Sci* **27**, 1123 (2002).

33. Hiltunen, K.; Harkonen, M.; Seppala, J. V.; Vaananen, T.*Macromolecules* **29**, 8677 (1996).

34. Hiltunen, K.; Seppala, J. V.; Harkonen, M. *J. Appl. Polym.Sci* **64**, 865 (1997).

35. Tuominen, J.; Seppala, J. V. *Macromolecules* **33**, 3530 (2000).

36. Teomim, D.; Domb, A. J. *Biomacromolecules* **2**, 37 (2001).

37. Teomim, D.; Nyska, A.; Domb, A. J. *J. Biomed. Mater. Res.* **45**, 258 (1999).

38. Zhang, L.; Eisenberg, A. *Science* **268**, 1728 (1995).

39. Zhang, L.; Yu, K.; Eisenberg, A. *Science* **272**, 1777 (1996).
40. Discher, D. E.; Eisenberg, A. *Science* **297**, 967 (2002**)**.
41. Discher, B. M.; Won, You-Yeon.; Ege, D. S.; Lee, James C-M.; Bates, F. S.; Discher, D. E.; Daniel A. H. *Science* **284**, 1143 (1999)**.**

42. Oda, R.; Huc, R. I.; Schmutz, M.; Candau, S. J.; Mackintosh, F. C. *Nature* **399**, 566 (1999).

43. Stupp S. I.; LeBonheur, V.; Walker, K.; Li, L. S.; Huggins, K. E.; Keser, M.; Amstutz, A. *Science* **276**, 384 (1997).

44. Hartgerink, J. D.; Beniash, E.; Stupp, S. I. *Science* 294, 1684 (2001).

45. Kato, T. *Science* 295, 2414 (2002).

46. Wong, Gerard C. L.; Tang, J. X.; Lin, A.; Li, Y.; Janmey, Paul A.; Safinya , C.R. Science **288**, 2035 (2000).

47. Thomas, B. N.; Safinya, C. R.; Plano R. J., Clark, N. A. *Science* **267**, 163(1995).

48. Schnur, J. M. *Science* 262, 1669 (1993).

49. Shyamroy, S. Dissertation No- Th-1365, 2003.

50. For mechanism of catalysis of esterification and transesterifications, see (a) Otera, J.; Dan-oh, N.; Nozaki, H. Tetrahedron **49**, 3065 (1993). (b) Otera, J.; Dan-oh, N.; Nozaki, H. *J. Chem. Soc.* 1742 (1991).

51. (a) Sawyer, A. K.; Frey, C. Synth. React. Inorg. Met. -Org. Chem. **13**, 259 (1983). (b) Shandilya, P. R.; Srivastava, G.; Mehrotra, R.C. *Synth. React. Inorg. Met.Org. Chem.* **13**, 899 (1983).

52. Bockstaller, M.; Kholar, W. Wegner.; Vlassopoulos, D.; Fytas, G. *Macromolecules* **31**, 6359 (2001).

Chapter-6

CHAPTER 6: GRAFTING OF POLY (L-LACTIC ACID) AND COPOLYMER OF L-LACTIC ACID WITH 12- HYDROXY STEARIC ACID ON THE SURFACE OF MWCNTS

6.1. Introduction:

The functionalization of carbon nanotubes (CNTs) and covalent grafting using monomers and polymers has attracted much recent attention for their potential application. The surface modification of carbon nanotubes has mainly been focused to enhance their chemical compatibility and dissolution properties [**1-5]**. The carbon nanotubes are classified as SWNTs, DWNTs and MWNTs depending upon number of rolled sheets and are conducting or semi conducting depending upon the chirality of the tubes. The CNTs can be dispersed in the polymer matrix by a variety of techniques, such as direct mixing, insitu polymerization, solution blending and also melt blending. Carbon nanotubes particularly MWCNTs have diameter in the range of 2-60 nm for the innermost tubular layer and in additional thickness of 0.7 nm for every extra layer. The covalent grafting of organic or polymeric molecules on to the MWCNTs has been accomplished by the "grafting to" technique by using esterification and amidation reactions **[1]**. However the loss in conformational entropy of the polymer significantly suppresses chains from diffusing to and reacting with carboxylic acid sites of MWCNTs, which leads to insufficient grafting. The polymer wrapping and "pi-pi' stacking on the surface of carbon nanotubes due to non covalent functionalization methods are difficult to correlate quantitively with properties due to the presence of excess polymer chains from covalently attached surface functional groups by using the "grafting from" method is the best way to produce polymer brushes on any surface.

Sun and coworkers showed that esterification of carboxylic acid can also be applied to functionalize and solubilize nonotubes of any length **[1, 6-7]**. An advantage with ester linkages is that they can be facilely difunctionalized via acid or base- catalyzed hydrolysis, allowing the recovery of carbon nanotubes from the soluble samples **[7]**. There is now ample experimental evidence for the conclusion that the nanotubes bound carboxylic acid is the site to attach a variety of functional groups for the solubilization of both shortened and full-length carbon nanotubes.

Carbon nanotubes are considered to be ideal reinforcing agent for high strength polymer composite, because of their tremendous mechanical strength (Pan et al. **[8]** obtained Young's modulus of 0:45±0:23 TPa, tensile strength of 1:72±0:64 GPa. and strain (12 %) **[9]**, high electrical conductivity (0.1 $S.cm^{-1}$) **[10]** and high aspect ratio.

Biocompatible polymers such as poly caprolactone, chitosan and poly lactide have also much attention because of their biomedical applications for example, and electric field is known to stimulate the healing of various tissues. In case of bone fracture healing, the use of an electric field was based on the observation that, when a bone was subjected to mechanical load (stress) deformation of bone (strain) is normally accompanied by an electrical signal bearing the strain characteristics.

Poly (L-lactide) (PLA) is the unique biodegradable polymer, which can replace all the conventional plastic so far available as their properties are concerned. At the same time, PLA has been limited to biomedical application as resorbable implant materials, because of its biodegradability and high production cost. Carbon nanotubes have noncreative surfaces and have not been used for dehydropolycondensation of PLA and related copolymers. To our knowledge, dehydropolycondensation of L-lactic acid, L-lactic acid oligomers and copolymers with 12-hydroxy stearic acid has not been previously attempted, and this is the first report that demonstrates the growth of homopolymers and copolymers with 12-hydroxystearic acid in the levels up to 88 % from the surface of MWCNTs.

Methodology for chemical modification of CNT with polymer can be classified in to 'grafting to' and 'grafting from' methods. "Grafting to" means that polymer first prepared and then linked through a covalent bond to the surface of CNT, 'grafting from method' means polymerization of monomers on the surface through functional groups.

In this study, we highlight the grafting of L-lactic acid, L-lactic acid oligomer and copolymer of L-lactic acid and 12-hydroxy stearic acid to multiwalled carbon nanotubes (MWCNTs) using dehydropolycondensation techniques. In order to introduce functional groups, MWCNTs were functionalized. The functionalized MWCNTs were reacted with L-lactic acid, oligomers of L-lactic acid and copolymers through insitu polymerization. The attachment of PLA homopolymer and copolymer (L-lactic acid-co-12-hydroxystearic acid) chains to the MWCNTs were confirmed by FT-IR, TGA, scanning electron

microscopy (SEM), transmission electron microscopy (TEM) and ^{13}C CP/MAS (cross polarization/ magic angle spinning).

6.2. Experimental:

6.2.1. Materials: The MWCNTs used in this study were synthesized by thermal chemical vapour deposition (CVD) method. The purity of the pristine MWCNTs was > 95 %. L-lactic acid (88% aqueous solution) was purchased from PURAC, USA. 12-hydroxy steraric acid was purchased from Aldrich Sigma, tin chloride dihydrate from Aldrich Sigma, xylene and chloroform from SD Fine Chemicals (India).

6.2.2. Purification of MWCNTs: To eliminate the impurity in the MWCNTs such as metallic catalyst, they were treated in a mixture of 3 M HNO_3 and 1M H_2SO_4 at 60 ^{0}C for 12 h, followed by refluxing in 5 M HCl at 120 ^{0}C for 6h. The purity of acid treated MWCNTs was measured to be 99 % using TGA (TGA-7 Perkin Emmler). These acid treatments are known to introduce carboxylic and hydroxylic functional groups onto the surface. The functionalized MWCNTs (FMWCNTs) were filtered and washed with large amount of water and then vacuum dried at room temperature overnight.

6.3. Characterization:

6.3.1. FT-IR: As discussed in chapter 5.

6.3.2. Molecular weight determination: As discussed in chapter 3.

6.3.3. Thermogravimetric Analysis: Thermal stability was analyzed using Perkin-Elmer TGA-7, by heating the samples from 50–700 ^{0}C with a heating rate of 10 ^{0}C/min under nitrogen atmosphere with a flow rate 20 mL/min.

6.3.4. Scanning Electron Micrograph (SEM): SEM was taken on a gold-coated surface of polymer sample after careful washing and drying by using a Leica Cambridge Stereo scan Model 440.

6.3.5. Transmission Electron Microscopy (TEM*):* Samples solution in DMF after sonication for TEM imaging were made on copper grids were kept overnight on filter paper for drying. TEM imaging was done using a JEOL 1200EX electron microscope operating at an accelerating voltage of 80 kV-120 kV. Images were captured using charged couple detector camera and viewed using Gatan Digital Micrograph software.

6.3.6. Atomic force microscopy: AFM experiments were conducted with a PicoSPM equipped with a fluid cell and an environmental chamber (Molecular Imaging, Phoenix, AZ) and controlled by a Nanoscope III electronics (Digital Instruments, Santa Barbara, CA). We used silicon nitride cantilevers with a nominal spring constant of 0.1 N m^{-1} and an integrated pyramidal tip whose nominal apex radius was typically equal to 50 nm (Microlever, Thermo Microscopes, and Sunnyvale, CA). All AFM measurements were performed in either nitrogen atmosphere or water rather than in air to eliminate or at least significantly reduce capillary forces. The adhesive interaction between tip and sample was determined from force vs. cantilever displacement curves. In these measurements the deflection of the cantilever is recorded as the probe tip approaches, contacts, and is then withdrawn from the sample. The observed cantilever deflection is converted into force using the nominal cantilever spring constant. Force-displacement curves were obtained using the "force volume imaging" mode. In this mode an array of force curves over the entire probed area can be obtained. A force curve is measured at each *x-y* position in the area, and force curves from an array of *x-y* points are combined into three-dimensional array of force data. Force volume enables the investigation of the spatial distribution of the interaction force between the tip and the surface. Using a program developed under Igor Pro (Wave metrics, Portland, OR), the force volume data were treated in order to extract from every curve the pull-off force, or adhesion force, and to generate adhesion maps of the probed areas. To eliminate possible changes that could affect the measured pull-off forces, experiments were realized with two independent tips at three different locations for each sample. For every experiment, the average value of adhesion forces was determined from 1024 force-distance curves. The reported values of adhesion force correspond to the average of the values measured for at least two independent tip-sample combinations.

6.3.7. ^{13}C Cross Polarization /Magic Angle spinning (^{13}C CP/MAS): ^{13}C CP/MAS NMR spectra were measured with Bruker MSL-300 NMR Spectrometer (75.5 MHz) with ^{13}C CP/MAS accessory at room temperature (25 ^{0}C). The sample powder (ca. 200 mg) was placed in a cylindrical ceramic rotor and spun at 3 KHz. Contact time and repetition time were 2ms and 5s respectively. Spectral width and data points were 27 KHz and 8 K, respectively. The ^{1}H field strength was 2mT for both the CP and decoupling processes.

The number of accumulations was 160-200. ^{13}C Chemical shifts were calibrated indirectly with reference to the higher field adamantane peak (29.5 ppm relative to tetramethly silane ($(CH_3)_4Si$). The Hartmann-Hann condition was matched using adamantane in each case. The experimental errors for the chemical shifts were within ± 0.1 ppm for broad peaks as described.

6.4. Result and Discussion:

The surface bound carboxylic groups on MWCNTs was used as template and L-lactic acid, L-lactic polymers and L-lactic acid-co-12-hydroxy stearic acid were attached to the MWCNTs through ester linkage using dehydropolycondensation method. Using a silylated reaction flask equipped with a Dean and Stark type condenser, requisite amount of 88 % L-lactic acid was azeotropically dehydrated using equal volume of xylene solvent for 6 hr using at reflux temperature without any catalyst. After removal of water in the trap of the Dean and Stark condenser, the reaction was cooled at 50 ^0C. Subsequently functionalized multiwalled carbon nanotubes (FMWCNTs) and catalyst (tin chloride dihydrate 0.2 wt %) were added followed by heating the reaction mixture slowly up to the refluxing temperature of the solvent (xylene) under mild stirring. The reaction was allowed to proceed at a temperature of 145 ^0C for 20 h. Similar methodology was adopted to attach L-lactic acid-co-12- hydroxyl stearic acid to MWCNTs through ester linkage. Poly (L-lactic acid, $\bar{M}_n$ = 14,000) was prepared in our laboratory by dehydropolycondensation method and also used. Poly (L-lactic acid) was also grafted on functionalized carbon nanotubes by dehydropolycondensation method. The amount of catalyst and reaction time are same in all cases. The reaction mixture was washed with chloroform several times to remove the unbound PLA and filtered under vacuum through 0.22 μm polytetrafuloroethylene (PTFE) membrane to yield corresponding grafted polymers and copolymers.

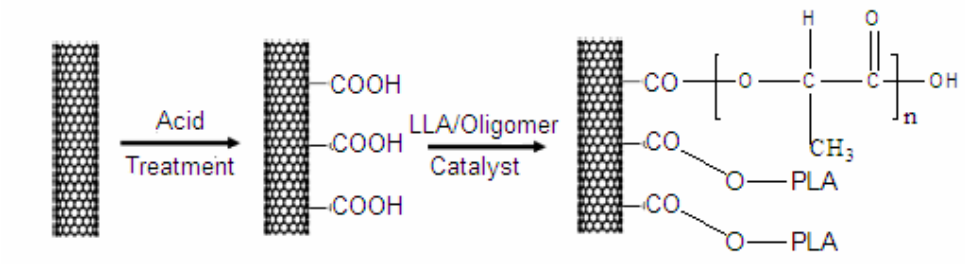

Figure 6.1: Reaction scheme for grafting of L-LA and oligomers of L-lactic acid.

L-lactic acid (88 % aqueous solution) was azeotropically dehydrated using equal volume of xylene solvent for 6 hr using at reflux temperature without any catalyst. After removal of water in the trap of the Dean and Stark condenser, the reaction was cooled at 50 ^{0}C. Catalyst (tin chloride dihydrate 0.2 wt %) was added followed by heating the reaction mixture slowly up to the refluxing temperature of the solvent (xylene) under mild stirring. The reaction was allowed to proceed at a temperature of 145 ^{0}C for 20 h (in case of PLA oligomer 20 h). The resulted polymer was dissolved in chloroform and precipitated in n-hexane and dried in vacuum oven and used for comparison with grafted PLA polymers attached on the surface of MWCNTs.

6.4.1. Molecular weight determination: Molecular weight of blank samples without nanotubes was measured by GPC and shown in Figure 6.2. Figure 6.2 A shows chromatogram of oligomer of PLA ($\bar{M}_n$= 14,000). The chromatogram showed the molecular weight of PLA prepared by L-lactic acid (Figure 6.2 B) having number average molecular weight 3500.

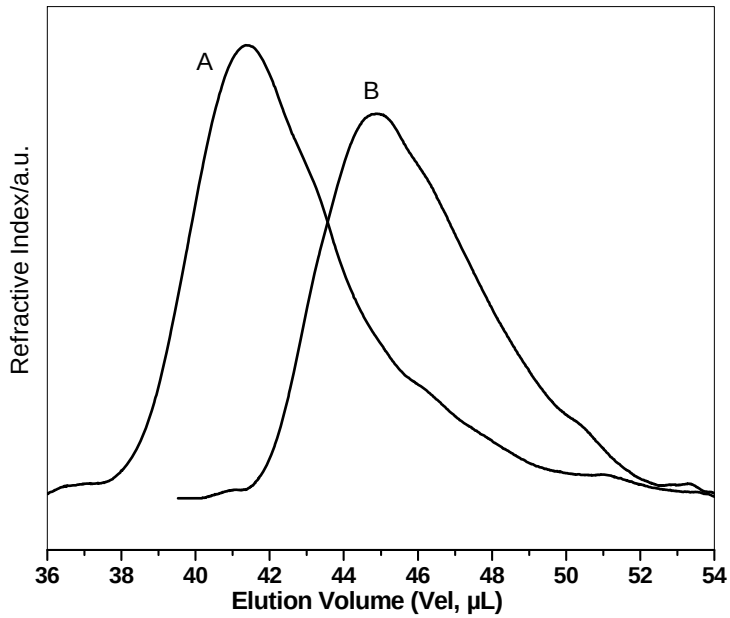

Figure 6.2: (A) PLA oligomer used for the preparation of sample PLA oligomer and (B) SEC chromatogram of PLA prepared by L-lactic acid.

6.4.2. FT-IR: Figure 6.3A shows the IR spectra of the functionalized nanotubes. As it is clearly evident, there is a broad absorption at 3370 cm^{-1}due to the free hydroxyl groups for Figure 6.3A and also peaks between 1354 and 1366 cm^{-1} are attributed to -OH

deformation. The peak at 1717-1723 cm^{-1} is attributed to the C=O stretching mode of carboxylic acids, **[11]** whereas the peaks at 3180 and 3329-3335 cm^{-1} are attributed to -OH stretching of carboxylic acid monomers and carboxylic acids with intermolecular hydrogen bonds, respectively. Because of carbon nanotubes texture (black powder) the quality of the spectra is not the desired, nevertheless the spectroscopic data presented make clear that -COOH groups have been introduced. No C-C bond vibration was observed due to the fact that C-C bonds of the tubes are of high symmetry and therefore inactive in the infrared. The attachment of homopolymers was confirmed from the characteristic C-H and carbonyl stretching vibration centered at 2922 cm^{-1} and 1737 cm^{-1} respectively in the FT-IR spectrum. Figure 6.3A showed an absorption band at 1720 due to the C=O stretching mode of the carboxylic group (MWCNTs-COOH).

Figure 6.3Ba shows the FT-IR of PLA without nanotubes. The peak at 1760.73 cm^{-1} is attributed due to carbonyl group and a broad peak around 3500 cm^{-1} is due to –OH stretching. Figure 6.3Bb depicts the FT-IR spectra of the grafted PLA-1 and showed an absorption at 2870 cm^{-1} (-CH stretching), 1751cm^{-1} (-C=O stretching) **[11]**. Similarly grafted PLA-2 (Figure 6.3Bc) also showed 2876cm^{-1} (-CH stretching) and 1756 (-C=O stretching). It was observed that -CHs frequency of grafted PLA-1 and grafted PLA-2 shifted considerably lower frequency ($\Delta\nu$ = 7 and 1 cm^{-1}) as compared to PLA (Figure 6.3b). The carbonyl stretching frequency of both grafted PLA-1 and grafted PLA-2 has also shifted to lower frequency ($\Delta\nu$ = 6 and 1 cm^{-1}). The Low frequency shift may be attributed to non-covalent interaction of PLA with MWCNTs [**12].** As the residual MWCNTs were thoroughly washed several times with chloroform and dried under vacuum for 40 ^{0}C for 3h, the presence of polymer absorption in the IR spectrum supports the occurrence of a grafting reaction.

6.4.3. Thermogravimetric analysis: TGA provides a measure of the degree of functionalization. The relative content of grafted PLA-1 and PLA-2 and L-lactic acid-co-12-hydroxy stearic acid, compared with that of MWCNTs-COOH was investigated by TGA. The TGA curve of MWCNTs-COOH is shown in Figure 6.4A and different from the grafted MWCNTs samples. Figure 6.4A showed that MWCNTs-COOH is stable around 600 ^{0}C. The weight loss above 600 ^{0}C is likely to be due to the decomposition or oxidation of MWCNTs **[13]**. The PLA grafted MWCNTs were pyrolyzed from 50 to

700 ^{0}C at rate of 10 ^{0}C/min under an atmosphere of nitrogen. After 5 min at 700 ^{0}C, the weight percentage curve leveled up at 286 ^{0}C (Figure 6.4 b). The weight loss was determined to be 90 % (Figure 6.4 b) of PLA-1. In controlled experiment all of the bulk PLA (typically by $\bar{M}_n$ =3500) was lost below 300 ^{0}C (Figure 6.4 a) suggesting that the entire PLA component of PLA grafted MWCNTs sample was lost during the TGA analysis. The weight loss percentage in case PLA-2 was 12 %. The temperature derivative percentage weight loss curve showed two main weight loss peaks. According to the heating profile the first weight loss occurred at 146 ^{0}C and the second at 236 ^{0}C. Cleavage of the polymer chain from sidewall of the carbon nanotubes would account for this observation since it is not possible to determine the molecular weight of the polymer chain grafted on to the MWCNTs.

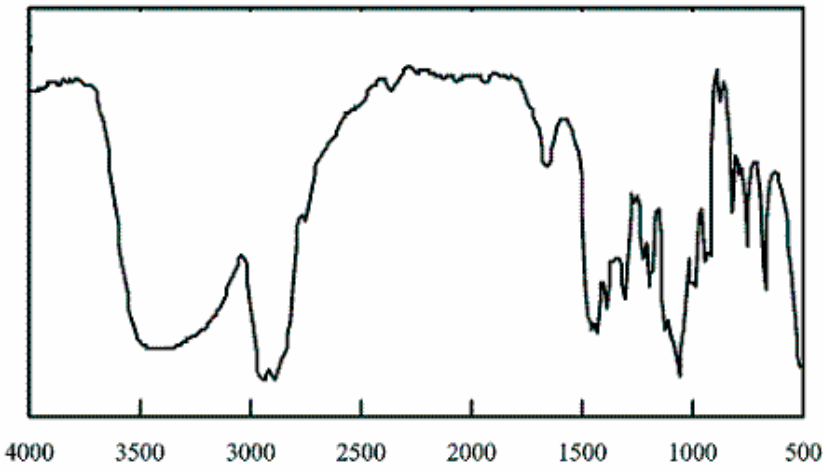

Figure 6.3 A: FT- IR spectra of FMWCNTs,

But in case of oligomer around 4 % (Figure 6.4 c) grafting was observed (PLA-2). Figure 6.4 B depicts the differential curve of grafted materials. PLA-1 (Figure 6.4Bb') clearly demonstrated two melting points at respective places as observed in TGA curve. Similar observations were obtained in case of PLA-2 (Figure 6.4Bc').

It is very essential to mention here that the work-procedure in this investigation involves washing and removal of free polymer using filtration in order to characterize unambiguously the grafting reaction. The amount of polymer present on the tubes (4-8 %) is considerably lower than the amount of precursor acid groups on the MWNTS. Low level of grafting was observed when equimolar or higher amounts of PLA oligomers

were used. It appears that the reaction of high molecular weight PLA polymer chain ends with active sites of the nanotubes is hindered because of the entropy constraints of the polymer. It is also difficult to ascertain the extent of polymer wrapping or coating contributing to the grafting efficiency. Conditions such as absence of solvent and high temperature (above the polymer's Tg) would, in general, increase the grafting efficiency as reported elsewhere **[12, 14-15]**.

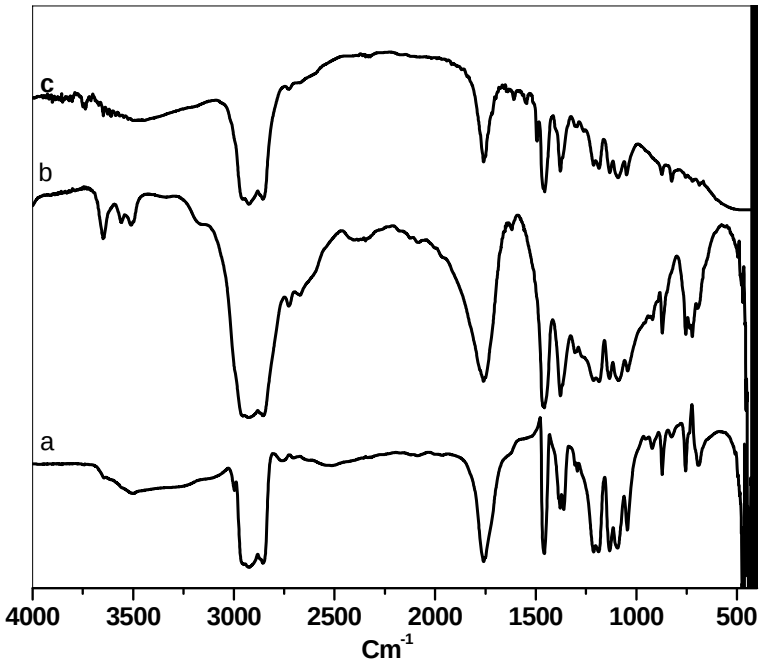

Figure 6.3 B: FT- IR spectra of (a) PLA without nanotubes, (b) PLA-1 and (c) PLA-2.

To access the effect of MWCNTs on the thermal behavior of PLA matrix in the DSC experiment were conducted and results were shown in Figure 6.5. PLA polymer exhibited glass transition temperature (T_g) 39.49 ^{0}C, the crystallization isotherm (T_c) 88.24 ^{0}C, peaks in the second heating cycle and 135.21(T_m) was estimated from first heating curve. The values of T_g, T_c and T_m are decreased up to 36.49, 88.06 and 125.74 ^{0}C. The melting temperature of PLA-g-MWCNTs was calculated from second heating curve and showed a shoulder along with main melting peak. The shoulder T_m peak is attributed due to induced crystallization behavior because of the presence of MWCNTs in the PLA matrix by covalent ester linkage **[11]**.

6.4.4. Scanning electron microscopy: SEM images of grafted PLA1-MWCNTs of these materials were illustrated in Figure 6.6 a. These images demonstrate a low MWCNTs

content. The Figure 6.6 b (PLA-2) also showed high content of MWCNTs because PLA chain is anchored to the surface of MWCNTs and the polymer chain arranged in a particular configuration. Finally, the PLA in the grafted polymers and copolymers remain semicrystalline, as indicated from FTIR studies (-CH_3 (920.6 cm^{-1}, C=O stretching (1750-1789 cm^{-1} and C-H stretching modes (2880-3005 cm^{-1}) and also confirmed α-helical structure **[10]**.

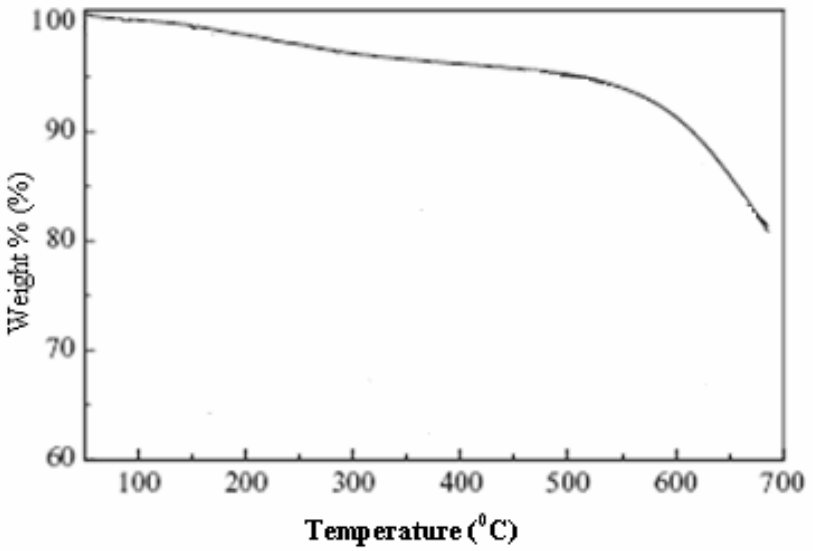

Figure 6.4A: TGA curve of MWCNT-COOH.

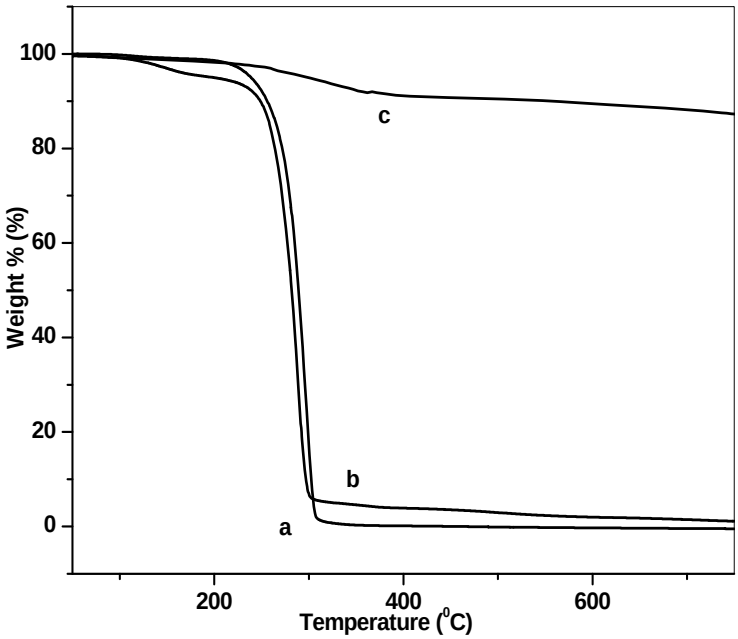

Figure 6.4B: (a) TGA curve of PLA, (b) TGA curve of PLA-1 and (c) TGA curve of PLA-2.

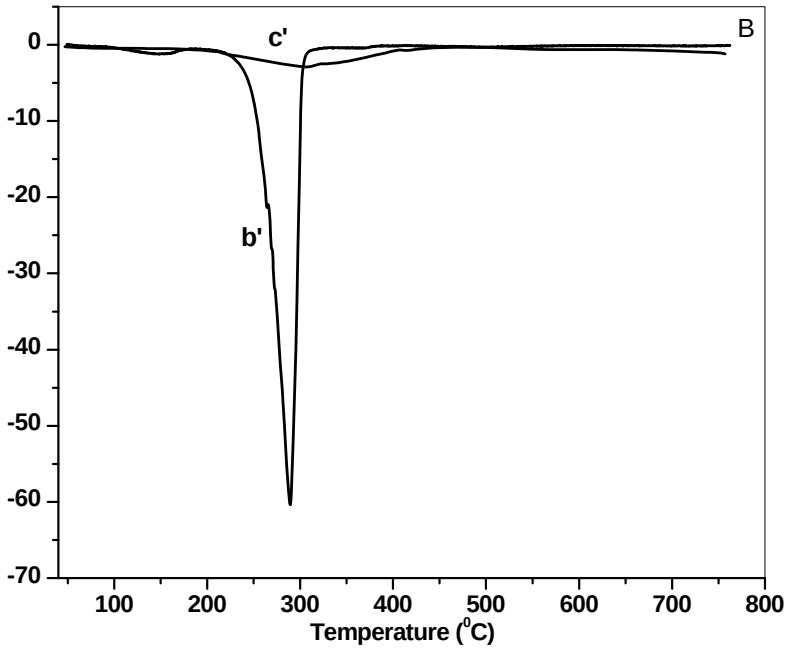

Figure 6.4 C: (b') DTA of sample PLA-1 and (c') derivative curve TGA plot of sample PLA-2.

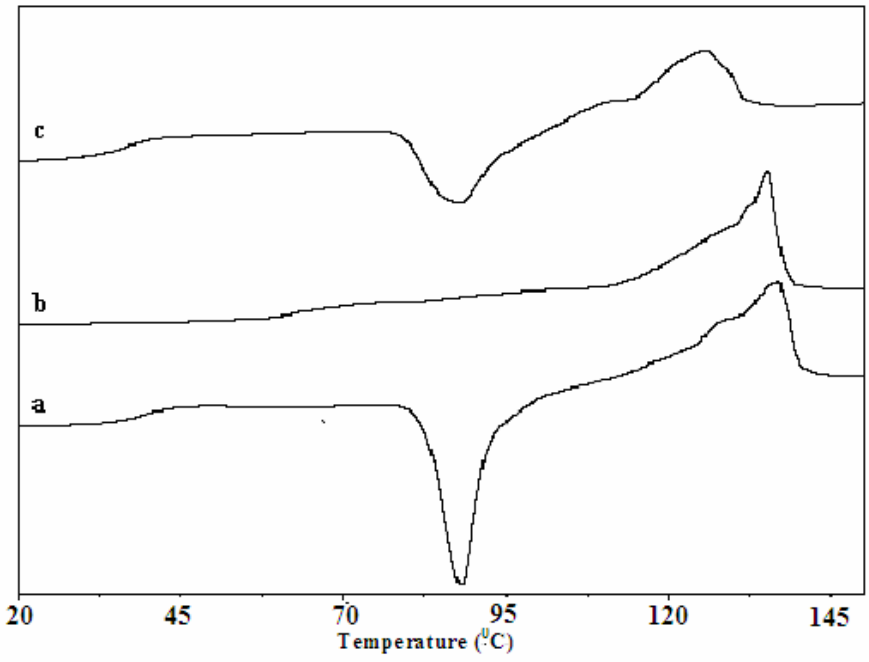

Figure 6.5: (a) Second heating of PLA, (b) First heating of PLA and (c) second heating of PLA-1(grafted on MWCNTs).

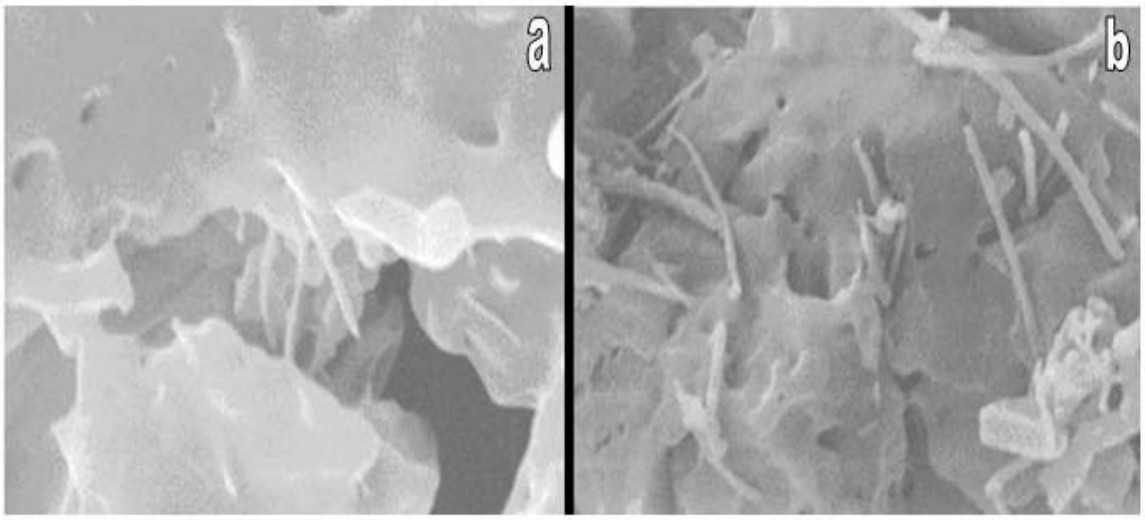

Figure 6.6: (a) SEM images of PLA-1 and (b) SEM images of PLA-2.

6.4.5. Transmission electron microscopy: TEM images provide conformation for the unbundling of the PLA grafted MWCNTs (Figure 6.7 a). The nanotube exhibits a morphology that can be attributed to the polymer that grafted on to the MWCNTs. Figure 6.7 b shows that PLA oligomers are also grafted on to the surface of MWCNTs. However, the chemical attachment points on the MWCNTs are less in comparison with grafted PLA-1.

6.4.6. Atomic force microscopy: Figure 6.8 a shows the AFM image of the L-lactic acid grafted MWCNTs and topographic patterns comprised of variable height ranging from 20-40 nm and side lengths ranging from 0.0 to 1.5 μm. Figure 6.8 b displays the AFM image of PLA oligomer grafted MWCNTs and topography patterns comprised of height from 0-250 nm and the side lengths ranging from 0.0 to 7.7 μm. These are clearly distinct AFM images observed in case of L-lactic acid grafted MWCNTs; grafting reaction occurred and clearly reflected between the two carbon nanotubes. The PLA grafted on MWCNTs appeared as oval shaped randomly distributed indicating grafting reaction occurred on the surface of MWCNTs. The grafted PLA oligomers form α helical conformation and intimately appeared as oval patches and also strongly supported by FTIR and TGA results. The percentage grafting of PLA oligomer is lower in comparison with LA-MWCNTs grafting which was evidenced by TGA results.

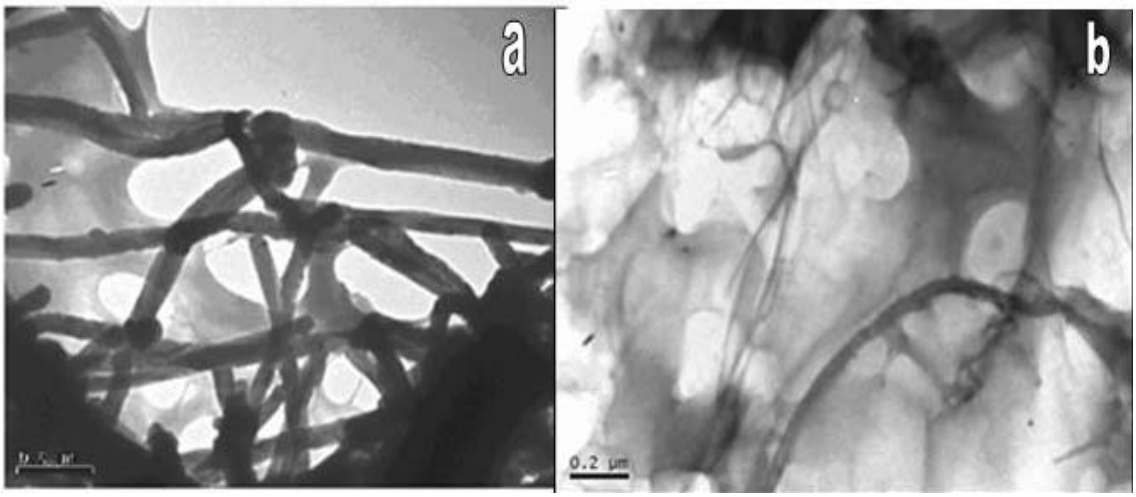

Figure 6.7: (a) TEM image of PLA-1 and (b) TEM image of PLA-2.

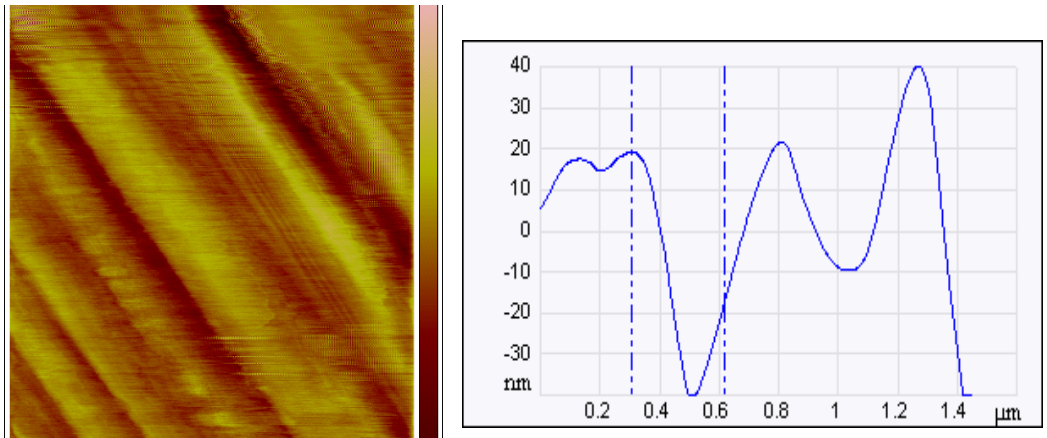

a

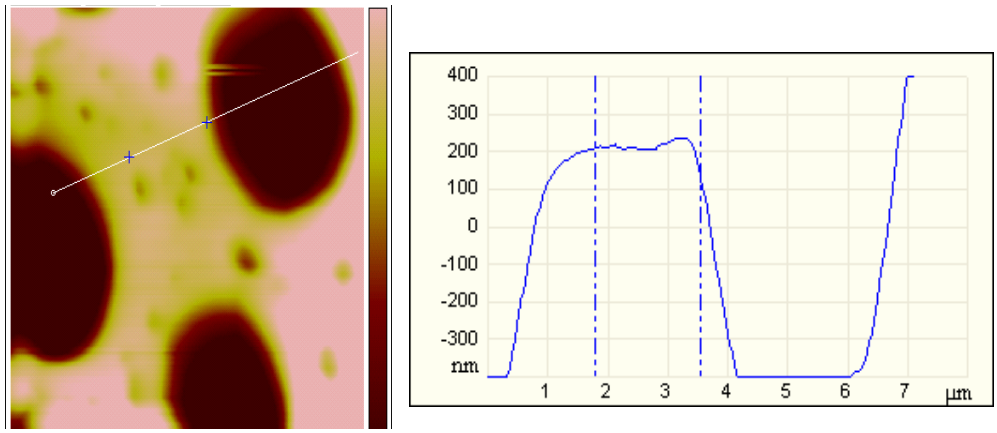

b

Figure 6.8: AFM of grafted materials (a) PLA-1 and (b) PLA-2.

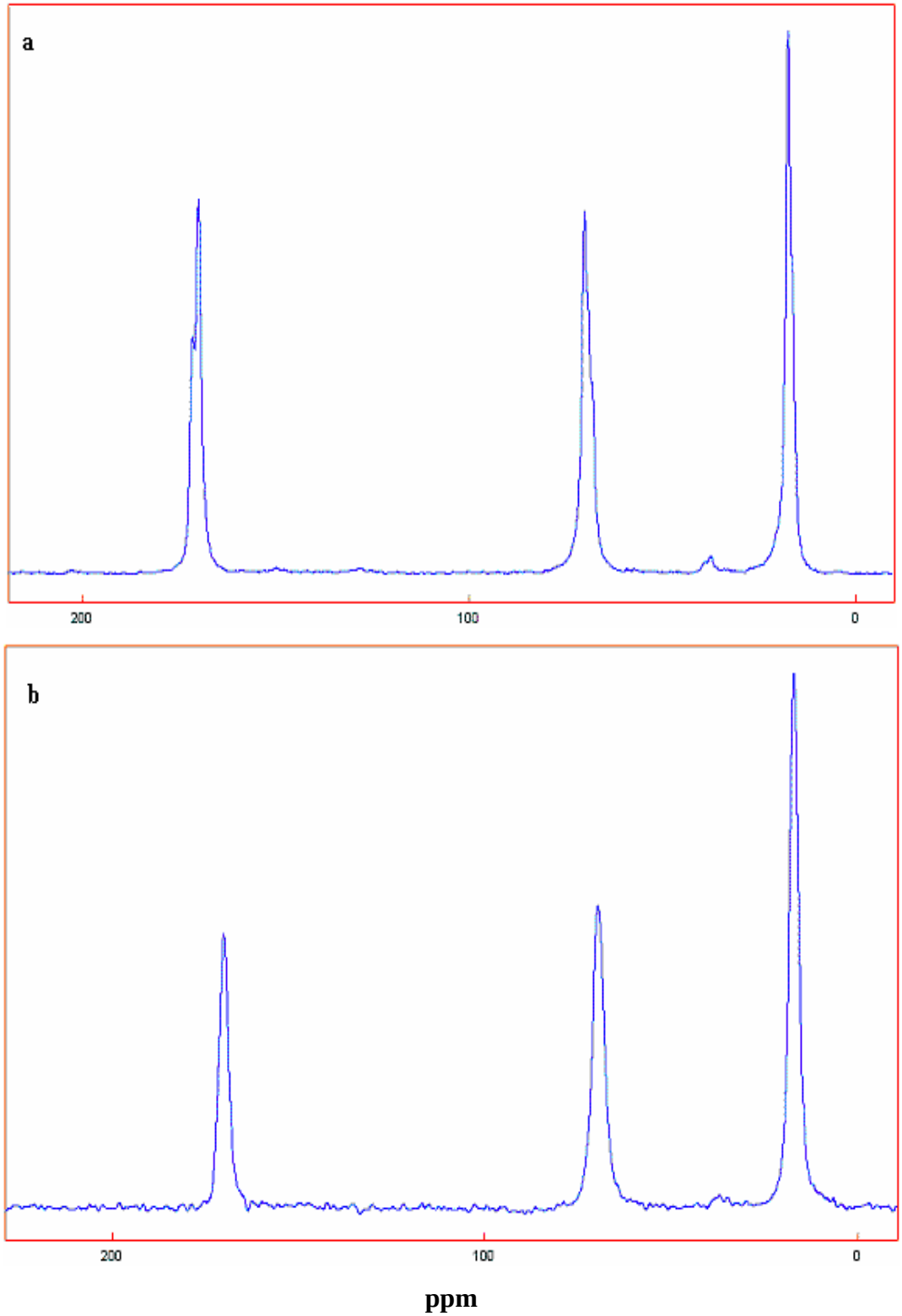

Figure 6.9: (a) ^{13}C CP/MAS of grafted PLA-1 and (b) ^{13}C CP/MAS of PLA without nanotubes.

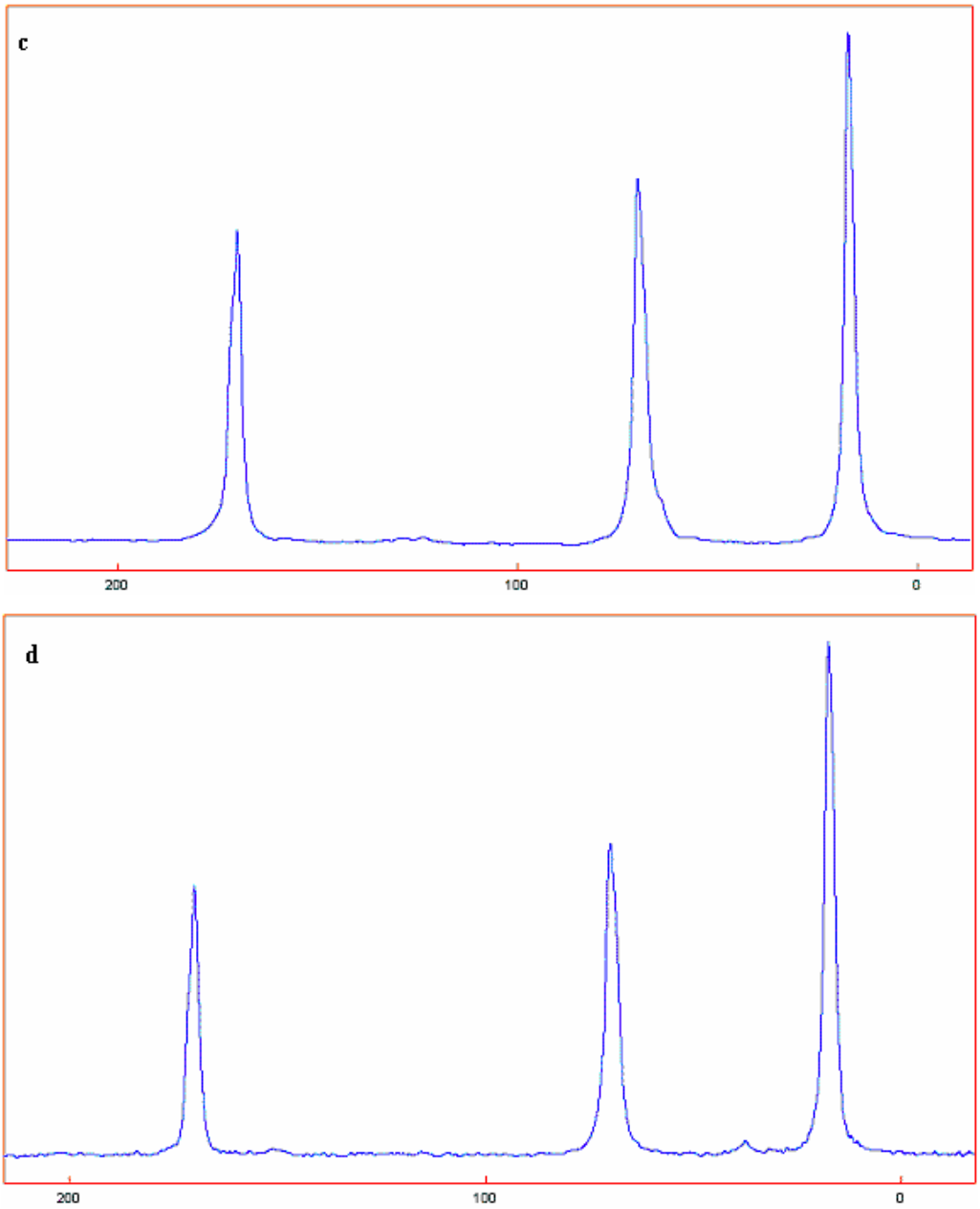

Figure 6.10: (c) ^{13}C CP/MAS of grafted olgiomer of PLA-2 and (d) ^{13}C CP/MAS of PLA oligomer.

6.4.7. ^{13}C Cross Polarization /Magic Angle Spinning (^{13}C CP/MAS): Figure 6.9a shows ^{13}C CP/MAS of grafted PLA where as Figure 6.9 b shows ^{13}C CP/MAS of PLA starting from L-lactic acid. The ^{13}C resonance appeared at approximately 17, 70 and 170 ppm corresponds to the methyl, methane and carbonyl carbon respectively in the polymer. ^{13}C

NMR signals of PLA become very broad upon the attachment of MWCNTs via the esterification of nanotubes bound carboxylic acid. Results from the determination of NMR nuclei spin-lattice (T_1) and spin-spin (T_2) relaxation times suggest that the broaden signals are associated with diamagnetic species namely the nanotubes attached polymer moieties **[15]**. Similar line broadening appeared in case of grafted PLA oligomers in comparison with PLA oligomers.

6.5. Grafting of copolymer on the surface of MWCNTs: The grafting of copolymer was carried out by taking silylated three-neck flask reactor L-lactic acid refluxed with xylene for 6 h using Dean stark apparatus. The reaction mixture was cooled up to 50 ^{0}C and 5 mol % of 12-hydroxystearic acid, FMWCNTs and tin chloride dihydarte were added in to it. The polymerization reaction was carried out for 20 h under stirring condition under the envelope of dry argon atmosphere (Figure 6.11).

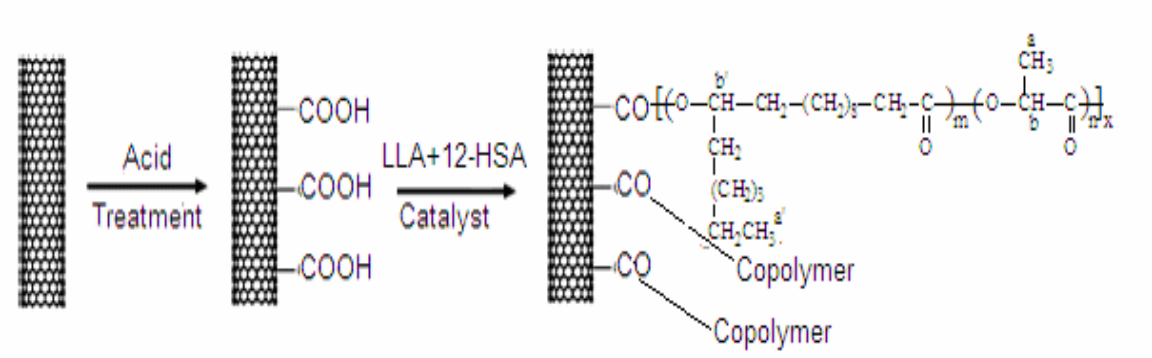

Figure-6.11: In situ grafting and copolymerization of L-LA and 12-hydroxy stearic acid on the surface of MWCNTs by using dehydropolycondensation.

6.5.1. Molecular weight determination: The blank copolymerization of L-lactic acid and 12-HSA using same method (dehydropolycondensation) without nanotubes. Figure 6.11 show the chromatogram of copolymer, having $\bar{M}_n = 3400$, $\bar{M}_w = 8200$ and PDI = 2.4 respectively.

6.5.2. ^{1}H NMR of copolymer: Figure 6.13 shows the ^{1}H NMR of copolymer. ^{1}H NMR confirmed the structure of the copolymer and incorporation of 12-hydroxystearic acids in the copolymer chain was calculated as 4.92 %.

6.5.3. FT-IR: Figure 6.14 a shows the FT-IR of copolymer without nanotubes. As is clearly evident, there is an absorption at 3504 cm^{-1} due to the free hydroxyl groups. The

characteristic stretching bands of ester group appeared at 1749 cm^{-1} (C=O) and 1134 cm^{-1} (C-O). The bands at 2997 and 2944 cm^{-1} are due to C-H stretching mode. Figure 6.14 b shows the IR spectra of MWCNTs grafted copolymer. The characteristic stretching band of carbonyl peak appears at 1726 cm^{-1} (C=O) and 1130 cm^{-1} for C-O stretching. The bands appeared at 2944 and 2863 cm^{-1}, which are assigned due to C-H stretching modes. There are more absorptions around 1458, 1377 and 1060 cm^{-1}, which can be attributed to the alkyl C-H and C-C bending modes. The peaks appeared in Figure 6.14 b slightly shifted with respect to copolymer peaks shown in Figure 6.14 a.

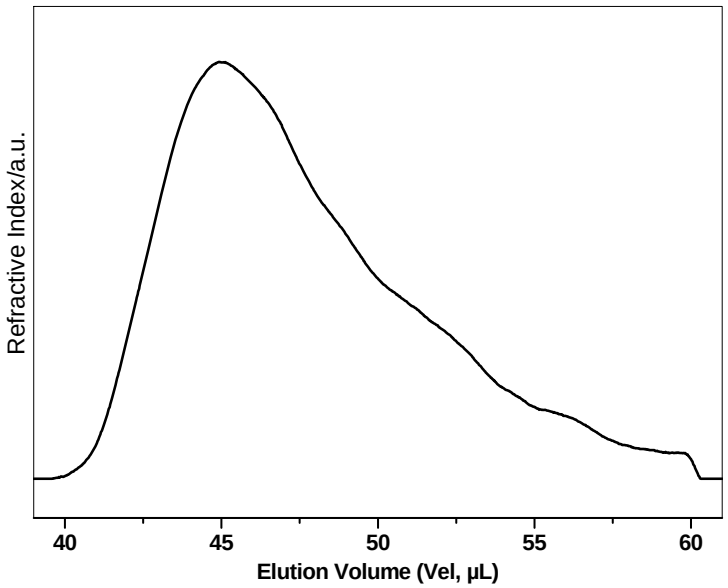

Figure 6.12: Size Exclusion Chromatography (SEC) elugram of copolymer (L-LA-co-12-HSA).

6.5.4. Thermo gravimetric analysis: The copolymer- grafted MWCNTs were pyrolyzed under an atmosphere of nitrogen and shown in Figure 6.15 a. The copolymer began to degrade around 220 ^{0}C and complete degradation occurred around 315 ^{0}C. After 700 ^{o}C, the weight percentage curve leveled at 12 % (Figure 6.15 a). The weight loss was determined to be 88 %. Figure 6.14b displays TGA curve of copolymer, degradation began around 135 ^{0}C and completed at 315 ^{0}C. Differential TGA curve (Figure 6.15 a) also confirmed that complete weight loss occurred around 315 ^{0}C in the case of copolymer as well as grafted copolymer on the surface of MWCNTs.

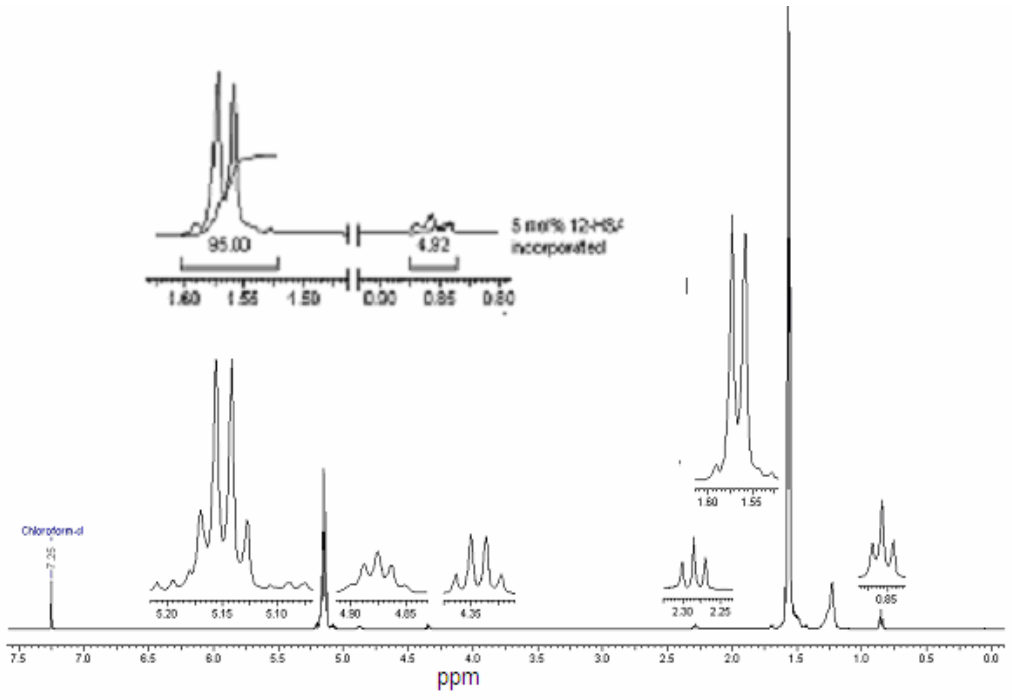

Figure 6.13: ^{1}H NMR (500 MHz) of copolymer (L-LA-co-12-HSA).

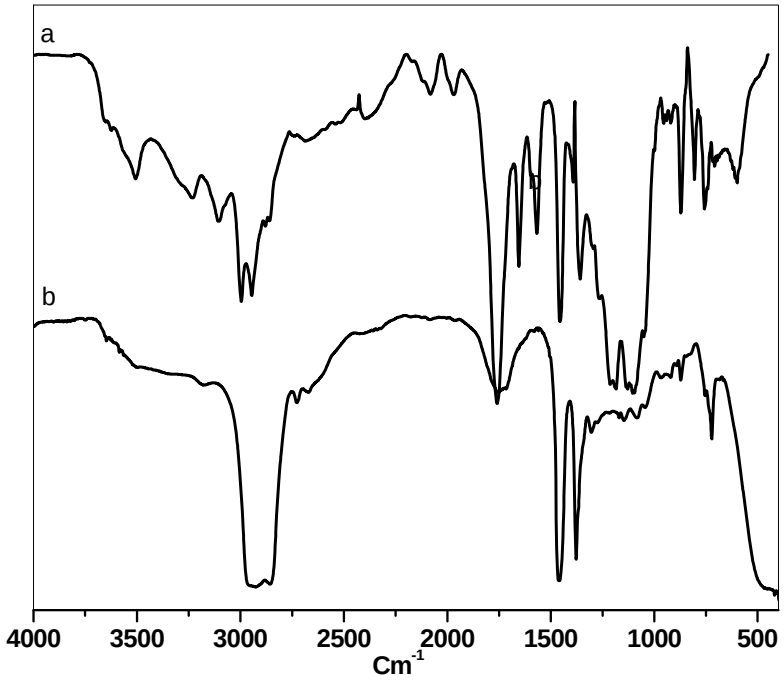

Figure 6.14: (a) FT-IR of copolymer sample (L-LA-co-12HSA) without nanotubes and (b) FT-IR of grafted copolymer on FMWCNTs.

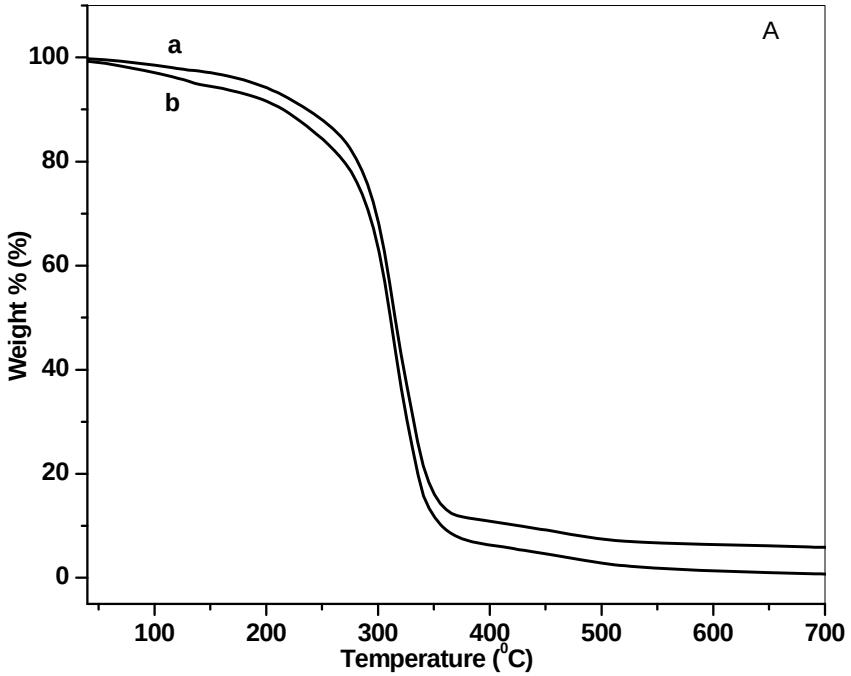

Figure 6.15 A: (a) TGA curves of grafted copolymer and (b) TGA curve of copolymer.

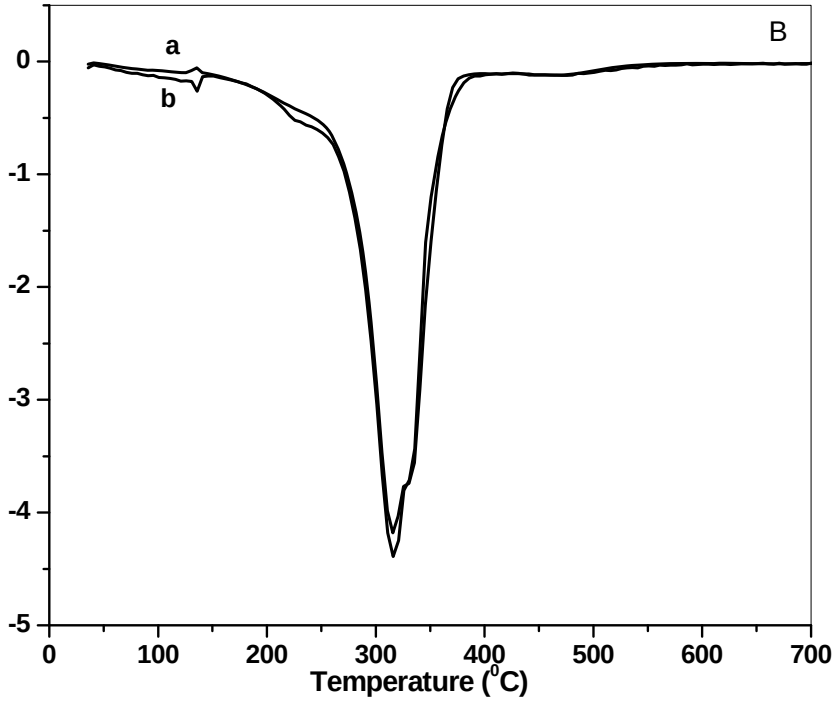

Figure 6.15 B: (a) DTA curve of grafted materials and (b) DTA curve of copolymer.

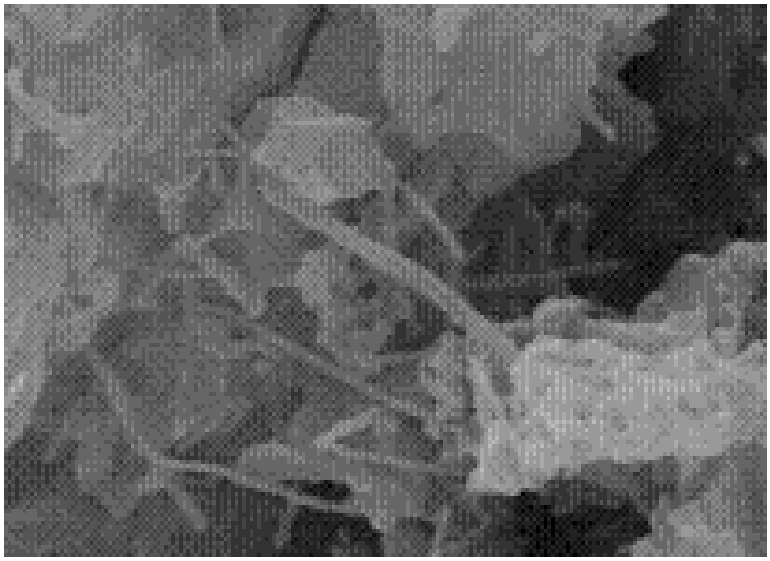

Figure 6.16: SEM of grafted copolymer (L-LA-co-12-HSA) on MWCNTs.

6.5.5. Scanning electron microscopy: Figure 6.16 shows the SEM image of grafted copolymer (L-LA-co-12-HSA). The images provided evidence of chemical linkage between copolymer and MWCNTs. The individual MWCNTs were exfoliated and separated by copolymer molecules. It is clearly evident from spectral analysis that the copolymer molecules were grafted on the surface of MWCNTs during dehydropolycondensation. These images demonstrated high MWCNTs content, for the material samples showed good dispersibility in chloroform, dichloromethane and acetone.

6.5.6. Transmission electron microscopy: Transmission electron microscopy was used to directly image of grafted copolymer on MWCNTs. The TGA traces indicate that the grafted copolymer content in the grafted copolymer was approximately 88%. TEM images provide confirmation of unbundling of grafted copolymer on MWCNTs. The nanotubes can be attributed to copolymer that is grafted on to MWCNTs. These results were supported by spectral data and TGA analysis.

6.5.7. Atomic Force Microscopy: Figure 6.18 displays AFM image of the surface of copolymer grafted MWCNTs formed on the topographic patterns comprised of 10 nm in height and side length ranging from 0.5 nm to 4 μm. Surface patches are formed

randomly distributed employing that the presence of side chain hanged at 12-postion in the copolymer grafted on MWCNTs.

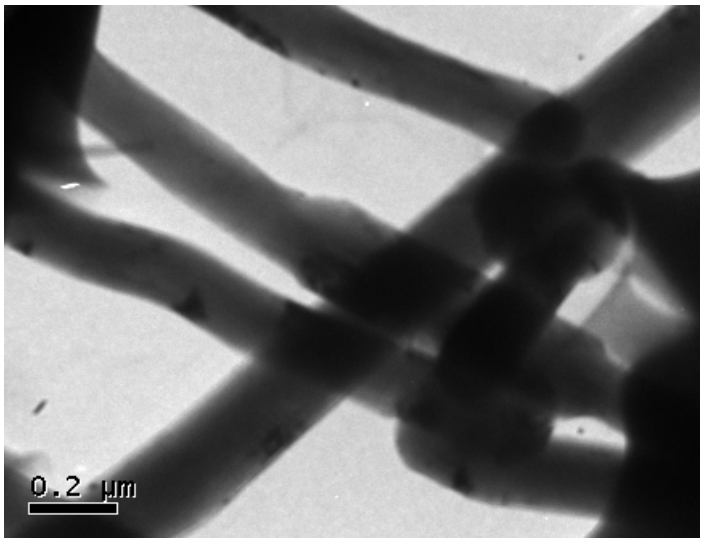

Figure 6.17: TEM of grafted copolymer (L-LA-co-12-HSA) on MWCNTs.

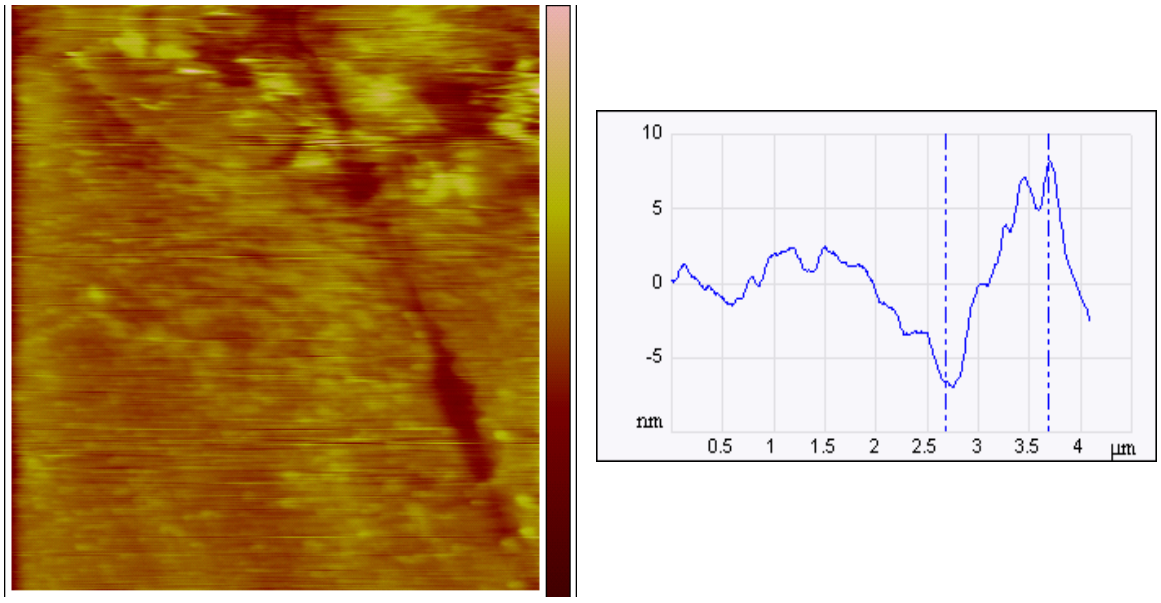

Figure 6.18: AFM images of copolymer grafted on MWCNTs.

The random distribution of patches on the surface was maintained and arrangement of the patches was distinctly different considering that the averaged center to outer distance between neighboring patches is approximately 80 nm on a flat surface.

6.5.8. *^{13}C Cross Polarization /Magic Angle Spinning (^{13}C CP/MAS):* Figure 6.19 A and A' show the ^{13}C CP/MAS NMR spectra of grafted copolymer (L-lactic acid-co-12 hydroxyl stearic acid) on MWCNTs surface and copolymer respectively. As expected, the solution NMR resonances are narrower than the solid- state NMR resonances. The ^{13}C resonances at approximately 17, 70 and 170 ppm corresponds respectively to the methyl, methane and carbonyl carbon in the polymer. The line broadening of methyl, methane and carbonyl groups increased when the copolymer grafted on the surface of MWCNTs. The line broadening suggested the formation of new crystallites, which is likely to be induced in the proximity of MWCNTs. Experiments were performed to compare the cross- polarization efficiency for the crystalline and amorphous domains in the polymer. They were assumed to be identical with in the errors in the NMR measurements. Since the CP/MAS measurements were made at 35 ^{0}C below the Tg of the PLA polymer. The mobility differences (in the kilo hertz region) are expected to be minimal. The shape of the resonance in the spectra of partially crystalline PLA did not change with varying contact times. The integrated intensity of the various partially crystalline PLA did not change with varying contact times. The integrated intensity of the various partially crystalline and amorphous polymers was found to be proportional to the weight of the polymer in the rotor when the identical instrumental condition was employed. The ^{1}H T_1 line for this sample was between 0.96 to 1.0s, shorter for amorphous and larger for crystalline component while Gaussian peak corresponds to the amorphous content in the sample.

The fraction of polymer chains in the folds in between lamellae also contributes to amorphous composition. The cross polarization efficiency is identical in the amorphous and crystalline domains of the polymer; the normalized integrated area of the peaks represents the molecules in that particular environment. Therefore, the narrow line broadening in case of grafted copolymer on MWCNTs is attributed due to the contribution of MWCNTS matrix.

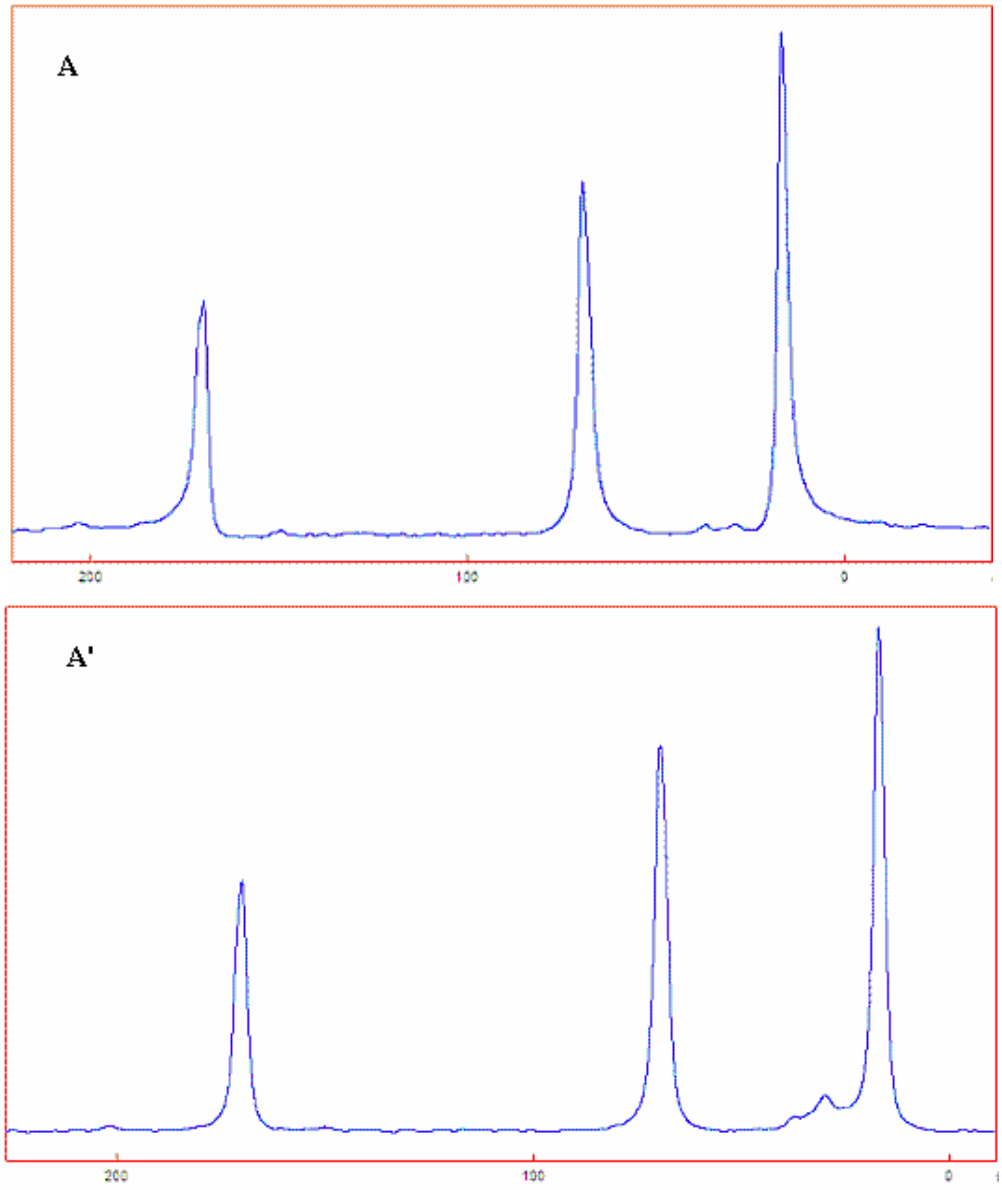

Figure 6.19: (A) ^{13}C CP/MAS of grafted copolymer and (A') ^{13}C CP/MAS of copolymer.

6.6. Conclusion:

In conclusion, L-Lactic acid, PLA oligomers and copolymers of L-LA and 12-HSA have been successfully grafted on the surface of MWCNTs by dehydropolycondensation and thoroughly characterized. The maximum level of grafting was observed as 15 wt %. In principle, this insitu dehydropolycondensation is feasible for a wide range of biocompatible and biodegradable monomers (aliphatic hydroxyl carboxylic acid). A smooth surface was detected by AFM for grafted homopolymers. Such microstructure

would account for the homogeneous distribution of MWCNTs and improve mechanical and electrical properties of the polymer. DSC study reveals that the L-LA-g-MWCNT has the effect of plasticizing the PLA matrix, which resulted in the lower of T_g, T_c and T_m than those of the PLA. The appearance of a shoulder of the melting endothermic peak on the second heating cycle suggested the formation of new crystallites, which is likely to be induced in the proximity of MWCNTs and also strongly supported by ^{13}C CP/MAS NMR study.

References

1. (a) Chen, J.; Hamon, M. A.; Hu, H.; Chen, Y.; Rao, A. M.; Eklund, P. C.; Haddon, R. C. *Science* **282**, 95 (1998). (b) Sun, Y. -P.; Fu, K.; Lin, Y.; Huang, W. *Acc. Chem. Res.* **35**, 1096 (2002).
2. Star, J. F.; Stoddart, D.; Steuerman, M.; Diehl, A.; Boukai, E. W.; Wong, X.; Yang, S.-W.; Chung, H.; Choi, J.; Health, R.; *Angew. Chem.* 2001, **113**, 1771-1775; *Angew. Chem. Int. Ed.* 2001, **40**, 1721-1725.
3. Georgakilas, V.; Kordatos, K.; Prato, M.; Guldi, D. M.; Holzinger, M.; Hirsch, A. *J. Am. Chem. Soc.* **124**, (2002).
4. Dyke, C. A.; Tour, J. M. *Nano. Lett.* **3**, 1215 (2003).
5. (a) Viswanathan, G.; Chakrapani, N.; Yang, H.; Wei, B.; Chung, H.; Cho, K.; Ryu, C. Y.; Ajayan, P. M. *J. Am. Chem. Soc.* **125**, 9258 (2003). (b) Banerjee, S.; Kahn, M. G. C.; Wong, S. S. *Chem. Eur. J.* **9**, 1898 (2003).
6. Riggs, J. E.; Guo, Z.; Carroll, D. L.; Sun, Y.-P. *J. Am. Chem. Soc.* **122**, 5879 (2000).
7. Fu, K.; Huang, W.; Lin, Y.; Riddle, L. A.; Carroll, D. L.; Sun, Y.-P. *Nano. Lett.* **1**, 439 (2001).
8. Pan, Z. W.; Xie, .S. S.; Lu, L.; Chang, B. H.; Sun, L. F.; Zhou, W. Y.; Wang, G.; Zhang, D. L. *Appl . Phy Lett.* **74**, 3152 (1999).
9. Yu, M. F.; Lourie, O.; Dyer, M. J.; Moloni, K.; Kelly, T. F.; Ruoff, R. S. *Science* **287**, 637 (2000).
10. Zhang, D. ; Kandadai, M.A.; Cech, J.; Roth, S.; Curren S. A. *J. Phys. Chem. B.* **110**, 12910 (2006).

11. Hamon, M.A.; Hui, H.; Bhowmik, P.; Itkis, H. M. E.; Haddon, R. C. *Applied Physics A Materials Science and Processing* **74,** 333 (2001).
12. Lin, Y.; Rao, A. M.; Sadanadan, B.; Kenik, E. A.; Sun, Y.-P. *J. Phys. Chem. B.* **106**, 1294 (2002).
13. Chen, X.; Chen, X.; Lin, M.; Zhong, W.; Chen, X,; Chen, Z. Macromolecular Chemistry and Physics **208,** 964 (2007).
14. Hill, D. E.; Lin, Y.; Rao, A. M.; L. Allard, F.; Sun, Y.-P. *Macromolecules* **35**, 9466 (2002).
15. Huang, W.; Fernando, S.; Allard, L. F.; Sun, Y.-P. *Nano. Lett.* **3**, 565 (2003).
16. Sun, Y-P.; Hung, W.; Lin, Y.; Fu, K.; Kitaygorodskiy, A.; Riddle, L.A.; Yu, Y.J.; Carroll, D. L. *Chem. Mater.* **13**, 2864 (2001).

Chapter-7

CHAPTER 7: HOMOPOLYMERIZATION AND COPOLYMERIZATION OF L, L-LACTIDE WITH ε-CAPROLACTONE IN PRESENCE OF NOVEL ZINC PROLINATE DERIVATIVES

7.1. Introduction:

In the recent year, there are enormous catalysts have been used for the polymerization of lactide and other lactones **[1-4]**. Some studies of variable catalyst have also been carried out. These catalysts are absolutely non-toxic, because they have been used and no adverse effect has been observed in polymeric product. Poly lactide (or poly lactone) polymer prepared using such catalyst does not require to be purified from the catalysts prior to a medical (implantation of various body parts and other accessories) or pharmaceutical application. The widely used catalyst such as salts or complexes of aluminum, tin or lanthanide ions for the polymerization of lactides or lactones, do not meet the above requirements. Zinc metal or its derivative was considered as a potential catalyst for lactides or lactones polymerization. Several difficulties have also been encountered. Zinc metal or zinc containing compound has been studied by several research groups with mixed results. Basic compound such as zinc oxide or carbonate favors partial racemization of L-lactide and termination steps. Use of diethyl zinc catalyst during polymerization of lactide and lactones has caused technical problem because it is highly moisture sensitive and self-inflammable liquid. Zinc powder is removed from the polylactones by ultra filtration. There are some literature reports about the use of organo zinc in polymerization of lactide and lactones, but nothing is known about the toxicity of the legend, which does not belong to the human metabolism. Although numerous amino acids and their derivatives belong to the human metabolism, zinc salts of amino acids have rarely been used as catalysts for the polymerization of lactides and lactones **[4]**.

Recently, poly (lactide) (PLA) and poly (ε-caprolactone) (PCL) and their copolymer have attracted more attention in the fields of surgery, sustained drug delivery and tissue engineering **[5-7]**. These polymers have shown their potential applications in a variety of fields because of their biodegradability, biocompatibility and permeable properties. Poly (ε-caprolactone) shows low melting temperature (T_m~60 ^{0}C) and high decomposition

temperature (T_d= 350 ^{0}C) and degrades very slowly due to its high hydrophobicity and crystallinity. It is known that block copolymerization allows combination of the chemical properties of the main components and physical properties of the resulted copolymers can be tailor made by adjusting the molecular weights and the composition of the constituting blocks. Though several strategies have been used for preparation of PLA and PCL, the particular convenient method to synthesize these polymers is the ring opening polymerization (ROP) of lactide/lactones and their functionally related compounds. The ring opening polymerization of lactide and ε-caprolactone give polymers with wider spectrum of properties than the polymers synthesized by copolymerization of the corresponding hydroxyacids, which have been reported in the literature. Such ring opened copolymers yield tough polymers with properties from rigid thermoplastics to elastomeric rubbers [**8, 9]**, with tensile strengths ranging from 0.6 to 48 Map and also elongation **[10]**. The larger reactivity of lactide over ε-caprolactone leads to copolymers that are blocky, where the block lengths depend on the starting co-monomer composition, catalyst **[11]** and polymerization temperature.

The copolymer of pure L-lactide with ε-caprolactone obtained by ROP contributes flexibility behavior because of the ε-caprolactone segment and high crystalline melting points from PLA blocks. Many metal complexes (e.g. Al **[12]**, Li **[13]**, Mg **[14],** Fe **[15]**, Son **[16]** and Or **[17]** have been used as initiator/catalyst in the ROP of cyclic ester. β-diketiminato ligands have emerged as one of the most versatile ligands and these ligands are readily tunable to access derivatives containing a range of substituents around ligands skeleton **[18]**.

A highly efficient initiator (complexation of zinc with β-diketiminato ligands) for the ring opening polymerization of lactides and ε-caprolactone has been studied **[19]**.

zinc metal or zinc containing compounds were studied by several groups **[20-25]**, with mixed results. Zinc oxide or carbonate favors partial racemization of L, L-lactide and termination steps. Diethyl zinc is a highly moisture sensitive and self-inflammable liquid Which is inconvenient for up scaling and technical productions of polylactides. zinc powder needs to be removed by ultra filtration. Zinc bis (2, 2-dimethyl –3, 5-heptanedionate) give high molecular weights, but nothing is known about toxicity of the ligand, which doesn't belong to the human metabolism.

Zinc L-lactate posses several useful and promising properties, but poly (L-lactide) with a molecular weight 100,000 can seemingly not to be obtained with this zinc salt **[25]**. The present work highlights on zinc salts of amino acids. Although numerous amino acids and their derivatives belong to the human metabolism, zinc salts of proline have never been used as catalysts for the polymerization of lactides and ε-caprolactone. Zinc prolinate was selected because of its biocompatibility in comparison with other reported catalyst. Therefore, zinc salts of L-proline, D-proline and were used in homopolymerization of L, L-lactide and D, L-lactide and copolymerization with other lactones, such as ε-caprolactone. The resulting copolymers were characterized by ^{1}H NMR, ^{13}C NMR, Size exclusion chromatatography (SEC), Infrared spectroscopy (IR), Differential scanning calorimetry (DSC), thermo gravimetric analysis (TGA) and MALDI ToF-MS.

7.2. Experimental:

7.2.1. Materials and methods: L, L-lactide, ε-caprolactone, L-proline, D-proline and zinc acetate were purchased from Aldrich sigma, dichloromethane (DCM) and methanol were purchased from SD-Fine Chemical India.

7.2.2. Synthesis of zinc prolinate catalysts: The catalyst zinc L-prolinate was easily synthesized by stirring zinc acetate Zn $(OAc)_2$ (1 equiv.), L-proline (2 equiv.) and triethylamine (2 equiv.) in methanol (Figure 7.1). The complex (white sluggish) was precipitated out from the methanolic solution and can be easily isolated. Zinc D-prolinate was prepared by using similar procedure. The spectroscopic data **[26]**, the mononuclear zinc $(prolinate)_2$ derivatives are shown to be the prevailing species. FTIR (Figure 7.2) also confirmed the structure before and after the complexation with proline.

$C_{10}H_{16}N_2O_4Zn$ (291.60), calculated, C 40.91, H 5.48, N 9.54 and found C 40.90 H 5.53 N 9.4. This catalyst was shown possessing low hygroscopic. The crude product was recrystallized and $[\alpha]_D^{20}$= -53 .68 concentration 2.59/dl in water.

The complex was resulted from the reaction of zinc acetate with either (L or D) proline. The two L-proline molecules are coordinated to the zinc atom via their N and carboxylic O atom. The two bidentate ligands are trans with respect to each other. The zinc atom is pentacoordinate, fifth coordination site being occupied by the symmetry related O (4') (symmetry code: (i) 2-x, y-1/2, -z) of a neighboring proline molecules, so that an infinite

polymeric chain is generated. The polymer shows a helical structure along the 2^1 direction. The zinc coordination here is unique as most zinc amino acid complexs are hexadentate.

FT-IR showed the N-H stretching at ~3750 cm^{-1}, C=O ketonic (ν CO) = 1590 cm^{-1} and antisymmetric and symmetric carbonyl stretching frequency at 1720 and 1350 cm^{-1}. The stretching ν (CO) and ν N-H bands of L-praline after coordination with zinc were observed at 3250 and 1550 cm^{-1}. The antisymmetric and symmetric carbonyl stretching frequency were observed at 1550 and 1350 cm^{-1} respectively. The difference between the antisymmetric and symmetric stretching frequencies ν (COO^-) was calculated as 168 cm^{-1} and found similar to the stretching frequency of M-O bond. Similarly IR spectra of zinc D-prolinate showed the frequency at 3250 cm^{-1} and 1550 cm^{-1}. The peaks at 1680 and 1382 cm^{-1} were observed due to carbonyl antisymmetric and symmetric stretching frequency respectively.

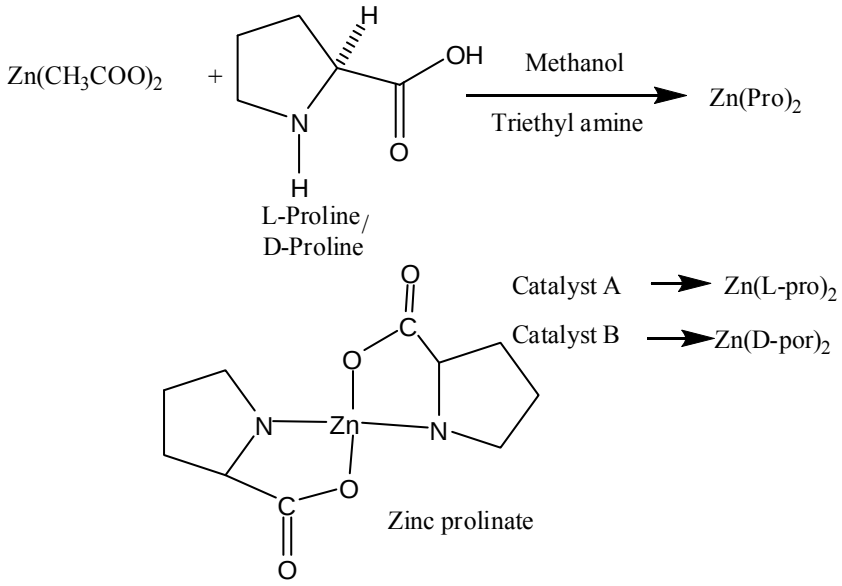

Figure 7.1: Synthesis of catalysts.

7.3. Characterization method:

7.3.1. FT-IR: As discussed in chapter 6.

7.3.2. Exclusion Chromatography: As discussed in chapter 3.

7.3.3. Differential Scanning Calorimetry (DSC): As discussed in chapter 3.

7.3.4. Thermo gravimetric Analysis: As discussed in chapter 5.

7.3.5. X-Ray Analysis: As discussed in Chapter 3.

7.3.6. Nuclear Magnetic Resonance Spectroscopy (NMR): As discussed in chapter 3 and chapter 5.

7.3.7. ^{13}C Cross Polarization /Magic Angle Spinning (^{13}C CP/MAS): As discussed in chapter 4.

7.3.8. MALDI-ToF MS Analysis: As discussed in Chapter 4.

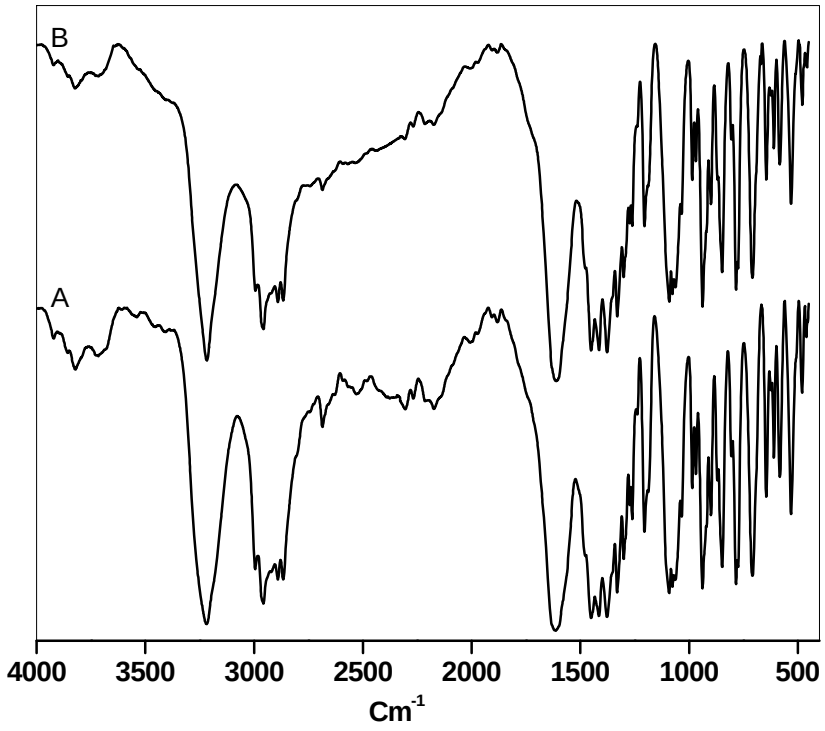

Figure 7.2: FT-IR spectra of (A) zinc L-prolinate and (B) zinc D-prolinate.

7.4. Results and Discussion:

The zinc salts of proline having two configurations (L- and D-) were prepared and used as potential catalysts of the polymerization of L-lactide and D, L-lactide. These catalysts showed low hygroscopic. Zinc salt of L-proline should be compared with that of zinc D-prolinate in term of their structure. The catalysts can also be recovered by dissolving product (PLA) in dichloromethane and precipitating using deionised water because catalysts are water soluble. Zinc salts of L-proline and D-proline dried over P_4O_{10} and composition were rechecked by elemental analysis prior to further use.

7.4.1. General procedure for synthesis of PLA by ring opening polymerization: 2g (0.0138 mmol) of lactide (L and D, L-lactide) was taken for each reaction, requisite concentration of zinc prolinate (L or D) was taken and polymerization was carried out in sealed glass reactor previously passivated with trimethyl silyl chloride. Thermodynamic and kinetic parameters were altered to examine their effect on ring opening polymerization. The type of catalyst was also varied. The reaction scheme is shown in Figure 7.3.

7.4.2. Molecular weight determination: Table-7.1 shows the ring opening polymerization of L, L–lactide in presence of Zn (L–prolinate)$_2$. The homopolymers (L-1 to L-5) were prepared in presence of zinc L-prolinate catalyst at various temperatures ranging from 150 ^{0}C to 240 ^{0}C, keeping fixed monomer to catalyst ratio. The yield and molecular weight increased monotonously up to 195 ^{0}C and thereafter became steady. The maximum yield obtained was 93 %, which is close to the realistic maximum. Because the conversion of L, L-lactide cannot be higher than 96±1% due to thermodynamic reason. PLA was prepared at 195 ^{0}C in 1h and showed $\bar{M}_n$ and $\bar{M}_w$ values as 5100, 9200 Da and polydispersity as 1.8 respectively, which was obtained at 675 monomer to catalyst ratio. Polymers L-6 to L- 9 is shown in Table 7.2 varying [monomer]/ [catalyst] ratios.

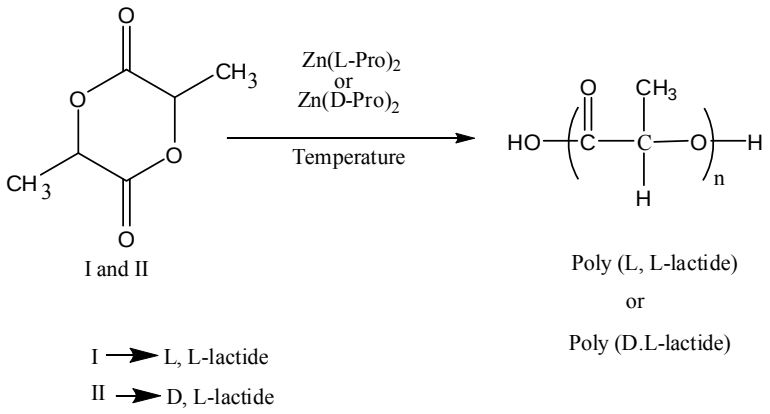

Figure 7.3: Homopolymerization of L, L-lactide and D, L-lactide.

Table 7.3 depicts polymers L-9 to L-13, which showed the effect of polymerization time. The maximum molecular weight was obtained at 2 h of polymerization time at 195 ^{0}C. Polymer L-3 and L-13 showed comparative results of the catalytic activity of Zn (L-prolinate)$_2$ and Zn (D-prolinate)$_2$ respectively.

Table 7.1: Effect of temperature on ROP of L, L-lactide

Polymer samples	Temperature (^{0}C)	$\bar{M}_n$ (GPC)	$\bar{M}_w$ (GPC)	T_g (^{0}C)	T_m (^{0}C)	ΔH_f (J/g)	Tc (^{0}C)
L-1	150	850	2900	35.55	90.8	49.67	nd
L-2	180	3200	4200	34.12	144.13	39.63	70.08
L-3	195	5100	9200	55.15	138.99	29.69	103.29
L-4	210	4000	4600	21.31	124.93	18.38	nd
L-5	240	3800	4600	38.76	nd	nd	nd

L, L-lactide, zinc L-prolinate catalyst, [M]/[C] = 675, time of polymerization 60 min and nd –not detected.

The result confirmed that Zn (L-prolinate)$_2$ is more reactive in comparison to Zn (D-prolinate)$_2$. Similarly, catalytic activities of both zinc prolinate were studied in presence of the D, L-lactide. There were no remarkable effects of the catalyst in the polymerization reaction. The molecular weights of PLA polymers were low with narrow distribution. The molecular weights increased from samples (L_6-L_3) with the increase in [M]/ [C] ratio and decreased thereafter. Similar results have been observed using Zn L-lactate **[27]** catalyzed polymerization of 1, 4-dioxane-2-one, polymerizing L-lactate in presence of Sn(II) Octoate **[28],** using highly active zinc catalyst for the controlled polymerization of lactide **[29]** and also other examples. The result of Zn L-prolinate catalyzed polymerization showed the $[\eta]_{inh}$. increased with increase in [M]/ [C] ratio **[30]**. The increase in the temperature resulted increase in molecular weight. Polymer L-3 showed $\bar{M}_n$ and $\bar{M}_w$ values as 5100 and 9200 Da respectively and thereafter decreased with increase in temperature up to 240 ^{0}C.

7.4.3. Thermal Analysis: The results of thermal characterization are shown in Table-7.1 to Table 7.3 and thermograms are also shown in Figure 7.4 A and 7.4 B. T_g varied from 21.31 to 55 .15 ^{0}C for the polymers prepared with Zn (L-prolinate)$_2$. The melting temperature T_m of the polymers prepared with the Zn (L-prolinate)$_2$ catalysts (catalyst A) increased from 110 ^{0}C to 142.2 ^{0}C, whereas polymer (L-13) prepared in presence of the

Zn (D-prolinate)$_2$ showed T_g and T_m as 51.6 ^{0}C and 79.1 ^{0}C respectively. PLA prepared in presence of Zn (L-prolinate)$_2$ resulted less racemization reaction in comparison with Zn(D-prolinate)$_2$. The T_g obtained in case of D, L-lactate polymerization using Zn (L-prolinate)$_2$ imparts lower T_g than Zn (D-prolinate)$_2$. The degree of crystallinity calculated from powder patterns is typically between 45 to 65 % except for few samples.

Table 7.2: Effect of [M]/[C] ratio on the polymerization (ROP) reaction of L, L-lactide

Polymers samples	[M]/[C]	$\bar{M}_n$ (GPC)	$\bar{M}_w$ (GPC)	T_g (^{0}C)	T_m (^{0}C)	ΔH_f (J/g)	T_c (^{0}C)
L-6	337	4000	4700	31.66	131.51	22.1	102.2
L-7	405	4300	4900	35.15	132.09	23.0	103.5
L-8	506	4400	6200	42.28	139.28	20.7	98.3
L-3	675	5100	9200	55.15	145.99	31.7	103.3
L-9	1013	3400	8400	47.74	144.89	30.4	99.2

As all polymerization were conducted at 195 ^{0}C, monomer: L, L-lactide, catalyst: zinc L-prolinate and polymerization time: 60 min.

7.4.4. Nuclear Magnetic Resonance Spectroscopy (NMR): ^{13} C NMR has been utilized as a useful tool for determining the number average molecular weight, $\bar{M}_n$ quantitatively. Besides end group analysis, this technique has also used in other quantitative analysis for determination of residual L-lactic acid, lactide formed due to unzipping of chain ends **[31]**. ^{13}C NMR has also been used to study the crystallization and morphology **[32]**, and for direct observation of stereodefects in poly (L-lactide) **[33]**. In the present study, ^{13}C NMR was used to determine the end groups, residual lactic acid, lactide and stereosequence of poly (lactic acid) s in PLA samples. For this purpose, the PLAs were prepared by changing various parameters such as catalyst concentration, polymerization time, reaction temperature variation etc, and are shown in Table 7.1 to Table 7.3. The spectrum of L-3, L-5, L-9, L-12 and L-13 are depicted in Figure 7.5. The peaks appearing from 169.23 to 169.70 ppm are due to ester carbonyl groups and peaks arising from 172.9 to 173.4 ppm are due to carboxylic acid end functional groups. The accuracy

of DPn estimate was same in two consecutive NMR measurements. There is a peak at 167.2 ppm is due to lactide in the polymers and calculated for samples as L- 12 and L-13 are 1.2 and 0.8 respectively.

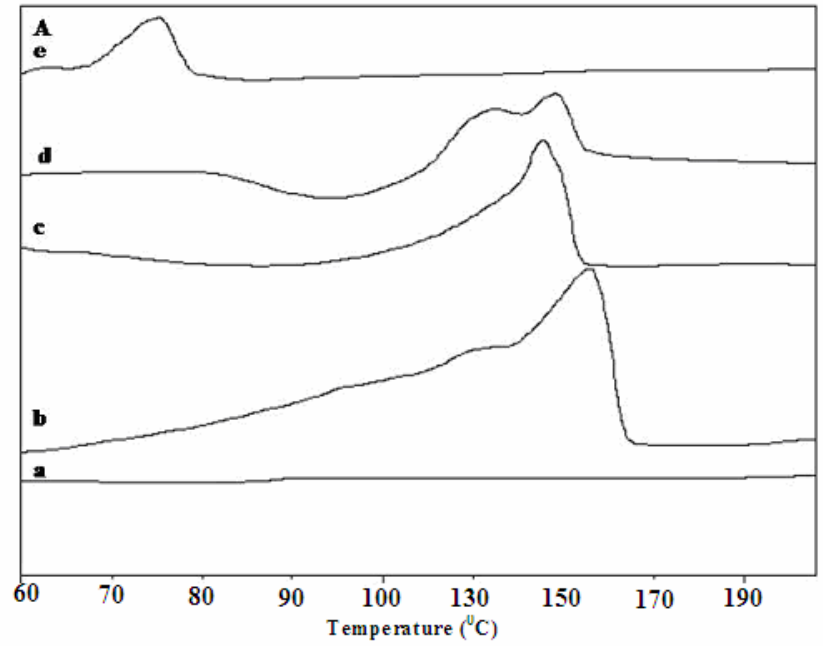

Figure 7.4A: DSC thermogram of PLA (a) L-5, (b) L-3, (c) L-9, (d) L-12 and (e) L-13.

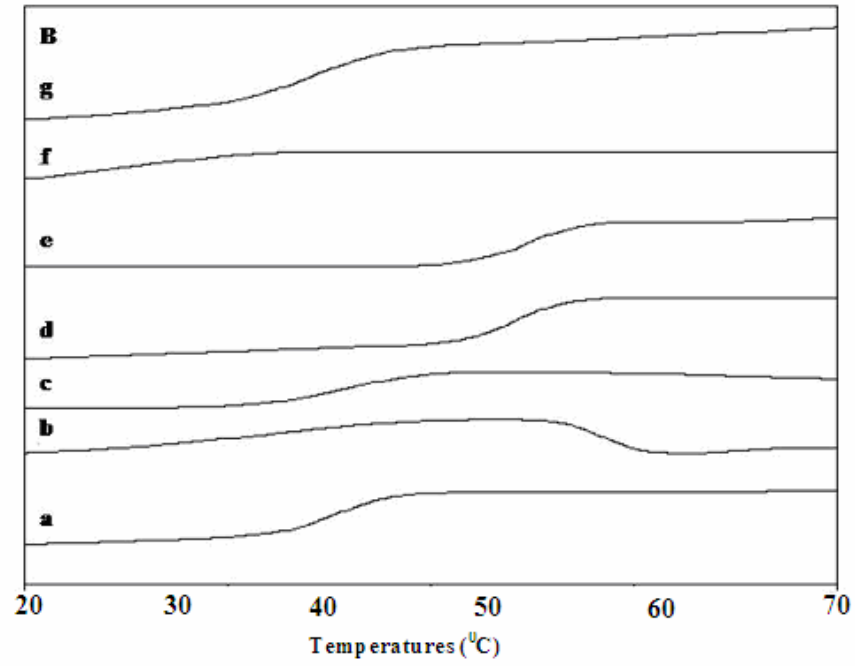

Figure 7.4 B: DSC thermogram of PLA (a) L-5, (b) L-3, (c) L-9, (d) L-12 and (e) L-13.

Figure 7.6 shows the ^{13}C spectra of L-14 and L-15. The peaks arising from 169.13 to 169.72 ppm and 168.9 to 168.7 (L-16) ppm appearing are due to ester carbonyl groups. The peaks arising from 172.9 to 173.4 ppm are due to carboxylic acid end functional groups. There was a peak at 167.9 (L-14) and 167.3 (L-15) ppm due to lactide in the polymers and was estimated 2 %.

7.4.5. 13C Cross Polarization /Magic Angle Spinning (13C CP/MAS): The 13C NMR spectrum of L-3 and L-13 are shown in Figure 7.7. The peaks at 109.1 and 110.5 ppm may be attributed due to C-2 carbon of the complex catalyst structure.

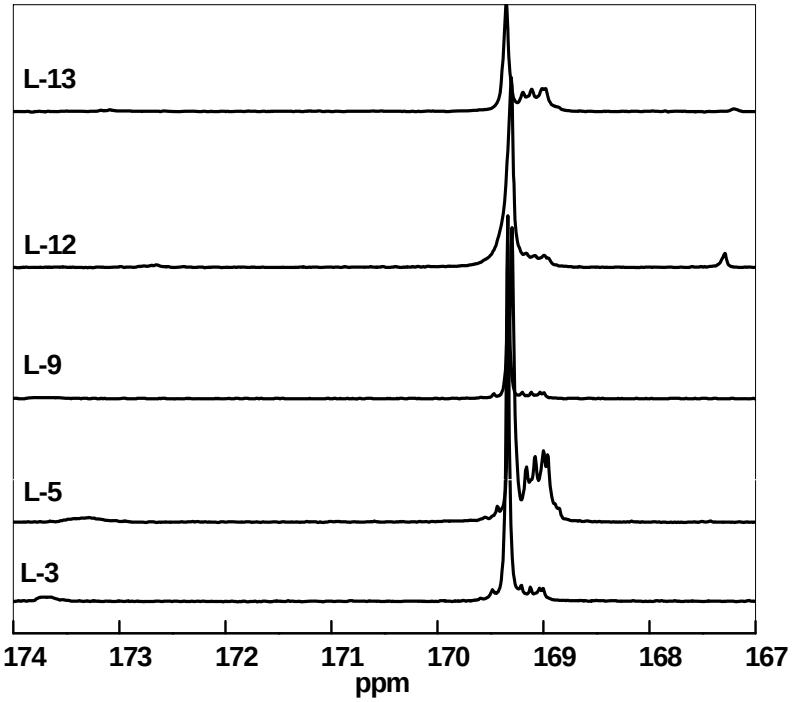

Figure 7.5: ^{13}C NMR spectra (500 MHz) around carbonyl (ester), carbonyl (acid) and carbonyl (lactide) areas of PLA oligomers L-3, L-5, L-9, L-12 and L-13.

7.4.6. MALDI-ToF-MS: MALDI-ToF-MS has been employed for the determination of molecular weights and the nature of end group. Using ring opening polymerization reactions, only low-molecular weight oligomers and high molecular weight PLA can be prepared. Therefore polymers prepared during this study were subjected to MALDI-ToF MS analysis and are shown in Figures 7.8-7.13. Polymer L-3 (Figure 7.8), showed peaks ranging from 689 to 1840 Da corresponding to sodiated adduct molecular ions H- [O-CH

(CH3) CO-]n-OH-Na+ (mass=72n+18+23); n found to be varying from 9 to 25, 23 being the mass number of sodium. The series ranging from 490 to 1497 Da corresponding potassiated adduct molecular ions of type H- [O-CH (CH3) CO-] n OH-K+.

Table 7.3: Effect of reaction time on polymerization ROP) of lactide

Sr.no.	Lactide	Catalyst	Time (min)	$\bar{M}_n$ (GPC)	$\bar{M}_w$ (GPC)	T_g (^{0}C)	T_m (^{0}C)	ΔH_f (J/g)	Tc (^{0}C)
L-10	L-LA	Zinc L-prolinate	30	4500	6500	16.24	110.02	15.26	68.77
L-11	L-LA	Zinc L-prolinate	90	4500	6600	49.75	133.69	17.09	nd
L-12	L-LA	Zinc L-prolinate	120	3600	6900	44.29	142.21	15.60	96.45
L-13	L-LA	Zinc D-prolinate	60	2500	5800	51.67	79.11	6.91	nd
L-14	D-LA	Zinc L-prolinate	60	1500	2700	20.65	Nd	nd	nd
L-15	D-LA	Zinc D-prolinate	60	1341	2500	37.44	Nd	nd	nd

[M]/[C]= 675 and polymerization temperature 195 ^{0}C.

Figure 7.9 depicts the MALDI-ToF mass spectrum of the L –5. As expected, the MALDI-ToF mass spectrum of the sample shows a series of intense molecular ion peaks ranging from a mass of 618 to 1769 Da, which are assigned to sodiated adduct molecular ion of the type H- [O-CH (CH_3) CO-]$_n$ OH-Na^+. There is another series ranging from 706 to 1498 Da, which are corresponding due to the potassiated adduct molecular ions, denoted by the structure H- [O-CH (CH_3) CO-]$_n$ OH K^+. The peaks ranging from 784 to 1215 Da correspond to oligomers of the structure H- [O-CH (CH_3) CO-]$_n$ OCH_2CH_3, with a molecular mass 72n+46+23. The MALDI-ToF spectrum of the L-9 and L-13 are presented in Figure 7.10 and Figure 7.11. The most intense peak of the L-9 ranging from 617 to 1626 Da, correspond to doped sodium ions of the linear oligomers with a mass of

72n +18+23 (n values varies from 8 to 22). The corresponding linear polymer doped with potassium ions can also see as peaks of mass 72n+18+39. Figure 7.11 depicts the MALDI-ToF spectrum of L-13. The most intense peaks, arising in the region from 545 to 1425 Da, correspond to linear oligomers, doped with sodium ions (n varies from 7 to 19).

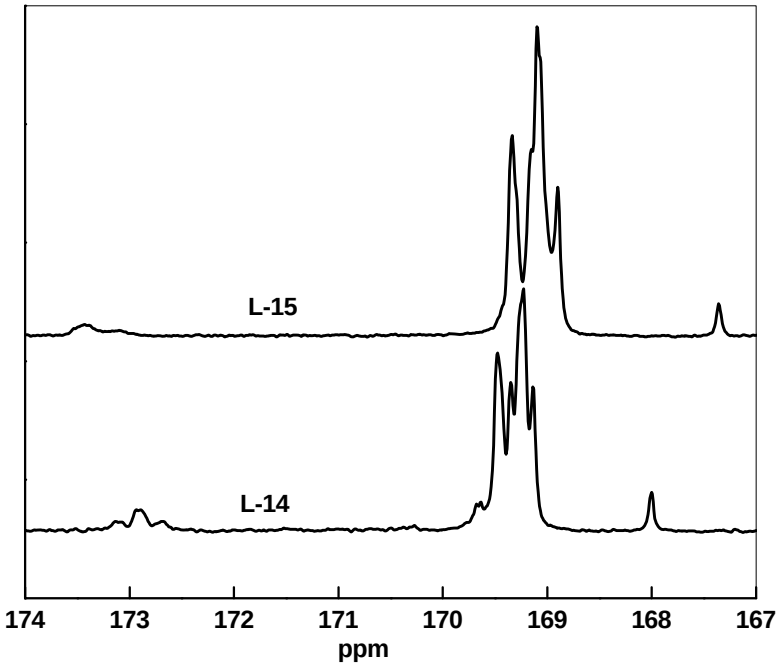

Figure 7.6: ^{13C} NMR spectra (500 MHz) around carbonyl (ester), carbonyl (acid) and carbonyl (lactide) areas of PLA oligomers L-14 and L-15.

The doped potassium ion that appears in the same region is also of linear oligomers. The peaks ranging from 599 to 959 Da, correspond to cyclic oligomers doped with sodium ions (n varies from 8 to 13). The doped potassium ions that appear in the same region are also of the cyclic oligomers. This confirms that few macrocyclic oligomers were present in this sample. The peaks ranging from 1283 to 1427 Da, corresponding to linear oligomers zipped with catalyst molecule with sodium mass of 72n+36+23 in the middle. The peaks are of the HO-(-CH(CH_3)COO)n-Zn-O-Zn-O(COCH(CH_3)n-OH-Na^+ type that is linear polymer molecules. Figure 7.12 presents the MALDI-ToF mass spectrum of sample L-14. The oligomers contained chains terminated by OH on one side and COOH on the other. The MALDI ToF spectrum is dominated by a series of intense peaks ranging from a mass of 560 Da to a mass of 1497 Da, corresponding to oligomers doped

with K^+ ions of type H- [O-CH (CH_3)CO-]$_n$ OH-K^+ (mass=(72n +18+39); n values varying from 7 to 20 were detected , 39 being the mass number of potassium.

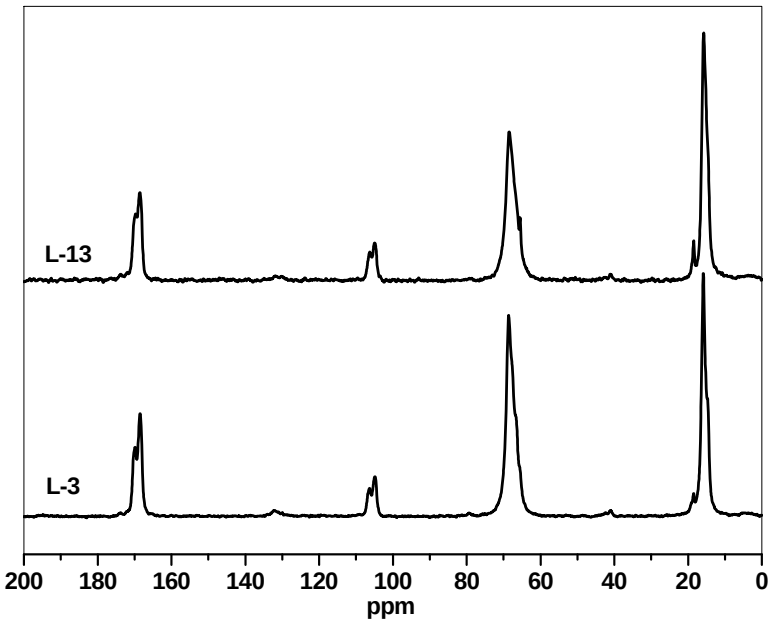

Figure 7.7: ^{13}C CP/MAS (300 MHz) L-3 and L-13.

The peak ranging from 545 to 1553 Da corresponding to oligomers doped with Na^+ ions of type H- [O-CH (CH_3) CO-]$_n$ OH-Na^+ (mass=72n +18+23), n values varying from 7 to 21 were detected, 23 being the mass number of sodium. There is another series ranging from 573 to 861 Da corresponding to oligomers doped with Na^+ ions of type H- [O-CH (CH_3) CO-]$_n$ OC_2H_5-Na^+ (mass=72n+46+23), n values ranging from 8 to 11 were detected, 23 being the mass number of sodium. This peak most likely appears in the spectrum because of the presence of impurity ethanol, which reacted during polymerization and formed chain ends of PLA. The peaks ranging from 779 to 1427 Da corresponding to a new structural formula, HO- [CH (CH_3) CO-]$_n$ Zn-O-Zn-(OCO-CH-CH_3)-OH. These chains have residual catalyst attached in the middle of the polymer chain. This result confirmed that a small amount of catalyst dissociates during polymerization reaction. Figure 7.13 shows the MALDI spectrum of polymer L-15. The most intense peaks belonging to this series, corresponding to oligomers doped with Na^+ ions of type H- [O-CH (CH_3) CO-]$_n$ OH-Na^+ (mass=72n+18+23); n values ranging from

7 to 20 were detected, 23 being the mass number of sodium. These peaks of linear oligomers doped with potassium ions that appear in the same region are also observed.

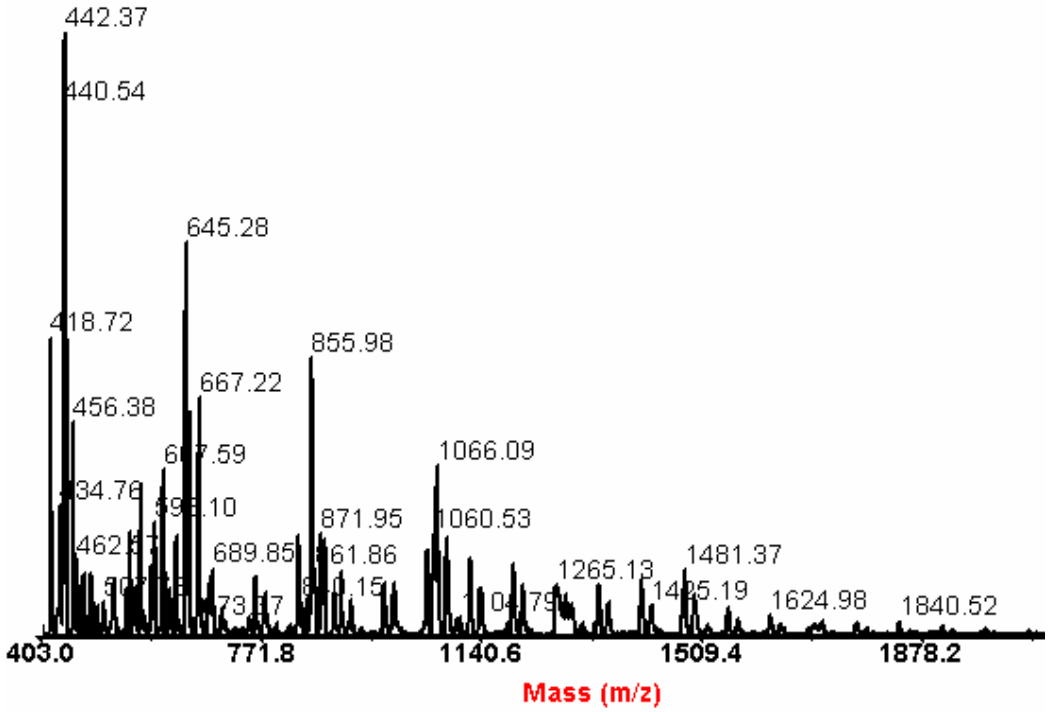

Figure 7.8: MALDI ToF-MS of L-3 oligomers.

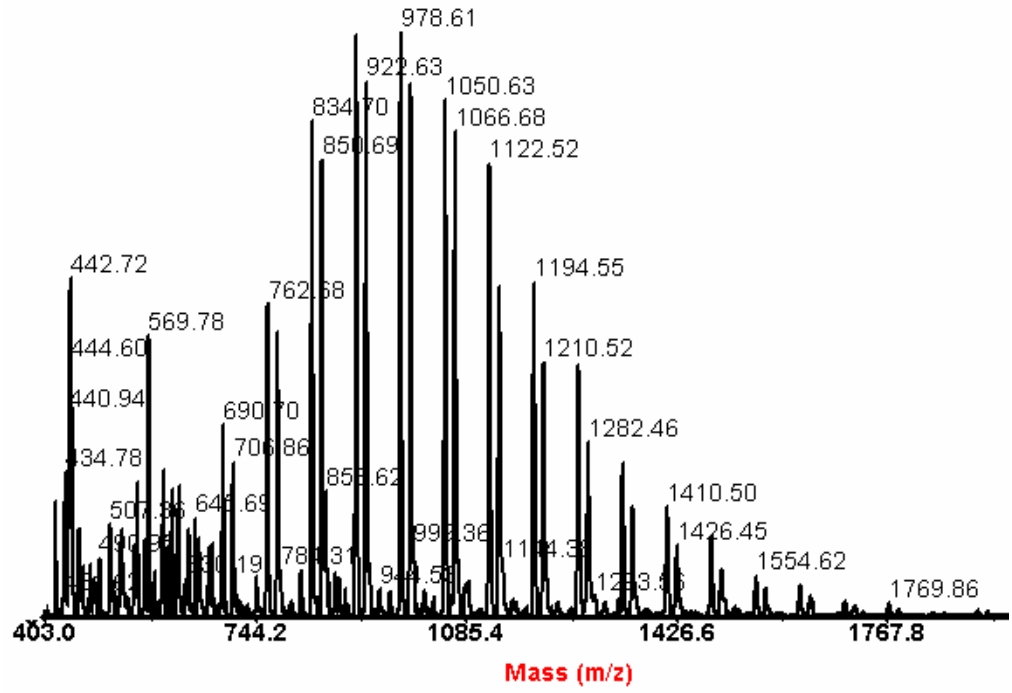

Figure 7.9: MALDI ToF-MS of L-5 oligomer.

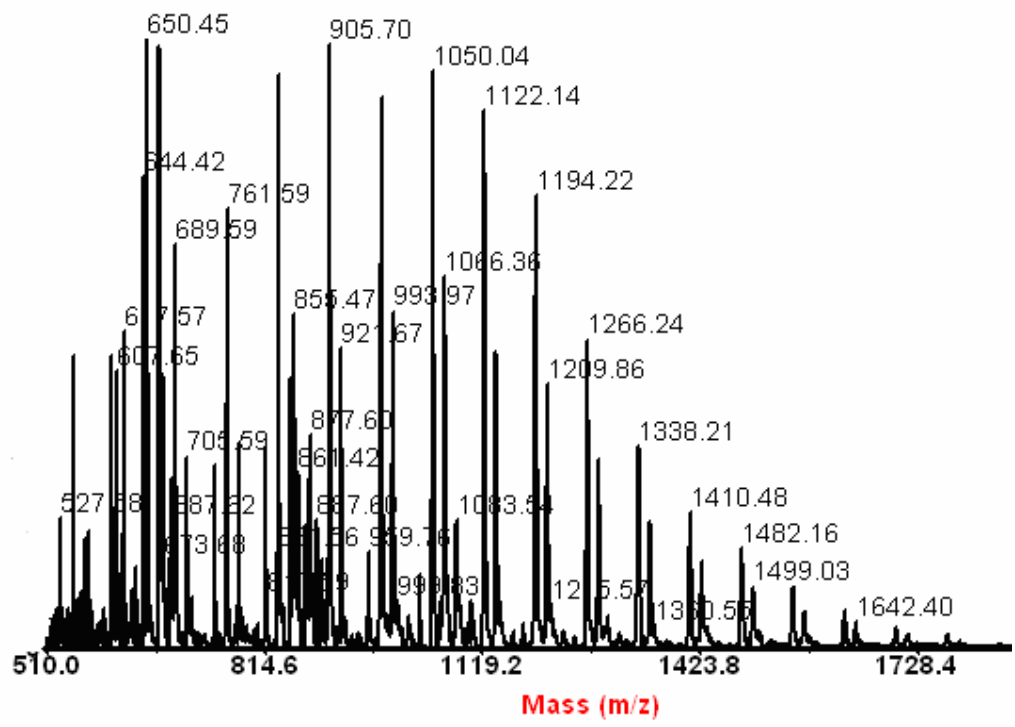

Figure 7.10: MALDI ToF-MS of L-9 oligomer.

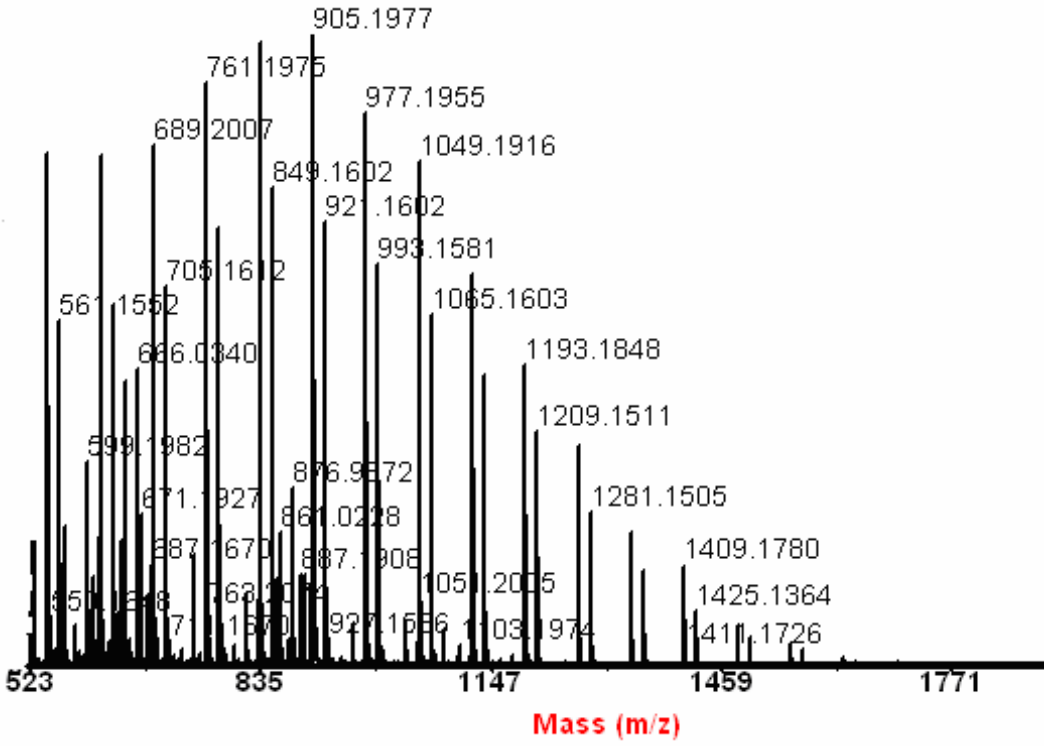

Figure 7.11: MALDI ToF-MS of L-13 oligomer.

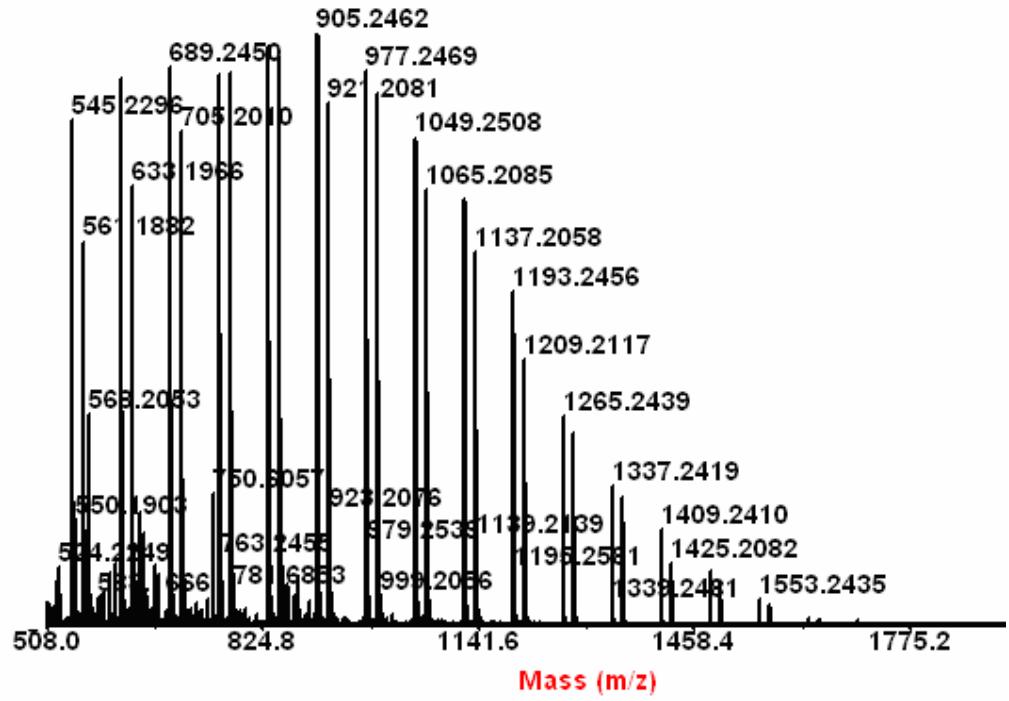

Figure 7.12: MALDI ToF-MS of L-14 oligomer.

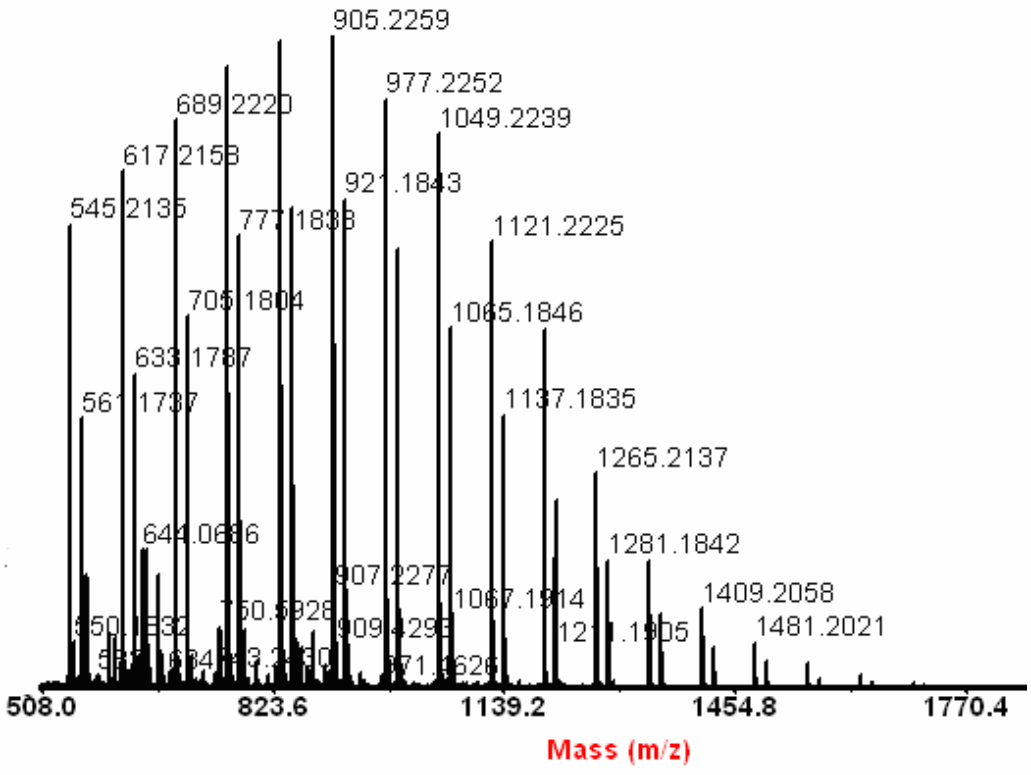

Figure 7.13: MALDI ToF-MS of L-15 oligomer.

7.5. *Synthesis of copolymer of L, L-lactide with ε-caprolactone:* Ring opening polymerization of L, L- lactide and ε-caprolactone initiated using zinc (L-prolinate)$_2$ catalysts are shown in Figure 7.14. Ring opening polymerization of L, L-lactide (L-LA) and ε-caprolactone (ε-CL) employing zinc (L-prolinate)$_2$ as an initiator was systematically examined. Copolymer of L, L-lactide and ε-caprolactone are amorphous, transparent and film-forming materials, which are of interest as resorbable wound dressing **[34]**. In the present work, all the copolymerization reactions carried out using break seal technique. Conversion of LA and ε-CL was determined on the basis of ^{1}H NMR spectroscopic studies. The molecular weights and polydispersity of copolymers were measured by gel permeation chromatography (GPC).

7.5.1. FT-IR: Figure 7.15 shows the IR spectra of the P (LA- ε-CL) copolymers. The copolymer exhibited the band at 1725 cm^{-1} due to C=O stretching and at 2943 and 2869 cm^{-1} due to C-H stretching of poly (ε-caprolactone) (PCL) units. The another C=O stretching band appeared at 1757 cm^{-1} and C-H stretching at 2822 cm^{-1} are in the agreement with the presence PLA units. CP-3 showed a single C=O stretching at 1748 cm^{-1}, which may be attributed due to random nature of the copolymer. CP-4 showed a doublet splitting at 1708 and 1748 cm^{-1}, which may be attributed due to blocky nature of the copolymer.

7.5.2. Molecular weight determination: Figure 7.16 illustrates the SEC trace of PLA, PCL homopolymers and LA-ε-CL copolymers ranging from 80:20 to 50:50 (CP-1 to CP-3 and CP-4) prepared by sequential addition of L, L-lactide followed by ε-caprolactone monomer. All purified homo and copolymers showed single peak in the GPC curve and with molecular distribution ranging from 1.5 to 1.9 as shown in Table 7.4. Size exclusion chromatograph of copolymers showed the absence of homopolymers. PCL represented broader distributions in comparison with other peaks. (Figure 6.20) PCL shows $\bar{M}_n$ = 43,000 and $\bar{M}_w$= 85,000 and distribution = 1.9. CP-1 showed $\bar{M}_n$ = 15,000 and $\bar{M}_w$ = 30,000 and distribution is 1.8. CP-2 showed $\bar{M}_n$ = 14,000 and $\bar{M}_w$ = 25,000 and distribution 1.7. Similarly CP-3 showed $\bar{M}_n$ = 5,100 and $\bar{M}_w$ = 9,800 and distribution as 1.8. It is observed from Table 7.4 that $\bar{M}_n$ and $\bar{M}_w$ gradually decreased from CP-1 to CP-3. A similar observation was made by Domb et al **[35]**, for L-lactic based

copolymers. CP-4 showed $\bar{M}_n$ = 33,000 and $\bar{M}_w$ = 51,800 and distribution =1.7 which may be attributed due to the sequential addition of comonomers.

7.5.3. Thermal characterization: TGA thermograms of the polymers were obtained from 50 ^{0}C to 700 ^{0}C at the heating rate of 10 ^{0}C/min as shown in Figure 6.17. PCL exhibited a uniform thermal degradation behavior. In case of (LA- ε -CL) copolymers, two-step degradation was detected. It is assumed that the first step degradation step was due to PLA blocks. A T_d value at 432 ^{0}C was obtained for PCL and 323-382 ^{0}C ranges for the copolymers. The TGA curves of the copolymers shifted slightly lower temperature as compared to PCL, i.e. overall stability decreased due to the incorporation of PLA segments. CP-4 showed two characteristic peaks at 323.4 ^{0}C and 424.0 ^{0}C respectively due to its blocky nature. The copolymers with different compositions (CP-1 to CP-4) along with PLA and PCL were characterized by DSC analysis as shown in Figure 7.18 A and Table 7.4. The T_g and T_m values of the copolymers were in proximity to the T_g of PLA and T_m of PCL. With the increase of L, L-LA sequences in the copolymers, glass transitions were shifted to higher temperatures. In case of CP-4, two melting temperatures (T_ms) were observed at 57.41 and 131.33 ^{0}C respectively. These results may be attributed due the larger length of lactide and ε-caprolactone, which are confirmed by TGA and ^{13}C NMR. The second heating thermograms of DSC were shown in Figure 6.18 B. The glass transition temperature, T_g of the copolymer varied from – 14.9 to 27.3 ^{0}C. The T_g value decreased with increase in incorporation of ε-caprolactone. In other words T_g increased with incorporation of L, L-lactide units.

7.5.4. Determination of polymer structure by NMR: In general, polymerization was carried out at 195 ^{0}C using zinc L-prolinate as the initiator, and the results are tabulated in the Table 7.4. Figure 7.19 shows the spectrum of PLA-PCL copolymer at various compositions in the range of 100:0, 80:20, 70:30, 50:50 and 0:100.

Signals at 1.5 (-CH_3) and 5.1 ppm (-CH) were assigned to PLA blocks, 1.3, 1.6, 2.3 and 4.0 ppm due to different methylene protons (-CH_2-) of PCL blocks. The [ε-CL]/ [LA] molar ratio of the product were determined from the integration of the signals due to PCL block at 4.0 ppm and PLA block at 5.1 ppm.

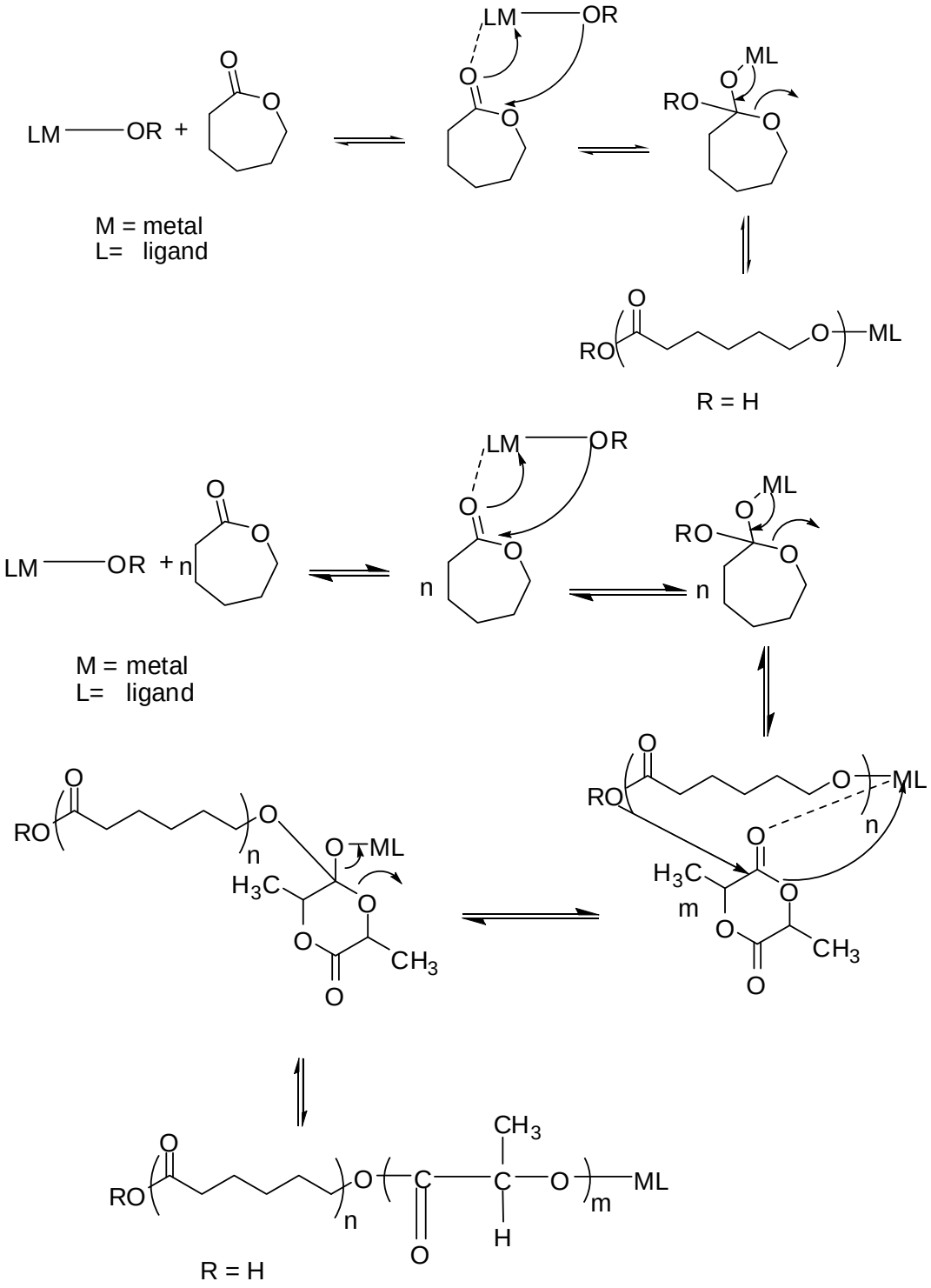

Figure 6.14: Reaction scheme for homopolymerization (PCL and PLA) and copolymerization.

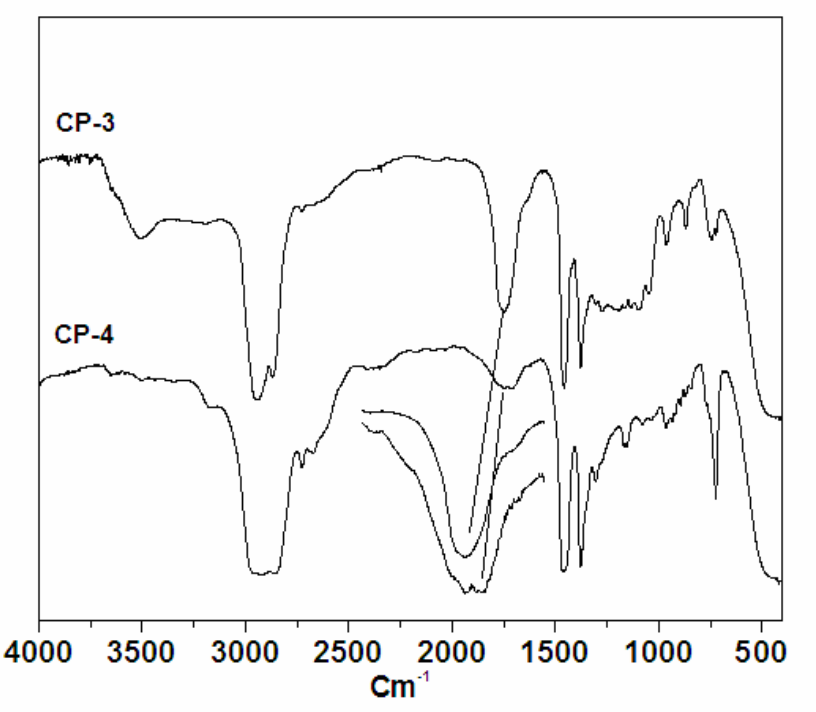

Figure 6.15: FT-IR spectra of copolymers CP-3 and CP-4.

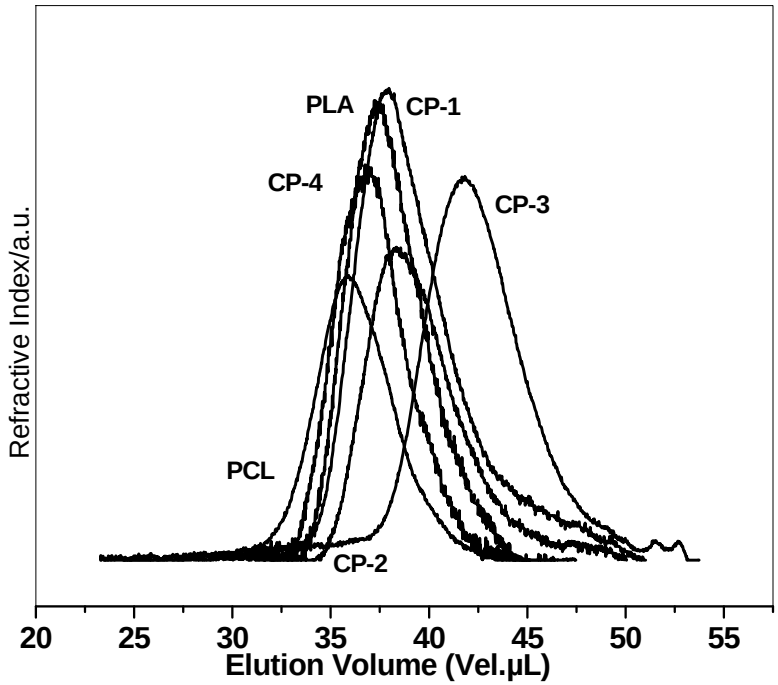

Figure 6.16: SEC chromatograms of PLA, PCL and CP-1 to CP-4.

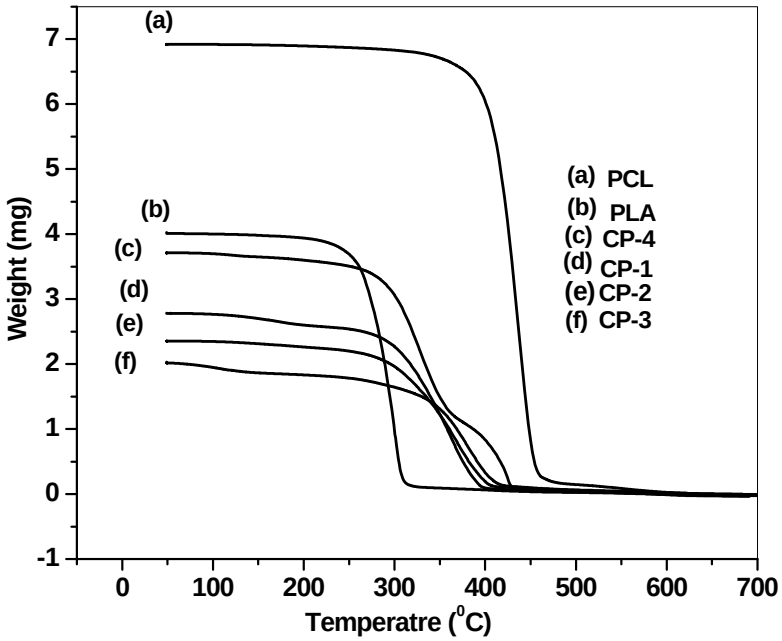

Figure 6.17: TGA curve of copolymer samples.

6.5.4a Determination of copolymer structure: A series of P (LA-ε-CL) were synthesized by ring opening polymerization using zinc L-prolinate as a catalyst. The results were summarized in Table 7. Copolymer composition was verified by ^{1}H NMR by the integration of the peaks at 5.15 ppm due to PLA units and the peaks at 4.0 ppm due to PCL units. The relative degree of crystallinity of the copolymer depends directly on the PLA block size-degree of randomness. ^{1}H NMR spectra of CP-1, CP-2, CP-3 and CP-4 are shown in Figure 7.19A. To correlate the NMR spectra to the composition and the frequency of occurrence of specific comonomer sequence and the number average sequence mathematics calculation models was used. If the copolymers not strictly alternating or block like/a randomly selected pair of co monomer units in the polymer chain may be represented as follows ε-CL-ε-CL. ε-CL-LA, LA-ε-CL, LA-LA. To simplify the calculations, only the last three options were considered. An examination of the ^{13}C quantitative NMR spectra of P (LA-ε-CL) revealed four well-separated peaks at different spectral ranges. The carbonyl peaks of PLA photopolymers appeared in the range of 169.28 to 169.64 ppm. The lactide formation was around 1 %. The carbonyl ester peak of PCL appeared at 173.55 ppm. As the mole ratio and preparation method of the copolymers varied, the integration ratios of those peaks were changed. Figure 7.19A

represents the relevant peaks for P (LA-ε-CL) synthesized by ROP along with PLA and PCL homopolymers using the same ROP techniques and zinc L-prolinate catalyst.

1. Unconditional probability. [p (LA) and p (ε-CL)] are the probabilities of a randomly selected monomer unit in the polymeric chain to be either LA or ε-CL. This could be determined by the overall integration of LA to ε-CL.

$$\mathbf{p(LA)+p(\varepsilon\text{-}CL) = 1 \text{------} (1)}$$

2. Probability, p(LA-LA), p(LA-ε-CL) and p(ε-CL-LA) are the probabilities that the randomly selected connection was p(LA-LA), p(LA-ε-CL) or p(ε-CL-LA). The probability could be determined from the integration ratio of the relevant peaks as presented in Figure 7.20 B. From these probabilities and the feed ratios it is possible to calculate the following:

I. Degree of Randomness (h) of the formed polymer

$$\mathbf{h = p(LA\text{-}\ \varepsilon\text{-}CL\ /p(LA)\ p(\varepsilon\text{-}CL) \text{----------} (2)}$$

h<1 means block character of the copolymer; h = 1 means the polymer takes a random distribution; h>1 means alternating tendency; and h=2 means a full alternating copolymer.

II. Number average sequence length of monomer sequence (Ln)

$$\mathbf{L_{LA} = 1/p\ (\varepsilon\text{-}CL\text{-}LA) \text{--------} (3)}$$

For the p (LA-ε-CL) synthesized by ROP using zinc proline catalyst with mole ratio from 80:20 to 50:50, the results can be presented in Table 7.5. The result can be summarized in the following way. In case of all the copolymers, the h value approaches to 1 irrespective of various compositions ranging from 80:20 to 50:50. The h value clearly attributes that the polymer takes a random distribution. In case of 50:50 molar compositions, the result means alternating tendency of the copolymer. The alternating tendency of P (LA-ε-CL, 50:50 molar ratios) is a result of the relatively higher ε-CL content. In case of block copolymerization (60:40), the h values are 0.13, which is less than 1.0, confirming block character of the copolymer.

The number average sequence length (L_{LA}) of L, L-lactide decreased from 14.0 to 5.2 for p (LA-ε-CL) from 80:20 to 50:50 respectively. Sequential length is additional evidence to random and blocks character to the copolymers. ^{1}H NMR spectra of PLA and PCL are shown in Figure 7.19B (a) and Figure 7.19B (b). The h value was calculated using equation 2.

Table 7.4: Zinc (L-prolinate)$_2$ catalyzed homopolymerization and copolymerization of L, L-lactide and ε-caprolactone

Sr.No.	Feed ratio (LA-ε-CL)	Incorporation ratio (LA- ε-CL)	$\bar{M}_n$ (GPC)	$\bar{M}_w$ (GPC)	PDI	T_m (^{0}C)	ΔH_f (J/g)	T_g (^{0}C)	ΔC_p J/(g. ^{0}C)
PLA	100	100	24,200	38,800	1.6	146.9	20.7	53.4	0.41
CP-1	80:20	83:17	15,800	30,000	1.8	nd	nd	27.3	0.40
CP-2	70:30	74:26	14,000	25,000	1.7	nd	nd	14.4	0.45
CP-3	50:50	56:44	5,100	9,800	1.9	nd	nd	-14.9	0.38
CP-4	BL60:40	65:35	33,000	51,800	1.5	T_m –a 57.41	25.89	T_{g-}a -46.1	0.04
						T_{m2}-b 131.33	12.34	T_{g2}-b -9.98	0.45

Reaction time 8h, nd-not determined, a 1st Tg (-46.1 ^{0}C) and Tm (57.41 ^{0}C) and b- 2nd Tg (-9.98 ^{0}C) and Tm (131.33 ^{0}C).

7.5.5. MALDI-ToF-MS analysis: MALDI-TOF MS has been employed for the determination of molecular weights and the nature of end groups [33, 34]. With ring opening polymerization, poly (L, L-lactide), poly (ε-caprolactone) and copolymers of L, L-lactide ε–caprolactone can be prepared. The homopolymers, copolymers prepared during this study were subjected to MALDI-ToF analysis. The results of the analysis are shown in Figures 7.21 which presents the MALDI-ToF mass spectrum of sample PLA.

The polymer contained chains terminated by –OH on the one side and –COOH on the other side. The MALDI spectrum is dominated by series of intense peaks ranging from a mass 542 Da to 1622 Da, corresponding to polymers doped with Na^+ of type H- [O-CH

(CH_3)-CO-]$_n$-OH-Na^+ (mass = 72n+18+23); n values varying from 7 to 22 were detected, 23 being the mass number of sodium ion.

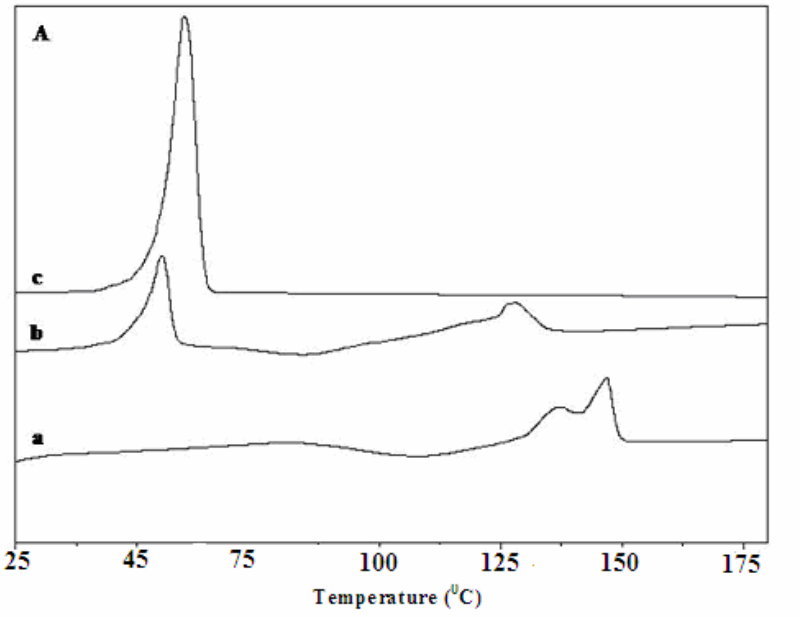

Figure 7.18 A: DSC thermograms of polymer samples (a) PLA, (b) CP-4 and (c) PCL.

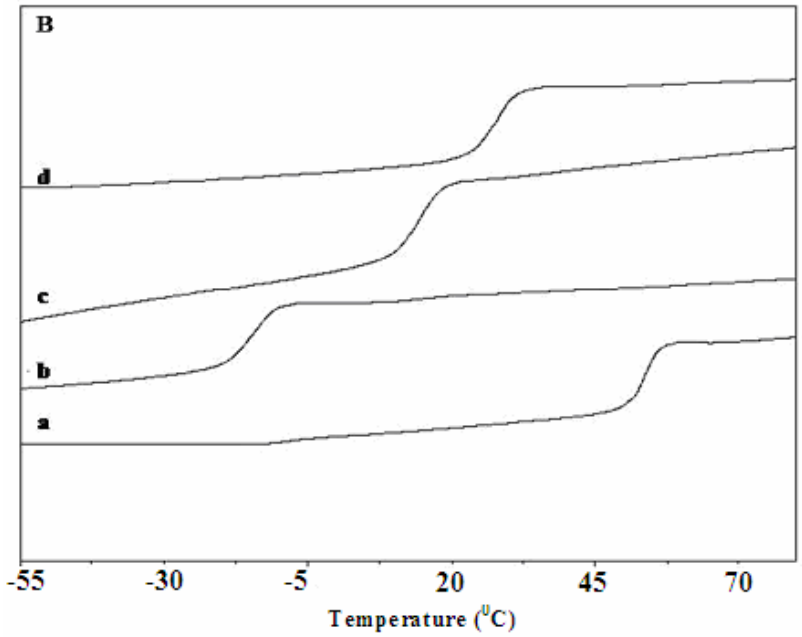

Figure 7.18 B: DSC thermograms of polymer samples (a) PLA, (b) CP-3, (b) CP-2 and CP-1.

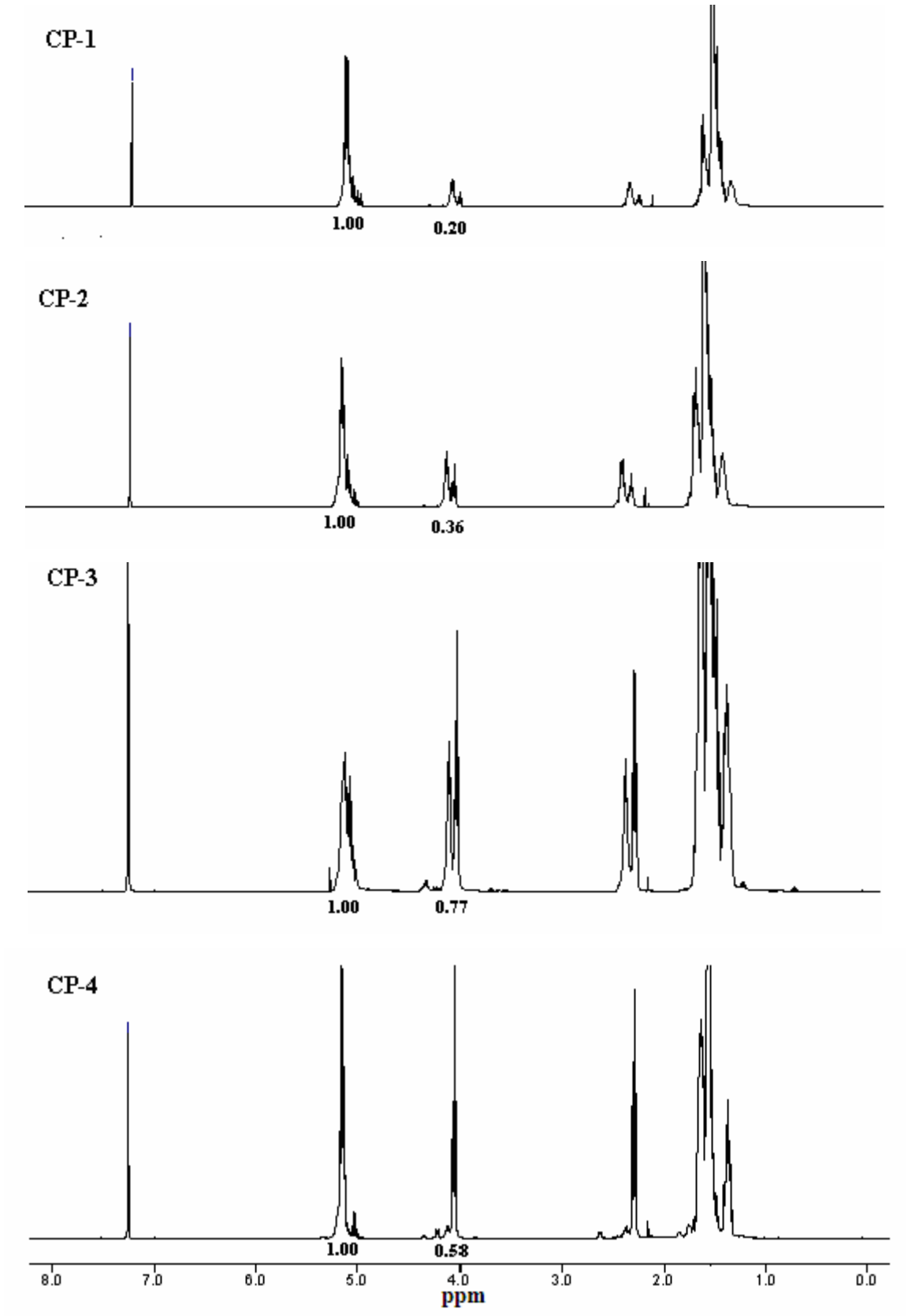

Figure 7.19A: ^{1}H NMR spectra CP-1, CP-2, CP-3 and CP-4.

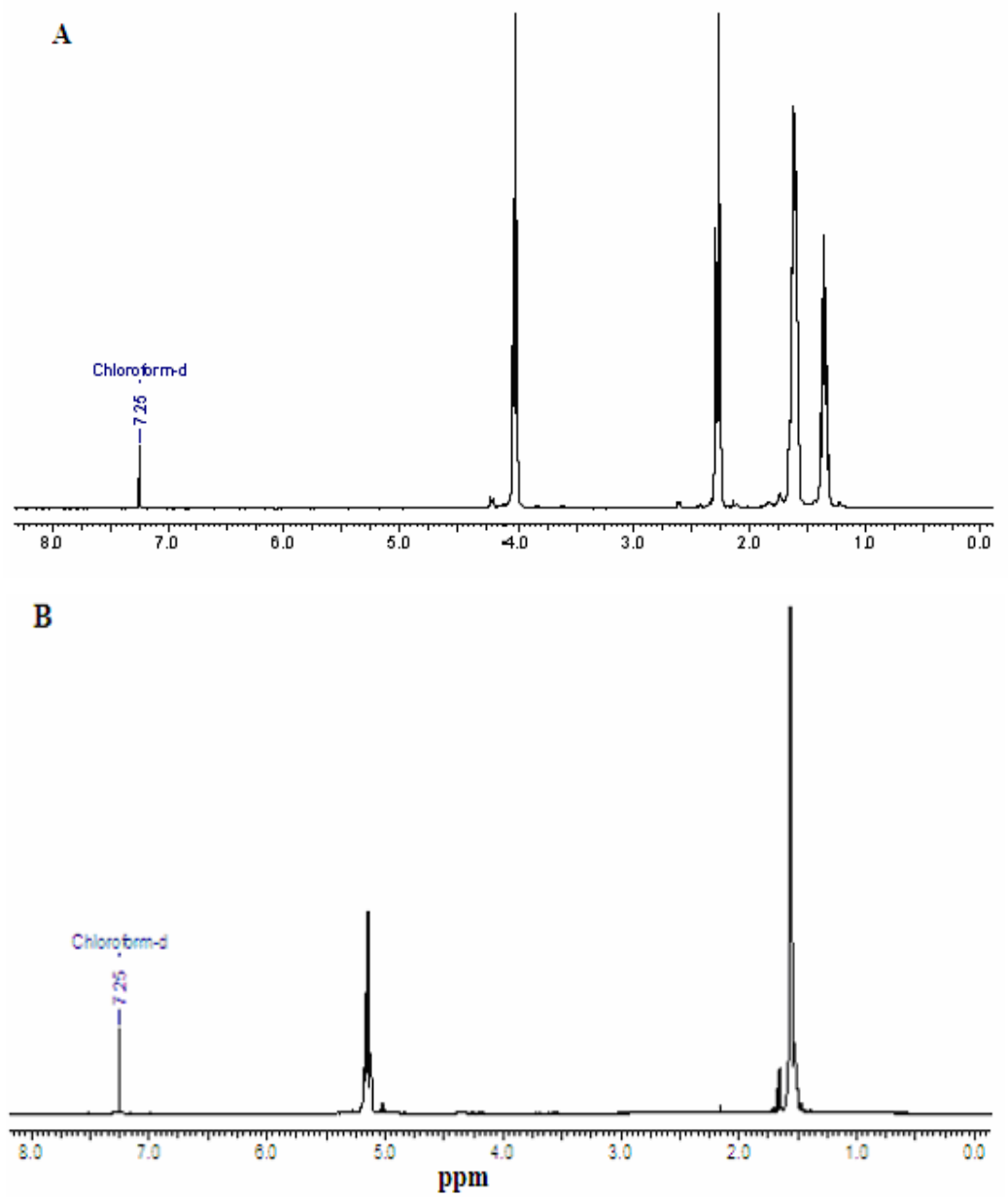

Figure 7.19 B: ^{1}H NMR spectra (A) PCL and (B) PCL.

Some of the peaks ranging from 526 to 742 correspond to macrocyclic structures with n = 7-10 (mass = 72n+23) can be observed. The macrocyclic structures were formed by intramolecular transesterification or esterification between chain ends. In the region from 703 to 1207 Da, the lower intense peaks correspond to polymers doped with Na^{+} and terminated with -OCH_3 and H, most likely generated from the impurities present in the catalyst. The peak corresponds to polymer of the structure H- [O-CH (CH_3)-CO-] $_n$-OCH_3, with a molecular mass of 72n +23 +32. Figure 7.22 shows the MALDI-TOF

spectrum of poly (ε-caprolactone). The spectrum shows the chemical heterogeneity, which consist of linear and cyclic oligomers.

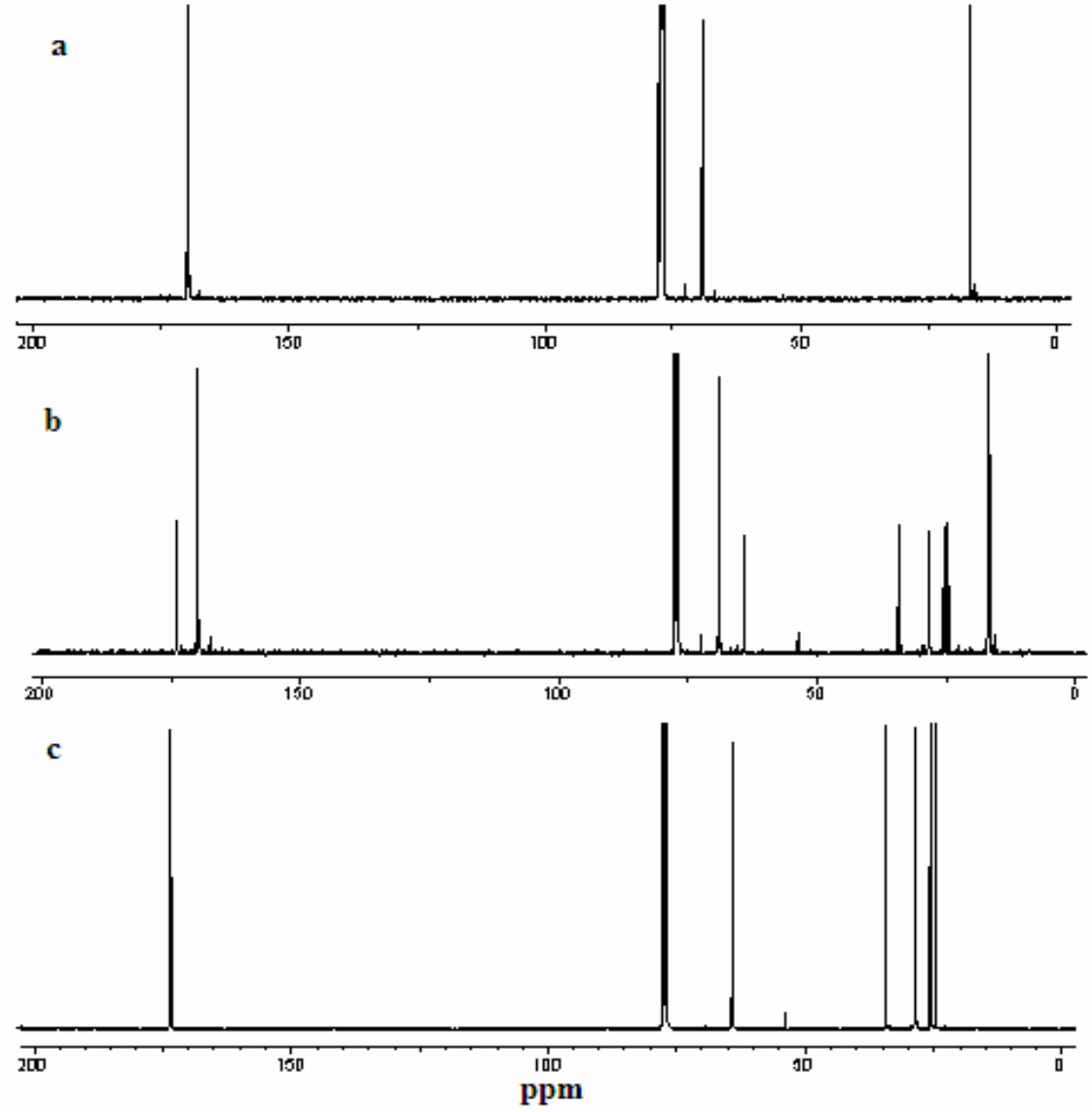

Figure 7.20 A: ^{13}C NMR of polymer samples (a) PLA, (b) CP-5 and (c) PCL.

The spectrum is dominated by a series of intense peaks ranging from 593 to 1618 Da with n<15 correspond to cyclic polymers doped with sodium ions. The peaks at moderate intensities ranging from 609 Da to 1750 Da, correspond to linear polymers doped with sodium ions (mass = 114n+23+18) denoted by the structure H- [-O-$(CH_2)_5$-CO-]-OH-Na^+. In the region from 626 to 1196 Da, the lower intensity peaks correspond to polymers

doped with potassium ions and terminated with OH and H. These polymers bearing OH and H as terminal groups contribute to general formula H- (-O- $(CH_2)_5$-CO-)-OH-K^+.

Table 7.5: Comonomer sequence distribution by using ^{1}H NMR

Copolymer samples	Feed ratio (LA- ε CL)	Probability of finding the [LA-LA] unit P[LA-LA]	Probability of finding the [LA-CL] unit P[LA-CA]	Probability of finding the [CL-LA] unit P[CL-LA]	Average block length L_{LA}	Degree of randomization
CP-1	80:20	0.750	0.162	0.070	14.0	1.01
CP-2	70:30	0.368	0.163	0.075	13.3	0.78
CP-3	50:50	0.290	0.324	0.191	5.2	1.29
CP-4	BL60:40	0.692	0.033	0.921	83.0	0.13

A-Probability degree of randomness and average block length calculated based on LA: CL (mol/mol) feed ratios (8:2 to 5:5), according to equation 1, 2 and 3 different as presented in the text
B- L, L lactide and caprolactone were added at a time in the reaction.

7.5.5a. Determination of comonomer incorporation as well as end groups by MALDI-TOF MS: The MALDI-ToF-MS spectrum of copolymer with 20 mol% ε-caprolactone incorporation (CP-1) is shown in Figure 7.23 and the empirical formula of such copolymer will be H-(-OCH(CH_3)-CO-)m-(-O-$(CH_2)_5$-CO-)n-OH. The more intense peaks at 598, 784, 856, 1208 etc. are due to such sodiated adducts, when m varies 1 to 8 and n varies from 1 to 4 corresponding potassiated adducts were also located. The peaks at 527, 598, 670 Da are also due to copolymers, but the empirical formula H- (O-CH (CH_3) CO) $_m$- (O- $(CH_2)_5$-CO-)$_n$-OCH_3, that is methyl ester ended instead of carboxylic acid and they desorbed as sodiated adducts, so that the molecular weights can be calculated as (72m+114n+32+23), when value of m varied from 3-4 and n varied from 1-3. The impurity methyl alcohol may be contaminated through zinc prolinate catalyst. Figure 7.23 shows the MALDI-ToF mass spectrum of copolymer CP-2. The spectrum shows the chemical heterogeneity, which consists of linear and cyclic oligomers. The most intense peaks, ranging from 545 to 666 Da correspond to doped with sodium ions

cyclic polymers with a mass 72m + 114n+23 (m varies from 4-5 and n varies from 2-5). The corresponding cyclic polymers doped with potassium ions can also be seen as peaks of a mass 72m + 114n +39. The peaks of a cyclic oligomer doped with potassium ions overlap with the corresponding peaks of another cyclic polymer with a mass of 72m +114n+23 (m =1, n =5). The linear copolymer peaks ranging from a mass of 629 to 672 Da, corresponding to copolymer doped with Na^+ ions of type H-(O-CH(CH_3)CO)$_m$-(O-(CH_2)$_5$-CO-)$_n$-OH-Na^+ (mass=72m+114n+18+23) m values varying from 4 to 8 and n values from 2-3. The peaks ranging from 860 to 892 Da correspond to copolymer of the structure H-(O-CH (CH_3) CO)$_m$-(O-(CH_2)$_5$-CO-)$_n$-OCH_3 with a molecular mass of 72m+114n+23+32.

Figure 7.25 shows the MALDI-ToF mass spectrum of CP-3. Similar pattern of splitting were observed as in CP-2. The macrocyclic peaks appeared at 550, 568, 666 Da corresponding to the mass 72m+114n+23, where m varies from 1-4 and n from 2-5. The sample expected to be formed by copolymers bearing –OH and H as terminal groups corresponding to the general formula H[-O-CH(CH_3)CO)-(O-(CH_2)$_5$ –CO)]OH –Na^+, shows peaks in the region 629 to 672 Da, from which the molecular mass of each copolymer can be calculated as 72m+114n+18+23. The peaks ranging from 860 to 892 Da correspond copolymers of the structure H (-O-CH_3)-CO-)$_n$- (O-(CH_2)$_5$-CO)-OCH_3, with a molecular mass of 72 m+114n+32+23, where m varies from 8 to 10 and n varies from 1 to 2. Figure 6.26, shows the MALDI ToF spectrum of copolymers (CP-4). The spectrum is dominated by a series of intense peaks ranging from 568 to 1276 Da correspond to linear copolymers doped with masses of 72 m+114n+32+23. These peaks are assigned to H- (O-CH (CH_3)$_n$-(O-(CH_2)$_5$-CO)$_n$-OH where m varied from 6 to 14 and n from 1 to 2.

The linear chains doped with potassium ions appeared as peaks at 585, 671, 934, 1292 (see the inset). There are few peaks at 665 and 689 Da which correspond to cyclic copolymer. The peak at 665 Da corresponds to doped with potassium ion of cyclic copolymer with a mass of 72m+114n+39, where m=7 and n=1. The peak at 689 Da corresponds to doped with sodium ion of cyclic copolymer with a mass of 72m+114n+23, where m=6 and n=1

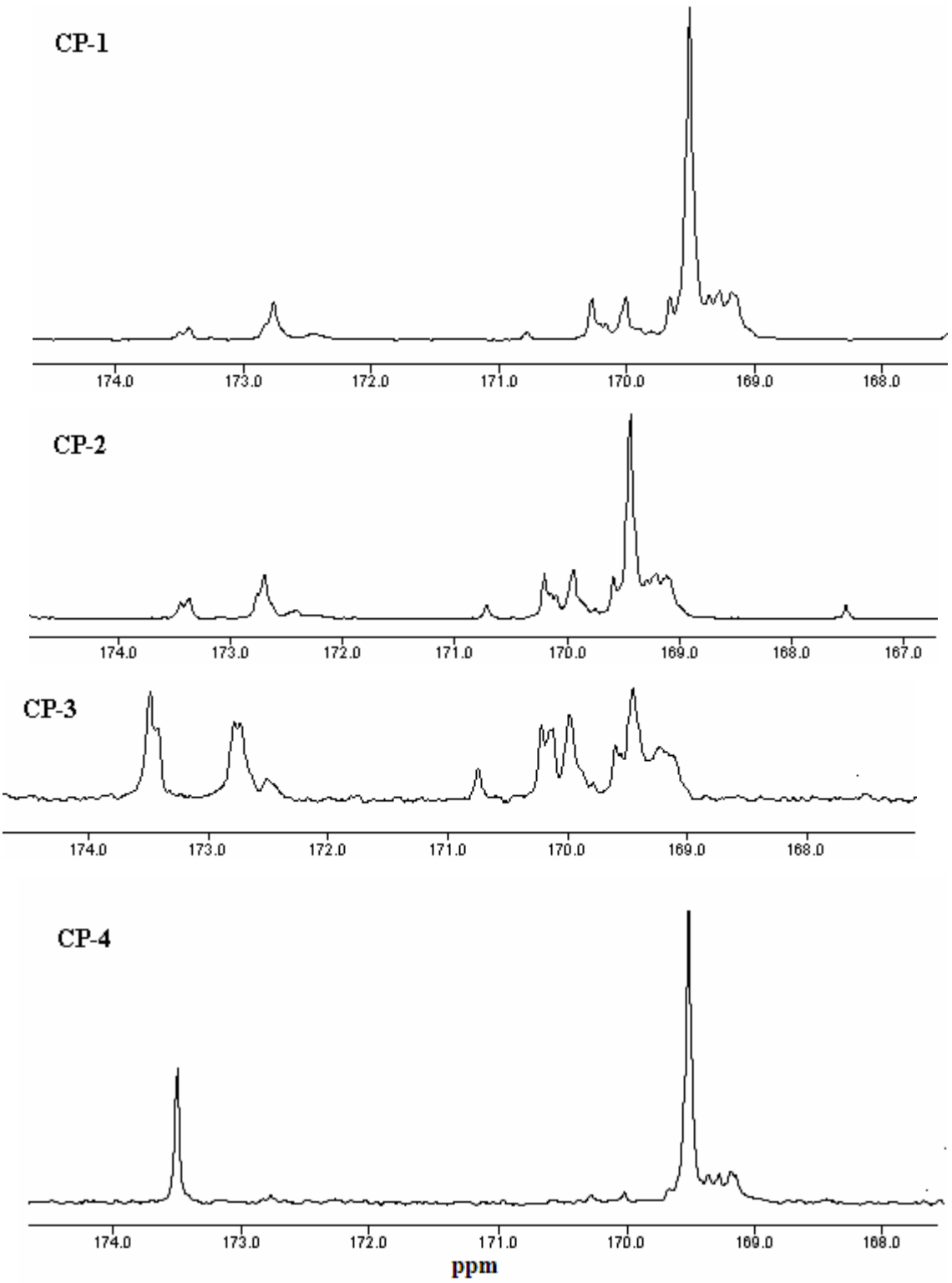

Figure 7.20B: ^{13}C NMR (500 MHz) spectrum (C=O signal only) of the CP-1, CP-2, CP-3 and CP-4.

The peak at 860 Da corresponds to copolymer of structure H-(O-CH (CH_3)-CO)$_m$-(O-(CH_2)-CO-)n-OCH_3, with a molecular mass of 72m+114n+32+23, where m=6 and n=2. The peak corresponds to copolymer doped with sodium ions and terminated with OCH_3 and H, most likely generated from the impurities present in the catalyst.

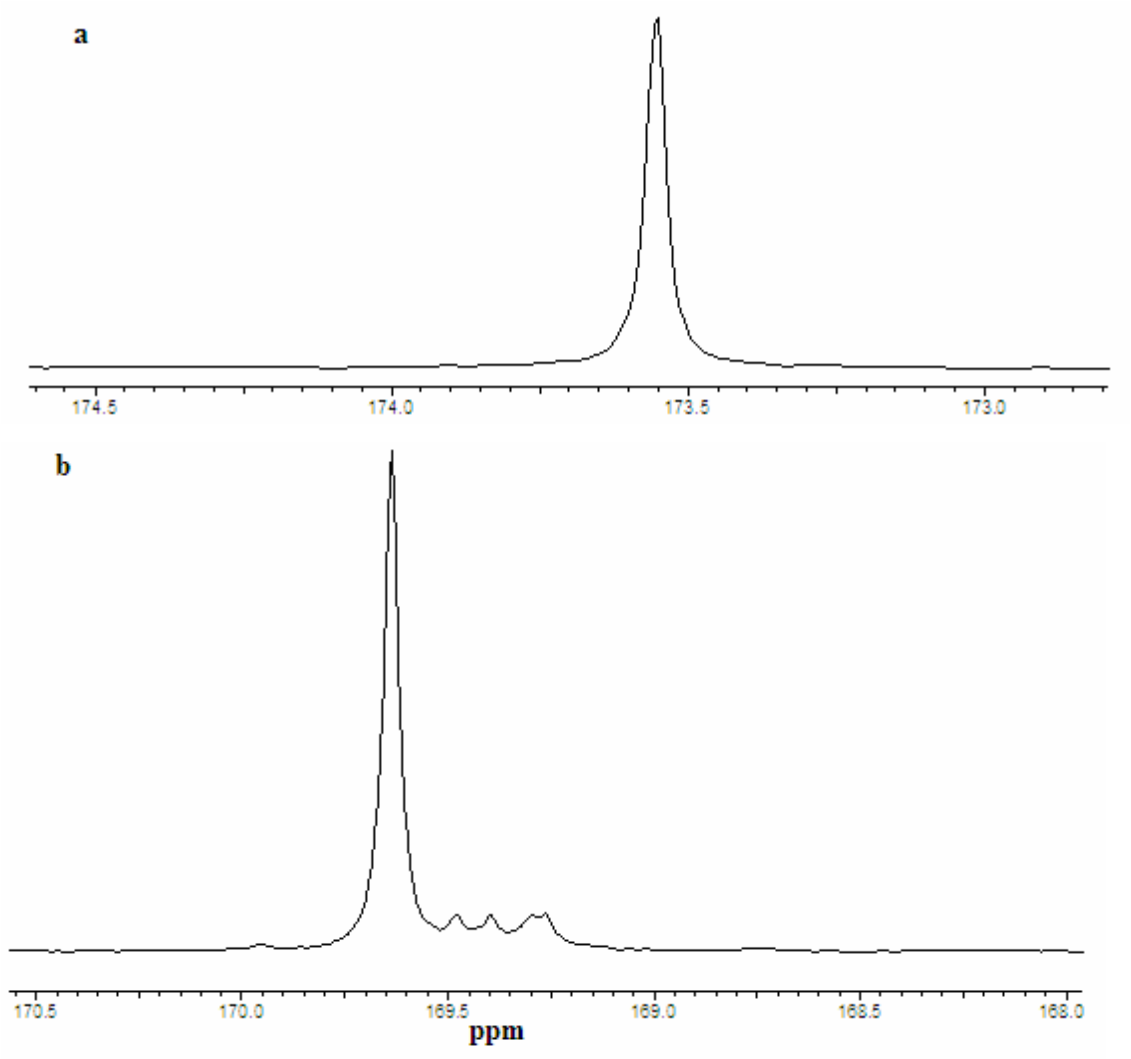

Figure 7.20C: ^{13}C NMR (500 MHz) spectrum (C=O signal only) of the (a) PCL and (b) PLA calculation performed using deconvulation method using X WIN-PLOT software.

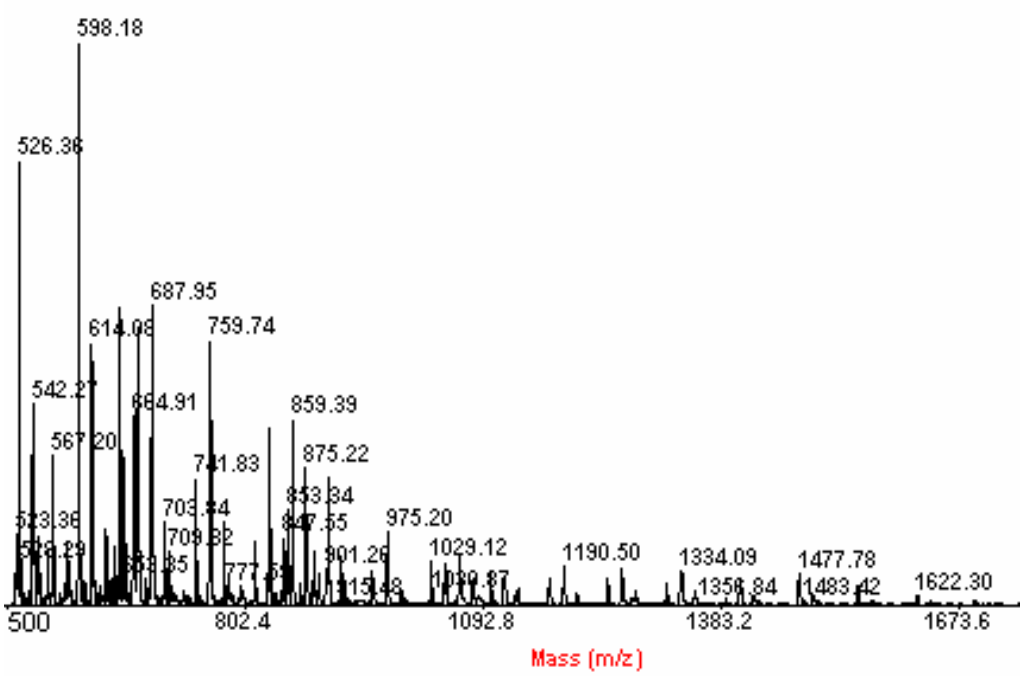

Figure 7.21: MALDI ToF spectra of polymer sample PLA.

.

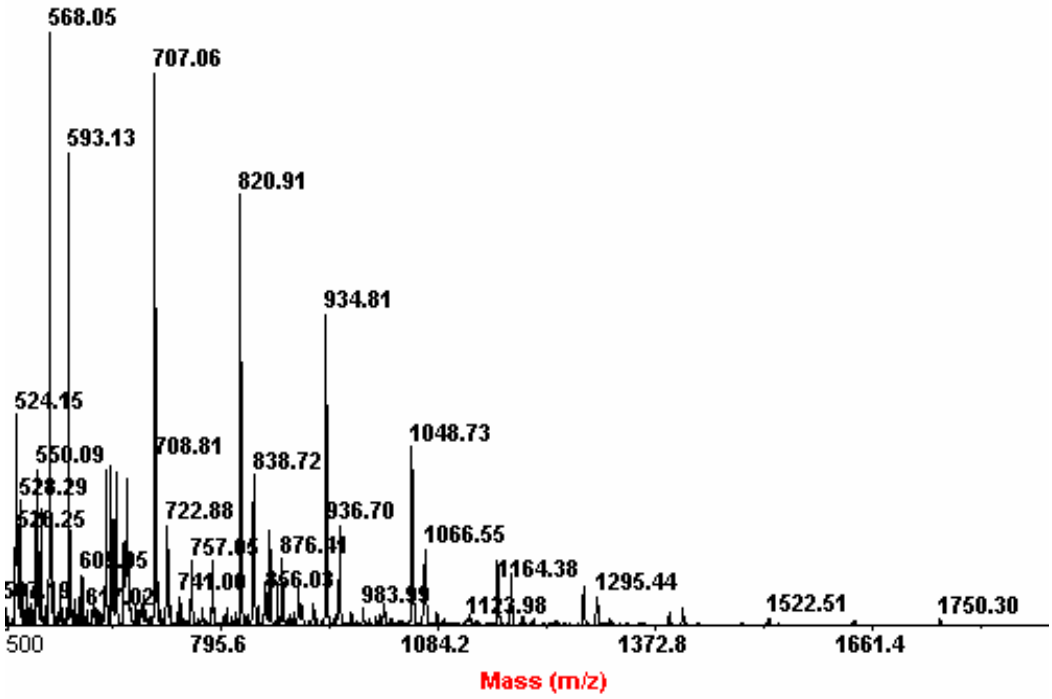

Figure 7.22: MALDI ToF spectra of polymer sample PCL.

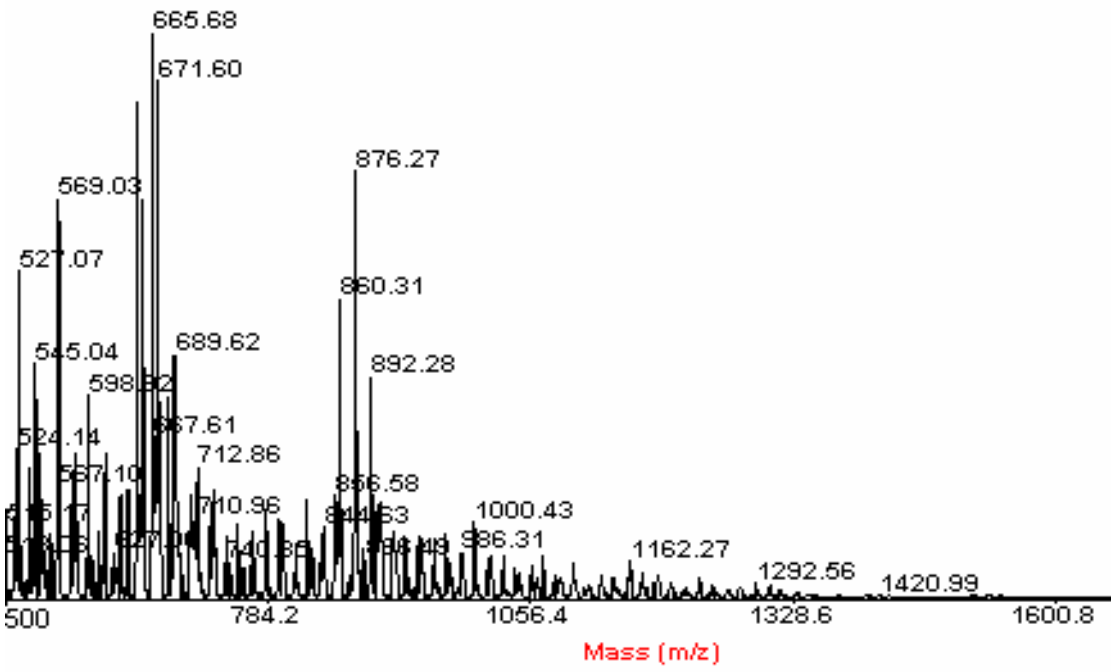

Figure 7.23: MALDI ToF spectra of polymer sample CP-1.

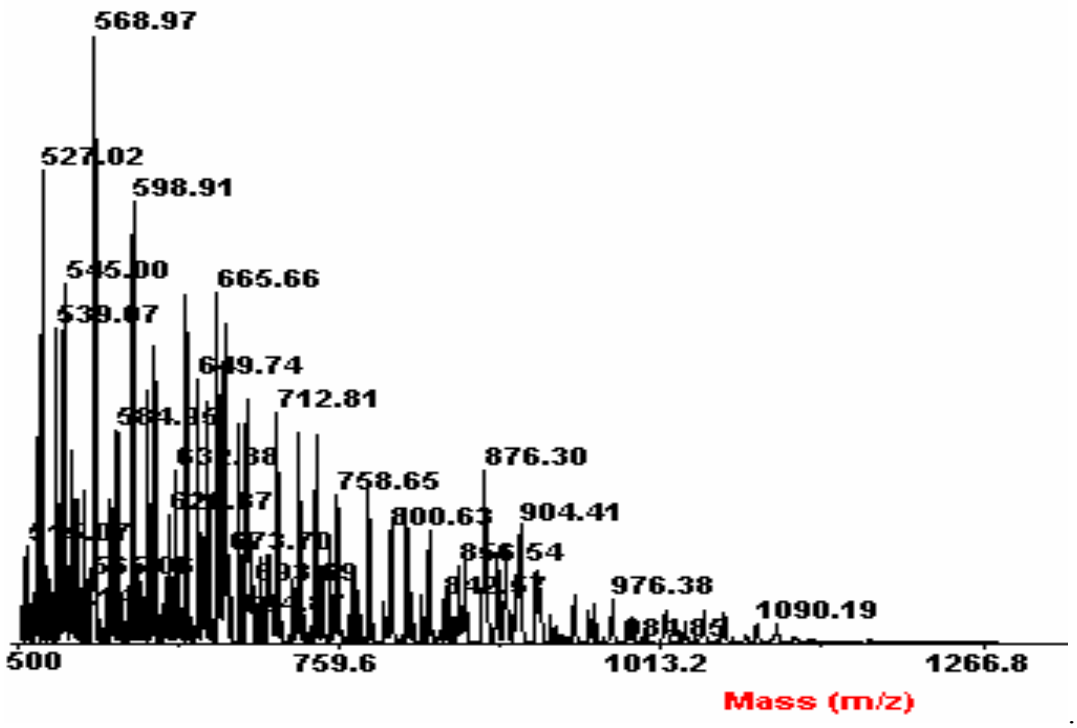

Figure 7.24: MALDI ToF spectra of polymer sample CP-2.

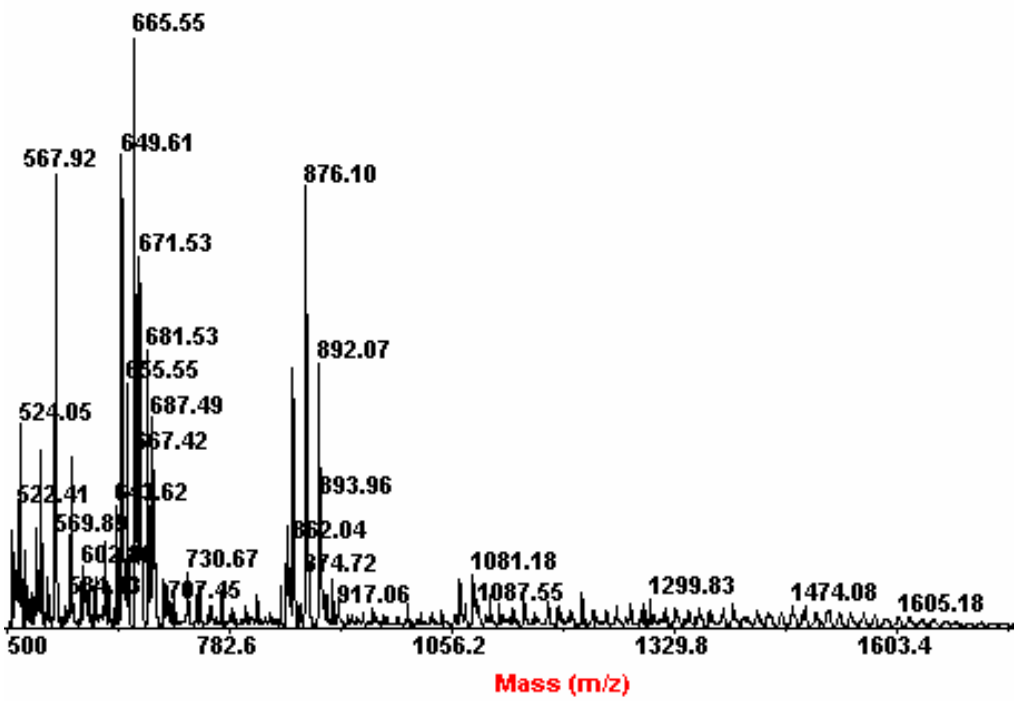

Figure 7.25: MALDI ToF spectra of polymer sample CP-3.

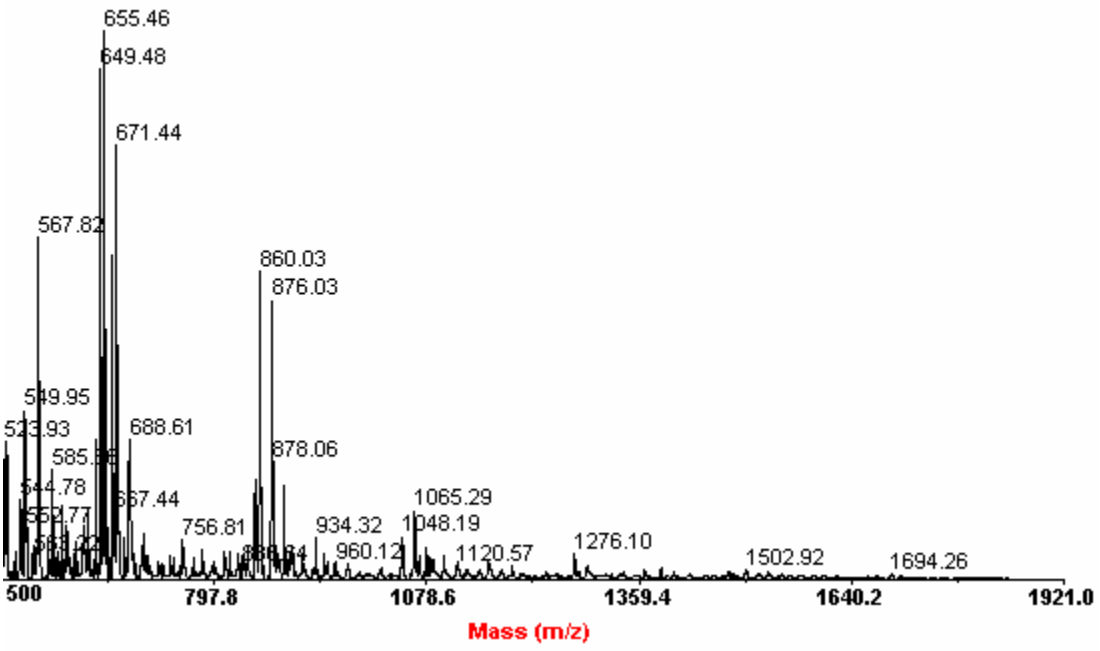

Figure 7.26: MALDI ToF spectra of polymer sample CP-4.

7.5.6. Mechanistic discussion: Zinc prolinate formed polymer and showed α-helical structure. Zinc atom showed trigonal bipyramidal geometry and the pyrrolidine rings adopted envelope conformations **[26]**. The zinc atom is pentacoordinate, the fifth

coordination side being occupied by symmetry related oxygen atom of a neighboring molecule to generate an infinite helical structure along the 2, direction. Lactide molecule behaves like ligand and replace L-proline molecule and forms complex with zinc atom. Thereafter, the reaction may occur as shown in Figure 6.14.

7.6. Conclusion:

The structure and properties of low molecular weight PLA oligomers and L, L- LA-ε-caprolactone copolymers produced by ring opening polymerization were determined in term of the nature of the catalyst, polymerization time, and temperature. Results showed that linear PLA oligomers with $\bar{M}_n$ 2900-3400 Da, can be prepared with zinc (L-prolinate)$_2$ catalyst. The failure to obtain high molecular weight polymers in bulk can be attributed to the competitive formation of small amount of macrocycles. A small part of catalyst dissociate during the course of polymerization. Less racemization reaction was occurred in presence of Zn (L-prolinate)$_2$ than Zn (D-prolinate)$_2$. The catalyst structure of Zn (L-prolinate)$_2$ and Zn (D-prolinate)$_2$ remains intact after polymerization, shown in L-3 and L-14. ^{13}C solid-state NMR confirmed the presence of catalyst in the L-3 and L-14 polymers.

Biodegradable random and block copolymers L, LA-ε-CL synthesized by ring opening polymerization of ε-caprolactone and L, L-lactide in presence of Zn (L-prolinate)$_2$ catalyst. PLA/PCL block copolymer was synthesized by ROP by sequential addition of ε-caprolactone and L, L-lactide. Break seal techniques were used in all the experiments of copolymerization reaction. Zn (L-prolinate)$_2$ caused partial racemization. The isolated copolymer posses a reasonable composition matching with feed ratio. Results showed that linear copolymer with $\bar{M}_w$~9,000- 30,000 can be prepared with Zn (L-prolinate)$_2$ catalyst. Block copolymer of ε-caprolactone with L, L-lactide resulted $\bar{M}_w$~ 52,000. The various copolymers conserved the excellent thermal behavior inherent to PCL, thus providing a wide range of processing temperatures for thermal treatments. ^{13}C NMR results proved the nature of copolymers (CP-1, CP-2 and CP-3) is random and CP-4 showed blocky nature, which were further supported by FT-IR and TGA data. The L_{LA} chain length decreased from 14.0 to 5.0 due to decrease in feed ratio in the copolymer.

MALDI-ToF also confirmed the linear copolymers with expected end groups and also the presence of some cyclic oligomers.

References

1. Kricheldorf, H .R. Boettcher. C. *Makromol. Chem*. **194**, 463 (1993).
2. Kricheldorf, H .R.; -Saunder. I. Kreisers. *Polymer* **35**, 4175 (1994).
3. Kricheldorf, H. R.; Damrau, D.-O. *Macromol. Chem. Phys*. **198**, 1767 (1997).
4. Kricheldorf, H. R.; Damrau, D.-O. *Macromol. Chem. Phys.* **199**, 1747 (1998).
5. Li, S.; Vert, M. *"Biodegradable Polymers: Polyesters" in: The Encyclopedia of Controlled Drug Delivery",* E. Methiowitz, Ed. J. Wiley & Sons, New York, P-71 (1999).
6. Li, S.; Vert, M. "*Biodegradation of Aliphatic polyesters" in; Degradable Polymers: Principles and Applications",* G. Scott, D. Gilead, Eds. Chapman and Hall, London**,** p-43 (1995).
7. Moore, G. F.; Saunders, S.M.; *Advances in biodegradable polymers" in Rapra Review Reports* **98**, 1 (1997).
8. Sinclair, R.G. *USP 4045418* (1977).
9. Sinclair, R.G. *USP 40457537*, **1977**.
10. Wehrenberg, *R.H. ME*. **9**, 3 (1981)
11. Vion, J. M.; Jerome, R.; Teyssie, P.; Aubin, M.; Prudhomme, R. E. *Macromolecules*, **19**, 1828 **(1986).**
12. (a) Ovitt, T. M.; Coates, G. W. *J. Am. Chem. Soc.* **124**,1316 (2002). (b) Huang, C.-H.; Wang, F.-C.; Ko, B.-T.; Yu, T.-L.; Lin,C.-C. *Macromolecules* **34**, 356 (2001). (c) Liu, Y.-C.; Ko, B.-T.; Lin, C-C. *Macromolecule*s **34**, 6196 (2001). (d) Chen, H.-L.; Ko, B.-T.; Huang, B.-H.; Lin, C.-C. *Organometallics* **20**, 5076 (2001). (e) Hsueh, M.-L.; Huang, B-H.; Lin, C.-C. *Macromolecules* **35**, 5763 (2002). (f) Zhong, Z.; Dijkstra, P. J.; Feijen, J. *J. Am. Chem. Soc*. **125**, 11291 (2003).
13. (a) Kricheldorf, H. R. *Makromol. Chem*. **194**, 1665 (1993). (b) Ko, B-T.; Lin, C-C. *J. Am. Chem. Soc*. **123**, 7973 (2001). (c) Chisholm, M. H.; Lin, C-C.; Galluccia, J. C.; Ko, B-T. *DaltonTrans* 406 (2003).

14. (a) Kricheldorf, H. R.; Berl, M.; Scharnagl, N. *Macromolecules* **21**, 286 (1988). (b) Chisholm, M. H.; Eilerts, N. W.; Huffman, J. C.; Iyer, S. S.; Pacold, M.; Phomphrai, K. *J. Am. Chem.Soc*. **12**, 11845 (2000). (c) Chisholm, M. H.; Gallucci, J.; Phomphrai, K. *Inorg. Chem.* **2002**, 41, 2785. (d) Chisholm, M. H.; Phomphrai, K. *Inorg. Chim. Acta.* **350**, 121 (2003).
15. (a) O'Keefe, B. J.; Breyfogle, L. E.; Hillmyer, M. A.; Tolman, W. B. *J. Am. Chem. Soc.* **124**, 4384 (2002). (b) Duda, A.; Penczek, S. In Polymers from Renewable Resources: Biopolyestersand Biocatalysis; Scholz, C., Gross, R. A., *Eds. ACS Symp. Ser*., 764. (c)Dobrzynski, P.; Kasperczyk, J.; Janeczek, M.; Bero, M. *Polymer* **43**, 2595 (2002).
16. Kricheldorf, H. R.; Sumbbl, M. V.; Saunders, I. K. *Macromolecules* **24**, 1944 (1991).
17. (a) Schwach, G.; Coudane, J.; Engel, R.; Vert, M. *Polym. Int*. **46**, 177 (1998). (b) Bero, M.; Kasperczyk, J.; Jedlin, ski. J. *Macromol. Chem*. **191**, 2287 (1990). (c) Bero, M.; Kasperczyk, J.; Adamus, G. *Macromol. Chem.* **194**, 907 (1993). (d) Cheng, M.; Moore, D. R.; Reczek, J. J.; Chamberlain, B. M.; Lobkovsky, E. B.; Coates, G. W. *J. Am. Chem. Soc*. **123**, 8738 (2001). (e) Rieth, L. R.; Moore, D. R.; Lobkovsky, E. B.; Coates, G. W. *J. Am. Chem. Soc*. **124**,15239 (2002). (f) Moore, D. R.; Cheng, M.; Lobkovsky, E. B.; Coates, G. W. *J. Am. Chem. Soc*. **125**, 11911 (2003). (g) Allen, S. D.;Moore, D. R.; Lobkovsky, E. B.; Coates, G. W. *J. Organome. Chem*. **683**, 137 (2003). (h) Chamberlain, B. M.; Cheng, M.; Lobkovsky, E. B.; Coates, G. W. *J. Am. Chem. Soc.* **123**, 3229 (2001).
18. Lewinski, J.; Ochal, Z.; Bojarski, E.; Tratkiewicz, E.; Justyniak, I.; Lipkowski, *J. Angew. Chem. Int. Ed.* **42**, 4643 (2003).
19. Chen, Hsuan-Ying.; Huang, Bor-Hunn.; Lin, Chu-Chieh. *Macromolecules* **38**, 5400 (2005).
20. Kricheldrof , H. R .; Serra, A. *Polymer Bull.* **14**, 497 (1985).
21. Kleine, I.; Kleine , H. *Makromol Chem.* **30**, 23 (1959).
22. Dittrich, W.; Schutz, R. C. *Makromol Chem.* **15**, 109 (1971).
23. Chabot, F.; Vert, M.; Chapelle, St.; Granger. P. *Polymer* **24**, 53 (1983).

24. Bero, M.; Kasperczyk, J.; Jedlinsky, Z. J. *Makromol. Chem. Phys*. **191**, 2287 (1990).
25. Nijehuis, A. J.; Grijpma, D. W.; Pennings, A. J. *Macromolecules* **95**, 6419 (1992).
26. For the crystal structure of Pro_2Zn: Ng. C-H.; Fun, H. –K.; Teo, S-B.; Teoh, S-G.; Chinnakali, K. *Acta Crystallogr* C **51**, 244 (1995).
27. Leensing, J. W.; Gogolewski, S.; Pennings, A. J. *J. Appl. Polym. Sci.* **29**, 2829 (1984).
28. Kricheldrof, H.R.; Damrau, D.O. *Macromol.Chem. Phys.* **199,** 1089 (1998).
29. Kricheldrof, H.R.; Saunders, K.I..; Boettcher, C. *Polymer* **36,** 1253 (1995).
30. Willams, C. K.; Breyfogie, L. E.; Choi, S.K.; Nam, W.; Young, V.G.; Hillmyer, M. A.; Tolman, W. B. *J. Am. Chem. Soc.*1**25**, 11350 (2003).
31. Kricheldrof, H.R.; Damrau, D.O. *Macromol.Chem. Phys.***199**, 1747 (1998).
32. Wachsen, O.; Reichert, K. H.; Kruger, R. P.; Much, H.; Schulz, G. *Poly. Degrad. Stab.* **55**, 225 (1997).
33. Chabot, F.; Vert, M. *Polymer* **24**, 53 (1993).
34. Kricheldrof, H.R.; Saunders, K.I. *Macromol. Symp*. **103**, 85 (1996).
35. Slivniak, R.; Domb, A. J. *Macromolecules* **38**, 5545 (2005).

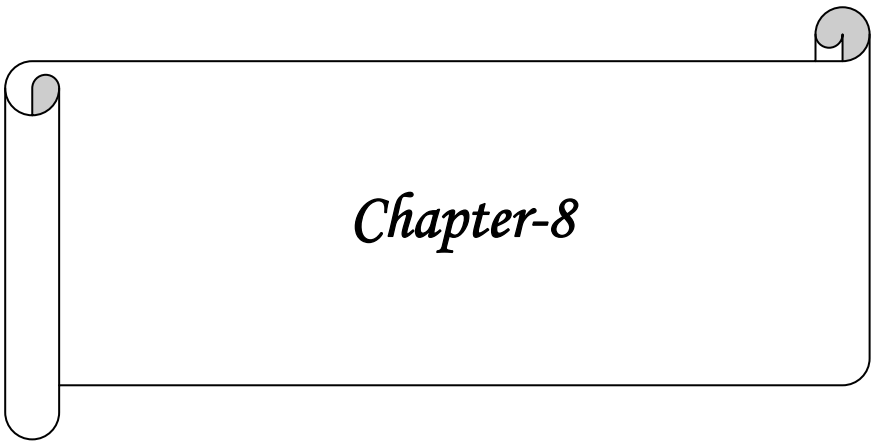
Chapter-8

CHAPTER 8: SUMMARY AND CONCLUSIONS

In the present work, poly (L-lactic acid) oligomers were synthesized, starting from L-lactic acid monomer obtained as 88 % aqueous solution. Monomer purity was determined by gas liquid chromatography and the total amount of impurities such as methanol, ethanol, acetic acid, pyruvic acid, fumaric acid and succinic acid were detected to be less then 30 ppm.

Linear PLA oligomers of controlled number average molecular weight and having both hydroxyl and carboxyl end groups were prepared as PLA oligomer by dehydropolycondensation and ring opening polymerization of lactide.

A range of PLA oligomers starting from linear to macro cyclic were obtained by dehydropolycondensation of L-lactic acid under various reaction conditions and using Lewis acid catalysts. Properties of the PLA oligomers were found to be more dependent on the polymerization temperature (140-190 ^{0}C) and also somewhat the nature of the catalyst. PLA oligomers are strictly linear in the polymerization temperature in to the temperature range (140-145 ^{0}C). Both linear and macro cyclic PLA oligomers were obtained in the range of 160-165 ^{0}C. Macro cyclic structures were predominant in the higher temperature (~190 ^{0}C). Incorporation of D-lactic acid units in the backbone due to racemization was also observed at 190 ^{0}C.

Post-polymerization of linear oligomers were performed in the presence of various zeolites i.e. ZSM-5, ZSM-12 and β-zeolite. Stereosequence analysis of the PLA polymers were examined using quantitative ^{13}C NMR spectra.

Homopolymer of aleuritic acid and copolymers of aleuritic acid with L-lactic acid at various compositions were prepared and the aggregation behavior due to pendent hydroxyl groups were studied.

Functionalized multiwalled carbon nanotubes were further modified using L-lactic acid, PLA oligomers ($\bar{M}_n$ -13,200) and L-lactic acid with 12-hydroxy stearic acid copolymer by graft polymerization technique.

Zinc prolinate catalysts were prepared by using L and D-proline precursor and used for the homopolymerizaton of lactides and copolymerization of lactide with ε-caprolactone.

Salient achievements of the present work:

1. Although PLA oligomers using Lewis acid catalysts have widely studied, the post polymerization in presence of zeolites have not been carried out. **Molecular weight of PLA oligomers was found to enhance 13 folds in presence of β-zeolites. Zeolites act as a Lewis acid as well as desiccating agents. β-zeolite was found to be best among other zeolites studied because of its large surface area. Polymer PLA prepared with $SnCl_2.2H_2O$ exhibited lower transestrification values in comparison with other catalysts. A stereo specificity favoring long isotactic block was detected.**
2. There are few literature reports here and there regarding poly aleuritic acid by enzymatic method. Poly (aleuritic acid) has also been carried out by condensation method and resulted infusible masses due to side reaction and crosslinking reaction etc. **Poly (aleuritic acid) and L-lactic acid-co-aleuritic acid were prepared by dehydropolycondensation for the first time using protection and deprotection method. A linear poly (aleurtic acid) with $\bar{M}_w$ 120,000 was prepared. Aggregation behavior of PAA showed micelle type structure in various solvents. The copolymers of L-lactic acid and aleuritic acid are soluble in organic and also mixed solvents. The copolymers also assembled in to micelle like structures.**
3. Multiwalled carbon nanotubes were functionalized by treating with nitric acid and sulphuric acid mixture. The graft copolymerization of L-lactic acid, PLA oligomes and L-lactic acid with 12-hydroxy stearic acid copolymer were carried out on the surface of functionalized MWCNTs using different Lewis acid catalysts. **Grafting reaction of L-LA, PLA oligomers and copolymers on the surface of functionalized MWCNTs was achieved for first time by dehydropolycondensation. Thermal studies reveal that PLA-g-MWCNTs have the effect of plasticizing the PLA matrix and also suggest the formation of new crystalline domains, which is likely to induce in the proximity of the functionalized MWCNTs. The homogeneous distribution of MWCNTs was**

observed by AFM and ultimately improve the mechanical and electrical properties of PLA polymers.

4. An enormous amount of research work has been carried out in the field of ring opening polymerization (ROP) of lactones using zinc derivatives. The amino acids and their derivatives belong to human metabolism. However, zinc salt of proline have never been used as catalyst for the polymerization of lactide, ε-caprolactone and also their copolymerization reaction. **PLA oligomers with $\bar{M}_n$ 2900-5100 Da was also obtained with zinc L-prolinate catalyst. A linear copolymer of L, L-lactide with ε-caprolactone with $\bar{M}_w$ 9000 to 30,000 was obtained. Block copolymer of ε-caprolactone with L, L-lactide were prepared by sequential addition of ε-caprolactone and lactides and the $\bar{M}_w$ as found to be 52,000.**

Future directions:

For arriving at a higher molecular weight PLA from direct dehydropolycondensation, the only way is to synthesize higher molecular weight oligomers than achieved in the present work and then perform various post-polymerization reactions in presence of other zeolites having matching pore size and higher surface area. But, higher molecular weight of PLA oligomers can definitely not be achieved through dehydropolycondensation of L-LA by increasing the reaction temperature, because of competitive cyclization.

Silicate and organo modified alumino-silicates (clays) have generally been used for compositing with PLA and copolymers with other monomer, where PLA and copolymers with other monomer is the main matrix and clay is the minor component. Such compositing is expected to bring about changes in mechanical properties of the polymers.

Functionalization of carbon nanotubes by treating with ethylene glycol to produce primary hydroxyl group on the surface of carbon nanotube. Grafting of lactides and other lactone on the surface of functionalized MWCNTs, SWCNTs and fullerene by using ring opening polymerization technique.

Kinetic study of copolymerization of lactide with other lactone in presence of zinc prolinate as ROP catalyst. Prepration of other amino acid salt of zinc and study the homo and copolymerization of lactones.

P U B L I C A T I O N S

1. Homopolymerization and Copolymerization of L, L-Lactide in Presence of Novel Zinc proline Organocmetallic Catalyst **Proceedings of International Conference (BIO) DEGRADABLE POLYMERS FROM RENEWABLE RESOURCES, Vienna, 18-21 November 2007, p-69-76.**

   A. Pandey and B. Garnaik

2. Synthesis of poly (L-lactic acid) by dehydropolycondensation using various pore size zeolites

   e-polymer (Manuscript under communication)

   Asutosh K. Pandey, B. Garnaik

3. Synthesis and Characterization of Novel Value Added Biodegradable Poly (Aleuritic Acid) from Renewable Resources (Shellac) and Invertible Amphiphilic Behaviors in Various Solvents

   e-polymer (Manuscript under communication)

   Asutosh K Pandey, Baijayantimala Garnaik

4. Synthesis and Characterization of L-Lactic and Aleuritic Acid Based Copolyesters

   Journal of Applied Polymer Science (Manuscript under communication)

   Asutosh K. Pandey, Baijayantimala Garnaik

5. Sequences Determination by ^{13}C NMR of Poly (L-Lactic acid) Prepared by Dehydropolycondensation Method

   Macromolecular Rapid Communication (Manuscript under communication)

   Asutosh K. Pandey, B. Garnaik

6. Biocompatible Biodegradable Polymer grafted Multiwalled Carbon Nanotubes through Dehydropolycondensation

   Macromolecules (Manuscript under communication)

   Asutosh K. Pandey, Baijayantimala Garnaik

7. Copolymerization of L, L-lactide with ε-caprolactone by zinc derivative of L-proline

   J. Polym. Sci, Chem. Edn. (Manuscript under communication)

   Asutosh K. Pandey, Baijayantimala Garnaik

PAPER PRESENTATIONS IN NATIONAL AND INTER NATIONAL CONFERENCES

1. Presented a poster in **Macro 2004 in Kerala** entitled: "Synthesis of Biodegradable Poly lactic acid by using various pore zeolites." A. K. Pandey, B. Garnaik
2. Presented a poster in **Macro 2006 in National Chemical Laboratory,** entitled: "Synthesis and Characterization of Novel Biodegradable Polymer Poly (Aleuritic acid) and study the aggregation behavior of hydroxyl pendant groups." A. K. Pandey, B. Garnaik
3. Presented a poster in **NMRS-2007 National Chemical Laboratory,** entitled: "Polymerization of L-lactic acid with various organotin catalysts and it's a stereo chemical aspect." A. K. Pandey, B. Garnaik
4. Presented a poster in **NMRS-2007 National Chemical Laboratory, e**ntitled: "Solid-State ^{13}C CP/MAS studies of the crystallinity and morphology of biodegradable polymers and grafted on Mulltiwalled carbon nanotubes."

   A. K. Pandey, B. Garnaik
5. Presented a poster in **Polymer 2007 Vienna- Austria**, entitled "Homopolymerization and Copolymerization of L, L-Lactide in presence of Novel Zinc proline Organocmetallic Catalyst" A. K. Pandey, B. Garnaik
6. Presented a paper **"Recent Advanced in Drug Discovery Research" 2008 Poona college,** entitled "Synthesis of drug molecule precursor using polymer supported with lithium aluminum hydride (LAH) by complexation " Asutosh K. Pandey, B. Garnaik.
7. Presented a paper **2nd International symposium on Advanced Materials and polymers for Aerospace and Defence Applications "SAMPADA-2008"** entitled "Biocompatible and Biodegradable Polymers Sandwich Between Multiwalled carbon nanotube (MWCNTs)" Asutosh K. Pandey and Baijayantimala Garnaik

8. Presented a poster in **Macro 2009 in Chennai,** entitled "Polymer-Grafted Multiwalled Carbon Nanotubes through Dehydropolycondensation" Asutosh K. Pandey, Baijayantimala Garnaik